Aus dem Institut für Molekularbiologie und Tumorforschung
Geschäftsführender Direktor: Prof. Dr. Rolf Müller
des Fachbereichs Medizin der Philipps-Universität Marburg

# Identification and functional characterisation of dL(3)mbt-containing complexes in *Drosophila melanogaster*


Inaugural-Dissertation
zur Erlangung des Doktorgrades der Naturwissenschaften
(Dr. rer. nat.)

dem Fachbereich Medizin der Philipps-Universität Marburg
vorgelegt von

Karin Meier

aus Amberg

Marburg 2012

Angenommen vom Fachbereich Medizin der Philipps-Universität Marburg am:

4.5.2012

Gedruckt mit Genehmigung des Fachbereichs.

| | |
|---|---|
| Dekan: | Prof. Dr. Matthias Rothmund |
| Referent: | Prof. Dr. Alexander Brehm |
| 1. Korreferent: | Prof. Dr. Renate Renkawitz-Pohl |

*Für meine Eltern*

"*The important thing is not to stop questioning,*

*curiosity has its own reason for existing.*"

Albert Einstein

# Table of contents

# 1 Summary

## 1.1 Abstract

The *Drosophila* Lethal (3) malignant brain tumour (dL(3)mbt) protein is the founding member of the family of MBT domain proteins. The MBT domain is a 'chromatin reader', a module that specifically recognises mono- and di-methylated lysines within histone tails. *In vitro* studies suggest that these domains compact nucleosomes to form higher order chromatin structures. Importantly, MBT domain-containing proteins were previously shown to have critical functions in developmental processes, maintenance of transcriptional repression and tumour suppression. Accordingly, mutation of the gene that encodes the dL(3)mbt protein leads to the development of a malignant and invasive tumour in the brain of third instar larvae.

Data from both *Drosophila melanogaster* and human implicate that MBT domain proteins cooperate with or are part of multi-subunit protein complexes. Therefore, the goal of this thesis was to identify novel interaction partners and protein complexes of dL(3)mbt.

In the first part of this thesis, dL(3)mbt has been shown to associate with enzymatic histone deacetylase activity. dRpd3 was identified as a histone deacetylase specifically associating with dL(3)mbt. Interestingly, the three MBT domains were sufficient to mediate interaction with dRpd3. This dL(3)mbt-dRpd3 complex has been linked to the maturation of newly synthesised chromatin.

In the second part of this study, the multi-subunit complex LINT, consisting of dL(3)mbt, the co-repressor protein dCoREST and the novel protein dLint-1, was isolated by FLAG immunoaffinity purification and classical biochemical chromatography. These factors interacted stably with each other in extracts from cell lines, embryos and larval brain. On polytene chromosomes the two LINT subunits dL(3)mbt and dLint-1 co-localised extensively at many binding sites. Subsequent microarray analysis led to the identification of hundreds of genes that were co-regulated by dL(3)mbt and dLint-1. Among these target genes was a subset of germline-specific genes that were stably repressed by all three LINT complex components. Strikingly, there is a significant overlap with genes that have been demonstrated to drive tumour growth in *l(3)mbt* mutant brains. Moreover, this study confirmed that the LINT complex

bound directly to promoter regions of these target genes to repress transcription. A reporter gene assay revealed that the recruitment of dL(3)mbt and dLint-1 to the promoter of a luciferase gene was sufficient to repress its transcription and that maximal repression was dependent of the presence on all LINT subunits.

The upregulation of LINT target genes was accompanied by changes in histone modifications, namely an increase in active and a loss of repressive histone modifications. However, since the LINT complex itself does not contain histone-modifying enzymes these changes are likely to occur co-transcriptionally.

Collectively, the results of this thesis lead to a model, in which the LINT complex maintains transcriptional repression of germ cell-specific target genes by hindering access of RNA Polymerase II and other activating transcription factors to their promoters.

## 1.2 Zusammenfassung

Das *Drosophila* Protein Lethal (3) malignant brain tumour (dL(3)mbt) war das Gründungsmitglied der Familie der MBT-Domänen Proteine. Die MBT-Domäne ist ein sogenannter "Chromatin-Leser", ein Modul, das spezifisch an mono- und di-methylierte Lysine, die in Histon-Schwänzen lokalisiert sind, bindet. *In vitro* Studien legen nahe, dass diese Domänen Nukleosomen kompaktieren, um dichter gepacktes Chromatin zu erzeugen. Bedeutenderweise wurde im Vorfeld gezeigt, dass MBT-Domänen enthaltende Proteine entscheidende Funktionen in Entwicklungsprozessen, der Erhaltung von transkriptioneller Repression und Tumorsuppression übernehmen. Dementsprechend führt die Mutation des Gens, das für dL(3)mbt kodiert, zur Entwicklung eines malignen und invasiven Tumors im Larvengehirn des dritten Larvenstadiums.

Daten sowohl aus *Drosophila melanogaster* als auch dem humanen System implizieren, dass MBT-Domänen Proteine im Allgemeinen Proteinkomplexen, die mehrere Untereinheiten enthalten, angehören oder mit ihnen zusammenwirken. Daher war das Ziel dieser Arbeit neue Interaktionspartner und Proteinkomplexe von dL(3)mbt zu identifizieren.

Im ersten Teil dieser Arbeit wurde gezeigt, dass dL(3)mbt mit enzymatischer Histondeacetylaseaktivität assoziiert. dRpd3 wurde als eine Histondeacetylase identifiziert, die spezifisch mit dL(3)mbt interagiert. Interessanterweise waren die drei MBT-Domänen ausreichend, um die Bindung mit dRpd3 zu vermitteln. Die Funktion dieses dL(3)mbt-dRpd3-Komplexes wurde in Zusammenhang gebracht mit der „Reifung" von neu synthetisiertem Chromatin.

Im zweiten Teil dieser Studie wurde der Proteinkomplex LINT, der aus dL(3)mbt, dem Korepressor dCoREST und einem neu identifizierten Protein namens dLint-1 besteht, mittels FLAG-Immunoaffinitäts-Aufreinigung und klassischer Chromatographie isoliert. Diese Faktoren interagieren stabil miteinander in Extrakten, die von Zelllinien, Embryonen und larvalen Gehirnen gewonnen wurden. Auf Polytän-Chromosomen kolokalisierten die beiden LINT-Untereinheiten dL(3)mbt und dLint-1 in hohem Umfang an vielen Bindungsstellen. Anschließende *Microarray*-Analyse führte zur Identifizierung Hunderter Gene, die von dL(3)mbt und dLint-1 koreguliert wurden. Innerhalb dieser Zielgene war eine Untergruppe von Keimbahn-spezifischen Genen, die

stabil von allen drei LINT-Komponenten reprimiert wurden. Auffallend ist, dass es einen signifikanten Überlapp mit Genen gibt, die das Tumorwachstum in *l(3)mbt* mutanten Gehirnen fördern. Weiterhin, bestätigte diese Arbeit, dass der LINT-Komplex direkt an die Promotoren dieser Zielgene bindet, um die Transkription zu unterbinden. Die Untersuchung eines Reportergen-Systems machte deutlich, dass die Rekrutierung von dL(3)mbt und dLint-1 an den Promotor eines Luciferasegens ausreicht, um dessen Transkription zu reprimieren und dass die maximale Repression abhängig ist von der Anwesenheit aller LINT-Untereinheiten.

The Hochregulierung von LINT-Zielgenen wurde von Veränderungen von Histon-modifikationen begleitet, nämlich dem Anstieg von aktiven und dem Verlust von repressiven Histonmodifikationen. Allerdings ist es, da der LINT-Komplex keine Histon-modifizierenden Enzyme enthält, wahrscheinlich, dass diese Veränderungen kotranskriptionell auftreten.

Zusammengefasst, führen die Resultate dieser Arbeit zu einem Modell, in welchem der LINT-Komplex die Repression von Keimzell-spezifischen Zielgenen aufrechterhält, indem er den Zugriff von RNA Polymerase II und anderen aktivierenden Trans-kriptionsfaktoren auf ihre Promotoren behindert.

# 2 Introduction

## 2.1 Regulation of chromatin

### 2.1.1 Chromatin structure

In all eukaryotes the genetic information is encoded by DNA and packaged into chromatin, in a way that allows cellular processes, such as transcription, replication and DNA repair, to take place. The fundamental unit of chromatin is the nucleosome, which is composed of 146 base pairs (bp) of superhelical DNA wrapped around a protein octamer. This protein complex consists of the four core histones (each in two copies) H3, H4, H2A and H2B (Figure 2.1). The core histones are predominantly globular with the exception of the unstructured N-terminal 'tails', which stick out of the nucleosome (Luger et al., 1997).

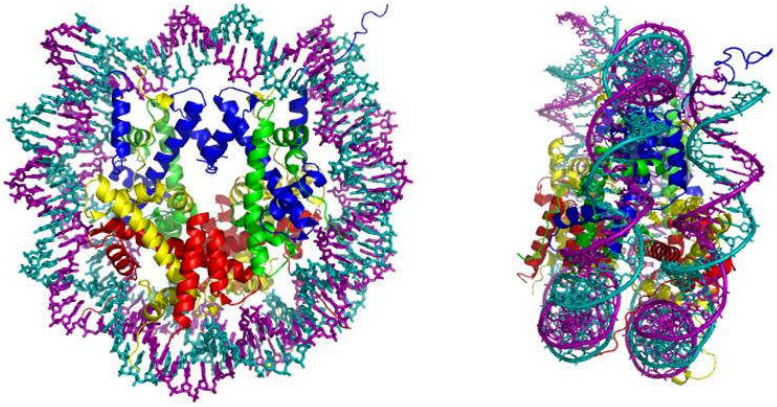

**Figure 2.1: Crystal structure of the nucleosome core particle.** Histone octamer core consisting of H3 (blue), H4 (green), H2A (blue) and H2B (red) (each two copies) and a 146 bp DNA superhelix (turquoise and purple). Left panel: View down the DNA superhelix. Right panel: View perpendicular to the DNA superhelix. The figure was generated using PyMOL software from the pdb file [1AOI] (Luger et al., 1997), available at the RSCB protein data base (http://www.rcsb.org/pdb/home/home.do).

The repeating nucleosome core particles are separated from each other by a stretch of linker DNA and therefore occur on average every 200 bp throughout the eukaryotic genome (Kornberg, 1977). Under non-physiological conditions, nucleosome arrays including the linker DNA can form an approximately 10 nm fibre, referred to as 'beads-on-a-string' structure (Thoma et al., 1979). In the nucleus, however, chromatin is

progressively compacted into higher-order chromatin structures, such as the 30 nm fibre. The assembly of higher-order structures is stabilised by the linker histone H1, which is attached to the nucleosome core where the DNA enters and leaves the histone octamer. In addition a multitude of non-histone proteins participate in the formation of higher-order chromatin structures, such as the heterochromatin protein 1 (HP1) (Eissenberg et al., 1990; James and Elgin, 1986).

Dependent on the degree of compaction, chromatin can be divided into two general types, euchromatin and heterochromatin (Huisinga et al., 2006). Whereas hetero-chromatin is typically highly condensed, relatively gene-poor and transcriptionally inert, euchromatin is less condensed, gene-rich and generally associated with higher transcriptional activity.

Aside from the overall level of compaction the activity of chromatin is determined by various parameters, which play important roles during distinct cellular processes:

First, the spacing between nucleosomes can vary and thereby influence nucleosome occupancy and positioning, which is for instance implicated in the regulation of gene expression by allowing or inhibiting the access of sequence-specific regulatory factors (Schnitzler, 2008). A genome-wide analysis in yeast revealed that most transcription factor binding sites are depleted of nucleosomes (Yuan et al., 2005). In general, the nucleosome architecture can be altered by chromatin remodeler factors, which utilise the energy of ATP-hydrolysis to loosen DNA-histone interactions (Varga-Weisz and Becker, 1998).

Second, in addition to canonical histones, different variants exist that have evolved specialised functions in biological pathways. For instance, an alternative form of H3 is the histone variant H3.3 that is structurally very close to canonical H3 since they differ only in four amino acid residues (McKittrick et al., 2004). Despite this similarity, the histone variant H3.3 has been found to be specifically enriched in transcriptionally active chromatin and is the key substrate of replication-independent nucleosome assembly (Ahmad and Henikoff, 2002; McKittrick et al., 2004). The deposition of H3.3 appears to be coupled to transcription (Schwartz and Ahmad, 2005).

Third, DNA can be methylated on cytosines ($m^5C$) within CpG dinucleotides, which is the major target for DNA methylation in eukaryotes (Bird, 2002). An exception is *Drosophila melanogaster* (*D. melanogaster*), where DNA methylation was found

mostly on CpTs in early embryos (Lyko et al., 2000). In general DNA methylation is associated with chromatin silencing (Bird et al., 2002).

Finally, also histone proteins are targets for modifications that have roles both in activation and repression of transcription (for more details see 2.1.2).

### 2.1.2 Histone modifications

A remarkable feature of histones is their large number of residues that can be post-translationally modified. These modifications include acetylation, methylation, phosphorylation, ubiquitylation, sumoylation, ADP-ribosylation, deimination, proline-isomerisation (Kouzarides, 2007), propionylation, butyrylation (Zhang et al., 2009) and glycosylation (Sakabe et al., 2010). While some modification types, such as acetylation, methylation, phosphorylation and ubiquitylation (Figure 2.2), have been more intensively studied (see below), the biological nature of other post-translational histone modificaions (PTMs), such as propionylation, butyrylation and glycosylation, remains to be determined. In general, histone modifications have been shown to be important in many chromatin associated cellular processes, such as gene regulation, DNA replication, DNA repair, and chromosome condensation (Kouzarides, 2007). Just recently, a direct role of histone modifications in the regulation of alternative splicing has been demonstrated (Luco et al., 2010).

The role of distinct histone modifications will be discussed below, with a special focus on their function in gene regulation. The mode of action of histone modifications is thought to rely on two basic mechanisms. Firstly, they act indirectly by recruiting non-histone proteins, which in turn regulate corresponding processes through their chromatin-associated activities. Secondly, they act directly by influencing inter- or intranucleosomal DNA-histone contacts and thereby impacting higher-order chromatin structure (Kouzarides, 2007).

The latter mechanism is documented best for histone acetylation, which occurs on several lysine residues within all four core histones (Figure 2.2). The covalent attachment of an acetyl group to a lysine residue will neutralise the positive charge of the ε-amino group in the lysine side chain. *In vitro* assays have suggested that this neutralisation of histone tails by hyperacetylation prevents the formation of higher-order chromatin compaction and thereby can promote transcription (Annunziato et al., 1988;

Tse et al., 1998). Furthermore, it has been shown that acetylation of H4K16 alone can also cause defects in chromatin folding, substantiating that H4K16ac is a critical determinant of the degree of chromatin compaction (Shogren-Knaak et al., 2006; Shogren-Knaak and Peterson, 2006). Generally speaking, acetylation of histones is associated with gene activation, while deacetylated chromatin is linked to transcriptional repression (Shahbazian and Grunstein, 2007).

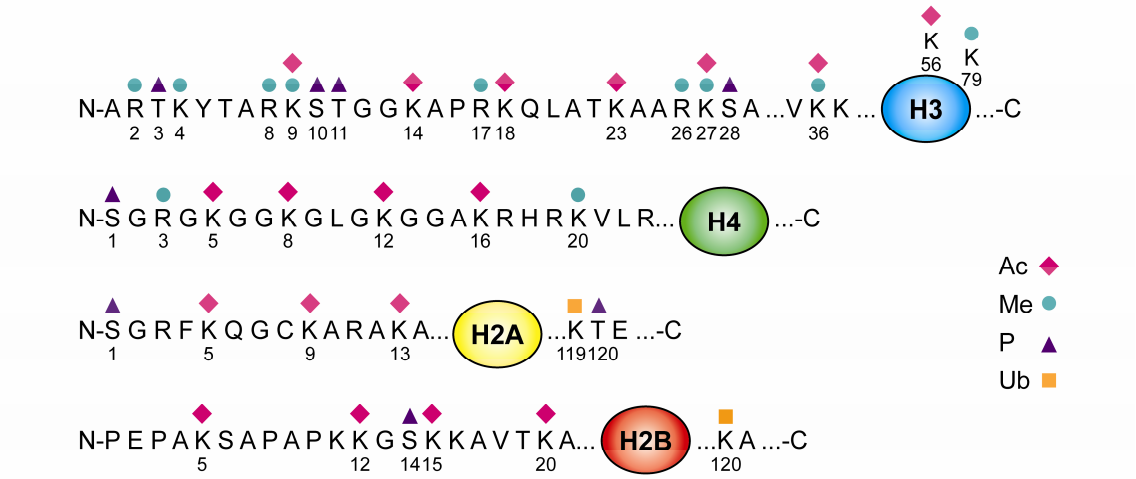


**Figure 2.2: Histone modifications: Acetylation, methylation, phosphorylation and ubiquitylation of H3, H4, H2A and H2B.** Schematic illustration of PTMs on canonical histones. The majority of histone modifications occur in the N-terminal tails of histones. Exceptions from this rule are methylation of K56 and K79 in H3 and ubiquitylation of K119 and K120 in H2A and H2B, respectively, as well as phosphorylation of T120 in H2A, which are located in the globular histone domains (modified from Bhaumik et al., 2007).

Phosphorylation of several histone H3 residues (such as S10: Wei et al., 1998; T11: Preuss et al., 2003; S28: Goto et al., 1999) has a well established role in chromosome condensation during mitosis (Nowak and Corces, 2004). Therefore it is striking that histone phosphorylation occurring during interphase has also been linked to transcriptional activation, which is thought to require an open chromatin state (Nowak and Corces, 2004; Pérez-Cadahía et al., 2009).

Unlike acetylation, which in general is associated with actively transcribed genes, histone lysine methylation is associated with either active or repressive transcription, depending on the chromatin context and the residue it occurs on (Li et al., 2007a; Kouzarides, 2007). The complexity of this modification is further enhanced by the existence of three methylation states: mono- (me1), di- (me2) and tri-methylation (me3). In H3 several lysines have been found to be methylated, four of them are located in the

N-terminus (K4, K9, K27, K36), while K79 resides within the globular domain. In histone H4 only K20 is known to be targeted by lysine methylation. Whereas methylation on H3K9, H3K27 and H4K20 has been implicated in chromatin silencing, H3K4 and H3K36 methylation has been associated with actively transcribed chromatin. A genome-wide analysis in yeast revealed that specific histone methylation marks, associated with actively transcribed genes, exhibit specific patterns relative to the gene body (Pokholok et al., 2005). Thus, H3K4me3 peaks at the promoter-proximal regions, whereas H3K36me3 is enriched throughout the transcribed region with highest levels at the 3' end.

In addition to lysines, arginines are also targets for methylation and are modified either by mono- or di-methylation (Di Lorenzo and Bedford, 2010). The latter can be either symmetric or asymmetric with one methyl group on each terminal nitrogen or both methyl groups on one terminal nitrogen, respectively. Histone arginine methylation can be associated with both transcriptional activation and repression.

The dynamics of histone modifications is dependent on enzymes catalysing the covalent attachment of PTMs, so called 'writers', and their removal, so called 'erasers' (see 2.1.4) (Figure 2.3; Gardner et al., 2011). Furthermore, there are 'readers', also referred to as effector proteins, that specifically recognise histone modifications and accordingly associate with chromatin via specific binding modules (see 2.1.3).

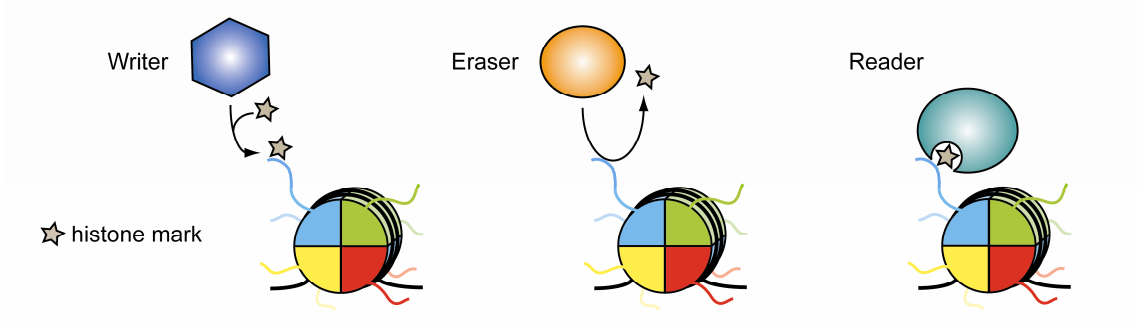


**Figure 2.3: Activities of chromatin factors associated with histone modifications.** Writers attach PTMs (asterisk) covalently to histones (left panel), while erasers remove them (middle panel), and readers (also termed effectors) bind to specific modifications (right panel) (modified from Gardner et al., 2011).

The discovery of a large number and variety of histone modifications in recent years, also led to the finding that distinct histone modifications can influence each other, either synergistically or antagonistically (Suganuma and Workman, 2008). This kind of

communication between PTMs is called 'cross-talk' and can occur at different levels. For example, lysine residues can be modified by different PTMs, such as acetylation and methylation (compare H3K9, Figure 2.2), which is why these modifications are mutually exclusive. Whereas acetylation of H3K9 is associated with transcriptional activation (Liang et al., 2004; Roh et al., 2005), H3K9 methylation, a specific binding site for HP1, is a marker of silenced genes and heterochromatic regions (Bannister et al., 2001; Stewart et al., 2005). Moreover, the binding of factors to specific histone marks can be either inhibited or enhanced by an additional modification of an adjacent residue. An example that illustrates inhibition is the disruption of HP1 binding to methylated H3K9 during M-phase of the cell cycle by phosphorylation of H3S10 (Fischle et al., 2005). On the other hand, H3S10 phosphorylation can also promote K14 acetylation by the Gcn5 enzyme to activate transcription (Clements et al., 2003).

As a model of how histone modifications can regulate diverse processes associated with chromatin, the 'histone code hypothesis' has been put forward (Strahl and Allis, 2000; Jenuwein and Allis, 2001). Thus, a histone code is established by the combinatorial nature of distinct histone modifications that are read by effector proteins to bring about a corresponding downstream biological event.

### 2.1.3 Histone modification readers

The histone code is becoming continuously more elaborate due to the discovery of novel histone modifications and 'cross-talks' between various modifications (Winter and Fischle, 2010). Although the exact mechanisms of how this code is deciphered in the cell remains to be investigated in more detail, the binding of reader proteins (or effector proteins) that interpret histone modifications and translate them into a proper downstream event, is one favoured model (Strahl and Allis, 2000). In order to specifically bind to distinct histone modifications, reader proteins harbour histone binding modules (Figure 2.4). In the past decade, a large number of crystal structures of histone binding modules, either in the free form or bound to their histone peptide substrate, and *in vitro* binding studies have contributed to the mechanistic understanding of specific recognition of PTMs by these domains (Taverna et al., 2007). Some of these insights into specific readout mechanisms will be discussed in the following.

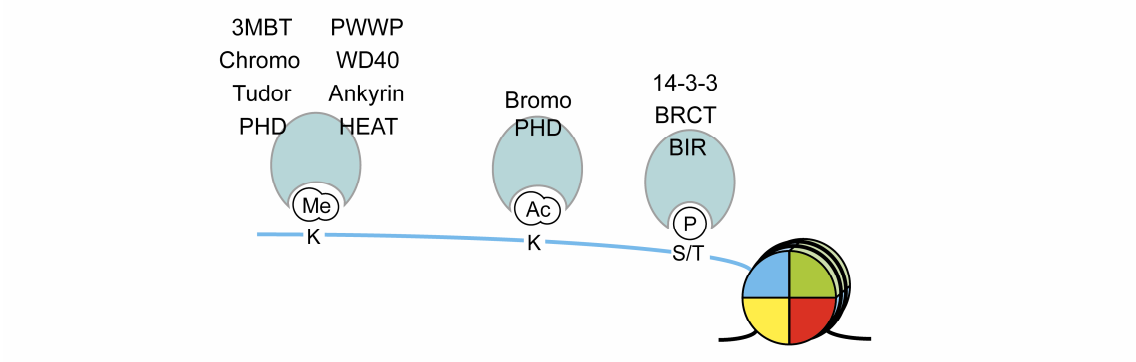


**Figure 2.4: Histone modification binding modules.** Domains that specifically bind to methylated lysines, acetylated lysines or phosphorylated serines/threonines (modified from Kouzarides, 2007 and complemented with novel binding modules: Brent and Marmorstein, 2008; Han et al., 2006; Kelly et al., 2010; Liu et al., 2010; Sofueva et al., 2010; Wang et al., 2009; Zeng et al., 2010).

*The Bromo domain*

The Bromo domain, originally identified in the *Drosophila* protein Brahma (Tamkun et al., 1992), is a module known to bind to acetylated lysines. This highly conserved domain is found in many chromatin-associated proteins, such as chromatin remodelling factors, as well as in most histone acetyl transferases (Jeanmougin et al., 1997). Detailed insight into the mechanism of acetyl-lysine recognition was first gained from the solution of an NMR structure of the Bromo domain of HAT co-activator p300/CBP-associated factor (P/CAF) and from a high-resolution crystal structure of the *Saccharomyces cerevisiae* (*S. cerevisiae*) acetyl-transferase Gcn5 Bromo domain complexed with H4K16ac (aa 15-29) (Dhalluin et al., 1999; Owen et al., 2000). Bromo domains adopt a conserved structural fold that is composed of a left-handed anti-parallel bundle of four helices (Z, A, B and C) with inter-helical loops ZA and BC. These loops accommodate a hydrophobic binding pocket, in which the acetyl-lysine inserts. In addition to hydrophobic interactions, acetyl-lysine forms a specific H-bond between the oxygen of the acetyl carbonyl group and the amide nitrogen of a conserved asparagine. Further contacts with the binding pocket derive from a network of water-mediated H-bonds between the protein backbone carbonyl groups and acetyl-lysine.

*The 'Royal family' of histone binding domains*

The methylation state of lysines can be recognised by various binding modules (Figure 2.4). Among them are Tudor, Chromo, PWWP and MBT domains, which all belong to the so-called 'Royal family' and share a β-stranded core region (Maurer-

Stroh et al., 2003). Members of the Royal family can read out both higher (Kme2, Kme3) and lower (Kme1, Kme2) lysine methylation states. A common mechanism of these domains is the formation of hydrophobic cavities or cages for the specific recognition of differentially methylated lysine residues (Taverna et al., 2007). Typically, Chromo domains belong to the group of modules that bind higher methylation states of lysines. In this context, the Chromo domain of HP1 binds preferentially to di- and tri-methylated H3K9, while the Chromo domain of Polycomb (Pc) specifically binds to H3K27me3 (Fischle et al., 2003). Interestingly, Tudor domains can target both higher and lower methylation states. While the tandem Tudor domain of human JMJD2A was found to bind to H3K4me3 (Huang et al., 2006), the tandem Tudor domain of 53BP1 recognises H4K20me1 and -me2 (Botuyan et al., 2006). The binding specificity and structural mechanism of malignant brain tumour (MBT) domains as low methylation histone lysine readers will be described in detail below (see 2.2.1).

*The PHD finger domain*

Another domain able to bind histone lysines is the plant homeo domain (PHD), which was first described in the *Arabidopsis* homeo domain protein HAT3.1 (Schindler et al., 1993), but is also conserved in many other eukaryotic chromatin-related proteins with roles in transcription regulation (Aasland et al., 1995). Characteristic for canonical PHD fingers, spanning 50 to 80 amino acids on average, is a Cys4HisCys3 (C4HC3) signature that coordinates two zinc ions (Pascual et al., 2000; Capili et al., 2001).

On the one hand, PHD fingers exhibit nucleosome-binding activity. This was demonstrated for the PHD finger of the acetyltransferase p300 that cooperates with the adjacent Bromo domain to bind to hyperacetylated nucleosomes in a robust manner (Ragvin et al., 2004). Moreover, it was reported that the two PHD fingers of *Drosophila* ATP-dependent chromatin assembly factor 1 (Acf1) can bind to the central domains of core histones and thereby increase the efficiency of nucleosome mobilisation activity of the ATPase ISWI (Eberharter et al., 2004).

On the other hand, PHD domains were shown to function as specific histone modification binding modules, recognising lysines of different methylation states. Thus, the PHD finger of human BPTF, the largest subunit of the chromatin remodelling complex NURF, binds to tri-methylated H3K4 (Li et al., 2006; Wysocka et al., 2006), whereas the PHD domain of human BHC80, a LSD1 complex component (Shi et al.,

2005), targets the unmethylated H3 tail (Lan et al., 2007b). In both cases, the histone H3 peptide binds to the surface of the PHD finger by extending the PHD anti-parallel β-sheet by an additional strand. In the BPTF PHD finger the tri-methyl group of H3K4me3 is positioned within a cage of four aromatic residues. Furthermore, the specific binding of BPTF to H3K4me3 results from the simultaneous binding of H3R2 in a second binding channel (Li et al., 2006). The BHC80 PHD domain lacks an aromatic cage. Instead, recognition of the unmethylated K4 residue through a pair of H-bonds with the ε-ammonium group and steric exclusion of methyl groups contribute to its specificity (Lan et al., 2007b). Recently, PHD fingers have been shown to be an alternative module to bromo domains to bind to acetylated lysines. Thus, the tandem PHD finger of human DPF3b, which cooperates with the BAF chromatin remodelling complex, specifically recognises the H3K14ac modification (Zeng et al., 2010).

Remarkably, histone binding modules, such as Bromo, Chromo, Tudor, MBT and PHD domains frequently occur in multiple repeats or in combination within the same protein or a protein complex (Ruthenburg et al., 2007). This observation supports the idea that many chromatin factors bind to multiple histone modifications in a multivalent fashion (Figure 2.5).

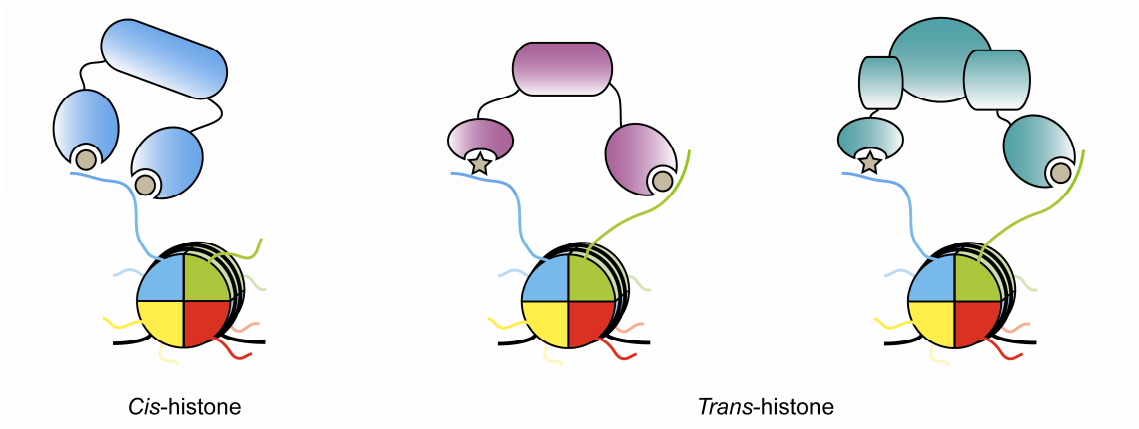


**Figure 2.5: Modes of intranucleosomal binding to multiple histone modifications.** Left panel: A chromatin protein binds to two histone modifications within the same histone tail (*cis*-histone). Middle panel: A protein interacts with two histone modifications located in different histone tails (*trans*-histone). Right panel: Two distinct proteins as part of a complex associate with two histone modifications located in different histone tails (*trans*-histone) (modified from Ruthenburg et al., 2007).

### 2.1.4 Histone modification writers and erasers

Histone modifications are thought to be dynamic, since for most modifications writers, which specifically set the mark, and erasers, which catalyse selective removal, exist.

The extent of histone acetylation is regulated by histone acetyltransferases (HATs) and histone deacetylases (HDACs) (Shahbazian and Grunstein, 2007).

Most histone lysine methyltransferases (HKMTs) belong to a class of proteins containing a catalytic SET domain (named after the *Drosophila* proteins Su(var)3-9, E(z) and Trx), which possesses a selective substrate specificity (Upadhyay and Cheng, 2011). An HKMT that lacks the SET domain is Dot1, which specifically methylates H3K79 (Feng et al., 2002). The removal of lysine methylation is carried out either by lysine specific demethylase (LSD) enzymes (Shi et al., 2004; Karytinos et al., 2009) via a flavin-dependent amine oxidation reaction or members of the Jumonji C (JmjC) domain-containing dioxygenases in a $Fe^{2+}$- and α-ketoglutarate-dependent reaction (Tsukada and Zhang, 2006).

The methylation of arginines is catalysed by protein arginine methyltransferases (PRMTs), a family of enzymes that transfer a methyl-group of S-adenosylmethionine (SAM) to a guanidino nitrogen of arginines (Di Lorenzo and Bedford, 2010). There are two major classes of PRMTs, namely type I and II. Both produce mono-methylation as an intermediate towards di-methylation. Type I and II PRMTs further catalyse the formation of asymmetric and symmetric di-methylation, respectively. To date, it is unclear, whether arginine demethylases exist. Previously, human JMJD6 has been reported to be the first identified arginine demethylase (Chang et al., 2007). However, a study from Webby and co-workers (2009), as well as a structural analysis (Mantri et al., 2010), suggest that the dominant catalytic activity of JMJD6 is lysyl-hydroxylation. Besides, a modification that can block arginine methylation is the conversion of arginine to citrulline by peptidylarginine deiminases (PADIs) (Cuthbert et al., 2004).

The role of enzymatic activities of writers and erasers will be exemplified by the two opposing histone lysine methylation marks H3K27 (repressive) and H3K4 (active), mainly focusing on the *Drosophila* system. Among the enzymes that regulate these two histone modifications are Polycomb group (PcG) and trithorax group (trxG) proteins, which are required for the proper maintenance of restricted homeotic gene (*Hox*) expression patterns during metazoan development (Kennison, 1995), whereby trxG and PcG proteins maintain the active or silent chromatin state of *Hox* genes, respectively.

The expression of *Hox* genes in turn is essential for the specification of the anterior-posterior body axis and segment identity. The system of PcG and trxG proteins has been studied in the past extensively and the investigation in *D. melanogaster* as a model organism has contributed to a great extent to our current understanding.

#### 2.1.4.1 Dynamics of H3K27 methylation

*Methylation of H3K27*

Tri-Methylation of H3K27 is a hallmark of Polycomb silenced chromatin and is catalysed by the PcG member Enhancer of zeste (E(z)) (Czermin et al., 2002; Müller et al., 2002). The SET-domain HKMT E(z) is a subunit of the Polycomb repressive complex 2 (PRC2), which further contains the proteins Extra sex combs (Esc) (or Esc-like, Escl), Nucleosome remodelling factor 55 (Nurf-55, also termed chromatin assembly factor 1, Caf1), and Suppressor of zeste 12 (Su(z)12) as core subunits. A homologous PRC2 complex was also identified in human (Cao et al., 2002; Kuzmichev et al., 2002). Interestingly, biochemical analyses of E(z) reveal that the enzyme on its own is virtually inactive. To effectively methylate K27 within the histone H3 tail E(z) needs to associate with the three above-mentioned non-enzymatic subunits of the PRC2 complex (Czermin et al., 2002; Ketel et al., 2005; Nekrasov et al., 2005). While Nurf-55, Su(z)12 and Esc contribute to nucleosome binding, Esc is also crucial to boost the enzymatic HKMT activity of E(z) as part of the PRC2 complex (Nekrasov et al., 2005). A specific role of the human homologue of Esc, the WD40 domain protein EED, was identified recently. EED was demonstrated to bind specifically via an aromatic cage to tri-methylated lysines in histone tails associated with repressive functions, among them H3K27me3 (Margueron et al., 2009). In methylation assays the addition of H3K27me3 histone tails increased the HKMT activity of PRC2 on unmodified nucleosomes significantly. It is noteworthy that these observations provide a mechanism of how the H3K27me3 mark could be propagated following DNA replication. Biochemical purification of Polycomb-like (Pcl) interacting proteins, led additionally to the identification of a PRC2 complex variant, Pcl-PRC2, which also catalyses mono-, di- and tri-methylation of H3K27 *in vitro* (Nekrasov et al., 2007). *In vivo* data in *Drosophila* mutants lacking Pcl suggest that Pcl-PRC2 is critical for the generation of high H3K27 tri-methylation levels at Polycomb target genes, but appears to be dispensable for genome-wide H3K27me1/2 levels.

*Demethylation of H3K27*

The E(z) activity is counteracted by H3K27 specific demethylases. In human the two related JmjC-domain proteins JMJD3 and UTX have been identified to specifically demethylate H3K27me2/3 (Agger et al., 2007; De Santa et al., 2007; Lan et al., 2007a; Lee et al., 2007a). A role of UTX in the regulation of *Hox* genes was demonstrated upon differentiation of the pluripotent embryonal carcinoma cell line NT2/D1 with retinoic acid. UTX was shown to be recruited to the promoters of *HOXA* and *B* loci coinciding with the loss of H3K27me3 and gene activation (Agger et al., 2007; Lee et al., 2007a). The homologue H3K27me2/3 demethylase in *Drosophila* was termed dUTX (Smith et al., 2008). Consistent with a role of dUTX in gene activation, its co-localisation with the elongating form (C-terminal domain (CTD) phosphorylated at Ser2) of RNA polymerase II (Pol II) was observed. Using the heat shock gene *Hsp70* as a model for inducible gene activation, dUTX was found to be recruited along with Pol II to the *Hsp70* gene upon heat shock. Interestingly, the investigation of histone modification changes in *Utx* mutant clones revealed in addition to an increase in H3K27me3 a reduction of H3K4me1 levels (Herz et al., 2010). In this context it is important to note, that the human UTX demethylase was found to associate with H3K4 methyltransferases of the mixed-lineage leukemia (MLL) family (Cho et al., 2007; Issaeva et al., 2007; Lee et al., 2007a).

### 2.1.4.2 Dynamics of H3K4 methylation

*Methylation of H3K4*

The methylation of H3K4, which antagonises PcG gene silencing in *Drosophila*, has been reported to be catalysed by the SET domain and trxG proteins Trithorax (Trx) and Absent, small or homeotic discs 1 (Ash1) (Breen and Harte, 1991; Klymenko and Müller, 2004; LaJeunesse and Shearn, 1995; Milne et al., 2002).

However, the specificity of Ash1 as a methyltransferase is controversial. Initially, Ash1 was shown to be a multi-catalytic HKMT methylating H3K4, H3K9 and H4K20 *in vitro* (Beisel et al., 2002). An independent study found that the SET domain of Ash1 specifically methylates H3K4 *in vitro* and that H3K4 methylation is widely lost on polytene chromosomes of *ash1* mutant *Drosophila* larvae *in vivo*, while H3K9 methylation is only slightly reduced and H4K20 or H3K36 methylation is unaffected (Byrd and Shearn, 2003). Therefore, in the past the effect of Ash1 on *Hox* gene

expression has been discussed in light of its H3K4 methyltransferase activity. However, two research groups report that *Drosophila* and human Ash1 specifically methylate H3K36 and that pre-existing H3K36 methylation inhibits the enzymatic activity of PRC2 on nucleosomes (Tanaka et al., 2007; Yuan et al., 2011).

Nevertheless, consistent with a role as trxG proteins, which are generally considered to function as transcriptional activators, expression of the *Hox* gene *Ubx* is lost in *ash1* or *trx* mutant imaginal discs within its normal expression domain (Klymenko and Müller, 2004). Surprisingly, the *Ubx* expression is restored in these mutants, when additionally PcG function is removed. Furthermore, such trxG and PcG double mutants display strong mis-expression of *Hox* genes comparable to observations made in PcG single mutant clones. These results led to a model, in which Trx and Ash1 HKMTs do not function as 'co-activators', but as 'anti-repressors' preventing PcG silencing of *Hox* genes in their normal expression domains.

*Demethylation of H3K4*

In *Drosophila*, demethylation of the active histone mark H3K4 is catalysed by dLsd1 (also referred to as Su(var)3-3) (Di Stefano et al., 2007; Rudolph et al., 2007) and the JmjC-domain protein Little imaginal discs (Lid) (Eissenberg et al., 2007; Lee et al., 2007b). dLsd1 specifically demethylates H3K4me1/2, whereas the substrate of Lid has been shown *in vivo* to be tri-methylated H3K4. Recently, dKDM2 has been identified as an additional potential H3K4me3 demethylase (Kavi and Birchler, 2009).

Previously, mutant alleles of *Su(var)3-3* have been reported to suppress positional-effect variegation (PEV) (Di Stefano et al., 2007; Rudolph et al., 2007). In *D. melanogaster* PEV is an experimental system to identify genes controlling higher-order chromatin formation. In PEV a euchromatic gene becomes subjected to transcriptional silencing as a result of its placement into the vicinity of heterochromatin by chromosomal rearrangements (Schotta et al., 2003). Therefore, the suppressor function of dLsd1 suggested its requirement for heterochromatic gene silencing (Di Stefano et al., 2007; Rudolph et al., 2007). Upon mutation of *Su(var)3-3* early embryos display elevated levels of H3K4me2 in somatic and germline precursor cells, resulting in a reduction of heterochromatic H3K9me2/3 (Rudolph et al., 2007). These results support a role of dLsd1 in controlling the boundaries between eu- and heterochromatin during early embryogenesis.

Opposite to what one would expect from an enzyme removing a histone modification correlated with transcriptional activation, *lid* was first identified as a member of the trxG of genes, since *lid* mutations enhanced the homeotic phenotypes caused by mutations in other trxG genes (Gildea et al., 2000). In line with Lid-mediated H3K4me3 demethylation contributing to *Hox* gene activation, expression of *Ubx* in haltere discs upon *lid* mutation and in S2 cells upon Lid knockdown was reduced (Lee et al., 2007b; Lloret-Llinares et al., 2008). Moreover, heterozygous *lid* mutant flies show a strong enhancement of PEV indicating a role of Lid in antagonising heterochromatin-dependent gene silencing (Lloret-Llinares et al., 2008).
Although dLsd1 and Lid cooperatively increase global levels of H3K4 methylation, the opposing functions in regulating euchromatin-heterochromatin boundaries were confirmed in double mutant flies (Di Stefano et al., 2011). Nevertheless, both dLsd1 and Lid were also shown to be directly involved in the repression of euchromatic Notch target genes (*E(spl)*) in a synergistic manner, by modulating the H3K4 methylation levels (Di Stefano et al., 2011; Moshkin et al., 2009).

Taken together, the findings above illustrate that there is a complex functional interplay between histone lysine methylases and demethylases *in vivo* and that the biological role of distinct chromatin-modifying enzymes depends very much on the chromatin context.

## 2.2 MBT domain proteins

### 2.2.1 MBT domains as histone modification readers

The MBT domain was originally named after the *D. melanogaster* tumour suppressor gene *lethal (3) malignant brain tumour* (*l(3)mbt*). Upon the identification and cloning of the *l(3)mbt* gene sequence, Wismar et al. (1995) noticed that the 1477 aa long sequence of the predicted protein MBT163 (referred to as dL(3)mbt in the following), encoded by *l(3)mbt*, comprised three tandem repeats of a novel motif encompassing 100 aa in average. This motif was termed ‘mbt-repeat’. A decade later the MBT domains have been found to belong to a new class of methyl-lysine binding modules (Kim et al., 2006), which has contributed to a growing interest in the functional analysis of MBT domains.

#### 2.2.1.1 Structural basis of histone peptide binding by MBT domains

The first crystal structure of MBT domains has been solved for human L3MBTL1, which like dL(3)mbt contains three MBT repeats (Wang et al., 2003). In addition, the MBT domains of L3MBTL1 have been crystallised in complex with two potential physiological ligands, the histone peptides H1.5K27me1/2 (aa 23-27) (Li et al., 2007b) and H4K20me2 (aa 15-25) (Min et al., 2007). Since then several other MBT domains have been crystallised and their structure solved at atomic resolution (Eryilmaz et al., 2009; Grimm et al., 2007; Grimm et al., 2009; Guo et al., 2009; Santiveri et al., 2008; Sathyamurthy et al., 2003).

The three-dimensional structure of the human three MBT (h3MBT) domains comprises three similar globular modules (Figure 2.6). Each MBT domain consists of a C-terminal globular β-subunit core with a barrel-like fold and a long N-terminal arm that forms extended contacts with the β-subunit core of the preceding neighbour. This architecture adopts a stable propeller-like structure with three leaves arranged around a central cavity (Wang et al., 2003) (Figure 2.6, left panel). The structural observation that the N-terminal arm of each MBT domain interacts extensively with its neighbouring MBT core is a likely explanation for why these domains are commonly found in repeats of at least two domains (Bonasio et al., 2010; Sathyamurthy et al., 2003).

The crystal structure of h3MBT uncovered potential binding pockets in all three structural equivalent β-subunit cores, which were occupied by the morpholino ring of MES (2-(N-morpholino)ethane sulfonic acid; a component of the crystallisation buffer) (Wang et al., 2003). Strikingly, crystal structures of h3MBT bound to H4K20me2 (Min et al., 2007) and H1.5K27me2 (Li et al., 2007b) revealed that only one of the MBT domains, namely the second, accommodates di-methylated lysine. A fact that interestingly also applies to modules with two (Grimm et al., 2007; Santiveri et al., 2008) or four MBT domains (Grimm et al., 2009; Guo et al., 2009).

The binding pocket of the second MBT domain of h3MBT that accommodates the di-methyl-lysine (Kme2) is formed by residues Phe379, Trp382, Tyr386, Leu361, Thr411 and Asp355 (Figure 2.6, right panel). The first four residues form an ‘aromatic cage’, with the side chains of Phe379, Trp382 and Tyr386 orientated approximately perpendicular to one another. This aromatic cage interacts with Kme2 via van-der-Waals and cation-π interactions (Min et al., 2007). Moreover, the negatively charged

Asp355 residue stabilises the Kme2 binding through formation of a salt bridge and a hydrogen bond to the di-methylammonium group.

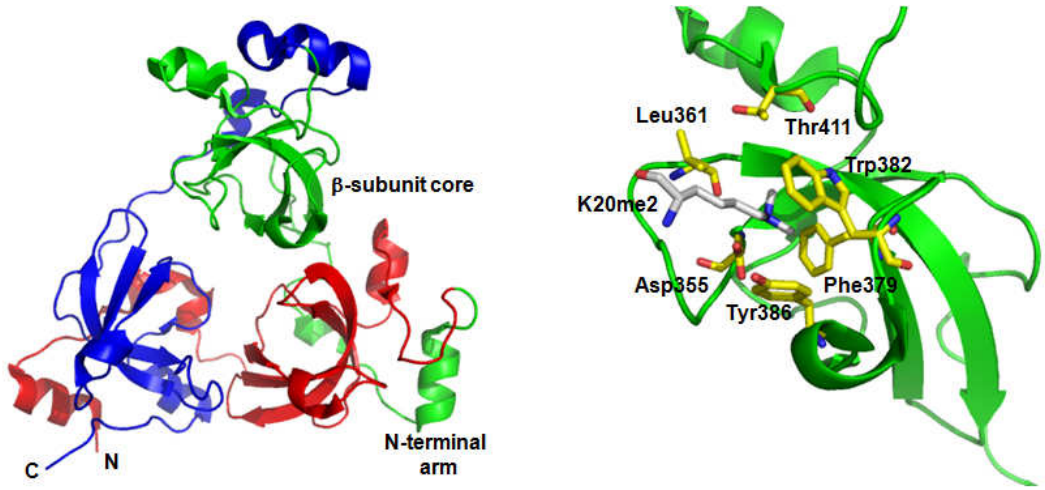


**Figure 2.6: Crystal structure of the three MBT domains of human L3MBTL1.** Left panel: Propeller-like structure of the three MBT domains MBT1 (red), MBT2 (green) and MBT3 (blue). The labelling of the β-subunit core and the N-terminal arm refers to MBT2. N: N-terminus; C: C-terminus. Right panel: Binding of di-methylated lysine K20 of H4 peptide (aa 17-25) to the binding pocket of MBT2. Residues forming the lysine-binding pocket and the K20me2 are shown as stick models (in yellow and gray, respectively). The figure was generated using PyMOL software from the pdb file [2PQW] (Min et al., 2007), available at the RSCB Protein data base.

An explanation for the exclusive peptide binding of the second MBT domain was found by superimposition of the three MBT modules: In the first and the third MBT domain the relatively small side chain of Cys363 inside of the binding site is substituted by a long or bulky side-chain of arginine or phenylalanine, respectively. Hence, steric hindrance prevents the binding of methyl-lysine to the binding pockets.

Although peptide association is only observed for one domain of the MBT repeats, all MBT domains seem to have the structural potential to bind ligands, which remain to be identified. In h3MBT the first MBT domain was found to coordinate the proline of an adjacent MBT molecule (Min et al., 2007). Whether this interaction is important under physiological conditions needs to be further analysed.

#### 2.2.1.2 Specificity of histone peptide binding

Qualitative peptide pulldown assays and quantitative methods, such as isothermal titration calorimetry (ITC) and fluorescence polarisation measurements, demonstrated a preferential binding of MBT domains to mono- and di-methylated lysines within histone tails, including H4K20, H1.4K26, H3K9, H3K27, H3K4 and H3K36 methylation marks (Bonasio et al., 2010; Kalakonda et al., 2008; Li et al., 2007b). While the three MBT domains of L3MBTL1 bind equally well to mono- and di-methyl states in some cases (H4K20, H1.4K26), in others the binding affinity for mono-methyl-lysine is greater by a factor of two (H3K9, H3K27, H3K36) or even by an order of magnitude (H3K4) (Li et al., 2007b). Despite the low selectivity concerning the sequence context surrounding the lysines, a higher specificity in the *in vivo* context seems to be likely. For instance, PR-SET7-mediated H4K20 mono-methylation, but not G9a-catalysed H3K9 methylation, is involved in the recruitment of L3MBTL1 to the *cyclin E* promoter (Kalakonda et al., 2008).

*Discrimination between differentially methylated lysines*

The discrimination of MBT domains between Kme1/2 and Kme0/3 is based on the chemical nature of the different methylation states of lysine. Thus, weaker van-der-Waals and cation-π interactions of the aromatic cage with unmethylated lysine are likely to account for favoured binding of higher methylation states (Min et al., 2007). In case of the tri-methyl modification, loss of the hydrogen bond with Asp355 and a weakening of ionic interactions between Kme3 and Asp355, as well as steric hindrance of the bulky tri-methyl-lysine, provide an explanation for the exclusion from the binding pocket.
An exception concerning the peptide specificity of MBT domains mentioned above is the module of the four MBT domains of the *C. elegans* protein LIN-61. In *in vitro* assays LIN-61 shows a strong preference for histone peptides containing di- and tri-methylated H3K9 over other peptides with methylated lysines, including H4K20, H3K27, H3K4 and H3K36 (Koester-Eiserfunke and Fischle, 2011). Furthermore, mutagenesis of conserved residues, known to be important for histone peptide binding (see above), implies a binding mode that differs from other MBT modules.

*Methylation-dependent chromatin compaction*

Another striking feature of the MBT domains, shown for the three MBT domains of human L3MBTL1 *in vitro*, is their ability to compact oligo-nucleosomal arrays in an

H4K20me1/2- and H1bK26me1/2-dependent manner (Trojer et al., 2007). In agreement with structural data (Li et al., 2007b; Min et al., 2007) mutation of residues critical for histone peptide recognition confirmed that the second MBT domain was essential for binding of methylated H4K20 or H1bK26 (Trojer et al., 2007). Trojer et al. provide two models of how MBT domains could compact chromatin in a monomeric or dimeric form by bringing nucleosomes into closer vicinity through binding to the respective histone modifications. However, the mechanism of how MBT domains compact chromatin exactly and the physiological relevance of this activity *in vivo* remain to be determined.

### 2.2.2 MBT domain proteins in *Drosophila melano*gaster

*The dL(3)mbt tumour suppressor protein*

The founding member of the MBT domain protein family is dL(3)mbt (Wismar et al., 1995). The corresponding *l(3)mbt* gene, mapping to the right arm of chromosome 3, was first identified in a genetic screen for mutant alleles causing malignant transformations in the developing fly (Gateff et al., 1993). A recessive-lethal and temperature sensitive (ts) mutation of *l(3)mbt* (*l(3)mbt*$^{ts1}$), induced by the mutagen ethyl methane sulfonate (EMS), resulted in the malignant transformation of adult optic neuroblasts and ganglion mother cells in the larval brain at the restrictive temperature of 29°C. In addition to the malignant phenotype in the larval brain, a (non-malignant) epithelial overgrowth of the imaginal discs was observed. The penetrance of the mutant allele is 100% and larvae die at the end of the third instar stage without giving rise to adult flies. The malignant cells were shown to grow in an autonomous, invasive and lethal fashion after transplantation into wild-type adult hosts. The time period, in which *l(3)mbt* gene activity was sensitive to the restrictive temperature and led to 100% brain tumour growth (but normal imaginal disc development), spanned the first six hours of embryonic development. At the permissive temperature of 22°C mutant flies developed normally without any apparent phenotype.

Additional *l(3)mbt* alleles were recovered in a maternal-effect screen with the objective to identify genes involved in pole/germ cell formation in the early embryo (Yohn et al., 2003). As a result, mutations in *l(3)mbt* were demonstrated to result in a reduced number of germ cells. There are two critical processes during the development of germ

cells in the *Drosophila* embryo: 1. The assembly of the germ plasm, characterised by special components, such as *oskar*-mRNA, at the posterior end of the egg. 2. The migration of nuclei into the germ plasm prior to pole cell formation. In embryos laid by females mutant for *l(3)mbt* a disruption of the synchrony of nuclear divisions in the early embryo was observed, which very likely accounts for the defect in germ cell development. Interestingly, by sequencing *l(3)mbt* mutant alleles, displaying defects in mitotic divisions, Yohn et al. (2003) could show that four out of five mutations (Missense mutations: GM79, ts1; Nonsense mutations: GM76, E2) map to the MBT domains, supporting their importance for dL(3)mbt function.

In line with a role of MBT domain proteins during cytokinesis, the human homologue L3MBTL1 was found to be associated with condensed chromosomes in mitotic cells (Koga et al., 1999). Overexpression of L3MBTL1 caused defects in proper chromosome segregation and cytokinesis, resulting in multi-nucleated U251MG cells.

*The Polycomb proteins Scm and Sfmbt*

In addition to dL(3)mbt, *D. melanogaster* contains two other MBT domain containing proteins: Sex comb on midleg (Scm) and Scm-related gene containing four mbt domains (Sfmbt) (Figure 2.7; see also 2.2.4). Both belong to the PcG group of proteins (Simon et al., 1992; Klymenko et al., 2006). In *Drosophila* many PcG genes were identified because of segmental transformation phenotypes produced by their mutation or mis-expression. For instance, in $Scm^{-/-}$ embryos, which lack both maternal and zygotic *Scm* product, all body segments from T1 (thoracic) to A7 (abdominal) were shown to be transformed into copies of segment A8 (Breen and Duncan, 1986). $Sfmbt^{1}$ (knockout allele) homozygous animals die as larvae (Klymenko et al., 2006), but mis-expression of the *Hox* gene products Ubx and Scr could be observed in induced $Sfmbt^{1}$ homozygous cell clones in imaginal discs of otherwise heterozygous animals.

It is worth noting that dL(3)mbt, Scm and Sfmbt protein sequences do not only share MBT domains as a structural motif, but also Zn fingers of the $C_2C_2$ type and the SPM domain (Bornemann et al., 1996) (Figure 2.7). The latter Scm, Ph and MBT homology (SPM) domain belongs to the superfamily of sterile alpha motif (SAM) domains (Kim and Bowie, 2003; Ponting, 1995) and might have a role in homo- and hetero-dimerisation/oligomerisation (Kim et al., 2002; Kim et al., 2005; Peterson et al., 1997). In this context, the SPM domains of Scm and Polyhomeotic (Ph) can mediate direct binding of the two proteins *in vitro* (Peterson et al., 1997). Genetic rescue experiments

*in vivo* revealed that mutations within the SPM domain of Scm that disrupt protein interactions *in vitro* correlate with a loss of Scm function (Peterson et al., 2004). Moreover, overexpression of the isolated wild-type SPM domain causes PcG loss-of-function homeotic transformation phenotypes in flies, supporting the idea that the SPM interaction module can efficiently compete with endogenous Scm for binding to other PcG partners *in vivo*.

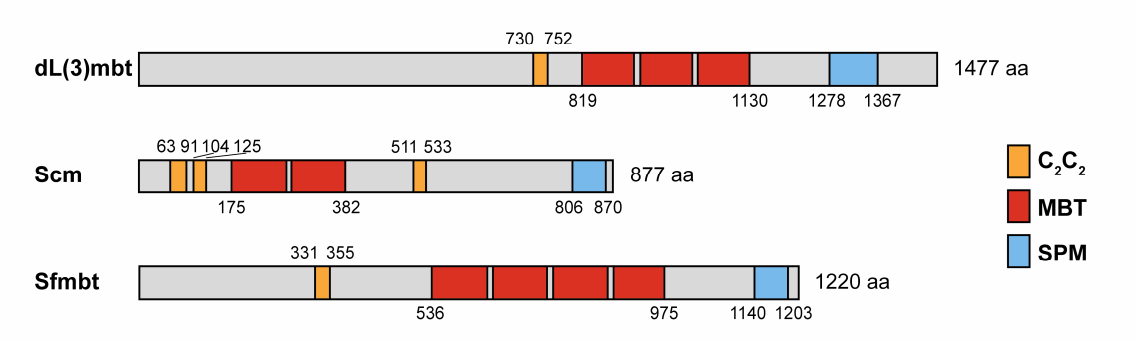


**Figure 2.7: Schematic depiction of protein domain structures of *Drosophila* MBT proteins.** Functional domains of dL(3)mbt, Scm and Sfmbt (transcript B) are displayed: MBT domains (red), SPM domains (blue) and putative Zn-fingers of the $C_2C_2$-type (orange). The positions of the domains are indicated below (MBT, SPM) or on top ($C_2C_2$). Protein lengths are indicated on the right.

### 2.2.3 MBT domain proteins in other species

The discovery of dL(3)mbt in the fly led to the identification of homologues from *Caenorhabditis elegans* (*C. elegans*) to man.

*MBT domain proteins in C. elegans*

In *C. elegans* three genes encode MBT domain containing proteins: *lin-61*, *mbtr-1* (Harrison et al., 2007) and *sor-3* (Yang et al., 2007). The LIN-61 and MBTR-1 proteins have a similar protein domain structure, being composed almost exclusively of four MBT domains and lacking other functional domains (Harrison et al., 2007). Mutational studies identified *lin-61* as a class B synthetic multivulva (synMuv) gene. In *C. elegans* vulval development is negatively regulated by the redundant functions of the synMuv genes, which are subdivided into three classes, namely A, B and C. The multivulva phenotype is caused by the mutation of at least two alleles from two different classes (Fay and Yochem, 2007). Several of the class B synMuv proteins act together in either one of the two protein complexes, DRM (DP, RB, MuvB) or NuRD-like (nucleosome

remodelling and histone deacetylase) (Harrison et al., 2006). However, LIN-61 was found to interact with neither of them (Harrison et al., 2007). Furthermore, despite their similar domain structure, MBTR-1 was not found to be involved in vulval development and its biological function remains unknown. Compared to other MBT domain containing proteins the Sor-3 protein in *C. elegans* is unique as it possesses only a single MBT domain (Yang et al., 2007). The corresponding *sor-3* gene was identified because of its role in regulating the specification of neuronal identities, including neurotransmitter patterning and axon pathfinding. In the same study, *sor-3* was shown to function as a PcG-like gene in maintaining the repression of the *Hox* gene *egl-5* outside of the restricted expression domain.

*MBT domain proteins in the mammalian system*

In mammals, at least nine MBT domain containing proteins exist (Bonasio et al., 2010). Two resemble *Drosophila* Scm, possessing two MBT domains: SCMH1 (Berger et al, 1999) and SCML2 (Montini et al., 1999). Three contain three MBT domains, like dL(3)mbt: L3MBTL1 (also known as L3MBTL) (Koga et al., 1999), L3MBTL3 (previously named MBT-1) (Arai and Miyazaki, 2005) and L3MBTL4 (Addou-Klouche et al., 2010). Four proteins are homologous to Sfmbt harbouring four MBT domains: L3MBTL2 (Wismar, 2001), SFMBT1 (Usui et al., 2000), SFMBT2 (Kuzmin et al., 2008) and MBTD1 (Eryilmaz et al., 2009). It is worth mentioning that L3MBTL2, unlike most other MBT domain proteins, does not contain an SPM domain.

**Table 2.1: Homologous MBT domain proteins in *D. melanogaster*, human and *C. elegans*.**
For evolutionary relationship and domain organisation see Bonasio et al., 2010.

| Number of MBT domains | *D. melanogaster* | Human | *C. elegans* |
|---|---|---|---|
| **1** | - | - | SOR-3 |
| **2** | Scm | SCMH1<br>SCML2 | - |
| **3** | dL(3)mbt | L3MBTL1<br>L3MBTL3<br>L3MBTL4 | - |
| **4** | Sfmbt | L3MBTL2<br>SFMBT1<br>SFMBT2<br>MBTD1 | LIN-61<br>MBTR-1 |

*MBT domain proteins and diseases*

The fact that mutation of the *Drosophila l(3)mbt* gene leads to a strong tumourigenic phenotype awoke interest in the potential tumour suppressor function of homologous human genes. Strikingly, the *l3mbtl1* gene maps to chromosome 20q12, a region that is commonly deleted (del(20q12)) in hematopoietic malignancies, such as myelo-proliferative disorders (MPD), like polycythaemia vera (PV), myelodysplastic syndromes (MDS) and acute myeloid leukemia (AML) (Bench et al., 2004; MacGrogan et al., 2004). In addition, L3MBTL1 is expressed in $CD34^+$ hematopoietic stem progenitor cells (HSPCs), which enclose the hematopoietic progenitor cells from which myeloid disorders arise (MacGrogan et al., 2004). Therefore, *l3mbtl1* has been assumed to be a good candidate tumour suppressor gene within this region, whose inactivation or haploinsufficiency could account for the pathogenesis of these disorders (Perna et al., 2010). However, two mutation analyses of a limited number of myeloid leukemia cell lines and samples from MPD and MDS patients did not identify any significant mutations (Bench et al., 2004; MacGrogan et al., 2004). Furthermore, the *l3mbtl1* gene has been previously identified as an imprinted gene locus in normal hematopoietic cells, in which monoallelic methylation of CpG islands is associated with transcriptional silencing. However, the analysis of methylation patterns revealed that the 20q12 deletion does not correlate with the preferential loss of one specific allele and retention of the methylated allele did not correlate with reduction in *l3mbtl1* mRNA levels (Bench et al., 2004; Li et al., 2004). Nevertheless, MacGrogan et al. (2004) found that eight leukemia cell lines (from 35 tested) showed significantly lower *l3mbtl1* expression (at least 3-fold; mRNA was not detectable in five cell lines) and two samples from AML patients (from 15 tested) exhibited aberrant expression (significantly lower and higher compared to normal cell population). This might indicate a relevance of L3MBTL1 expression in some cases of myeloid leukemia.

Recently, Perna et al. (2010) investigated the role of the L3MBTL1 protein in normal hematopoiesis in more detail by knockdown and overexpression experiments in $CD34^+$ cells. Thus, the knockdown of L3MBTL1 resulted in an accelerated differentiation of hematopoietic progenitor cells towards the erythroid lineage, whereas overexpression of L3MBTL1 impaired erythroid differentiation. Additionally, L3MBTL1 depleted cells showed an increased activation of the STAT5, AKT/FOXO and MAPK signalling pathways, even in the absence of erythropoietin (Epo), which is characteristic of myelo-

proliferative disorders, in particular polycythaemia vera. These results supported the idea that L3MBTL1 is critical for normal hematopoiesis.

A study investigating the role of L3MBTL1 during the cell cycle revealed that its chromatin association is most prominent during S-phase and mirrors the appearance of the H4K20 mono-methylation mark, suggesting a possible role of L3MBTL1 related to DNA replication (Koga et al., 1999). Following this up, Gurvich et al. (2010) found that cell proliferation is inhibited in L3MBTL1 depleted U2OS cells, which arrest in G2/M phase. Moreover, knockdown of L3MBTL1 in these cells caused double strand breaks (DSBs), activation of the DNA damage response (DDR) pathway and genomic instability. In agreement with a function of L3MBTL1 during DNA replication, the protein was demonstrated to interact with various components of the DNA replication machinery and to be required for proper replication fork progression. The involvement of L3MBTL1 in DNA replication and maintenance of genomic stability might provide another mechanism for the role of *l3mbtl1* as a tumour suppressor. However, given the non-redundant defects upon L3MBTL1 depletion in cell lines described above, it was somewhat surprising that L3MBTL1$^{-/-}$ mice developed normally and did not display any apparent phenotype (Qin et al., 2010). This might be attributed to a difference between an acute loss of L3MBTL1 upon knockdown versus a chronic absence in knockout mice, where functional compensation by another MBT family member could take place (Gurvich et al., 2010).

In addition to L3MBTL1 also other MBT domain proteins have been linked to cancer in human. For instance, focal homozygous and hemizygous deletions of *l3mbtl3*, *l3mbtl2* and *scml2* genes were identified in a subset of medulloblastomas (Northcott et al., 2009). Furthermore, *l3mbtl4* is a candidate tumour suppressor gene in breast cancer (Addou-Klouche et al., 2010) and AML (Veigaard et al., 2011). Loss of the 18p11 region that *l3mbtl4* maps to was found in approximately 20% of breast cancer tumours and 40% of breast cancer cell lines (Addou-Klouche et al., 2010). The *l3mbtl4* gene was shown to be targeted by deletion, breakage and mutations and its mRNA was down-regulated in a significant number of breast tumours. In addition, the 18p11 region was identified as a common deleted region in a subset of AML patients, characterised by a complex aberrant karyotype and poor prognosis (Veigaard et al., 2011).

## 2.2.4 MBT domain proteins in transcriptional repression

### 2.2.4.1 Transcriptional silencing by Polycomb group proteins

The two *Drosophila* MBT proteins Scm and Sfmbt act in concert with other PcG family members to maintain transcriptional repression of *Hox* genes (Simon et al., 1992; Klymenko et al., 2006). Since the discovery of PcG factors and their role in *Hox* gene regulation, genome-wide studies have greatly increased the number of target genes beyond *Hox* genes, both in *D. melanogaster* (Oktaba et al., 2008; Schwartz et al., 2006) and mammalian cells (Boyer et al., 2006; Lee et al., 2006b). In the fruit fly, several PcG protein complexes have been identified, among them PRC1 and PRC2, as well as the Pho-repressive complex (PhoRC) (Müller and Verrijzer, 2009). PcG proteins have been found to be associated with so called *cis*-regulatory Polycomb responsive elements (PREs) that are required for silencing (Müller and Kassis, 2006).

*Scm and the PRC1 complex*

Biochemical studies have established Pc, Ph, Posterior sex combs (Psc) and Sex combs extra (Sce)/Ring1 as core subunits of PRC1 (Francis et al., 2001; Saurin et al., 2001; Shao et al., 1999). The PRC1 complex combines writer and reader activities through Ring1 and Pc: The enzymatic activity of Ring1 facilitates H2A ubiquitylation, while the Chromo domain of Pc was reported to specifically bind to tri-methylated H3K27 (Fischle et al., 2003; Min et al., 2003), which is catalysed by E(z) and is a hallmark of PcG-silenced chromatin (Cao et al., 2002; Müller et al., 2002). Additional biochemical activities of PRC1 *in vitro* comprise chromatin compaction (Francis et al., 2004) and inhibition of chromatin remodelling (Francis et al., 2001; Shao et al., 1999). The nature of the Scm association with PRC1 (Figure 2.8), initially suggested by *in vitro* interaction assays between the SPM domains of Scm and Ph (Peterson et al., 1997), is controversial. *In vivo* reporter gene assays demonstrate the repressor function of Scm, when tethered to DNA, that requires functional Ph (Roseman et al., 2001). Further evidence derives from biochemical purifications that consistently detect sub-stoichiometric amounts of Scm in PRC1 complexes in both fly and human (Saurin et al., 2001; Levine et al., 2002). However, co-immunoprecipitations detect little or no association between Scm and PRC1 components (Klymenko et al., 2006; Peterson et al., 2004). Additionally, although Scm can stably assemble into a reconstituted PRC1 complex upon baculoviral co-expression, in gel filtration analysis the bulk of Scm in fly

embryo extract elutes in a peak that separates from Ph containing fractions (Peterson et al., 2004).

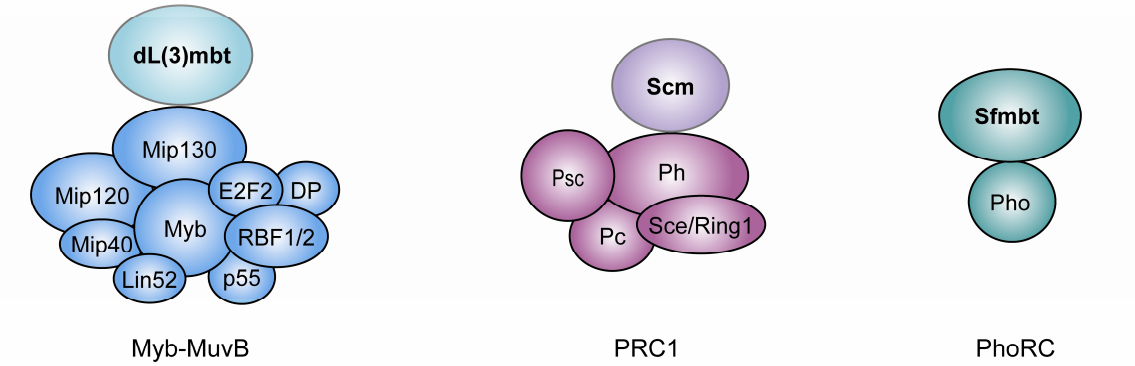


**Figure 2.8: *Drosophila* MBT domain proteins in multi-subunit complexes:** Left panel.: dL(3)mbt and the Myb-MuvB complex. Middle panel: Scm and the PRC1 complex. Right panel: Sfmbt within the PhoRC complex. dL(3)mbt and Scm are associated with the corresponding complexes in sub-stoichiometric amounts. See text for more detail.

*Targeting of Polycomb complexes*

Recently, in order to functionally characterise the relationships between Scm and the three PcG complexes, PRC1, PRC2 and PhoRC, in the context of chromatin, ChIP studies of distinct PcG components have been carried out upon RNAi in S2 cells and larval imaginal discs (Wang et al., 2010). In this study, Scm was found to co-occupy a PRE upstream of *Ubx* together with PRC1, PRC2 and PhoRC. However, Scm association was retained upon knockdown of Pho (PhoRC), E(z) (PRC2) or Pc (PRC1). In contrast, knockdown or mutation of *Scm* did not affect Pho binding, but dislodged PRC1 and PRC2 subunits. Similarly, upon Sfmbt knockdown, Scm remained bound, whereas PRC1 and PRC2 levels were reduced. These results are in agreement with biochemical studies suggesting that Scm is not a core subunit of PRC1 (see above), although it might be involved in the recruitment of PRC1 and PRC2. Questions that remain to be answered are how Scm itself is recruited, since it lacks a DNA-specific binding motif, and how it executes its repressor function.

Another recent study identified conjugation of Small ubiquitin-like modifier (SUMO) as a negative regulation mechanism of Scm and PcG-mediated silencing (Smith et al., 2011). The Scm protein was found to be a novel substrate for SUMO modification,

whereby decreased SUMOylation correlated with elevated levels of Scm at the *bxd* PRE. In agreement with this, SUMO knockdown resulted in lower expression levels of *Ubx* in S2 cells and partial haltere-to-wing transformation phenotypes in flies.

The only known PcG proteins with specific DNA-binding activity are the redundant factors Pleiohomeotic (Pho; Brown et al., 1998) and Pho-like (Brown et al., 2003), which are required for anchoring the complexes PRC1 and PRC2 at PRE sequences (Wang et al., 2004). However, Pho is not a subunit of either PRC1 or PRC2, but was found to exist together with Sfmbt in a distinct complex, named PhoRC (Klymenko et al., 2006) (Figure 2.8). Analysis of genome-wide distribution of Pho and Sfmbt in embryos and larvae revealed that PhoRC associates with PREs of a large number of target genes, including key developmental regulators, many of which are co-occupied by PRC1 and PRC2 (Oktaba et al., 2008).

*Repressive activities of Scm and Sfmbt*

With regard to a role in silencing, transcriptional repressive activity of Sfmbt was demonstrated in embryos carrying an $UAS_{GAL4}$-*Ubx-LacZ* reporter gene, when tethering Sfmbt to DNA by fusion to GAL4 (Klymenko et al., 2006). As reported for other MBT domains protein, the MBT repeats of Scm (Grimm et al., 2007) and Sfmbt (Grimm et al., 2009) bind specifically to mono- and di-methylated lysines of various histone peptides, respectively. To study the importance of the MBT domains in *Hox* gene repression, Scm (ΔMBT or D324A) and Sfmbt (E947A/Y948F/D917A) transgenes with mutations in their MBT domains, that abolish histone peptide binding *in vitro*, were tested for their capacity to rescue *Hox* gene repression (*Ubx*) in homozygous null-mutant imaginal discs (Grimm et al., 2007; Grimm et al., 2009). In case of Scm, MBT mutant transgenes showed impaired functionality in the rescue experiment compared to wild-type protein. But surprisingly, $Scm^{\Delta MBT}$ and $Scm^{D324A}$ were able to rescue repression of *Ubx* in a fraction of cell clones. Similar results were obtained testing the $Sfmbt^{E947A/Y948F/D917}$ mutant in a homozygous *Sfmbt* null-background. These observations raised the question, whether Scm and Sfmbt function in a partially redundant fashion in *Hox* gene silencing, even though biochemical purifications suggest that they are present in distinct complexes (Grimm et al., 2009). In line with this hypothesis, Scm and Sfmbt co-occupied several PREs at common target genes. Furthermore, the functional redundancy between Scm and Sfmbt was tested by investigating the mis-expression of PcG target genes in clones lacking wild-type Scm

and Sfmbt function, but expressing $Scm^{D324A}$ instead. Interestingly, in these double mutant clones a strong synergistic effect between Scm and Sfmbt for the two target genes *Abd-B* and *en* was observed, suggesting that the two proteins cooperate to maintain PcG repression. Although Scm and Sfmbt were purified in different PcG complexes, co-expression in Sf9 cells revealed a potential physical association in addition to the known genetic interaction (Grimm et al., 2009). The relevance of this association *in vivo* and the role of histone modification binding by MBT domains in the Polycomb system are so far unclear.

#### 2.2.4.2 Transcriptional repression by dL(3)mbt and homologous proteins

*Repression mechanism of human MBT domain proteins*

Similar to Scm (Roseman et al., 2001) and Sfmbt (Klymenko et al., 2006), human L3MBTL1 (Boccuni et al., 2003), L3MBTL2 (Yoo et al., 2010) and SFMBT1 (Wu et al., 2007) were shown to function as transcriptional repressors, when tethered to DNA using UAS/GAL4 luciferase reporter assays. Analysis of different deletion mutants of L3MBTL1 revealed that the MBT repeats are required for full repressive activity, whereas the SPM domain and the Zn finger motif were dispensable (Boccuni et al., 2003). In accordance with this, a construct spanning only the four MBT domains of SFMBT1 was sufficient to mediate transcriptional repression (Wu et al., 2007). In contrast to L3MBTL1, whose transcriptional repression seemed to be independent of HDAC activity (Boccuni et al., 2003), L3MBTL2-mediated repression was inhibited by TSA treatment (Yoo et al., 2010). Involvement of HDAC activity in transcriptional repression by L3MBTL2 is also supported by demonstration of a physical and selective interaction between HDAC3 and L3MBTL2 (Yoo et al., 2010). Knockdown of HDAC3, but not other class I HDACs, significantly relieved transcriptional repression mediated by L3MBTL2, suggesting that HDAC3 is a key-modulator in the repression mechanism. Like Sfmbt, L3MBTL1 was found to associate with a DNA sequence-specific transcription factor, providing a potential recruitment mechanism for L3MBTL1 to target genes (Boccuni et al., 2003). Thus, L3MBTL1 was reported to interact *in vivo* with TEL, also known as ETV6, which belongs to the ETS family of transcription factors. Deletion of either the SPM domain of L3MBTL1 or the SAM domain of TEL completely abrogated the interaction between the two proteins. Therefore, this is another example of SPM/SAM domains mediating protein-protein interactions (see

2.2.2). The ability of TEL to repress a luciferase reporter gene under the control of a TEL-responsive promoter was enhanced upon co-expression of L3MBTL1. This supports the idea that in fact L3MBTL1 is recruited to the promoter of target genes in a TEL-dependent manner.

Another human transcription factor that was reported to recruit MBT domain proteins as co-repressors is Sp3. Aiming at identifying SUMO-dependent regulators of Sp3, Stielow et al. (2008a) made use of a genome-wide RNA interference (RNAi) screen in *D. melanogaster* Kc167 cells and identified Sfmbt as a corepressor of Sp3 acting downstream of SUMO conjugation. In line with a SUMO-specific regulation mechanism, Sfmbt has been shown to be capable of binding to SUMOylated Sp3 and to be recruited to a luciferase reporter gene carrying Sp3 binding motifs in a SUMOylation-dependent manner (Stielow et al., 2008a). In agreement with the assumption that the co-repressor function of MBT domain proteins is conserved in the human system, L3MBTL1 and L3MBTL2 were recruited to a luciferase reporter gene by GAL4-Sp3-WT, but not a SUMOylation-deficient GAL4-Sp3-KEEm mutant (Stielow et al., 2008b). In addition to MBT proteins, Mi-2, HP1 proteins and methyl-transferases SETDB1 and SUV4-20H were recruited in a SUMO-dependent manner, together with the silencing histone marks H3K9me3 and H4K20me3, leading to a model in which SUMOylated Sp3 represses target genes by establishing a local hetero-chromatic environment.

*MBT domain proteins and the E2F/pRB system*

Interestingly, several studies suggest the involvement of MBT domain proteins in the E2F/pRB pathway to repress E2F target genes. The pocket proteins, such as the tumour suppressor protein pRB, and heterodimeric E2F/DP transcription factors cooperate in the regulation of cell cycle, but also differentiation (Blais and Dynlacht, 2007; Frolov and Dyson, 2004; Korenjak and Brehm, 2005). In $G_0/G_1$ pRB-family members interact with E2F transcription factors to repress genes required for S-phase entry and cell cycle progression through S-phase. Phosphorylation of pRB-family members induced by Cycline-dependent kinases (CDKs) causes the release of E2F repressor complexes from occupied promoters and results in binding of activator E2Fs and the expression of E2F target genes. The modulation of chromatin structure is thought to play an important role underlying pRB-mediated repression. Aside from core histones and the linker histone H1B, Trojer et al. (2007) identified HP1γ and the retinoblastoma protein (pRB) as

proteins interacting with L3MBTL1 using α-FLAG affinity purification. In agreement with pRB-association, L3MBTL1 is bound to proximal promoter regions of E2F target genes *c-myc* and *cyclin E1* (Trojer et al., 2007). At the *cyclin E1* promoter mono-methylation of H4K20 has been shown to contribute to association of L3MBTL1 to chromatin (Kalakonda et al., 2008). In addition to L3MBTL1, L3MBTL2 has been co-purified with an E2F-6 complex (E2F6.com-1), including the E2F6 heterodimeric partner DP-1, the heterodimeric transcription factors Mga/Max, the PcG proteins RING1/2 and HP1γ (Ogawa et al., 2002). Subunits of the E2F6.com-1 were found to bind to E2F-responsive target genes in $G_0$ rather than $G_1$. Since the MBT domains of L3MBTL1/2 have the capability to compact nucleosomal arrays (Trojer et al., 2007; Trojer et al., 2011; Trojer and Reinberg, 2008) and human L3MBTL1/2 have been demonstrated to associate or co-localise with HP1 proteins (Ogawa et al., 2002; Stielow et al., 2008b; Trojer et al., 2007), a model has been put forward, in which MBT domain proteins repress target genes by chromatin compaction and local heterochromatin formation.

In *Drosophila*, there is data as well linking the action of MBT domain proteins with E2F transcription factors. During the isolation of the Myb-MuvB complex dL(3)mbt, just like the HDAC dRpd3, were co-purified, however, both in sub-stoichiometric amounts compared with the core components of the complex (Lewis et al., 2004). The Myb-MuvB core complex contains beside the heterodimeric transcription factor dE2F2/dDP, one of the two pocket proteins RBF1 and RBF2, members of the retinoblastoma protein family, p55/Caf1, a second transcription factor, called dMyb, and the dMyb-interacting proteins Mip120, Mip130 and Mip40, (Figure 2.8). An independent purification of the identical core complex, termed dREAM (*Drosophila* RBF, dE2F2, and dMyb-interacting proteins) complex, failed to recover dL(3)mbt, as well as dRpd3, as stable interaction partners (Korenjak et al., 2004). Moreover, in *C. elegans* even though the MBT domain protein LIN-61 acts as a class B synMuv gene in the same genetic pathway as the worm homologues of pRB and E2F, LIN-35 and EFL-1, which assemble together into the DRM complex, no physical interaction between LIN-61 and subunits of the DRM complex was detected (Harrison et al., 2006; Harrison et al., 2007).

However, in line with a functional interaction dL(3)mbt co-represses a significant number of E2F target genes with roles in developmental processes (Georlette et al.,

2007; Lewis et al., 2004). Additionally, dL(3)mbt and Sfmbt were identified to act as negative regulators of E2F in a reporter-based genome-wide RNAi screen in *Drosophila* cells (Lu et al., 2007).

## 2.3 Objectives

Past research on MBT domain-containing proteins has revealed that they are associated with chromatin and play critical roles in transcriptional repression, regulation of development and tumour suppression (see 2.2).

The presence of a limited number of homologous MBT proteins in the fly (dL(3)mbt, Scm and Sfmbt, see 2.2.2), results in a lower potential of redundancy within this family of proteins compared to mammals, which have at least nine homologous MBT proteins (Bonasio et al., 2010). Therefore, *D. melanogaster* is a valuable model organism for biochemical and functional investigation of these chromatin-related factors.

Previously, biochemical analyses have identified several MBT proteins associated with or as part of multi-subunit complexes (see 2.2.4). For dL(3)mbt an association with the Myb-MuvB complex has been reported (Lewis et al., 2004). However, the interaction between dL(3)mbt and the Myb-MuvB complex was only sub-stoichiometric. This raised the question, whether stoichiometric dL(3)mbt-specific protein complexes exist in the fly. Accordingly, one of the major goals of this PhD thesis was to address this question by identification and isolation of putative dL(3)mbt-specific protein complexes using gel filtration chromatography and α-FLAG immunoaffinity purification.

In the past, MBT proteins were shown to contribute to transcriptional repression in both human and fly. Thus, an additional objective of this study was to determine the impact of potential dL(3)mbt complexes on transcriptional regulation by identifying target genes on a genome-wide level using a combined RNA interference (RNAi) and microarray approach. Moreover, this study aimed at finding direct target genes of dL(3)mbt complexes by chromatin immunoprecipitation (ChIP) analysis and further unravelling the consequences of transcriptional control by dL(3)mbt and its interaction partners on the chromatin level.

# 3 Material and Methods

## 3.1 Material

### 3.1.1 Material sources

If not mentioned otherwise, all common chemicals and reagents as well as equipment and consumables used in this study were from the following companies and trademarks:

Abcam plc, Abgene Ltd., Aesculap AG, Agilent Technologies Inc., Amersham Biosciences, AppliChem GmbH, Bayer AG, B. Braun Melsungen AG, Beckman Coulter Inc., Biometra, Bio-Rad Laboratories Inc., Biozym Scientific GmbH, Boehringer Ingelheim, Calbiochem, Covance Inc., Diagenode, Eppendorf, Fermentas, Gilson Inc., GE Healthcare, G. Kisker, Greiner Bio-one, Heraeus, HMC Europe GmbH, Intas Pharmaceutical Inc., Invitrogen, Julabo Labortechnik GmbH, Otto E. Kobe AG, Kodak, Labnet International, Lauda Dr. R. Wobser GmbH & Co.KG, Leica Microsystems GmbH, Life Technologies Corporation, Merck Chemicals, Millipore, MWG Biotech, New England Biolabs, PAA Laboratories GmbH, Peqlab Biotechnologie GmbH, Perbio, Pierce, Promega, Qiagen, Roche, Roth, Santa Cruz Biotechnology, Sarstedt AG & Co., Sartorius AG, Scientific Industries, Serva GmbH, Sigma-Aldrich, Sorenson BioScience, Thermo Fisher Scientific Inc., Upstate, VWR International, Whatman and Zeiss.

#### 3.1.1.1 Enzymes

| | |
|---|---|
| Calf intestine alkaline phosphatase | Fermentas |
| DNase I (RNase-free) | Peqlab |
| Fast AP Thermosensitive Alkaline Phosphatase | Fermentas |
| M-MLV Reverse Transcriptase | Invitrogen |
| Proteinase K | Roth |
| Restriction endonucleases | Fermentas, New England BioLabs |
| RNase A (DNase-free) | Qiagen |
| Taq DNA Polymerase | Fermentas |
| T4 DNA ligase | Fermentas |

#### 3.1.1.2 Enzyme inhibitors

| | |
|---|---|
| Aprotinin | Roth |
| Leupeptin | Roth |
| Pepstatin | Roth |
| PMSF (phenyl-methane-sulfonyl-fluoride) | Roth |

| | |
|---|---|
| RNasin Ribonuclease Inhibitor | Promega |
| RiboLock RNase Inhibitor | Fermentas |

#### 3.1.1.3 Chromatography and affinity purification

| | |
|---|---|
| ÄKTApurifier system | GE Healthcare |
| ANTI-FLAG M2 Agarose | Sigma-Aldrich |
| Dialysis membranes | Spectra/Por |
| Glutathione Sepharose 4 Fast Flow | GE Healthcare |
| GSTrap FF column | GE Healthcare |
| HiTrap SP HP column | GE Healthcare |
| HiTrap Q Sepharose FF column | GE Healthcare |
| Mono Q 5/50 GL column | GE Healthcare |
| Protein A Sepharose 4 FF | GE Healthcare |
| Protein G Sepharose 4 FF | GE Healthcare |
| StrataClean Resin | Stratagene |
| SulfoLink Coupling Gel | Pierce |
| Superose 6 HR 10/30 gel filtration column | GE Healthcare |

#### 3.1.1.4 SDS-PAGE and Western blotting

| | |
|---|---|
| APS (ammonium persulfate) | Serva |
| Rotiphorese Gel 30 (Acrylamide-Bisacrylamide 37,5:1) | Roth |
| Immobilon Western Chemiluminescent HRP Substrate | Millipore |
| PageBlue | Fermentas |
| PageRuler Prestained Protein Ladder | Fermentas |
| Protein Assay (Bradford solution) | Bio-Rad |
| Roti-Load 1 | Roth |
| Roti-PVDF membrane | Roth |
| SuperRX Fuji Medical X-ray film | Fujifilm |
| TEMED (tetramethyl-ethylene-diamine) | Roth |
| Whatman-3MM paper | Whatman |

#### 3.1.1.5 Agarose gel electrophoresis

| | |
|---|---|
| 6x DNA Loading Dye | Fermentas |
| GeneRuler 1 kb DNA Ladder Plus | Fermentas |
| EtBr (ethidium bromide) | AppliChem |

### 3.1.1.6 Kits

**Table 3.1: Kits with corresponding application and supplier.**

| Kit | Application | Supplier |
|---|---|---|
| ABsolute SYBR Green Mix | qPCR | Thermo-Scientific |
| Attractene Reagent | Transient transfection of *Drosophila* cells | Qiagen |
| Bac-N-Blue Transfection Kit | SF9 cell transfection for baculovirus generation | Invitrogen |
| Colloidal Blue Staining Kit | Colloidal coomassie staining of SDS-PAGE gels | Invitrogen |
| Dual-Luciferase Reporter Assay System | Measurement of Firefly and Renilla luciferase enzymatic activities | Promega |
| Effectene Transfection Reagent | Transient transfection of *Drosophila* cells | Qiagen |
| Expand High Fidelity$^{PLUS}$ PCR System | PCR | Roche |
| HiSpeed Plasmid Maxi Kit | DNA isolation for cell transfection | Qiagen |
| Immobilon Western Chemiluminescent HRP Substrate | Detection of Western blot signals | Millipore |
| MEGAscript T7 Kit | *In vitro* transcription | Ambion |
| Nanofect Reagent | Transient transfection of *Drosophila* cells | Qiagen |
| peqGOLD Cycle-Pure Kit | DNA isolation after ChIP | Peqlab |
| peqGOLD Total RNA Kit | RNA isolation from *Drosophila* cells and larvae | Peqlab |
| QIAGEN Plasmid Midi Kit | DNA isolation for cell transfection and cloning | Qiagen |
| QIAquick Gel Extraction Kit | Extraction of DNA from agarose gels | Qiagen |
| TNT T3/SP6 Quick Coupled Reticulocyte Transcription-Translation System | Coupled *in vitro* transcription and translation | Promega |

Additional sources and suppliers are mentioned in the individual subsections of section 3.2. Methods.

### 3.1.2 Standard solutions

The most common solutions and buffers are listed below. Buffer preparation was carried out according to standard procedures. Additional buffers are described in the individual subsections of section 3.2. Methods.

| | |
|---|---|
| Phosphate Buffered Saline (PBS) | 140 mM NaCl<br>2.7 mM KCl<br>8.1 mM $Na_2HPO_4$<br>1.5 mM $K_2PO_4$<br>pH adjusted to 7.4 with HCl |
| TE buffer | 10 mM Tris-HCl, pH 8.0<br>1 mM EDTA, pH 8.0 |
| TAE buffer | 40 mM Tris-acetate, pH 8.0<br>1 mM EDTA, pH 8.0 |
| TBE buffer | 90 mM Tris-borate<br>2 mM EDTA |

### 3.1.3 Bacteria strains and culture media

The *Escherichia coli* (*E. coli*) XL1-Blue strain was used for cloning and the propagation of plasmid DNA. The *E. coli* BL21 strain was used specifically for recombinant protein expression of GST fusion proteins.

Transformed bacteria were selected, depending on the resistance gene encoded on the plasmid, with 100 µg/ml ampicillin (Ratiopharm) or 30 µg/ml kanamycin (AppliChem).

| | |
|---|---|
| Lysogeny Broth (LB) medium | 1% (w/v) Peptone<br>0.5% (w/v) Yeast extract<br>1% (w/v) NaCl |
| Agar plates | 1.5% (w/v) Agar-agar<br>in LB medium |

## 3.1.4 Cell lines and tissue culture media

### 3.1.4.1 Insect cell lines

**Kc167:** A female diploid *D. melanogaster* cell line, derived from 6 to 12 hr old *Drosophila* embryos (Echalier and Ohanessian, 1970).

**S2:** A male aneuploid *D. melanogaster* cell line, derived from a primary culture of 20 to 24 hr old *Drosophila* embryos (Schneider, 1972; Zhang et al., 2010).

**Sf9**: A cell line established from pupal tissue of *Spodoptera frugiperda*. Sf9 cells were used for the expression of recombinant proteins using the baculovirus system (Vaughn et al., 1977).

### 3.1.4.2 Stably transfected S2 cell lines

Below is a description of the two stable S2 cell lines established in this study (for generation, see 3.2.1.4).

**S2 pPacHAFLAG-dL(3)mbt (puromycin resistant)**: S2 cells were co-transfected with the plasmids pPacHAFLAG-dL(3)mbt and pBS-Puro. pPacHAFLAG-dL(3)mbt encodes the full length N-terminally HA-/FLAG-tagged dL(3)mbt protein under the control of the constitutive *actin 5C* promoter.

**S2 pPac-dLint-1-FLAG (puromycin resistant)**: S2 cells were co-transfected with the vectors pPac-dLint-1-FLAG and pBS-Puro. pPac-dLint-1-FLAG encodes the full length C-terminally FLAG-tagged dLint-1 protein under the control of the constitutive *actin 5C* promoter.

The pBS-Puro vector carries a resistance gene against the antibiotic puromycin. Therefore, stably transfected S2 cell lines were selected and maintained by the addition of 5-10 µg/ml puromycin (PAA) into the medium.

### 3.1.4.3 Tissue culture media

**Schneider's *Drosophila* Medium**: Tissue culture medium for *Drosophila* cell lines, used for both Kc167 and S2 cell lines.

The medium was supplemented with 10% (v/v) fetal bovine serum (FBS; purchased from Gibco or HyClone) and 1% (v/v) Penicillin-Streptomycin (10 mg/ml; PAA).

**Sf-900 II SFM**: Tissue culture medium for Sf9 cells that was supplemented with 10% (v/v) FBS and 0.1% (v/v) Gentamycin (10 mg/ml; PAA).

### 3.1.5 Fly strains

Fly stocks were generally maintained at room temperature (RT), while fly crosses were kept at 26°C in a fly incubator. Fly stocks and crosses were cultured on standard food as described previously (Kunert and Brehm, 2008).

**Table 3.2: Fly strains used in this study.**

| Fly strain | Description | Source |
|---|---|---|
| OrR | Oregon R wild-type fly strain | P. Becker |
| w[1118] isogenic | $w^{1118}$ isogenic fly strain, isogenised chromosomes 1, 2 and 3. | Bloomington (BL#5905) |
| *da*-GAL4 | P{*da-GAL4*}; GAL4 driver strain, expresses GAL4 in a *daughterless* pattern. | R. Renkawitz-Pohl |
| sgs-58AB-GAL4 | GAL4 driver strain, expresses GAL4 in salivary glands. | R. Renkawitz-Pohl |
| UAS-dL(3)mbt RNAi | Transgenic line carrying a UAS-RNAi construct directed against dL(3)mbt, inserted at the 2nd chromosome. | VDRC library (ID #104563) |
| UAS-dLint-1 RNAi | Transgenic line carrying a UAS-RNAi construct directed against dLint-1, inserted at the 2nd chromosome. | VDRC library (ID #105932) |
| UAS-HA-FLAG-dL(3)mbt | Transgenic line carrying UAS-HA-FLAG-dL(3)mbt, inserted at the 3rd chromosome. | This study |

### 3.1.6 Plasmids

**Table 3.3: Plasmids used in this study.**

| Plasmid name | Description | Source/Reference |
|---|---|---|
| LD05287 | cDNA encoding for full length dL(3)mbt in the pBluescript_SK(-) vector. | DGC gold BDGP collection |
| RE35228 | cDNA encoding for full length CG1908/dLint-1 in the pFLC-I vector. | DGC gold BDGP collection |
| pPac-HA-FLAG | Vector for expression of N-terminal HA-FLAG-tagged proteins under the control of the constitutive *actin 5C* promoter in *Drosophila* cells. | G. Suske (Braun et al., 2001) |
| pPac-FLAG-BACK | Vector for expression of C-terminal FLAG-tagged proteins under the control of the constitutive *actin 5C* promoter in *Drosophila* cells. | I. Vetter |
| pVL1392 | Baculovirus transfer vector for recombinant protein expression in Sf9 cells. | Invitrogen |
| pGex4T1 | Vector for IPTG-inducible (isopropyl-beta-D-thiogalactopyranoside) expression of GST-tagged proteins in *E. coli*. | GE Healthcare |
| pGex5X3-3MBT | Vector for IPTG-inducible expression of a GST fusion of the 3MBT domains of L3MBTL1 in *E. coli*. | G. Suske; Generated by the Reinberg lab (Trojer et al., 2007) |
| pBS-Puro | Expression vector for *Drosophila* cells: encodes a resistance gene against puromycin under the control of the *Drosophila* heat shock promoter. | (Benting et al., 2000) |
| pING14A | Vector for *in vitro* transcription containing a SP6 promoter. | (Hagemeier et al., 1993) |
| pUASTattB | Integration vector for UAS/GAL4-mediated expression of transgenes. The plasmid contains an *attB* element that is recognised by the φC31 integrase, which can integrate the construct into a transgenic fly genome at an *attP* landing site. The vector carries a *white*$^{+}$ marker gene for selection of transgenic flies. | H. Jäckle; Generated by the Basler lab (Bischof et al., 2007) |
| pAc 5.1-LexA | Expression vector for *Drosophila* cells, which encodes the DNA binding domain of LexA under the control of a constitutive *actin* promoter. | B. Thompson (Thompson and Travers, 2008) |

| | | |
|---|---|---|
| pAc 5.1-LexA-dL(3)mbt | Encodes full length dL(3)mbt, C-terminally fused to the DNA binding domain of LexA. For constitutive expression in *Drosophila* cells, driven by a constitutive *actin* promoter. | D. Pagliarini |
| pAc 5.1-LexA-dLint-1 | Encodes full length dLint-1, C-terminally fused to the DNA binding domain of LexA. For constitutive expression in *Drosophila* cells, driven by a constitutive *actin* promoter. | L. M. Reuter |
| pGL2-hse/lexA | Reporter gene vector for *Drosophila* cells, which encodes Firefly Luciferase. The luciferase reporter gene is under the control of the *Hsp70* promoter. Upstream of the promoter reside 4 repeats of a LexA-specific recognition motif and a heat shock element. | B. Thompson (Thompson and Travers, 2008) |
| pPacRNLuc | Expression vector for *Drosophila* cells, which encodes Renilla Luciferase under the control of a constitutive *actin* promoter. | G. Suske |

Continuation of Table 3.3.

**Table 3.4: Plasmids generated in this study.**

| Plasmid name | Description |
|---|---|
| pPac-HA-FLAG-dL(3)mbt | Encodes full length dL(3)mbt, tagged N-terminally with an HA-/FLAG-tag, for constitutive expression in *Drosophila* cells, cloned with XbaI and BamHI using oligos: l3mbt-5-fw and l3mbt-6-rv. |
| pPac-dLint-1-FLAG | Encodes full length dLint-1, tagged C-terminally with a FLAG-tag, for constitutive expression in *Drosophila* cells, cloned with NotI and XhoI, using oligos: CG1908-3-fw and CG1908-4-rv. |
| pVL1392-HA-FLAG-dL(3)mbt | Encodes full length dL(3)mbt, N-terminally HA-/FLAG-tagged, for generation of recombinant baculovirus, subcloned from pPac-HA-FLAG-dL(3)mbt with BglII and BamHI. |
| pVL1392-dL(3)mbt-FLAG | Encodes full length dL(3)mbt, C-terminally FLAG-tagged, for generation of recombinant baculovirus, cloned with EcoRI and BamHI using oligos: l3mbt-9-fw and Flag-l3mbt-10-rv. |
| pVL1392-FLAG-N-term-dL(3)mbt | Encodes the N-terminus (aa 2-786) of dL(3)mbt, N-terminally FLAG-tagged, for generation of recombinant baculovirus, cloned with EcoRI and BamHI using oligos: del-l3mbt-Nterm-fw and del-l3mbt-Nterm-rv. |

| | |
|---|---|
| pVL1392-FLAG-3MBT-dL(3)mbt | Encodes the 3MBT domains (aa 787-1171) of dL(3)mbt, N-terminally FLAG-tagged, for generation of recombinant baculovirus, cloned with EcoRI and BamHI using oligos: del-l3mbt-MBTreg-fw and del-l3mbt-MBTreg-rv. |
| pVL1392-FLAG-C-term-dL(3)mbt | Encodes the C-terminus (aa 1172-1477) of dL(3)mbt, N-terminally FLAG-tagged, for generation of recombinant baculovirus, cloned with EcoRI and BamHI using oligos: del-l3mbt-Cterm-fw and del-l3mbt-Cterm-rv. |
| pVL1392-dLint-1 | Encodes full length dLint-1 for generation of recombinant baculovirus, cloned with BglII and XbaI, using oligos: CG1908-5-fw and CG1908-6-rv. |
| pGex4T1-3MBT-dL(3)mbt | Contains GST fusion of 3MBT domains (aa 811-1140) of dL(3)mbt for IPTG-inducible expression in *E. coli*, cloned with EcoRI and SalI using oligos: 3MBT-prim1-fw and 3MBT-prim2-rv. |
| pGex4T1-dLint-1 | Contains GST fusion of full length dLint-1 for IPTG-inducible expression in *E. coli*, cloned with SalI and NotI using oligos: CG1908-8-fw and CG1908-Cterm-rv. |
| pGex4T1-Nterm-dLint-1 | Contains GST fusion of N-terminus (aa 1-301) of dLint-1 for IPTG-inducible expression in *E. coli*, cloned with SalI and NotI using oligos: CG1908-Nterm-fw and CG1908-Nterm-rv. |
| pGex4T1-Cterm-dLint-1 | Encodes GST fusion of C-terminus (aa 302-602) of dLint-1 for IPTG-inducible expression in *E. coli*, cloned with SalI and NotI using oligos: CG1908-Cterm-fw and CG1908-Cterm-rv. |
| pGex4T1-PHDlike-dLint-1 | Encodes GST fusion of PHD-like domain (aa 515-602) of Lint-1 for IPTG-inducible expression in *E. coli*, cloned with SalI and NotI using oligos: CG1908-9-fw and CG1908-Cterm-rv. |
| pING14A-dLint-1 | Encodes full length dLint-1 under the control of a SP6 promoter for *in vitro* transcription, cloned with XbaI using oligos: CG1908-1-fw and CG1908-1-rv. |
| pUASattB-HA-FLAG-dL(3)mbt | Full length dL(3)mbt N-terminally HA-/FLAG-tagged for UAS/GAL4-mediated expression of recombinant dL(3)mbt in transgenic flies, subcloned from pPac-HA-FLAG-dL(3)mbt with BamHI into BglII cut pUASattB. |

Continuation of Table 3.4.

Oligonucleotides that were used for PCR-cloning are listed in Table 3.5. PCR-cloned fragments were sequenced after cloning at LGC Genomics.

### 3.1.7 Oligonucleotides

Unmodified DNA oligonucleotides were purchased from Eurofins MWG Operon, diluted for stock solutions at a concentration of 100 pmol/µl in double distilled water ($ddH_2O$) and stored at -20°C.

#### 3.1.7.1 Primers for PCR cloning

**Table 3.5: Primers used for PCR cloning.** Recognition sites of restriction endonucleases are underlined and FLAG-tag sequences are depicted in bold.

| Primer name | Sequence |
|---|---|
| l3mbt-5-fw | CGCTCTAGACCTGCCATTGTCGATGGCCAG |
| l3mbt-6-rv | CGCGGATCCCTAAGAGGACGTGCGCAAGG |
| l3mbt-9-fw | GGCCGAATTCATGCTGCCATTGTCGATGGC |
| Flag-l3mbt-10-rv | TTAAGGATCCCTA**TTTATCGTCATCGTCTTTGTAG TC**AGAGGACGTGCGCAAGGG |
| del-l3mbt-Nterm-fw | TTAAGAATTCATG**GACTACAAAGACGATGACGATA AA**CTGCCATTGTCGATGGC |
| del-l3mbt-Nterm-rv | GGCCGGATCCCTATCTAGACAAATCTGGCGCTGTTC C |
| del-l3mbt-MBTreg-fw | TTAAGAATTCATG**GACTACAAAGACGATGACGATA AA**CCACAAAAGCGGCAAACC |
| del-l3mbt-MBTreg-rv | GGCCGGATCCCTACGGCGCATACGGACAGC |
| del-l3mbt-Cterm-fw | TAAGAATTCATG**GACTACAAAGACGATGACGATAA A**TCTAGAGAAAATTGGCGTCAGTGG |
| del-l3mbt-Cterm-rv | GGGCCGGATCCCTAAGAGGACGTGCGCAA |
| 3MBT-prim1-fw | GGCCGAATTCCAAAAGGATAAGCCCAGAAAGCC |
| 3MBT-prim2-rv | AATTGTCGACTTACATCACGGACTTGGGCTGAAG |
| CG1908-1-fw | CCGGTCTAGAAGCAAGTACCATAAGGAGCGCA |
| CG1908-1-rv | CCGGTCTAGACTACTTCTCCAACTTATCTTTTTC |
| CG1908-3-fw | TTAAGCGGCCGCAGCAAGTACCATAAGGAGCGC |
| CG1908-4-rv | GGCCCTCGAGGTCTTCTCCAACTTATCTTTTTCGC |
| CG1908-5-fw | GGCCAGATCTATGAGCAAGTACCATAAGGAGC |
| CG1908-6-rv | GGCCTCTAGACTACTTCTCCAACTTATCTTTTTC |
| CG1908-8-fw | GGTTGTCGACTCATGAGCAAGTACCATAAGGAGC |
| CG1908-9-fw | AATTGTCGACTCAGCAGCGCAGGAGGAGGAT |
| CG1908-Nterm-fw | GGCCGTCGACTCAGCAAGTACCATAAGGAGCGC |
| CG1908-Nterm-rv | TTAAGCGGCCGCCTAGATCTCCAGGTCCTCCTCGT |
| CG1908-Cterm-fw | GGCCGTCGACTCACCAGTTTGCAGAACGATCGC |
| CG1908-Cterm-rv | TTAAGCGGCCGCCTACTTCTCCAACTTATCTTTTTC |

### 3.1.7.2 Primers for sequencing

The inserts of all newly cloned constructs were sequenced before usage. Sequencing reactions were conducted by LGC Genomics.

**Table 3.6: Primers used for sequencing.**

| Primer name | Sequence |
|---|---|
| l3mbt-seq-1-rv | TCAACGGTCAGGCTGTTCTTG |
| l3mbt-seq-2-fw | TGTGTGCGAGTACATAGAGCG |
| l3mbt-seq-3-fw | TGGTGCCATCGCCCAGTAATC |
| l3mbt-seq-4-rv | CAGAATCAGGGAGTAGAGCTTC |
| l3mbt-seq-5-fw | CAGTGGCGCCAGTTGTTACATC |
| l3mbt-seq-6-rv | GTTTCCAGTTCGTGCGAGGTGG |
| l3mbt-seq-7-fw | CATCATCAAGGCGGAATCTCTG |
| CG1908-seq-5-rv | GCGACCCTTTCATCAGCTTCG |
| CG1908-seq-6-fw | GGATTGGGTCAGCAGATCGC |
| CG1908-seq-7-fw | TCC GGCAGCTCCGATGATTC |
| GEX-fw | CTTTGCAGGGCTGGCAAG |
| GEX-rv | GAGCTGCATGTGTCAGAGG |

### 3.1.7.3 Primers for generation of dsRNA by *in vitro* transcription

Primers that were used to generate gene-specific dsRNAs by *in vitro* transcription contained a T7 promoter at the 5' end. dsRNA probes were used for RNA interference (RNAi) experiments to knockdown specific proteins in *Drosophila* cell lines. RNAi probes were designed according to the GenomeRNAi database of the German Cancer Research Center (DKFZ) (http://www.dkfz.de/signaling2/rnai/) and the Gene Lookup tool of the *Drosophila* RNAi Screening Center (DRSC) (http://www.flyrnai.org/).

**Table 3.7: Primers for dsRNA synthesis by *in vitro* transcription:** The sequence of the T7 promoter is depicted in lowercase letters, whereas the gene-specific DNA sequence is shown in uppercase letters.

| Primer name | Sequence | ID/Reference |
|---|---|---|
| EGFP-RNAi-fw | gaattaatacgactcactatagggaGAGCTGGACGGC GACGTAA | (Stielow et al., 2008a) |
| EGFP-RNAi-rv | gaattaatacgactcactatagggagACTTGTACAGCT CGTCCATG | |
| dL(3)mbt-RNAi-BKN20998-fw | taatacgactcactatagggGTTGGTTTGGGTGCTG TCTT | BKN20998 |
| dL(3)mbt-RNAi-BKN20998-rv | taatacgactcactatagggGCGTCTAAAGTTCAGC CAGG | |
| dLint-1-RNAi-HFA19822-fw | taatacgactcactatagggATGAAAGGGTCGCTG GATT | HFA19822 |

| | | |
|---|---|---|
| dLint-1-RNAi-HFA19822-rv | taatacgactcactatagggGCTCGGCACTGGAATCAT | |
| dRpd3- RNAi-(2)-fw | taatacgactcactatagggCGACGGCGTCTAATACCAAT | (Stielow et al., 2008a) |
| dRpd3- RNAi-(2)-rv | taatacgactcactatagggCCGCCCACTGATTACTGATT | |
| dCoREST-RNAi-fw | taatacgactcactatagggCATTCGCTCAGTTTTCTGACG | (Dallman et al., 2004) |
| dCoREST-RNAi-rv | taatacgactcactatagggCCACCGAAATGTACTCCTCC | |
| dLsd1-RNAi-fw | taatacgactcactatagggAAAGAAACGTCAATCACCCG | DRSC24846 |
| dLsd1-RNAi-rv | taatacgactcactatagggCCTCTTCGTTGGGTGTCATT | |
| E(z)-RNAi-fw | taatacgactcactatagggTCTCCAGCGGTTCTTCAGTT | DRSC29388 |
| E(z)-RNAi-rv | taatacgactcactatagggTCCTCGATAAGGATGGCAA | |
| dPR-Set7-RNAi-fw | taatacgactcactatagggATGGTCTCCAAGTACGCCAC | DRSC27118 |
| dPR-Set7-RNAi-rv | taatacgactcactatagggCCAAAAACCAGTTTAGCCCA | |
| G9a-RNAi-fw | taatacgactcactatagggAAACCAAGTGTTACTTTGAGAG | DRSC18619 |
| G9a-RNAi-rv | taatacgactcactatagggTGTACAAAATATGCCACATCCT | |
| Pc-RNAi-fw | taatacgactcactatagggGAAGCCATAAACACAACGCC | DRSC24966 |
| Pc-RNAi-rv | taatacgactcactatagggACATTTGTTTGGGTCGAAGC | |

Continuation of Table 3.7.

#### 3.1.7.4 Primers for gene expression analysis by RT-qPCR

Oligonucleotides that were used for RT-qPCR were designed either by the Universal ProbeLibrary Assay Design Center (Roche) or using Primer3 as a tool. The Oligo-dT primer that was used to reversely transcribe polyadenylated mRNAs into cDNA contained 17 dT nucleotides.

Universal ProbeLibrary Assay Design Center:
(http://www.roche-applied-science.com/sis/rtpcr/upl/index.jsp?id=UP030000)
Primer3: (http://frodo.wi.mit.edu/primer3/)

**Table 3.8: Primers for RT-qPCR gene expression analysis.**

| Primer name | Sequence | Reference |
|---|---|---|
| Gapdh1-fw | GAGCAAGGACTAAACTAGCCAAA | (Kunert et al., 2009) |
| Gapdh1-rv | CAACAGTGATTCCCGACCA | |
| l(3)mbt-RT-7-fw | TTTCTGGCACCACATTTCTG | This study |
| l(3)mbt-RT-8-rv | CTCTCCTTCTGCGTACTCTGC | This study |
| lint-1-RT-fw | GCAGGAGCAGCAAAGACG | This study |
| lint-1-RT-rv | CTCAAAGAGGCCGAGGAAC | This study |
| piwi-RT-fw | CAGAAGTACAAGGCCGGATAA | This study |
| piwi-RT-rv | TTTGCCAATCAGCGTTTTCT | This study |
| nos-RT-fw | GCGCGATCCTTGAAAATCT | This study |
| nos-RT-rv | GCGAACTCCTGCATCACAT | This study |
| swa-RT-fw | GCTGATGGCAGCGGTAGT | This study |
| swa-RT-rv | GGCTGGTTTCCGAGTTGTT | This study |
| ea-RT-fw | CGAAAATGCTAAAGCCATCG | This study |
| ea-RT-rv | CGTTGGGGAAGTAGAACTGG | This study |
| tor-RT-fw | GCCTGCAGAACTTTTTACGTG | This study |
| tor-RT-rv | TGTCCACGTTCTGTTCAAGG | This study |
| bam-RT-fw | GAGCAATGCGGACAAGTTC | This study |
| bam-RT-rv | TAGCGGTGCTCCAGATCC | This study |
| zpg-RT-fw | CGTCTTCTGCGAAATACTCAATTT | This study |
| zpg-RT-rv | CACTGGTTATAGTCGCCATTGT | This study |
| spnE-RT-fw | CCATATTTCCGATGCACTCA | This study |
| spnE-RT-rv | ATGGGGTAAAGTGCCTTCG | This study |
| tud-RT-fw | AAGAAGCCTTTGCTGCTTTG | This study |
| tud-RT-rv | CCTCGTTCGGCTGAGTAGTT | This study |
| G9a-RT-fw | AACGATGACTTGGAGCGTGTA | This study |
| G9a-RT-rv | GGGAGTCAGCACGTTGAAGT | This study |
| Pc-RT-fw | TCCAAAAGCGCGTTAAGAAG | This study |
| Pc-RT-rv | TCGTTTGTTCGTAGATGTCGAT | This study |

### 3.1.7.5 Primers for ChIP-qPCR analysis

Oligonucleotides that were used for ChIP analysis were designed using Primer3 as a tool.

**Table 3.9: Primers for ChIP analysis by qPCR.**

| Primer | Sequence | Reference |
|---|---|---|
| swa-a-fw | CGAAGTCCTGGAACTCGAAG | This study |
| swa-a-rv | AGTCTCAGCACACGGAACG | This study |
| swa-b-fw | TTTCGCCAAAGGCAATAGATG | This study |
| swa-b-rv | GGCGAGATCGAGGAGTATG | This study |
| swa-c-fw | TGCAGAGAAGCAATTTCACG | This study |
| swa-c-rv | CAATTAAATATGGCAGCGAATTG | This study |
| swa-d-fw | GTTAGCACCGAAGCTGATGG | This study |

| | | |
|---|---|---|
| swa-d-rv | GCTGGTTTCCGAGTTGTTGG | This study |
| swa-e-fw | ATCATGTGGACACCTCATCC | This study |
| swa-e-rv | GCAAACGCTTCTGACTATCG | This study |
| swa-f-fw | AAGTGGTTGCTTGTCGGTTG | This study |
| swa-f-rv | TGACGACGCTGATATTGAGG | This study |
| piwi-a-fw | CTGGTTGACCAACGATTGC | This study |
| piwi-a-rv | CGATAACTGCAACCTGATCG | This study |
| piwi-b-fw | CTTACCAATGCTTGGATCGAC | This study |
| piwi-b-rv | GGAACCAATCCGAGGAGCTG | This study |
| piwi-c-fw | TAAGGCTCTTGCAACGATTG | This study |
| piwi-c-rv | TTTTTTGGTACTTCGAGCTTTG | This study |
| piwi-d-fw | CCGTGGGGTGACCAATATG | This study |
| piwi-d-rv | GATCCCAGAAGGTTAGCATG | This study |
| tok-b-fw | GCGACGCTTGGTGAGAATC’ | This study |
| tok-b-rv | GCAGAAAACTCTGCCGTAG | This study |
| tok-c-fw | TTTGGGAAATTTGCCTTACG | This study |
| tok-c-rv | AACCCTGGCACAAACGTATC | This study |
| tok-d-fw | TCTGATTTCGCTTTGTGTCG | This study |
| tok-d-rv | GGCCAGACAAGATGAGTTGG | This study |
| nos-b-fw | GTCATCGTTTCCGAAAGCTC | This study |
| nos-b-rv | AGGTATGGAGCTGCACAAGG | This study |
| nos-c-fw | CATGTGATGTTGTCACAGTGC | This study |
| nos-c-rv | ACTTGCTAAGAATATGTGCCAC | This study |
| nos-d-fw | ATGTCCTACGGGAGTGCTC | This study |
| nos-d-rv | CACACGTTGTTCAGATGCTC | This study |
| crb-b-fw | CTAAGCGCCCAATGCTACTC | This study |
| crb-b-rv | TTTTACCAGCCAGGAATTGG | This study |
| crb-c-fw | TGCTGCTTGCAGTTCAAAAG | This study |
| crb-c-rv | GCACGCGACACTTTCTAGC | This study |
| crb-d-fw | CCTCATTTGTCTGCATTTTCA | This study |
| crb-d-rv | CACAATCCGTTGGAAAAAGG | This study |
| ea-b-fw | GAATGAAGGCATTGCGACTC | This study |
| ea-b-rv | CCCACGGAATACGGGATAC | This study |
| ea-c-fw | AGGCGGGGATTAAATAATGG | This study |
| ea-c-rv | TGGCGAGTCTCCAAATCAG | This study |
| ea-d-fw | GTGCCAGAACGTCTACAGC | This study |
| ea-d-rv | GGAGTCGGTCCAAATGACAC | This study |
| spn-E-b-fw | TCTGTTTCTAATAACTGACCAGCAA | This study |
| spnE-b-rv | TTCCACGTTGTATTCGACAGA | This study |
| spnE-c-fw | GCTGGGTTTCTTTCGATTACC | This study |
| spnE-c-rv | TTTTTCTCACAGTCTTTCTGGATT | This study |
| spnE-d-fw | TTCTGCATCAAGGCACTCTG | This study |
| spnE-d-rv | GCTCTAGATCTGCGCAAGGA | This study |
| tud-b-fw | TTAACGAATGGCTTTCCTCCT | This study |
| tud-b-rv | CGGATTTCAGTAGCGTCCTC | This study |
| tud-c-fw | CACGGCGACGTACCTAAAAT | This study |
| tud-c-rv | TTCCACAAGACAACGAAACG | This study |

Continuation of Table 3.9.

| | | |
|---|---|---|
| tud-d-fw | TGGAAGGATAATCCGCAGTC | This study |
| tud-d-rv | CGGCAGATGTTTAGGCGTAT | This study |
| actin5C-ORF-fw | ACCGGTATCGTTCTGGACTC | M.Murawska |
| actin5C-ORF-rv | CGGTCAGGATCTTCATCAGG | M.Murawska |
| interg-2R-fw | TGCTGACTGCCATCAAATTC | This study |
| interg-2R-rv | TACTTGCTGTGACGGCTTTG | This study |

Continuation of Table 3.9.

## 3.1.8 Antibodies and antisera

### 3.1.8.1 Primary antibodies

The dL(3)mbt- and dLint-1-specific antibodies were established and tested in the course of this study. More details concerning these antibodies can be found in section 3.2.5.

**Table 3.10: Antibodies and antisera used in this study.** Antibodies are specified with their name, including clone number (if available) or order number (for commercial antibodies). Corresponding dilutions or amounts (in µg or µl) depending on the type of experiment are stated. WB: Western blot; IP: immunoprecipitation; ChIP: chromatin immunoprecipitation; IF: immunofluorescence; DSHB: Developmental Studies Hybridoma Bank.

| Antibody | Host origin | Experiment | Dilution or amount | Source/Reference |
|---|---|---|---|---|
| α-FLAG M2 (F3165) | Mouse, monoclonal | WB | 1:4000 | Sigma-Aldrich |
| α-FLAG (F7425) | Rabbit, polyclonal | WB<br>ChIP | 1:2000<br>1 µg | Sigma-Aldrich |
| α-GST R-6G9 | Mouse, monoclonal | WB<br>IP | 1:100<br>100 µl | E. Kremmer |
| α-LexA | Mouse, monoclonal | WB | 1:200 | Santa Cruz Biotechnology |
| α-dL(3)mbt #3 | Rabbit, polyclonal | WB | 1:1000 | Peptide Specialty Laboratories |
| α-dL(3)mbt P1 6E6 | Rat, monoclonal | IP<br>IF | 50µl<br>1:2 (conc.) | E. Kremmer |
| α-dL(3)mbt P3 8F10 | Rat, monoclonal | IP | 50µl | E. Kremmer |
| α-dLint-1 #1 | Rabbit, polyclonal | WB<br>ChIP<br>IF | 1:5000<br>8 µl<br>1:50 | Peptide Specialty Laboratories |
| α-dLint-1 #2 | Rabbit, polyclonal | WB<br>ChIP | 1:5000<br>7 µl | Peptide Specialty Laboratories |
| Pre-immune #1 | - | WB<br>ChIP | 1:5000<br>6 µl | Peptide Specialty Laboratories |
| Pre-immune #2 | - | WB<br>ChIP | 1:5000<br>6.5 µl | Peptide Specialty Laboratories |

| | | | | |
|---|---|---|---|---|
| α-Rpd3 | Rabbit, polyclonal | WB | 1:5000 | J. Müller (Brehm et al., 2000) |
| α-dCoREST | Rabbit, polyclonal | WB | 1:5000 | G. Mandel (Dallman et al., 2004) |
| α-dLsd1 (α-Su(var)3-3) | Rabbit, polyclonal | WB | 1:2000 | T. Rudolph (Rudolph et al., 2007) |
| α-dHDAC3 | Rabbit, polyclonal | WB | 1:1000 | B. Turner |
| α-dMi2 (N-term) | Rabbit, Polyclonal | WB | 1:10000 | (Kehle et al., 1998) |
| α-dMi2 4D8 | Rat, monoclonal | IP | 100 µl | (Murawska et al., 2008) |
| α-RBF2 DR6 | Rat, monoclonal | WB | 1:10 | N. Dyson |
| α-HP1 C1A9 | Mouse, monoclonal | WB | 1:50 | DSHB |
| α-dPR-Set7 | Rabbit, polyclonal | WB | 1:1000 | A. Imhof |
| α-E(z) | Mouse, monoclonal | WB | 1:50 | A. Imhof |
| α-E(z) TAF | Rabbit, polyclonal | WB<br>IP | 1:1000<br>2 µl | J. Müller |
| α-E(z) TAD | Rabbit, polyclonal | WB<br>ChIP | 1:1000<br>4 µl | J. Müller |
| α-Tubulin beta KMX-1 | Mouse, monoclonal | WB | 1:15000 | Millipore |
| α-Lamin C LC28.26 | Mouse, monoclonal | WB | 1:1000 | DSHB |
| α-H3 (ab1791) | Rabbit, polyclonal | WB<br>ChIP | 1:5000<br>1 µg | Abcam |
| α-H4K20me1 (ab9051) | Rabbit, polyclonal | WB<br>ChIP | 1:1000<br>3 µg | Abcam |
| α-H4K20me1 (17-651) | Rabbit, polyclonal | ChIP | 0.25 µg | Millipore |
| α-H4K20me2 (39173) | Rabbit, polyclonal | ChIP | 10 µl | Active Motif |
| α-H4ac (06-598) | Rabbit, polyclonal | ChIP | 7.5 µg | Millipore |
| α-H3K4me2 CMA303 (05-1338) | Mouse, monoclonal | ChIP | 3 µg | Millipore |
| α-H3K27me3 (ab6002) | Mouse, monoclonal | WB | 1:1000 | Abcam |
| α-H3K27me3 (07-449) | Rabbit, polyclonal | ChIP | 3 µg | Millipore |
| α-H3K27me3 C36B11 (#9733) | Rabbit, polyclonal | ChIP | 5 µg | Cell Signaling |

Continuation of Table 3.10.

#### 3.1.8.2 Secondary antibodies

**Table 3.11: Secondary antibodies used for Western blot analysis and immunofluorescence.** WB: Western blot; IF: immunofluorescence;

| Antibody | Host origin | Experiment | Dilution | Source |
|---|---|---|---|---|
| ECL α-Rabbit | Donkey, polyclonal | WB | 1:30000 | GE Healthcare |
| ECL α-Mouse | Sheep, polyclonal | WB | 1:30000 | GE Healthcare |
| ECL α-Rat | Goat, polyclonal | WB | 1:30000 | Jackson Immuno-Research |
| α-rabbit Alexa488 | Goat, polyclonal | IF | 1:200 | Invitrogen |
| α-rat Alexa546 | Goat, polyclonal | IF | 1:200 | Invitrogen |

## 3.2 Methods

If not stated otherwise reactions were performed at RT.

### 3.2.1 Cell biological methods

#### 3.2.1.1 Standard cell culture procedures

*D. melanogaster* S2 and Kc167 cells were propagated at 26°C in Schneider's insect medium, supplemented with FBS and Penicillin-Streptomycin (3.1.4.3). Sf9 cells were cultured at 26°C in Sf-900 II SFM medium, supplemented with FBS and Gentamycin (3.1.4.3). For splitting, S2 and Kc167 cells were shaken off the flask and re-seeded in a cell density of $1.5\text{-}2 \cdot 10^6$ cells/ml every 3-4 days. Cell densities were determined using a hemacytometer. The adherent Sf9 cells were removed from the flask surface using a cell scraper when they had reached confluency, and splitted in a 1:3 to 1:4 ratio. Cells were typically spun down at 1000 rpm for 5 min at RT (Heraeus Megafuge 1.0).

#### 3.2.1.2 Freezing and thawing of cells

For freezing, cells from one dense 75 $cm^2$ flask were resuspended in 0.5 ml freezing medium A and 0.5 ml freezing medium B was added dropwise. 1 ml of cell suspension was aliquoted into a cryovial and frozen in a container with isopropanol at -80°C for 48-72 hr, before stored at -80°C or in liquid nitrogen.

| | |
|---|---|
| Freezing medium A | Schneider's insect or Sf-900 II SFM medium<br>40% (v/v) FBS<br>1% (v/v) Penicillin-Streptomycin or<br>0.1% (v/v) Gentamycin |
| Freezing medium B | Schneider's insect or Sf-900 II SFM medium<br>20% (v/v) dimethyl-sulfoxide (DMSO)<br>1% (v/v) Penicillin-Streptomycin or<br>0.1% (v/v) Gentamycin |

For thawing, cell aliquots were thawed at RT and resuspended in 12 ml of Schneider's insect medium or Sf-900 II SFM medium. S2 and Kc167 cells were centrifuged to remove DMSO, diluted in fresh medium and transferred to a tissue culture flask. Sf9 cells were directly seeded into a flask and medium was exchanged after 15-30 min, after cells had attached to the flask surface.

#### 3.2.1.3 Transient transfection

To test for the expression of recombinant FLAG-tagged dL(3)mbt and dLint-1, S2 or Kc167 cells were transiently transfected with the corresponding pPac expression vector. For this, Nanofect transfection reagent (Qiagen) was used. 6-10·$10^6$ cells were seeded into 10 cm dishes 6-24 hr prior to transfection in 10 ml of supplemented medium. According to the manufacturer's instruction manual, 7 µg of plasmid DNA was diluted to a total volume of 300 µl with medium lacking supplements. 10 µl of Nanofect transfection reagent were added and mixed by pipetting up and down. This was followed by an incubation for 10-15 min to allow transfection complex formation. Thereafter, cells were incubated with the transfection mix for 48 hr, harvested and assayed for expression by analysing nuclear extract samples (3.2.3.5) by Western blot (3.2.3.4).

#### 3.2.1.4 Stable transfection

For the generation of monoclonal cell lines stably expressing recombinant proteins, S2 cells are more suited than Kc167 cells, because S2 cells adhere to the culture dish more tightly, which leads to the formation of cell clones after selection with antibiotic.

For this purpose, cells were transfected using the calcium phosphate method (Graham and van der Eb, 1973a/b). 8·$10^6$ S2 cells were seeded into a 10 cm dish in 10 ml of

supplemented medium. 24 hr later cells were co-transfected with 20 µg of the corresponding pPac expression vector (pPac-HA-FLAG-dL(3)mbt or pPac-dLint-1-FLAG) and 1 µg of pBS-Puro. The plasmid DNA was diluted in 500 µl $CaCl_2$ solution and added dropwise to 500 µl of 2x HeBS buffer while vortexing. After an incubation of 30 min the transfection mixture including precipitates was added dropwise onto the cells. Plates were swirled and incubated at 26°C. Two days post-transfection cells were selected for 4-6 weeks with 5-10 µg/ml puromycin (PAA). Clones were picked and expanded until finally tested for expression of recombinant protein by Western blot (3.2.3.4).

| $CaCl_2$ solution | HeBS buffer (2x) |
|---|---|
| 250 mM $CaCl_2$ | 16 g NaCl |
| 1 mM Hepes/KOH, pH 7.1 | 0.7 g KCl |
| sterile filtered | 0.5 g $Na_2HPO_4$ |
| | 2 g D-Glucose |
| | 10 g Hepes |
| | pH adjusted to 7.1 with NaOH |
| | up to 1 l with $ddH_2O$ |
| | sterile filtered |

#### 3.2.1.5 Luciferase reporter gene assay

The plasmid-based luciferase reporter gene system (Thompson and Travers, 2008), used in this study, allows measuring the influence of a potential transcriptional regulator on transcription. Proteins of interest were fused to the DNA binding domain of LexA and tethered to specific LexA binding sites upstream of a reporter gene encoding the Firefly luciferase protein.

$1.6 \cdot 10^6$ Kc167 cells in 2 ml of supplemented cell culture medium were transfected simultaneously with three plasmids:

1. 10 to 1000 ng of pAc5.1-LexA, pAc5.1-LexA-dL(3)mbt or pAc5.1-LexA-dLint-1
2. 250 ng of pGL2-hse/lexA
3. 100 ng of pPacRNLuc

As controls transfections without plasmid and with only 250 ng pGL2-hse/lexA or 100 ng pPacRNLuc vector were included. pAc5.1 vectors were used to express the DNA binding domain of LexA (LexA) alone or dL(3)mbt and dLint-1 fused to LexA,

respectively. The expression of LexA or LexA fusion proteins was driven by a constitutive *actin* promoter. pGL2-hse/lexA was the vector carrying the luciferase reporter gene encoding for Firefly luciferase. This reporter gene was under the control of the *Hsp70* promoter and a TATA box, located directly upstream of the transcription start site. Further upstream were multiple copies of specific recognition motifs for the LexA domain, tethering the LexA proteins in close proximity to the *luciferase* reporter gene promoter. The third plasmid, pPacRNLuc, was used to drive constitutive expression of Renilla luciferase (controlled by an *actin* promoter). The activity of the Renilla luciferase was needed for nomalisation to account for differences in transfection efficiencies.

Transient transfections were carried out using Attractene Reagent (Qiagen). 4.5 µl of Attractene were added to each plasmid mixture and filled up to 100 µl with cell culture medium without supplements. The transfection mixture was incubated for 10-15 min at RT. Then the transfection mixture was added dropwise to the cells and incubated at 26°C for 48 hr. In cases when the luciferase reporter gene assay was combined with RNAi, $0.8 \cdot 10^6$ cells were treated with 15 µg of dsRNA, as described elsewhere (3.2.2.4), incubated at 26°C and transfected 48 hr after RNAi treatment as described above. After 48 hr of transfection, cells were lysed to measure luciferase activities (see below), to extract protein for Western blot analysis (3.2.3.4) or to isolate RNA for RT-qPCR (3.2.2.6).

To measure the enzymatic activities of Firefly and Renilla luciferases in the cell lysates of transfected cells the Dual-Luciferase Reporter Assay System (Promega) was used according to manufacturer's instructions. In brief, cells were harvested, washed twice with 1 ml of PBS and lysed in 250 µl of 1x Passive Lysis Buffer for 15 min while shaking. Then 20 µl of cell lysate were transferred into 5 ml polystyrene tubes (Sarstedt) in triplicates and Firefly and Renilla luciferase activities were determined using a Luminometer (AutoLumat PLUS LB953, Berthold Technologies). First, 100 µl of LAR II reagent were dispensed and Firefly luciferase activity was measured. Second, 100 µl Stop & Glo reagent were added, which inhibits the activity of Firefly luciferase and allows the measurement of Renilla luciferase activity.

For each sample the mean from the triplicate measurements of Firefly and Renilla luciferase enzymatic activities and the standard deviation was determined. To calculate the repressive activity of LexA fusion proteins, the mean values of the Firefly luciferase activities ($a_F$) were normalised against the Renilla luciferase activities ($a_R$) (equation 1)

and referred to the activities of samples transfected with an equal amount of expression vector encoding LexA alone (equation 2).

(1) $b = \left(\frac{a_F}{a_R}\right)^{-1}$ (2) $x\text{-}fold\ repression = \left(\frac{b_{\text{LexA fusion protein}}}{b_{\text{LexA alone}}}\right)$

The calculation of errors for the fold repression was calculated according to the *Gaussian error propagation law* (equation 3).

(3) $\sigma_{(x_1, x_{2,\ldots})} = \sqrt{\left(\frac{\partial y}{\partial x_1} \cdot \Delta\sigma_1\right)^2 + \left(\frac{\partial y}{\partial x_2} \cdot \Delta\sigma_2\right)^2 + \cdots}$

### 3.2.2 Molecular biological methods

Standard procedures in molecular biology, including transformation of DNA into chemically-competent bacteria, amplification of plasmid DNA in bacteria, restriction enzyme digestion, dephosphorylation of DNA fragments, ligation of DNA fragments, determination of DNA concentration and analysis of DNA on TAE- or TBE-agarose gels were carried out according to standard protocols (Sambrook and Russell, 2001).
Plasmid DNA was prepared on a large scale using QIAGEN Plasmid Midi Kit (Qiagen). For small-scale preparation of plasmid DNA buffers P1 to P3 of the QIAGEN Plasmid Midi Kit were used and DNA was precipitated from the supernatant using isopropanol due to standard procedures. Furthermore, isolation of PCR products or other DNA fragments from agarose gels was conducted using QIAquick Gel Extraction Kit and purification of digested PCR products or other DNA fragments was carried out using QIAquick PCR Purification Kit.

#### 3.2.2.1 Total RNA isolation

When working with RNA precautions were taken to provide an RNase-free environment. Pipette tips and reaction tubes were autoclaved before usage. In addition benches and pipettes were wiped with the decontamination solution RNaseZap (Ambion). Nuclease-free $H_2O$ from Ambion was used to solubilise or dilute RNA samples.
Total RNA was purified from Kc167 cells or from 3rd instar larvae upon RNAi knockdown to examine changes in mRNA levels of target genes by RT-qPCR. RNA was purified using the peqGOLD Total RNA Kit (S-Line; Peqlab). For this purpose,

cells from one well (6-well plate) were lysed in 400 µl RNA Lysis Buffer T. In case of larvae, 15-20 animals, washed in PBS, were collected into a 1.5 ml reaction tube and frozen in liquid nitrogen. After removal from the liquid nitrogen 400 µl lysis buffer were directly added and larvae were homogenised with a pestle. After applying the lysate onto the DNA Removing Column RNA was isolated following the manufacturer's instructions, including an on-column digest with DNase using the peqGOLD DNase I Digest Kit (Peqlab).

#### 3.2.2.2 Complementary DNA (cDNA) synthesis

To quantify changes in transcription levels upon RNAi, the mRNA contained in the total RNA preparation (3.2.2.1) was reversely transcribed into first-strand cDNA. cDNA was synthesised using the M-MLV Reverse Transcriptase (Invitrogen), according to the manual's instructions, using 1-1.5 µg of total RNA as template. dNTPs were purchased from Fermentas, nuclease-free $H_2O$ from Ambion and oligo $(dT)_{17}$ primer from MWG Biotech. cDNA was used as template for RT-qPCR (3.2.2.6) or for the generation of *in vitro* transcription (*iv*T) template by PCR (3.2.2.5).

#### 3.2.2.3 Synthesis of double-stranded RNA (dsRNA) by *in vitro* transcription (*iv*T)

For the synthesis of dsRNA, first a template for *iv*T was generated by PCR (3.2.2.5) using gene-specific oligos amplifying a product, usually 300-600 bp in length, from a plasmid, cDNA or genomic DNA, containing the gene of interest. The forward and reverse primers used (Table 3.7), enclosed a minimal T7 polymerase promoter (TAATACGACTCACTATAGGG) situated at the 5' end.

To synthesise a sense and an anti-sense RNA strand from the gene-specific PCR product an *iv*T reaction was performed using the MEGAscript T7 Kit (Ambion) following the instructions of the manual with minor changes. In short, 500-1000 ng of PCR product (purified by gel extraction) were incubated with 2 µl of each rNTP and 2 µl of enzyme mix in 1x reaction buffer for 16 hr at 37°C, followed by a 15 min incubation with 1 µl of TURBO DNase at 37°C. Upon addition of stop solution (5 M ammonium acetate; 100 mM EDTA) in a 1:1 ratio, the RNA was precipitated with 2.5 volumes of absolute ethanol at -20°C for at least 30 min. The probe was centrifuged for 15 min at 13000 rpm (Heraeus BIOFUGE pico). The RNA pellet was washed with

70% ethanol and centrifuged again for 5 min. After removal of the supernatant the RNA pellet was dried using a vacuum centrifuge. For solubilisation, the RNA was resuspended in 40 µl of nuclease-free water. To obtain properly aligned dsRNA the samples were first incubated at 37°C for 60 min in a thermoshaker (G. Kisker TS-100, 400 rpm), afterwards denatured at 65°C without shaking and then renatured by turning off the thermoshaker, to achieve a slow temperature decrease down to RT. The RNA concentration was determined by measuring the absorption at 260 nm and integrity was judged by agarose gel electrophoresis on a 1.5% TBE-gel.

#### 3.2.2.4 Knockdown by RNA interference (RNAi)

RNAi is a valuable tool to knockdown protein expression in eukaryotic cells (Fire et al., 1998). For *Drosophila* cells, dsRNA molecules with a size of around 500 bp can be transfected directly into the cells (Clemens et al., 2000). Inside of the cells the dsRNA is processed into small RNA molecules that bind specifically to the messenger RNA (mRNA), thereby leading to mRNA cleavage and suppression of protein expression. The synthesis of dsRNA for RNAi in cells is described in subsection 3.2.2.3.

**RNAi in cell culture**

For knockdown of a specific gene 0.8-1.2·$10^6$ S2 or Kc167 cells were transfected with 15 µg of the corresponding dsRNA in a well of a 6-well plate. For this purpose, dsRNA was pre-pipetted into the well and cells were added in 1 ml of medium lacking supplements. After incubation for 40 min at 26°C 1 ml of medium containing 20% (v/v) FBS, 2% (v/v) Pen/Strep was added. To increase the efficiency of dsRNA uptake Effectene transfection reagent (Qiagen) was used. According to the manufacturer's instructions, 50 µl of EC buffer were mixed briefly with 1.6 µl of Enhancer and incubated for 5 min. Thereafter, 5 µl of Effectene were added, vortexed for 10 sec and incubated for another 10 min. Upon addition of the transfection mix, cells were incubated for 6 d at 26°C. Knockdown efficiency of proteins in the nuclear extract fraction (3.2.3.5) was confirmed by Western blot (3.2.3.4) and changes in mRNA levels of target genes were quantified by RT-qPCR (3.2.2.6).

**RNAi in flies**

Knockdown experiments in flies were conducted using stocks from the phiC31 RNAi Library (KK) of the Vienna Drosophila RNAi Center (VDRC) (Dietzl et al., 2007). UAS-RNAi flies were crossed with corresponding GAL4-driver strains and knockdown efficiencies were verified by measuring the mRNA levels in 3rd instar larvae by RT-qPCR (3.2.2.6) or protein level in brain extracts (3.2.3.7) in case of dLint-1. As control, GAL4-driver strains were crossed with the $w^{1118}$ host strain which the RNAi library was injected into. Expression changes of target genes at the mRNA level in 3rd instar larvae were quantified by RT-qPCR.

### 3.2.2.5 Polymerase chain reaction (PCR)

PCR is a method to amplify a specific DNA sequence exponentially from a template DNA using sequence-specific primer pairs (Saiki et al., 1988). DNA fragments required for cloning or as template for *iv*T were generated using Expand High Fidelity$^{PLUS}$ PCR System (Roche). Plasmid DNA containing the corresponding DNA sequence or cDNA from Kc167 was used as PCR template. According to the manufacturer's instructions PCR reactions were set up as follows:

| | | |
|---|---|---|
| 10 µl | Expand HiFi$^{PLUS}$ Reaction Buffer | (5x) |
| 1 µl | dNTP mix | (10 mM) |
| 2 µl | Forward primer | (10 pmol/µl) |
| 2 µl | Reverse primer | (10 pmol/µl) |
| x µl | Template DNA | (50 ng plasmid or 2 µl cDNA) |
| 0.5 µl | Expand HiFi$^{PLUS}$ enzyme | (5 U/µl) |
| x µl | dd$H_2O$ (up to 50 µl) | (up to 50 µl) |

The PCR was performed in a T3000 Thermocycler (Biometra) following the scheme below. The annealing temperature was dependent on the primers used and the elongation time was chosen corresponding to the length of the DNA sequence that had to be amplified. For PCR products up to 3 kb the elongation temperature was 72°C, whereas for products larger than 3 kb it was 68°C.

| | | | |
|---|---|---|---|
| Initial denaturation | 94°C | 2 min | |
| Denaturation | 94°C | 20 sec | 35 cycles |
| Annealing | 55-60°C | 30 sec | |
| Elongation | 68 or 72°C | 1 min/1 kb | |

| | | |
|---|---|---|
| Final elongation | 68 or 72°C | 7 min |
| Cooling | 4°C | ∞ |

#### 3.2.2.6 Quantitative PCR (qPCR)

The qPCR technique combines the amplification of a certain DNA sequence by common PCR with the sensitive detection of a fluorescent dye, incorporated into the DNA, after each round of amplification. The dye used was SYBR Green, which specifically intercalates into dsDNA.

As template, 6 µl of 1:10 diluted cDNA (3.2.2.2) or 6 µl of 1:6 diluted genomic DNA (eluted after ChIP; 3.2.3.11) were pipetted into a Thermo-Fast 96 non-skirted PCR plate (Thermo-Scientific). Template DNA was diluted with injection-grade $H_2O$ (Serumwerk). Subsequently, 19 µl of PCR mix were added and the PCR plate was sealed with an Adhesive PCR Film (Thermo-Scientific). The samples were mixed briefly by vortexing and collected by brief centrifugation.

| | | |
|---|---|---|
| PCR mix | 1 µl | Primerpair (1:1 mix of forward and reverse primers in 1:10 dilution) |
| | 12 µl | ABsolute SYBR Green Mix (Thermo-Scientific) |
| | 8 µl | injection-grade $H_2O$ |

The PCR reactions were carried out in an Mx3000P cycler from Agilent Technologies using the PCR program below:

| | | | |
|---|---|---|---|
| Initial denaturation | 95°C | 15 min | |
| Denaturation | 95°C | 15 sec | 40 cycles |
| Annealing | 60°C | 30 sec | |
| Elongation | 72°C | 20 sec | |
| Denaturation | 95°C | 1 min | |
| Dissociation curve | 55°C | 30 sec | |
| | 55°C → 95°C | gradually | |
| | 95°C | 30 sec | |

The MxPro software automatically calculates the Cycle threshold (Ct) value for each reaction. The Ct is defined as the number of cycles required for the fluorescent signal to cross a certain set threshold which exceeds the background level.

For gene expression analysis, the relative amount of cDNA in two samples (i.e. EGFP control and dL(3)mbt RNAi) was compared, after both samples had been normalised to a reference gene (*Gapdh1*). A ΔCt value was calculated for both samples:

$$\Delta Ct_{\text{sample 1}} = C_{\text{sample 1}} - C_{\text{reference}} \qquad \Delta Ct_{\text{sample 2}} = C_{\text{sample 2}} - C_{\text{reference}}$$

The subtraction of the two ΔCt values results in a ΔΔCt value:

$$\Delta\Delta Ct = \Delta C_{\text{sample 1}} - \Delta C_{\text{sample2}}$$

Since the fluorescent signal per amplification cycle increases in an exponential manner, the difference in expression is calculated as: $x = 2^{-\Delta\Delta Ct}$

To show relative changes in expression levels of genes, the control (i.e. EGFP RNAi) was set to 1 and all other samples (i.e. dL(3)mbt RNAi) were displayed normalised to the control.

All samples were measured in triplicates, which resulted in a standard deviation s for each sample, used to calculate a standard deviation $s_{\Delta Ct}$ of ΔCt:

$$s_{\Delta Ct} = \sqrt{s_{\text{reference}}^2 + s_{\text{sample}}^2}$$

and therefrom a standard deviation $s_{norm}$ for the normalised fold expression:

$$s_{norm} = \sqrt{(x_{norm} \cdot \ln(2))^2 \cdot s_{\Delta Ct}^2}$$

For chromatin immunoprecipitation (ChIP; 3.2.3.11), all samples were normalised to the corresponding ChIP-input sample ($\Delta Ct_{\text{sample}} = C_{\text{input}} - C_{\text{sample}}$) and displayed as a percentage of input: $\%\ \text{input} = 2^{\Delta Ct_{\text{sample}}}$

A standard deviation $s_{\%\text{input}}$, considering the standard deviations from triplicate measurements, was determined as follows:

$$s_{\text{input}} = \ln(2) \cdot \%\ \text{input} \cdot \sqrt{s_{\text{input}}^2 + s_{\text{sample}}^2}$$

In case of histone modifications, the results were normalised against % input values of H3 ChIPs to account for differences in the nucleosome density between different chromatin regions. The errors were calculated as described in 3.2.1.5 according to equation 3.

#### 3.2.2.7 Microarray analysis

RNAi in Kc167 cells to deplete dL(3)mbt and dLint-1 was conducted in three biological replicates as described above (3.2.2.4). Transfection of dsRNA directed against enhanced green fluorescent protein (EGFP) was included as a control. After 5 d of incubation, total RNA was extracted from RNAi-treated cells as described in subsection 3.2.2.1. Samples were prepared according to standard Affymetrix protocols using the GeneChip® Fluidics Station 450 (protocol FS450_0002) and hybridised to the Affymetrix GeneChip® *Drosophila* Genome 2.0 Array. Scans were carried out on an Affymetrix GeneChip Scanner GSC3000_7G and the fluorescence intensities were analysed with Affymetrix GCOS Software 1.4. The quality of the total RNA, as well as of cRNA samples, which were synthesised during the Affymetrix protocol, was analysed using Agilent 2100 Bioanalyzer and RNA Nano LabChips from Agilent Technologies.

Statistical analysis was conducted by Florian Finkernagel. Raw data were normalised with the gcrma package of Bioconductor (http://www.bioconductor.org) and gene lists were filtered with the following thresholds: fold change ≥ 1.5, adj. $p \leq 0.05$.

### 3.2.3 Biochemical methods

Generally, proteins were kept on ice, in the presence of protease inhibitors (Leupeptin, Pepstatin, Aprotinin, each 1 µg/ml and 0.2 mM PMSF) and the reducing agent DTT (1 mM). Protease inhibitors and DTT were added freshly to buffers.

#### 3.2.3.1 Determination of protein concentration

Protein concentration was determined using the Bio-Rad Protein Assay (Bio-Rad), which is based on the colorimetric method described by Bradford (1976), according to manufacturer`s instructions. The concentration of purified GST proteins was estimated according to protein standards with a known concentration (such as BSA) in SDS-PAGE (3.2.3.2) and subsequent Coomassie blue staining (3.2.3.3).

#### 3.2.3.2 SDS-polyacrylamide gel electrophoresis (SDS-PAGE)

Discontinuous SDS-polyacrylamide gel preparation and electrophoresis were carried out using disposable gel cassettes and the XCell SureLock Mini-Cell system from

Invitrogen. Resolving and stacking gels were prepared according to standard protocols using a ready-to-use acrylamide/bisacrylamide mixture from Roth (Rotiphoresegel 30; 37.5:1). The resolving gel contained 7.5-15% and the stacking gel 4% of polyacrylamide. Prior to loading, protein samples were supplemented with 1x SDS-PAGE loading buffer and boiled for 5 min at 95°C. As molecular weight standard PageRuler Prestained Protein Ladder (Fermentas) was loaded in addition. The electrophoresis was carried out in SDS-PAGE running buffer at a constant voltage of 100 V in the stacking gel and at 150-180 V in the resolving gel. After electrophoresis, gels were either subjected to Western blotting (3.2.3.4) or stained with Coomassie Blue or silver staining (3.2.3.3).

| SDS-PAGE running buffer | SDS-PAGE loading buffer (5x) |
|---|---|
| 25 mM Tris | 250 mM Tris-HCl, pH 6.8 |
| 192 mM glycine | 10% (w/v) SDS |
| 0.1% SDS (w/v) | 50% (v/v) glycerol |
| | 0.5% (w/v) bromophenol blue |
| | 0.5 M DTT |

### 3.2.3.3 Staining of SDS-polyacrylamide gels

**Coomassie Blue staining**

To visualise purified recombinant proteins after gel electrophoresis, gels were stained with PageBlue Protein Staining Solution (Fermentas), which is based on the Coomassie Brilliant Blue G-250 dye. For that purpose, the gel was washed in $ddH_2O$ for at least 10 min, typically incubated overnight in the staining solution and destained with $ddH_2O$ until the difference in intensity between protein bands and background was as requested.

**Colloidal Coomassie Blue staining**

This staining technique is a very sensitive detection method for proteins and is highly compatible with subsequent mass spectrometry analysis. Protein gels were stained using the Colloidal Blue Staining Kit from Invitrogen according to the manufacturer's instructions, with the maximum staining time of 12 hr.

**Silverstaining**

The staining of protein gels with silver nitrate solution was carried out based on the method of Blum (1987). The gel was fixed in 50% ethanol/10% acetic acid overnight and washed three times for 20 min each in 30% ethanol. Afterwards, the gel was incubated for 1 min in 0.02% $Na_2S_2O_3$, washed three times with $ddH_2O$ (20 sec each) and stained in 0.2% $AgNO_3$ solution for 1 hr. Subsequently, the gel was washed with $ddH_2O$ again (three times, 20 sec each) and developed for 5 to 10 min with developing solution (3% $Na_2CO_3$, 0.05% $H_2CO$ and 0.0004% $Na_2S_2O_3$) until the protein bands had the desired intensity. After a brief wash with $ddH_2O$ (1 min) the reaction was stopped by incubating the gel in 0.5% (w/v) glycine for 5 min and finally washed in $ddH_2O$ for at least 30 min.

### 3.2.3.4 Western blotting

For Western blot analysis, proteins were separated by SDS-PAGE (3.2.3.2) and transferred onto a polyvinylidene fluoride (PVDF) membrane (Roth) using the Bio-Rad 'Wet Blot' Module. The PVDF membrane was activated for some seconds in methanol, before being placed onto the gel and surrounded by gel-sized sponges and Whatman paper soaked in transfer buffer. The transfer was then carried out for 1.5 hr at 400 mA constant current. The transfer chamber was cooled by the addition of a block of ice inside of the chamber and kept on ice. After the transfer, the membrane was incubated for 45 min in blocking solution (5% dried milk in PBST) at RT or overnight at 4°C to reduce non-specific background.

| | |
|---|---|
| PBST | PBS with 0.1% Tween-20 |
| Transfer buffer | 25 mM Tris<br>192 mM glycine<br>20% (v/v) methanol<br>0.02% (v/v) SDS |

Incubations with antibodies, as well as washing steps, were carried out on a rocking platform. Blocking was followed by incubation with a primary antibody directed against the protein of interest in an appropriate dilution (Table 3.10) with blocking solution. Depending on the antibody this incubation lasted for 1-2 hr at RT or overnight at 4°C. Afterwards, the membrane was washed three times with PBST (5-10 min each) and

subsequently incubated with the appropriate HRP-coupled secondary antibody (Table 3.11) for 1 hr at RT. After three washes with PBST (see above), the antigen-antibody complexes were detected by chemiluminescence using the Immobilon Western Chemiluminescent HRP Substrate Kit (Millipore) and SuperRX Fuji Medical X-ray films. In order to re-probe membranes with another primary antibody they were 'stripped'. For stripping, membranes were incubated in 50 ml of stripping buffer for 30 min at 50°C in a water bath and then washed three times with PBST for 10 min each. Afterwards membranes could be blocked and immunoblotted as described above.

| | |
|---|---|
| Stripping buffer | 62.5 mM Tris/HCl, pH 6.8 |
| | 10% (v/v) β-mercaptoethanol |
| | 2% (w/v) SDS |

### 3.2.3.5 Nuclear extract preparation

For preparation of nuclear extract, Kc167 or S2 cells were harvested, washed twice with ice cold PBS and resuspended in low salt buffer (6 well plate: 100 µl; 10 cm plate: 500 µl; 75cm$^2$ flask: 1000 µl). The cells were incubated on ice for 10 min and collected at 13000 rpm for 1 min at 4°C. The cytosolic fraction was removed, nuclei were resuspended in high salt buffer (at least in 1.5x nuclei pellet volume), incubated for 20 min on ice and centrifuged at 13000 rpm for 10 min at 4°C. The supernatant (nuclear extract) was subjected to Western blot (3.2.3.4), immunoprecipitation (3.2.3.10) or frozen in liquid nitrogen and stored at -80°C. All centrifugations were carried out in BIOFUGE pico centrifuge from Heraeus.

| Low salt buffer | High salt buffer |
|---|---|
| 10 mM Hepes/KOH, pH 7.6 | 20 mM Hepes/KOH, pH 7.6 |
| 1.5 mM $MgCl_2$ | 1.5 mM $MgCl_2$ |
| 10 mM KCl | 420 mM NaCl |
| DTT, protease inhibitors | 0.2 mM EDTA |
| | 25 % glycerol |
| | DTT, protease inhibitors |

Nuclear extract from 0-12 hr old embryos were prepared as previously described by Kunert and Brehm (2008) and kindly provided by N. Kunert.

### 3.2.3.6 Acid extraction of histones

For extraction of histones the insoluble nuclear pellet (after the preparation of nuclear extract; 3.2.3.5) was resuspended in 0.4 M HCl (at least 2x pellet volume) and incubated overnight at 4°C with shaking (1000 rpm). After centrifugation (at 4°C, 15 min, 13000 rpm) extracted histones were present in the supernatant and could be used for Western blotting (3.2.3.4).

### 3.2.3.7 Tissue extracts from third instar larvae

For direct Western blot analysis (3.2.3.4) 20 brains or salivary glands were dissected from third instar larvae in PBS under a stereomicroscope (Askania GSZ 2T) and transferred into 20 µl collection buffer (20 mM Tris, pH 8.0, 150 mM NaCl, 10 mM EDTA and 1 mM EGTA). The organs were squashed using a pestle and boiled for 5 min at 95°C after the addition of Roti-Load 1 (Roth), before loaded onto an SDS-PAGE gel for Western blot analysis.

For Immunoprecipitation (3.2.3.10) 200 brains were dissected from third instar larvae in PBS. 40 brains were collected in 20 µl PBS at a time and frozen in liquid nitrogen and stored at -80°C. After thawing, PBS supernatants were removed (and kept on ice) and each brain aliquot was squashed in 100 µl LNB I buffer using a pestle and incubated for 10 min on ice. Then samples were centrifuged at 5000 rpm for 5 min at 4°C (Heraeus BIOFUGE pico) and the supernatants ('cytosolic fraction') were taken off and combined. Afterwards, pellets were resuspended in 25 µl LNB II, incubated for 30 min on ice and centrifuged at 13000 rpm for 10 min at 4°C. The supernatants were pooled ('nuclear fraction').

| LNB I buffer | LNB II buffer |
|---|---|
| 15 mM Hepes/KOH, pH 7.6 | 15 mM Hepes/KOH, pH 7.6 |
| 10 mM KCl | 385 mM KCl |
| 5 mM $MgCl_2$ | 5 mM $MgCl_2$ |
| 0.1 mM EDTA, pH 8.0 | 0.1 mM EDTA, pH 8.0 |
| 350 mM sucrose | 0.1% Tween 20 |
| DTT, protease inhibitors | 10% glycerol |
| | DTT, protease inhibitors |

The protein concentration of the PBS supernatant, as well as the extracts obtained with LNB I and LNB II buffer, were measured in a Bradford Assay and 10 µg of the total

protein amount were analysed by Western blot (3.2.3.4). Immunoblotting revealed that all three samples contained β-tubulin and the nuclear proteins dL(3)mbt and dLint-1 (Figure 3.1). This was not the case when dissected brains were directly subjected to extract preparation (data not shown). Probably, the freezing/thawing procedure led to an at least partial lysis of the tissue/cells. For this reason the PBS supernatants and all LNB I/II extracts were pooled and used for immunoprecipitations.

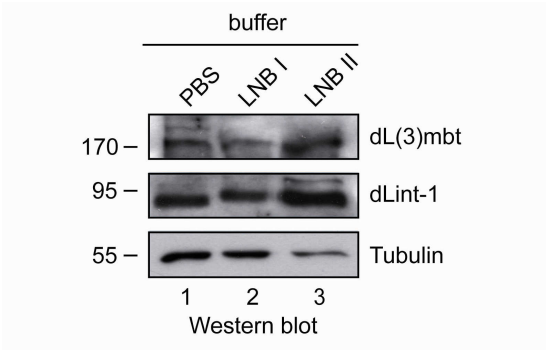


**Figure 3.1: Extract preparation from larval brains.** 10 µg of protein extracted with PBS, LNB I or LNB II buffer as indicated on top were analysed by Western blot using the corresponding antibodies as depicted on the right.

### 3.2.3.8 Whole cell extract preparation from Sf9 cells

To obtain whole cell extracts from Sf9 cells upon baculovirus infection (3.2.3.12), cells were harvested, washed in ice cold PBS and resuspended in 2 ml of LyBu-200 buffer per 15 cm dish. Cells were lysed by three repetitive freeze-thaw cycles in liquid nitrogen and subsequent sonication (2x15 sec, 25% output). Lysates were spun down at 13000 rpm for 15 min at 4°C (Heraeus BIOFUGE pico). The obtained whole cell extracts were used for various interaction assays.

| | |
|---|---|
| LyBu-x buffer | 20 mM Hepes/KOH, pH 7.6<br>x mM KCl<br>10 % glycerol<br>0.1 % NP-40<br>DTT, protease inhibitors |

### 3.2.3.9 FLAG affinity purification

For FLAG affinity purification of FLAG-dL(3)mbt and dLint-1-FLAG associated proteins, nuclear extracts from stable S2 cell lines (3.1.4.2) were prepared, as described before (3.2.3.5). 70 mg (total protein) of FLAG-dL(3)mbt extract and 150 mg (total

protein) of dLint-1-FLAG extract, as well as an equal amount of S2 mock extract, were incubated with 60 or 120 µl α-FLAG M2 agarose (FLAG beads; from Sigma-Aldrich; equilibrated in D-125), respectively, in D-125 buffer at 4°C for 3 hr with rotation. FLAG-beads were washed once with buffer D-125, three times with D-300 and once with D-125. Each wash was carried out with 10 ml of buffer at 4°C for 10 min on a rotating wheel. Bound proteins were eluted with 0.4 mg/ml FLAG-peptide (Sigma-Aldrich) in D-125 buffer. The beads were diluted 1:1 in elution buffer and elution was carried out for 2 hr on ice with regular resuspension of the slurry. Additionally, an elution was performed overnight at 4°C on a shaker. Eluates were combined, precipitated using StrataClean resin (Stratagene), subjected to SDS-PAGE and visualised by silver or Colloidal Coomassie Blue (Invitrogen) staining (3.2.3.2 and 3.2.3.3). In general, 10% of the eluates were visualised by silver staining, whereas 90% were loaded onto a gel for Colloidal Coomassie Blue staining. Protein bands were excised from Colloidal Coomassie Blue stained gels and analysed by peptide mass fingerprinting (Zentrum für Proteinanalytik, Munich, Germany).

| | |
|---|---|
| D-x buffer | 20 mM Hepes/KOH, pH 7.6<br>x mM mM KCl<br>2 mM $MgCl_2$<br>0.2 mM EDTA<br>0.05% NP-40<br>10% glycerol<br>protease inhibitors |

### 3.2.3.10 Immunoprecipitation

750 to 1000 µg of nuclear extract from *Drosophila* cells or 12 hr old embryos were incubated with an appropriate amount of the respective antibody (Table 3.10) diluted with IP buffer to a final salt concentration of 200 mM, and incubated for 2 hr at 4°C with rotation. 5 µl of Protein G or A beads (GE Healthcare) were added and incubation was continued for 1 hr. Beads were washed three times with IP buffer, before immunoprecipitates were subjected to Western blot (3.2.3.4) or HDAC assay (0).

α-FLAG-immunoprecipitations were carried out with S2 nuclear extracts (750 µg total protein) and 5 µl FLAG beads, diluted with IP buffer to a final salt concentration of 200 mM. Incubation was performed for 3 hr at 4°C on a rotating wheel. Beads were washed three times with IP buffer and analysed by Western blotting or HDAC assay.

For HDAC assays (0) nuclear extracts were optionally incubated with 50 µg/µl EtBr for 30 min on ice and centrifuged for 5 min at 13000 rpm (Heraeus BIOFUGE pico) to remove potential precipitates prior to IP. The supernatant was used for IP. EtBr was also present during washing steps.

For the interaction assays between recombinant proteins in Sf9 cells upon baculoviral co-infection, 200 µl of whole cell extract were incubated in 800 µl IP buffer with 10 µl FLAG beads for 3 hr at 4°C with rotation. Then, beads were washed three times in IP buffer and subjected to Western blotting (3.2.3.4).

| | |
|---|---|
| IP buffer | 25 mM Hepes/KOH, pH 7.6<br>150 mM NaCl<br>12.5 mM $MgCl_2$<br>0.1 mM EDTA, pH 8.0<br>10 % glycerol<br>0.1 % NP-40 |

#### 3.2.3.11 Chromatin immunoprecipitation (ChIP)

The ChIP technique was applied to investigate the direct association of proteins or histone modifications with a specific genomic region. The protocol was based on the Upstate Biotechnology ChIP assay protocol. In summary, $100 \cdot 10^6$ Kc167 cells were fixed with 1% formaldehyde (10% stock, methanol free from Polyscience) in culture medium for 10 min at RT. Fixation was stopped by the addition of 240 mM glycine (end concentration). Cells were harvested, washed in 20 ml ice cold PBS, resuspended in 1 ml SDS-lysis buffer and incubated for 10 min on ice. Lysates were sonicated using a Bioruptor (Diagenode) to obtain an average fragment length of 0.5 kb and centrifuged at 4°C for 15 min, 13000 rpm (Heraeus BIOFUGE pico). The supernatant (chromatin) was subjected to ChIP analysis. 140 µl of chromatin were used per ChIP, diluted 10x with ChIP buffer and pre-cleared with 40 µl of ProtG or ProtA beads (GE Healthcare) for 30 min with rotation. Prior to this, ProtG/A beads had been pre-blocked with 1 mg/ml BSA in TE buffer for at least 6 hr at 4°C. From the pre-cleared chromatin 14 µl were taken as an input sample and stored at 4°C. After adding antibody directed against the protein or histone modification of interest (Table 3.10) to the pre-cleared chromatin, samples were incubated overnight with rotation, prior to incubation with 35 µl of 1:1 ProtG/ProtA slurry for 2 hr at 4°C. As controls, ChIPs were performed without antibody (beads control), using pre-immune serum or a IgG control antibody. Precipitates were

washed successively for each 10 min on a rotating wheel at 4°C: three times with low salt wash buffer, three times with high salt wash buffer, once with LiCl wash buffer and twice with TE buffer. The last TE wash served to transfer beads into fresh reaction tubes for elution. All centrifugation steps to collect ProtG/ProtA beads were done with 2000 rpm for 4 min at 4°C (Heraeus BIOFUGE pico). Immunoprecipitates were eluted twice with 250 µl elution buffer (1% SDS, 0.1 M $NaHCO_3$) for each 15 min at RT. 500 µl of elution buffer were also added to input samples, which were then treated identically. Cross-links were reversed by addition of 20 µl 5 M NaCl and incubation at 65°C overnight. After addition of 10 µl 0.5 M EDTA, 20 µl 1 M Tris/HCl, pH 6.5 and 2 µl 10 mg/ml Proteinase K (Roth), samples were incubated for 1 hr at 45°C. DNA was purified with the peqGOLD Cycle-Pure Kit (Peqlab) and subjected to gene-specific qPCR (3.2.2.6).

| SDS-lysis buffer | ChIP buffer |
|---|---|
| 50 mM Tris/HCl, pH 8.0 | 16.7 mM Tris/HCl, pH 8.0 |
| 10 mM EDTA | 16.7 mM NaCl |
| 1% SDS | 1.2 mM EDTA |
| protease inhibitors | 0.01% SDS |
| | 1.1% Triton X-100 |
| | protease inhibitors |

| Low/high salt wash buffer | LiCl wash buffer |
|---|---|
| 20 mM Tris/HCl, pH 8.0 | 10 mM Tris/HCl pH 8.0 |
| 150 mM/500 mM NaCl | 250 mM LiCl |
| 2 mM EDTA | 1 mM EDTA |
| 0.1% SDS | 1% NP-40 |
| 1% Triton-X-100 | 1% sodium deoxycholate |

#### 3.2.3.12 Recombinant protein expression using the baculovirus system

The baculovirus system is an attractive tool to express proteins recombinantly in eukaryotic Sf9 cells. To generate recombinant viruses, coding sequences of the according proteins were cloned into the pVL1392 vector. pVL1392 constructs (Table 3.4) were transfected into Sf9 cells using the Bac-N-Blue Linear Transfection Kit (Invitrogen). For this purpose, $10^6$ Sf9 cells were plated into a 6 cm dish and incubated for 15 min at 26°C until cells attached to the dish surface. In the meantime, the transfection mix was prepared: 4 µg of plasmid DNA, 1 ml of Sf-900 II SFM medium

(without supplements) and at last 20 µl of Cellfectin Reagent were added to 0.5 µg of Bac-N-Blue DNA, mixed for 10 sec and incubated for 15 min. Meanwhile the medium was removed from the cells after settling and exchanged against 2 ml of medium without supplements. The transfection mix was added dropwise onto the Sf9 cells and incubated for 4 hr at RT on a rocking platform with moderate speed. After addition of 1 ml supplemented Sf9 medium, transfected cells were kept for 7 d at 26°C.

To amplify the virus titre, another two rounds of Sf9 infections were carried out. The supernatant was collected from the cells and centrifuged for 5 min at 1000 rpm to remove cell debris (Heraeus Megafuge 1.0). First, $7.5 \cdot 10^6$ Sf9 cells were plated into a 10 cm dish and incubated for 1 hr on a rocking platform with 1 ml of the first supernatant in 2.5 ml of supplemented medium. After addition of 10 ml of supplemented medium, infected Sf9 cells were incubated for 7 d at 26°C. Second, $12 \cdot 10^6$ Sf9 cells were plated into a 15 cm dish and incubated for 1 hr on a rocking platform with 1 ml of the second supernatant in 5 ml of supplemented medium. 15 ml of supplemented medium were added and infected Sf9 cells were incubated for 5-7 d at 26°C.

For protein expression the supernatant of the second amplification was used to infect Sf9 cells, described as above for the second amplification. But in contrast, cells were harvested after 48 hr and whole cell extract was prepared as specified in section 3.2.3.8. For protein expression a maximum amount of 1 ml of supernatant was used. In order to investigate interactions between proteins (FLAG-dL(3)mbt and dRpd3; dL(3)mbt and dLint-1-FLAG) volumes of baculoviruses to co-infect Sf9 cells had to be titrated (Table 3.12) to achieve optimal expression levels for both proteins.

**Table 3.12: Volumes of baculoviruses used for co-infection of Sf9 cells.** All baculoviruses in this table, except for His6-Rpd3 (provided by A. J. Courey; Chen et al., 1999), were generated in the course of this study.

| Baculovirus | Volume | Baculovirus | Volume |
|---|---|---|---|
| **dL(3)mbt-dRpd3 interaction assay** | | | |
| HA-FLAG-dL(3)mbt | 400 µl | $His_6$-dRpd3 | 200 µl |
| FLAG-N-term-dL(3)mbt | 400 µl | $His_6$-dRpd3 | 200 µl |
| FLAG-3MBT-dL(3)mbt | 200 µl | $His_6$-dRpd3 | 200 µl |
| FLAG-C-term-dL(3)mbt | 200 µl | $His_6$-dRpd3 | 200 µl |
| **dL(3)mbt-dLint-1 interaction assay** | | | |
| dL(3)mbt-FLAG | 900 µl | dLint-1 | 100 µl |

### 3.2.3.13 Histone deacetylase (HDAC) assay

As samples for measuring HDAC activity, immunoprecipitates of endogenous or recombinant FLAG-tagged proteins bound to ProtG or FLAG beads (3.2.3.10), were used. In case of FLAG-tagged protein, FLAG immunprecipitations from nuclear extract of mock S2 cells were used as negative controls. In case of endogenous proteins, control precipitations using α-GST antibody or no antibody (beads control) were carried out.

The sample volume was adjusted to 30 µl with HDAC buffer in siliconised reaction tubes and $^{3}$H-labelled chicken core histones (20000-50000 cpm; kindly provided by A. Imhof) were added. For HDAC inhibition 500 nM TSA were added. The samples were incubated for 90 min at 30°C and beads were resuspended every 15 min. After incubation, 200 µl $H_2O$ and 65 µl 1 M HCl/0.16 M HAc were added and mixed briefly. To extract radioactively labelled acetyl groups, which were set free by HDAC activity, the samples were mixed with 700 µl of ethyl acetate for 15 min by vortexing and centrifuged for 2 min at 13000 rpm (Heraeus BIOFUGE pico). 500 µl of the upper organic phase were transferred into a scintillation vial containing 5 ml of scintillation cocktail (PerkinElmer), mixed for 10 sec by vortexing and counted in a scintillation counter. A control with only histone substrate was included, which was then subtracted from all samples.

| | |
|---|---|
| HDAC buffer | 10 mM Tris/HCl, pH 8.0<br>1 mM $MgCl_2$<br>0.1 µg/µl BSA (added freshly) |

### 3.2.3.14 Coupled *in vitro* transcription and translation

For the synthesis of $^{35}$S-labelled dLint-1 the TNT Quick Coupled Reticulocyte Transcription/Translation System (Promega) was used, following the manufacturer's instructions. Radioactively labelled $^{35}$S-methionine was purchased from Amersham. In brief, a reaction was assembled on ice, as below. The reaction was kept at 30°C for 90 min. Aliquots were taken and analysed by autoradiography. Samples were separated by SDS-PAGE and the gel was treated with Amplify (Amersham) according to manufacturer's instructions, to increase signal intensity. After drying the gel, radioactively labelled proteins were visualised on a SuperRX Fuji Medical X-ray film. Residual protein was stored at -20°C.

| | | |
|---|---|---|
| 12.5 µl | Rabbit reticulocyte lysate | |
| 1 µl | Reaction buffer | |
| 0.5 µl | TNT RNA Polymerase | SP6 or T3 |
| 0.5 µl | Amino acid mixture without Met | 1 mM |
| 1 µl | [$^{35}$S] methionine | >1000 Ci/mmol at 10 mCi/ml |
| 0.5 µl | RNasin Ribonuclease Inhibitor | 40 U/µl |
| 2 µl | DNA template | 0.5 µg/µl |
| 7 µl | Nuclease-free dd$H_2O$ | (up to 25 µl) |

For *in vitro* transcription/translation of dLint-1, the ORF was cloned into the pING-14A vector under the control of a SP6 RNA polymerase-specific promoter. A control DNA encoding a *luciferase* gene under the control of a T3 RNA polymerase promoter served as a positive control for the reaction. The generated Luciferase protein was used in the following as a negative control for interaction studies (3.2.3.15).

### 3.2.3.15 Interaction assay of $^{35}$S-dLint-1 and FLAG-dL(3)mbt

To investigate the interaction between $^{35}$S-dLint-1 (3.2.3.14) and recombinant FLAG-dL(3)mbt, 12 ml of Sf9 extract, either mock or expressing FLAG-dL(3)mbt (3.2.3.12), were bound to 60 µl of α-FLAG M2 agarose. Beads were washed extensively, twice with 10 ml LyBu-200 and once with 5 ml LyBu-500 buffer (buffer composition, see 3.2.3.8) for each 5 min. Afterwards, 10 µl FLAG beads were equilibrated with IP buffer (3.2.3.10), blocked for 30 min with 0.2 µg/µl BSA in IP buffer and incubated with 8 µl of $^{35}$S-dLint-1 or 6 µl of $^{35}$S-Luciferase (similar protein amounts, estimated by signal strength on an X-Ray film) for 3 hr at 4°C in IP buffer. After extensive washing (four times 5 min with 1 ml IP buffer) samples were separated by SDS-PAGE and detected by autoradiography (3.2.3.14). All incubation and washing steps were carried out with rotation.

### 3.2.3.16 GST protein expression

Recombinant GST fusion proteins were expressed according to standard procedures. Generally, GST fusion proteins were expressed in *E. coli* BL21 (0.2-1 l total culture volume) for 2 hr at 37°C or overnight at 18°C after induction with 0.2-0.4 mM IPTG at $OD_{600}$ of 0.7-0.8. The bacteria were resuspended in 10-20 ml of PBS/1% Triton-X-100 (AppliChem) supplemented with protease inhibitors. After sonication (10 x 12 sec, 25% output), the suspension was centrifuged for 20 min at 15000 rpm at 4°C (Sorvall RC-

5B, SS34 rotor) to remove cell debris from the supernatant. GST proteins were bound to Glutathione Sepharose 4 Fast Flow (200-400 µl; GE Healthcare) and washed three times with PBS/1% Triton-X-100 and two times with PBS (each with 5-10 ml for 5 min at 4°C with rotation). If necessary GST proteins were eluted with 0.2-0.4 mM reduced glutathione in PBS and stored at -80°C.

#### 3.2.3.17 GST protein pulldown

GST fusion proteins were expressed and bound to Glutathione Sepharose as described above (3.2.3.16). If required GST proteins bound to Glutathione Sepharose beads were stored at -20°C in PBS/40% glycerol. Protein concentrations on beads were estimated after SDS-PAGE and Coomassie staining in comparison to a standard protein (such as BSA). For GST pulldown assays, beads with bound GST proteins (2-4 µg) were equilibrated in GST pulldown buffer and incubated with 200 µl of dL(3)mbt-FLAG containing Sf9 extract for 4 hr at 4°C with rotation in GST pulldown buffer. After extensive washing four times with 1 ml of GST pulldown buffer for 5 min at 4°C, samples were analysed by Western blotting and Ponceau staining.

| | |
|---|---|
| GST pulldown buffer | 25 mM Hepes/KOH, pH 7.6<br>150 mM KCl<br>12.5 mM $MgCl_2$<br>20% glycerol<br>0.1% NP-40<br>DTT, protease inhibitors |

#### 3.2.3.18 Histone peptide pulldown assay

Histone H4 peptides comprising amino acids 16-25 with lysine 20 either unmodified, mono-, di- or tri-methylated (purchased from Peptide Specialty Laboratories), were coupled to SulfoLink Coupling Gel (Pierce) via a C-terminal cysteine according to the manufacturer's protocol with minor changes. Instead of using columns, the batch method was applied. All centrifugations were carried out at 4000 rpm for 2 min (Heraeus BIOFUGE pico).

For the pulldown, immobilised peptides (0.5 µg each) were pre-blocked with 1 µg/µl BSA in binding buffer for 1 hr at 4°C. Recombinant FLAG-d3MBT, GST-d3MBT or GST-h3MBT was incubated with pre-blocked immobilised peptides for 2 hr at 4°C in

binding buffer with agitation. After extensive washing with binding buffer (4x with 1 ml for 5 min at 4°C with rotation), peptide-bound protein was analysed by Western blotting.

| | |
|---|---|
| Peptide pulldown binding buffer | 25 mM Tris, pH 8.0<br>150 mM NaCl<br>2 mM EDTA<br>0.5% NP-40 |

#### 3.2.3.19 GST protein purification for antibody generation

The recombinant GST fusion protein of dLint-1-Cterm (aa 302-602) was expressed in *E. coli* BL21 for 2 hr at 37°C after induction with 0.4 mM IPTG at $OD_{600}$ of 0.7-0.8. The bacteria of a 1 l culture were resuspended in 20 ml of PBS/1% Triton-X-100 (AppliChem) supplemented with protease inhibitors and 1 mM DTT. After sonication and centrifugation (see 3.2.3.16) the GST fusion protein was purified from the supernatant via affinity chromatography using a GSTrap FF column and the Äkta purifier system (GE Healthcare). Before loading the column, the bacterial lysate was filtered through a 0.2 µM filter. The GST fusion protein was eluted with elution buffer (40 mM reduced glutathione in 50 mM Tris-HCl, pH 8.5, 200 mM NaCl). Fractions containing the GST fusion protein were pooled and further purified via cation exchange chromatography using a HiTrap SP HP column (GE Healthcare). The protein was bound to the column in IEX-C-100 buffer and eluted with a salt gradient of 100 to 500 mM KCl in IEX-C-x buffer. Prior to injection, the purified GST-dLint-1-Cterm protein was diluted to a final salt concentration of 150 mM salt.

| | |
|---|---|
| IEX-C-x buffer | 25 mM Hepes/KOH, pH 7.0<br>x mM KCl |

## 3.2.4 Chromatographic fractionation of *Drosophila* cell nuclear extract

### 3.2.4.1 Gel filtration analysis

Gel filtration is a chromatographic technique to separate proteins and protein complexes on the basis of size. Generally, gel filtration was carried out in the presence of 300 mM salt, to eliminate or at least minimise the detection of protein complexes mediated by weak protein-protein interactions. Nuclear extract from Kc167 or S2 cells was loaded onto a Superose 6 HR 10/30 gel filtration column (GE Healthcare) and resolved in EX300 buffer on an Äkta purifier system and collected with a fraction collector Frac-950 according to the manufacturer's instructions. Upon sample injection 500 µl fractions were collected, precipitated using StrataClean resin (Stratagene) and subjected to Western blot analysis (3.2.3.4).

| | |
|---|---|
| EX300 gel filtration buffer | 10 mM Hepes/KOH, pH 7.6<br>300 mM KCl<br>1.5 mM $MgCl_2$<br>0.5 mM EGTA<br>10% glycerol<br>DTT, PMSF |

### 3.2.4.2 Ion exchange chromatography

Ion exchange chromatography was carried out according to standard procedures on an Äkta purifier system with a Frac-950 fraction collector using columns supplied by GE Healthcare according to the manufacturer's instructions. In general, samples were applied at slow flow rates of 250-500 µl/min, while washing and elution steps were carried out at flow rates of 1-2 ml/min, always considering the maximum back pressure of the corresponding columns.

In summary, 3.5 ml of Kc167 nuclear extract (6.0 µg/µl protein conc.) were diluted 4.2x with IEX-A-0 buffer to adjust the NaCl concentration of the sample to 100 mM. Subsequently, the sample was bound to a HiTrap Q Sepharose FF column (5 ml volume) that was prior to this equilibrated with IEX-A-100 buffer. The flow through was loaded once more to ensure efficient binding of proteins. Then the column was washed with 10-20 ml of IEX-A-100 buffer or until no protein (measured by absorption at 280 nm) appeared in the effluent.

| | |
|---|---|
| IEX-A-x buffer | 20 mM Tris/HCl pH 7.5<br>x mM NaCl<br>DTT, PMSF |

Elution was performed in two steps: First, applying IEX-A-500 buffer and second, applying IEX-A-1000 buffer. Peak fractions of the eluates were collected and tested together with the flow through by Western blotting. Next, the eluate (500 mM peak fraction), containing the proteins of interest, was diluted 5x with IEX-A-0 buffer. The sample was then bound to a Mono Q 5/50 GL column (GE Healthcare) and after the sample application the column was washed with 5-10 ml of IEX-A-100 buffer or until no protein was present in the effluent. For elution a continuous salt gradient was used, going from 100 mM up to 500 mM NaCl in IEX-A buffer, applied at a flow rate of 1 ml/min, collecting 50 fractions of 0.5 ml volume each. Finally, residual protein was eluted in one step with IEX-A-1000 buffer. 500 µl fractions were collected, precipitated using StrataClean resin (Stratagene) and subjected to Western blot analysis (3.2.3.4).

## 3.2.5 Antibody generation

### 3.2.5.1 dL(3)mbt-specific antibodies

The polyclonal α-dL(3)mbt (#3) antibody was raised against three dL(3)mbt-specific peptides (P1: PSGEDKTRSTQKNNKQNTSASC; P2: YFERPLYDRPGRRPSAC; P3:CLPEQSQTNGYKTDHDQELS). These peptides were synthesised and injected into rabbit by the Peptide Specialty Laboratories (Heidelberg).

The monoclonal α-dL(3)mbt antibodies (clones P1 6E6 and P3 8F10) were generously generated by E. Kremmer (Helmholtz Zentrum München). In short, Lou/C rats were immunised with dL(3)mbt-specific peptides (P1 and P3, see above) coupled to KLH (Keyhole Limpet Hemocyanin). After a series of immunisations, a final boost was given three days before fusion of the rat spleen cells with the murine myeloma cell line P3X63-Ag8.653. Subsequently, hybridoma supernatants were tested in ELISA using the corresponding peptides coupled to ovalbumin.

The specificity of the α-dL(3)mbt #3 antibody was tested by expressing a recombinant FLAG-tagged full-length protein of dL(3)mbt in S2 cells. The FLAG-tagged protein was immunoprecipitated using α-FLAG M2 agarose, subjected to Western blotting and detected using the α-dL(3)mbt #3 antibody (Figure 4.1 A). Moreover, the specificity

was confirmed by RNAi experiments in Kc167 cells and subsequent Western blot analysis (Figure 4.22 A). α-dL(3)mbt monoclonal P1 6E6 and P3 8F10 antibodies were used exclusively for immunoprecipitation and immunofluorescence. The specificity of the immunoprecipitate was tested in Western blot, using the α-dL(3)mbt #3 as primary antibody, which resulted in a band at the expected molecular weight of 170 kDa (Figure 4.2 C). Specificity in immunofluorescent stainings of polytene chromosomes was demonstrated by recognition of ectopically expressed recombinant dL(3)mbt (Figure 4.20 B).

#### 3.2.5.2 dLint-1-specific antibodies

The α-dLint-1 antibodies (#1 and #2) were raised against the C-terminal half of dLint-1 (aa 302-602), expressed and purified as a GST fusion protein (for purification, see 3.2.3.19). The injection of protein (0.5 mg/rabbit) and further antibody production was conducted by the Peptide Specialty Laboratories (Heidelberg).

To verify the specificity of these antibodies dLint-1 was depleted in Kc167 cells and the nuclear extracts were tested by Western blot (Figure 4.8 C). Both antibodies recognised a protein band between the molecular weight standards for 72 and 95 kDa that significantly decreased in intensity upon knockdown by RNAi.

#### 3.2.5.3 Antibody concentration

The cell culture supernatant, containing dL(3)mbt-specific rat antibody P1 6E6, was concentrated on Protein G Sepharose FF beads (ProtG beads) before being used in immunofluorescent staining of polytene chromosomes. 0.5 ml of ProtG beads were equilibrated in 100 mM Tris/HCl, pH 8.0. The pH of 8 ml of cell culture supernatant was adjusted to 8.0 by the addition of 1 M Tris/HCl, pH 8.0. Afterwards, the cell culture supernatant was incubated with the equilibrated ProtG beads on a rotating wheel for 2 hr at 4°C. Then ProtG beads were loaded into a 2 ml gravity flow column (Bio-Rad) and washed once with 5 ml of 100 mM Tris/HCl, pH 8.0 and once with 5 ml of 10 mM Tris/HCl, pH 8.0. Stepwise elution of the antibodies from the ProtG beads was carried out using 50 mM glycine, pH 3.0. 10 fractions of 500 µl volume were collected and neutralised immediately with 50 µl of 1 M Tris/HCl, pH 8.0. Eluates were separated on a 10-12.5% SDS-polyacrylamide gel and analysed by Coomassie staining. Fractions containing the bulk of antibodies were pooled and stored at 4°C.

### 3.2.6 Generation of a UAS-dL(3)mbt transgenic fly line

For fly transgenesis an integration system (Bischof et al., 2007) was used that is based on the ectopic expression of the φC31 integrase in the germline. φC31 integrase mediates the site-specific integration of a transgene encoded on the integration vector flanked by a bacterial attachment site (*attB*) into the transgenic fly genome at a phage landing site (*attP*) via recombination. The integration vector further contains a *white*$^{+}$ marker gene that can be functionally expressed upon correct integration. The pUASattB-HA-FLAG-dL(3)mbt plasmid (Table 3.4) was injected into the J5 strain (attP-zh86Fb/vas-phi-zh102D), which possesses an *attP* element inserted on the 3rd chromosome and showed the highest frequency of transgenesis (Bischof et al., 2007). Injection into embryos was performed in collaboration with the laboratory of Prof. R. Renkawitz-Pohl.

After injection, flies of the F0 generation were crossed to the $w^{1118}$ isogenic strain and the F1 generation was screened for flies with 'orange' eyes. Flies with 'orange' eyes were then crossed against each other to gain homozygous transgenic flies with red eyes, carrying the UAS-construct. Site-specific integration of the transgene was confirmed by PCR using genomic DNA as template (Figure 3.2). To isolate genomic DNA single flies (male and female) from the transgenic F2 generation were put into 50 µl of squashing buffer complemented by the addition of 1 µl ProteinaseK (10 mg/ml) and squashed with the aid of a 200 µl tip. Thereafter, the suspension was incubated for 30 min at 37°C and 10 min at 85°C. After a brief centrifugation 2 µl of the supernatant were used as DNA template for PCR (3.2.2.5). As negative controls identical PCR reactions were set up using genomic DNA, isolated from the J5 injection strain (attP-zh86Fb/vas-phi-zh102D) and $w^{1118}$ control flies, as template.

| | |
|---|---|
| Squashing buffer | 10 mM Tris/HCl, pH 8.0 |
| | 25 mM NaCl |
| | 1 mM EDTA, pH 8.0 |

To check the correct insertion of the UAS-dL(3)mbt construct via PCR a forward primer specific to the coding sequence of dL(3)mbt (l3mbt-insert-1-fw) and a reverse primer specific to the 3' end of the *attP* landing site (attPzh86Fb_rv) were used. A specific amplicon with a size above 2000 bp was present only in UAS-HA-FLAG-dL(3)mbt transgenic flies (Figure 3.2, lanes 1 and 2), but not in control flies (lanes 3, 4,

5 and 6). Furthermore, overexpression of recombinant dL(3)mbt in salivary glands was verified by Western blot and polytene stainings (Figure 4.20).

| | |
|---|---|
| l3mbt-insert-1-fw | GGACTCCCAACAAGAGATTGTC |
| attPzh86Fb_rv | GCCGAACGAAATTAAAAATTGA |

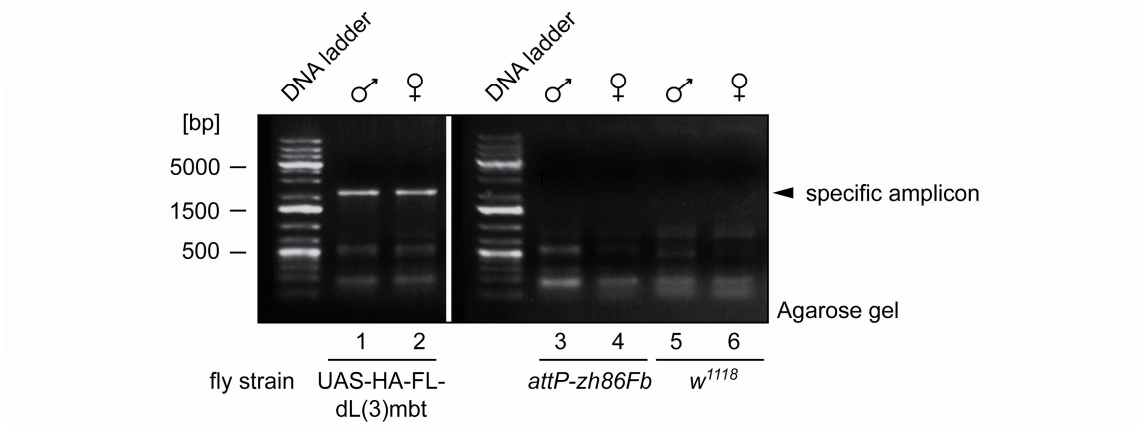


**Figure 3.2: Site-specific integration of the UAS-HA-FLAG-dL(3)mbt construct in the *attP* landing site.** Genomic DNA was isolated from single male and female flies (depicted on top) from transgenic flies carrying the UAS-HA-FLAG-dL(3)mbt (lanes 1 and 2), from the J5 injection strain (attP-zh86Fb; lanes 3 and 4) and from $w^{1118}$ control flies (lanes 5 and 6), as specified below. PCRs were carried out using the primer pair, l3mbt-insert-1-fw and attPzh86Fb_rv. PCR amplicons were analysed by agarose gel electrophoresis.

### 3.2.7 Immunofluorescent staining of polytene chromosomes

*Drosophila* larvae were raised under standard culturing conditions at 26°C. Third instar wandering larvae were washed and salivary glands were dissected in PBS under a stereomicroscope (Askania GSZ 2T). Dissected salivary glands (2 pairs at a time) were fixed in a drop of Polytene fixation buffer for 5 min on a siliconised cover slip (treated with dimethylchlorosilane solution). Then the cover slip was taken up by a glass microscope slide. In order to break up the glands, facilitate cell lysis and spreading of the polytene chromosomes, the tip of a pencil was used to gently tap onto the cover slip, while slightly moving it back and forth. Success of the squashing was verified quickly under a phase contrast microscope (Zeiss Primo Star) at 40x magnification. Squashed chromosomes were flattened by applying strong pressure on the cover slip by pressing the thumb onto the back side of the glass microscope slide. Subsequently, each glass slide was frozen in liquid nitrogen, the cover slip was removed using a scalpel and the glass slides were collected in PBS in a Coplin jar. Collected glass slides were washed

with PBS for 10 min while gently shaking. Subsequently glass slides were blocked in blocking solution (5% milk in PBS) for 30 min, while shaking was continued. After rinsing the slides with PBS again, they were placed in a humid chamber. Polytene chromosomes were covered with 40 µl of primary antibodies diluted in blocking solution and 2% normal goat serum (NGS; Sigma Aldrich) and fresh cover slips (concentrated rat α-dL(3)mbt P1 6E6: 1:2; rabbit α-dLint-1 #1: 1:50). Incubation with primary antibodies was carried out overnight at 4°C. After removal of the cover slips, glass slides were rinsed with PBS and washed three times with blocking solution. Chromosome squashes were incubated with the appropriate secondary antibodies (Table 3.10) diluted in blocking solution and 2% NGS for 1 hr at RT in the dark. Then the glass slides were washed once with wash buffer A and once with wash buffer B, each for 10 min in the dark, rinsed with PBS and DNA was stained with DAPI solution (0.2 µg/ml DAPI from Invitrogen in PBS) for 4-5 min. Slides were washed with PBS for 10 min in the dark, mounted with Fluoromount (SouthernBiotech), sealed with nail polish and stored at 4°C in the dark. Polytene chromosome stainings were analysed with a Zeiss fluorescence microscope (Axioplan).

| | |
|---|---|
| Polytene fixation buffer | 45% acetic acid<br>1% formaldehyde (10% stock, methanol-free from Polyscience) |
| Wash buffer A | PBS<br>300 mM NaCl<br>0.2% NP-40<br>0.2% Tween 20 |
| Wash buffer B | PBS<br>400 mM NaCl<br>0.2% NP-40<br>0.2% Tween 20 |

Overlays of dL(3)mbt and dLint-1 stained polytene chromosomes were assembled using Adobe Photoshop. Quantitative analysis of dL(3)mbt and dLint-1 binding sites was accomplished by visual inspection and counting was done with the aid of the Image J software (http://rsbweb.nih.gov/ij/).

# 4 Results

## 4.1 Purification of novel dL(3)mbt complexes

MBT domain-containing proteins have been previously reported to be part of or associate with multi-subunit complexes. In the model organism *D. melanogaster*, three MBT proteins have been identified, two of which are the PcG proteins Scm and Sfmbt. Although Scm can interact with the PRC1 complex, it is not a core component (Peterson et al., 2004), while Sfmbt is a stoichiometric subunit of the PhoRC complex (Klymenko et al., 2006). Both are involved in the maintenance of homeotic gene repression. Furthermore, dL(3)mbt as the third MBT protein in *Drosophila*, has been reported to be associated in sub-stoichiometric amounts with the Myb-MuvB complex (Lewis et al., 2004). However, an independent purification of the same core complex (dREAM) has failed to recover dL(3)mbt (Korenjak et al., 2004). In order to better understand the role of dL(3)mbt in the cell, this study aimed to investigate, whether dL(3)mbt is present in novel multi-protein complexes.

### 4.1.1 The dL(3)mbt repressor protein interacts with a histone deacetylase

#### 4.1.1.1 dL(3)mbt is associated with HDAC activity

At first to aid biochemical analysis of dL(3)mbt a polyclonal antibody (α-dL(3)mbt #3) was established. The specificity of this polyclonal antibody was confirmed by depleting the dL(3)mbt protein in Kc167 cells. After 5 d of RNAi, nuclear extracts of cells treated with double-stranded RNA (dsRNA) directed against dL(3)mbt and EGFP were analysed by Western blotting. A protein band with an apparent molecular weight of 170 kDa was detected that was no longer visible upon dL(3)mbt RNAi compared to cells treated with EGFP dsRNA (Figure 4.22 A, upper panel, compare lanes 1 and 2). This identified the antibody reactive band above 170 kDa as dL(3)mbt, which runs slower than expected from its theoretical molecular weight (163 kDa). Detection of β-tubulin around 55 kDa served as a loading control, to ensure that equal protein amounts have been applied.

In the past, numerous studies investigating the modulation of chromatin to regulate gene transcription have established that HDAC enzymes and their ability to deacetylate

histone tails are often required as co-repressive activities to shut down gene expression. In accordance with this, HDACs are important components of numerous transcriptional co-repressor complexes (Nagy et al., 1997; Shi et al., 2005; Xue et al., 1998). Moreover the activity of deacetylases is thought to play an important role to facilitate the formation of higher-order chromatin structures (Shahbazian and Grunstein, 2007; Shogren-Knaak et al., 2006; Shogren-Knaak and Peterson, 2006). Likewise, members of the MBT domain protein family have been implicated in chromatin compaction and transcriptional repression of genes. Therefore, the involvement of MBT and HDAC proteins in similar biological processes raised the question whether dL(3)mbt might interact with a histone deacetylase in *Drosophila*.

To address this question, first it was tested if dL(3)mbt associates with enzymatic HDAC activity. For this purpose, an expression vector for FLAG-tagged dL(3)mbt was generated, which drives the efficient expression of FLAG-dL(3)mbt, when transfected into S2 cells. To increase the chances that recombinant FLAG-tagged dL(3)mbt becomes incorporated into protein complexes, a stable monoclonal S2 cell line carrying the expression vector was established. The successful integration of the construct and expression of the recombinant protein in this S2 cell line was confirmed by FLAG immunoprecipitation and Western blot analysis using the α-dL(3)mbt #3 antibody (Figure 4.1 A, compare lanes 1 and 2 with 3 and 4). Overexpression of FLAG-dL(3)mbt was reflected in the input signals (compare lanes 1 and 3). Due to the high molecular weight of dL(3)mbt, addition of a comparatively small tag, such as in this case the HA-FLAG-epitope, did not result in a slower migration of the recombinant protein compared to endogenous dL(3)mbt in SDS-PAGE.

The enzymatic activity of HDACs can be measured using as a substrate core histones that were radioactively labelled with acetyl groups containing $^{3}H$ isotope (Brehm et al., 1998). In this set up HDAC activity corresponds to the radioactivity that is released upon incubation of a protein sample with the histone substrate. To test for the association of dL(3)mbt with HDAC activity, this assay was performed with FLAG immunoprecipitates of FLAG-dL(3)mbt, stably expressed in S2 cells (Figure 4.1 B). FLAG immunoprecipitations from control extract, lacking FLAG-tagged dL(3)mbt (mock), served as controls. Ethidium bromide (EtBr) was included in some assays to prevent unspecific interaction with HDAC activity mediated by DNA (Lai and Herr, 1992). The precipitation of FLAG-dL(3)mbt led to an enrichment of HDAC activity of about 30-fold, compared to controls. The interaction with HDAC activity, however, was

not affected by the addition of EtBr to the immunoprecipitation. To verify that the release of radioactivity relies on enzymatic HDAC activity, the class I- and II-specific HDAC inhibitor trichostatin A (TSA) (Yoshida et al., 1990) was added to the HDAC reaction, resulting in a 15-fold drop of the released radioactivity (Figure 4.1 B). Taken together, the FLAG-tagged dL(3)mbt protein precipitated HDAC activity and this association appeared to be mediated by protein-protein interactions. Moreover, the dL(3)mbt associated HDAC activity was sensitive to treatment with TSA, suggesting that the responsible enzyme belongs to HDAC classes I or II.

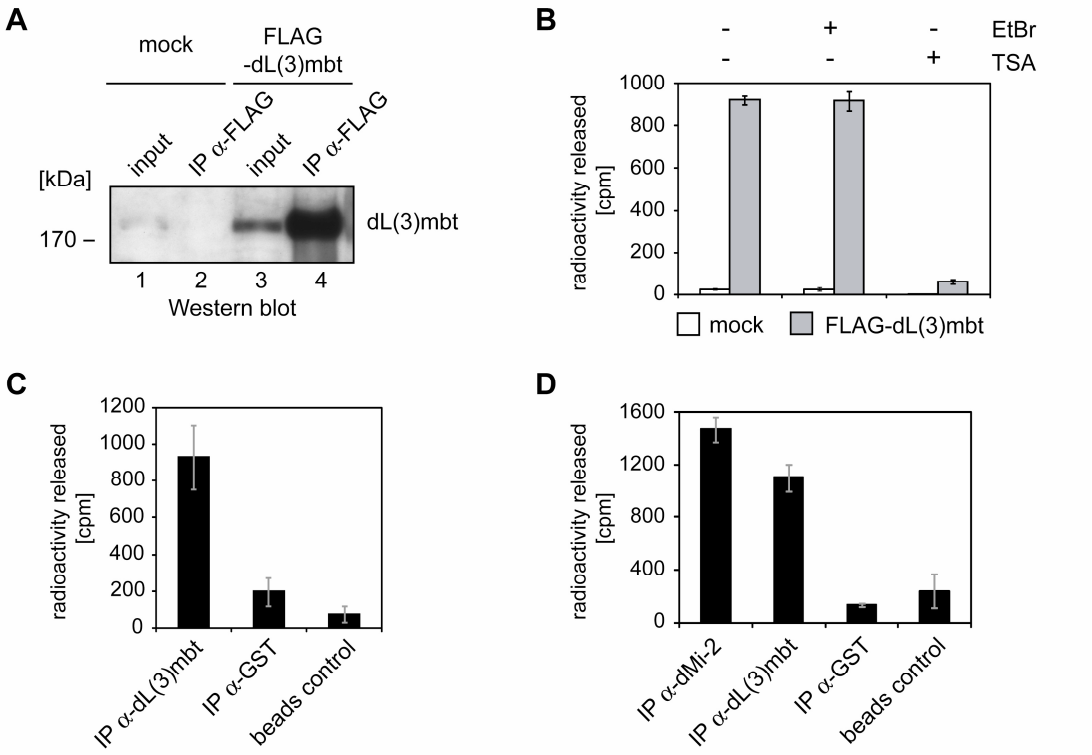


**Figure 4.1: Recombinant and endogenous dL(3)mbt are associated with HDAC activity.** (A) Stable expression of FLAG-tagged dL(3)mbt in S2 cells. Nuclear extracts from control S2 cells (mock, lanes 1 and 2) and cells stably expressing FLAG-tagged dL(3)mbt (lanes 3 and 4) were immunoprecipitated with α-FLAG M2 agarose (FLAG beads; lanes 2 and 4). Immunoprecipitates were analysed by Western blot using dL(3)mbt-specific antibody as indicated. 5% input (lanes 1 and 3). (B) HDAC assays were carried out with FLAG immunoprecipitates from nuclear extracts from control S2 cells (mock) and S2 cells stably expressing FLAG-tagged dL(3)mbt (FLAG-dL(3)mbt). Immunoprecipitations (IP) were carried out in the absence (-) or presence (+) of ethidium bromide (EtBr) and HDAC reactions were performed with (+) or without (-) the HDAC inhibitor trichostatin A (TSA), as indicated above. Data are means of triplicate experiments. (C) and (D) HDAC assays were carried out with α-dMi-2 (#4D8) and α-dL(3)mbt (#P1-6E6 and #P3-8F10, ratio 1:1) immunoprecipitates from S2 nuclear extract. Controls with α-GST (#R 6G9) antibody or no antibody (beads control) were included. Data are means of triplicate experiments. (B) and (C): Published in Scharf et al. (2009).

To ensure the significance of this interaction it was important to verify that also endogenous dL(3)mbt interacts with HDAC activity. However, despite its applicability in Western blot the α-dL(3)mbt #3 antibody did not work in immunoprecipitation. Hence, two monoclonal antibodies against dL(3)mbt were raised. When used in a 1:1 ratio these antibodies precipitated a significant proportion of dL(3)mbt that was detected by the polyclonal dL(3)mbt antibody in Western blot (Figure 4.2 C, upper panel, compare lanes 1 and 2). When using these dL(3)mbt-specific antibodies for immunoprecipitation, robust HDAC activity was indeed precipitated from S2 nuclear extract, corresponding to 4.6- and 12.5-fold more compared to precipitations using a control antibody or no antibody (beads control), respectively (Figure 4.1 C).

In order to assess, whether the amount of HDAC activity that was associated with dL(3)mbt was significant, an immunoprecipitation of the dMi-2 chromatin remodeler protein was carried out to serve as a positive control. As established previously, dMi-2 is the ATPase subunit of the stable *Drosophila* Nucleosome Remodelling and Deacetylation complex (dNuRD) that comprises among other proteins the HDAC dRpd3 (Kunert et al., 2009; Reddy et al., 2010). As expected, dMi-2 immunoprecipitates displayed a strong HDAC activity, when compared to precipitations using GST control antibody (10.7-fold more) or no antibody (beads control; 6.0-fold more) (Figure 4.1 D). Interestingly, the HDAC activity measured with dL(3)mbt precipitates, which were processed in parallel, was only 25% less than the activity interacting with dMi-2. Even though, the absolute values of HDAC activity levels precipitated by dL(3)mbt and dMi-2 antibodies are not directly comparable, since the antibodies might differ in their precipitation efficiencies, these results strengthen the idea, that endogenous dL(3)mbt interacts with one or more HDAC enzymes *in vivo*.

#### 4.1.1.2 dL(3)mbt and the histone deacetylase dRpd3 interact *in vivo*

HDAC assays revealed that dL(3)mbt is associated with enzymatic HDAC activity. This HDAC activity was sensitive to treatment with TSA, an inhibitor that targets class I and II HDACs. In *Drosophila*, there are two class I (dRpd3 and dHDAC3) and two class II histone deacetylases (HDAC6, isoforms S/L, and HDAC4). Of these, dRpd3, dHDAC3, HDAC4 and the isoform S of HDAC6 have been shown to be highly sensitive to TSA (Cho et al., 2005). Generally, dRpd3 is considered to be one of the most abundant HDACs, which is conserved from yeast (Rundlett et al., 1996) to human (Taunton et al.,

1996). To examine, whether dL(3)mbt was associated with dRpd3, immunoprecipitates of FLAG-tagged dL(3)mbt stably expressed in S2 cells were subjected to Western blot analysis (Figure 4.2 A).

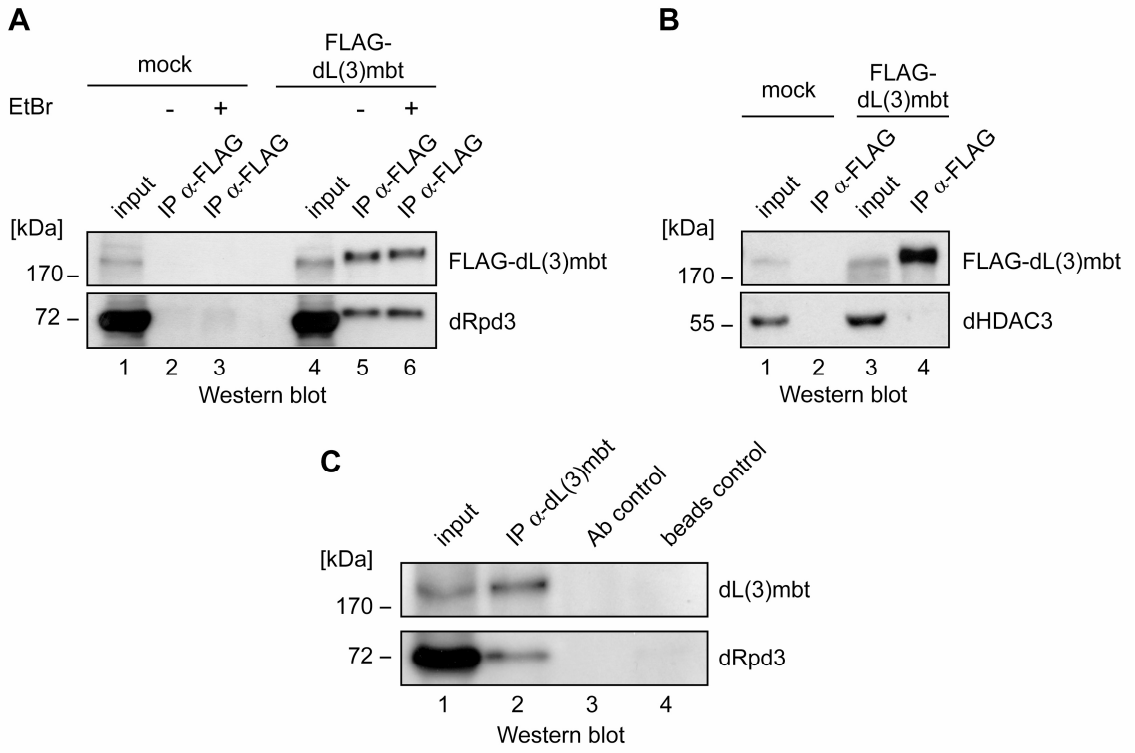


**Figure 4.2: Recombinant and endogenous dL(3)mbt are associated with the histone deacetylase dRpd3.** (A) Nuclear extracts from control S2 cells (mock, lanes 1, 2 and 3) and cells stably expressing FLAG-tagged dL(3)mbt (lanes 4, 5 and 6) were immunoprecipitated with FLAG beads (lanes 2, 3, 5 and 6). Immunoprecipitations were carried out in the absence (-) or presence (+) of ethidium bromide (EtBr). Immunoprecipitates (IP) were analysed by Western blotting using dL(3)mbt- (#3) and dRpd3-specific antibodies as indicated. Input: 5% of nuclear extracts (lanes 1 and 4). (B) Nuclear extracts from control S2 cells (mock, lanes 1 and 2) and cells stably expressing FLAG-dL(3)mbt (lanes 3 and 4) were immunoprecipitated with FLAG beads (lanes 2 and 4). Immunoprecipitates were analysed by Western blotting using dL(3)mbt (#3) and dHDAC3 antibodies as indicated. Input: 5% of nuclear extracts (lanes 1 and 3). (C) Nuclear extract from S2 cells was precipitated using a mixture of monoclonal dL(3)mbt antibodies (at a ratio of 1:1) or no antibody (lane 4, beads control). Immunoprecipitations were subjected to Western blot using dL(3)mbt (#3) and dRpd3 antibodies. Lane 3: Ab control using dL(3)mbt-specific antibody without extract. Input: 5% of nuclear extract (lane 1). Published in Scharf et al. (2009).

FLAG immunoprecipitation showed that dRpd3 co-precipitated with recombinant dL(3)mbt in an efficient manner in comparison with control precipitations conducted with extracts from cells lacking FLAG-dL(3)mbt expression vector (mock) (Figure 4.2

A, compare lanes 5 and 6 with 2 and 3). In agreement with the observations made in HDAC assays, the presence of EtBr did not interfere with the efficiency of dRpd3 co-precipitation (Figure 4.2 A, compare lanes 5 and 6).

In contrast to dRpd3, FLAG-dL(3)mbt did not bind the second class I histone deacetylase dHDAC3 (Figure 4.2 B, lower panel), even though a significant amount of recombinant FLAG-tagged dL(3)mbt was precipitated compared to the input (Figure 4.2 B upper panel, compare lanes 3 and 4 with 1 and 2). Unfortunately, antibodies against dHDAC4 and dHDAC6 were not available and a possible interaction with dL(3)mbt could not be investigated. Since the interaction with dRpd3 was detected using extracts from the S2 cell line stably expressing FLAG-dL(3)mbt, it was conceivable that this was only an observation seen upon overexpression of a recombinant protein. To exclude this possibility, endogenous dL(3)mbt was precipitated from S2 nuclear extract using monoclonal antibodies (Figure 4.2 C) and immuno-precipitates were assayed for endogenous dRpd3 in Western blot. In accordance with data obtained with FLAG-tagged dL(3)mbt, dRpd3 was clearly detected in immuno-precipitates of endogenous dL(3)mbt, suggesting that these proteins interact in a robust manner under physiological conditions.

Taken together, dL(3)mbt interacts with one or more enzymatically active HDACs belonging to either class I or II of this enzyme family. While association of dL(3)mbt with HDAC4 and HDAC6 could not be tested, no interaction with dHDAC3 was detected in Western blot (Figure 4.2 B). Nevertheless, it is likely that most of the HDAC activity that was shown to be associated with dL(3)mbt (Figure 4.1) is contributed by the robust interaction with dRpd3 (Figure 4.2).

#### 4.1.1.3 The three MBT domains of dL(3)mbt are sufficient for dRpd3 binding

As co-immunoprecipitations established that dL(3)mbt specifically interacts with the HDAC dRpd3, it was of interest to map the corresponding interaction module within dL(3)mbt. The amino acid sequence of dL(3)mbt exhibits three known protein domains, the 3MBT region, the SPM domain and a zinc finger motif (Figure 4.3 A, upper panel), which are all located in the C-terminal half of the protein. In contrast, the N-terminal half of the protein does not contain any established motifs. To map the region within dL(3)mbt that is important for binding of dRpd3, both proteins were expressed recombinantly in Sf9 insect cells via baculovirus infections and interaction studies were

carried out using FLAG immunoprecipitation. First, full length dL(3)mbt, which was N-terminally tagged with a FLAG epitope tag (Figure 4.3 A, upper panel), was co-expressed in cells together with full length dRpd3 (Figure 4.3 B, compare lanes 1 and 7). As controls, Sf9 cells were infected with no baculovirus or individual baculoviruses, encoding FLAG-dL(3)mbt or dRpd3, respectively (Figure 4.3 B, compare lanes 3, 5 and 7). FLAG affinity purification of FLAG-tagged dL(3)mbt reveals a robust co-precipitation of dRpd3 from Sf9 whole cell extracts compared to precipitations from extracts containing no or only one of the two recombinant proteins (Figure 4.3 B, compare lane 2 with lanes 4, 6 and 8).

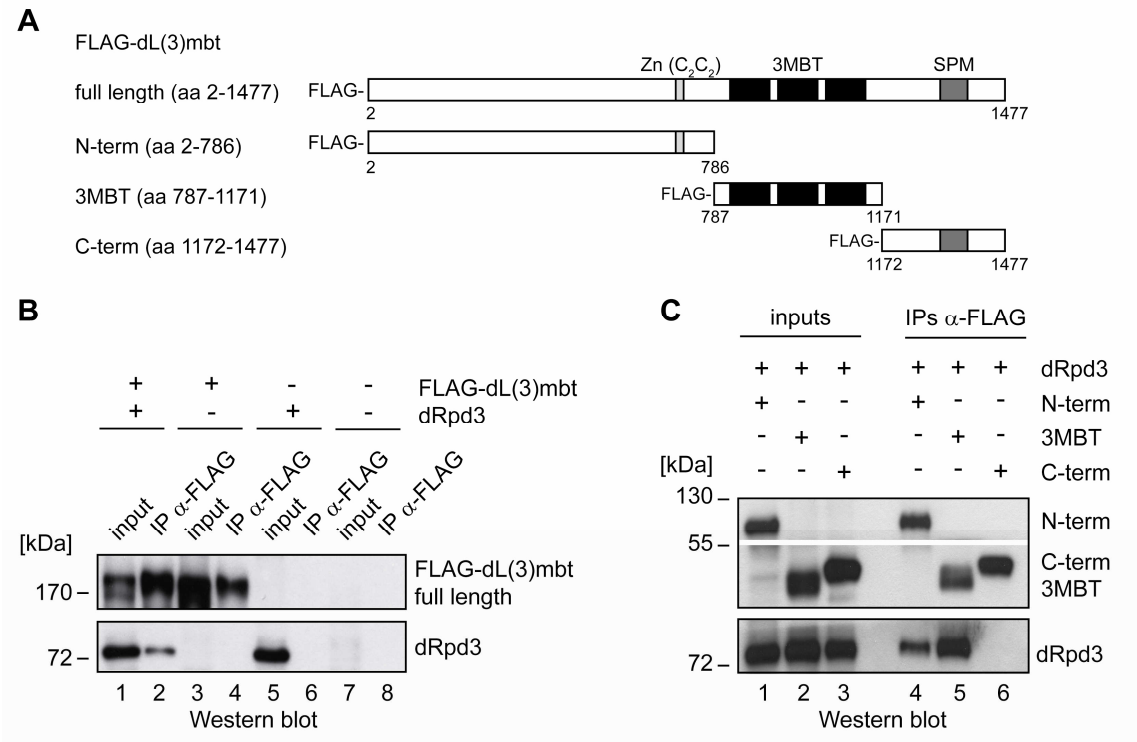


**Figure 4.3: The major dRpd3 interaction domain in dL(3)mbt maps to the MBT domains.** (A) Schematic representation of FLAG-tagged dL(3)mbt constructs used for baculoviral expression. Protein domains of dL(3)mbt are indicated on top: The Zn finger ($C_2C_2$-type) is depicted in light grey, the 3MBT domains in black, the SPM domain in dark grey and the remaining dL(3)mbt protein in white. (B) Sf9 cells were co-infected with baculoviruses expressing full length FLAG-dL(3)mbt or dRpd3 or as indicated on top. Extracts from infected cells were immunoprecipitated with FLAG beads (lanes 2, 4, 6 and 8). Immunoprecipitates were subjected to Western blot using α-FLAG (rabbit) and α-Rpd3 antibodies. Input: 5% of extracts (lanes 1, 3, 5 and 7). (C) Cells were co-infected with baculoviruses expressing one of the three FLAG-tagged dL(3)mbt deletion mutants, depicted in (A), or dRpd3 as indicated on top. Extracts from infected cells were immunoprecipitated with FLAG beads (lanes 4, 5 and 6). Immunoprecipitates were subjected to Western blot using α-FLAG (rabbit) and α-Rpd3 antibody. Input: 5% of extracts (lanes 1, 2 and 3). IP: Immunoprecipitation.

To determine which domain of dL(3)mbt is involved in the dRpd3 interaction, three FLAG-tagged dL(3)mbt mutants (depicted in Figure 4.3 A) were co-expressed with dRpd3. The three mutants tested in the interaction assay comprised: 1. most of the N-terminus including the zinc finger motif, 2. the three MBT domains and 3. the C-terminus of dL(3)mbt including the SPM domain. Western blot analysis using FLAG antibody verified that the different deletion mutants were produced with similar expression levels (Figure 4.3 C, upper panel, lanes 1, 2 and 3) and precipitated with comparable efficiencies upon FLAG affinity purification (Figure 4.3, upper panel, lanes 4, 5 and 6). Intriguingly, immunoblotting revealed strong binding of dRpd3 to the 3MBT domains and weaker binding to the N-terminal part of dL(3)mbt. In contrast, no interaction was observed between the C-terminus of dL(3)mbt and dRpd3.

In conclusion, both the N-terminus half, as well as the 3MBT motif of dL(3)mbt, contribute to dRpd3 association. However, the 3MBT region seemed to be the major dRpd3 interaction domain in dL(3)mbt. A construct including only the three MBT modules (aa 787-1171) was sufficient to bind dRpd3.

### 4.1.2 dL(3)mbt is part of a novel multi-subunit complex

#### 4.1.2.1 The bulk of dL(3)mbt is separated from RBF2 in *Drosophila* cells

Interestingly, HDAC assays and immunoprecipitations revealed that dL(3)mbt is associated with dRpd3, a very abundant histone deacetylase that also interacts with many other transcriptional regulators, as for instance Groucho (Chen et al., 1999) and is a subunit of multiple chromatin-associated complexes, like dNuRD (Kunert et al., 2009), the SIN3–RPD3 complex (Pile and Wassarman, 2000) or RLAF (Moshkin et al., 2009). Therefore it was conceivable that the dL(3)mbt-dRpd3 interaction was part of an association of dL(3)mbt with a larger complex. An alternative possibility was that dL(3)mbt was a subunit of other protein complexes independent of the interaction with dRpd3.

In order to assess the existence and distribution of dL(3)mbt protein in complexes nuclear extract from Kc167 cells was fractionated over a Superose 6 gel filtration column (Figure 4.4). Fractions were probed in Western blot with specific antibodies directed against dL(3)mbt and Retinoblastoma-family protein 2 (RBF2). The latter is one of the two retinoblastoma protein homologues in *Drosophila* and a specific subunit

of the Myb-MuvB/dREAM complex (Lewis et al., 2004; Korenjak et al., 2004). The bulk of dL(3)mbt was detected in fractions 16 to 20 (Figure 4.4, upper panel) with an apparent molecular weight of close to 2 MDa. By contrast, the major RBF2 peak eluted in fractions 20 to 24 close to an apparent molecular weight of 670 kDa (Figure 4.4, lower panel), which is consistent with previously published data on the size of the Myb-MuvB/dREAM complex (Korenjak et al., 2004). Hence, in this fractionation the bulk of dL(3)mbt is separated from the Myb-MuvB complex. Strikingly, it elutes in one major peak, with a higher apparent molecular weight than Myb-MuvB. Nevertheless, dL(3)mbt Western blot signals are also observed in RBF2-containing fractions, in agreement with a sub-stoichiometric association of dL(3)mbt with Myb-MuvB, as suggested by Lewis and co-workers.

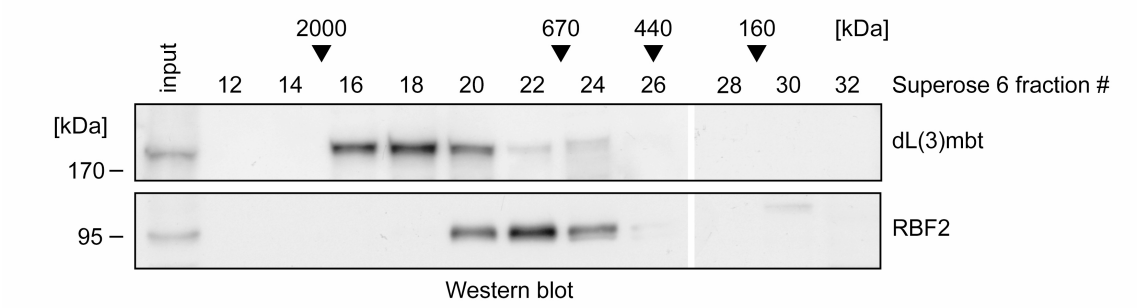


**Figure 4.4: The bulk of dL(3)mbt exists in a high molecular weight complex distinct from Myb-MuvB.** Nuclear extract from Kc167 cells was fractionated over a Superose 6 gel filtration column. Eluted fractions were analysed by Western blot for the presence of dL(3)mbt and RBF2 using antibodies as indicated. Fraction numbers and gel filtration molecular weight standards are denoted on top. Input: 5% of nuclear extract loaded on the column.

In summary, this supports the idea that dL(3)mbt is present in a so far uncharacterised high molecular weight complex, which is distinct from the Myb-MuvB complex.

#### 4.1.2.2 Recombinant FLAG-tagged dL(3)mbt incorporates into high molecular weight complexes

An unbiased approach to purify interaction partners of a protein of interest is to epitope-tag the polypeptide, express it in an appropriate cell/model system and subject it to immunoaffinity purification. To facilitate identification of unknown dL(3)mbt interacting proteins, the expression vector encoding N-terminally FLAG-tagged

dL(3)mbt under the control of the constitutive *actin 5C* promoter was used for stable expression in S2 cells (see Figure 4.1 A). Initially, to investigate the incorporation of recombinant FLAG-tagged dL(3)mbt into high molecular weight complexes, FLAG-dL(3)mbt was expressed by transient transfection into S2 cells and nuclear extract was fractionated over a Superose 6 gel filtration column (Figure 4.5). As a control, nuclear extract from untransfected cells, not expressing the FLAG-tagged protein, was also analysed by gel filtration.

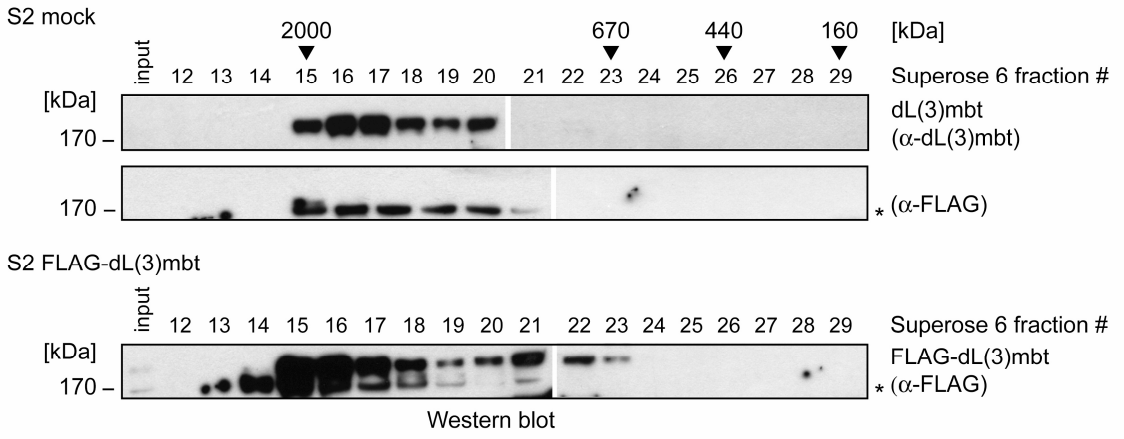


**Figure 4.5: Recombinant Flag-tagged dL(3)mbt integrates into high molecular weight complexes in S2 cells.** pPac-HA-FLAG-dL(3)mbt was transiently transfected into S2 cells. Nuclear extracts from S2 FLAG-dL(3)mbt (lower panel) and untransfected (mock, upper and middle panels) cells were fractionated over a Superose 6 gel filtration column. Eluted fractions were analysed by Western blot for the presence of endogenous dL(3)mbt (upper panel) and recombinant FLAG-tagged dL(3)mbt (middle and lower panels) using antibodies as indicated. Fraction numbers and gel filtration molecular weight standards are denoted on top. Input: 5% of nuclear extract loaded on the column. Cross-reacting proteins, detected by the FLAG antibody (mouse) are depicted with an asterisk.

Western blot analysis of the fractions using the dL(3)mbt antibody revealed that endogenous dL(3)mbt in S2 cells elutes in one major peak (Figure 4.5, upper panel, fractions 15 to 20) close to an apparent molecular weight of 2 MDa, in line with data obtained with Kc167 cell nuclear extract (Figure 4.4). Moreover, FLAG-tagged dL(3)mbt co-eluted in the same fractions as endogenous dL(3)mbt. Gel filtration analysis of FLAG-dL(3)mbt revealed a second peak in fraction 21, which is not apparent with endogenous protein. This could result from overexpression of FLAG-dL(3)mbt, upon which not all recombinant protein was incorporated into the major dL(3)mbt complex.

In conclusion, the gel filtration analysis suggests that recombinant FLAG-tagged dL(3)mbt incorporated into the same high molecular weight complex as endogenous dL(3)mbt. Therefore the cell line expressing FLAG-tagged dL(3)mbt (Figure 4.1 A) was a suitable tool to identify dL(3)mbt interacting partners.

#### 4.1.2.3 Identification of *Drosophila* L(3)mbt interacting protein 1 (dLint-1) as a novel interaction partner of dL(3)mbt

To scale up expression of FLAG-tagged dL(3)mbt for purification, the stable S2 cell line expressing FLAG-tagged dL(3)mbt was expanded (see Figure 4.1 A). Next, nuclear extract, obtained from this cell line, was subjected to FLAG affinity purification. In parallel, nuclear extract from cells not expressing FLAG-tagged dL(3)mbt, was processed as well. Aliquots of eluates obtained by FLAG-peptide competition were visualised by silver staining of an SDS-PAGE gel (Figure 4.6).

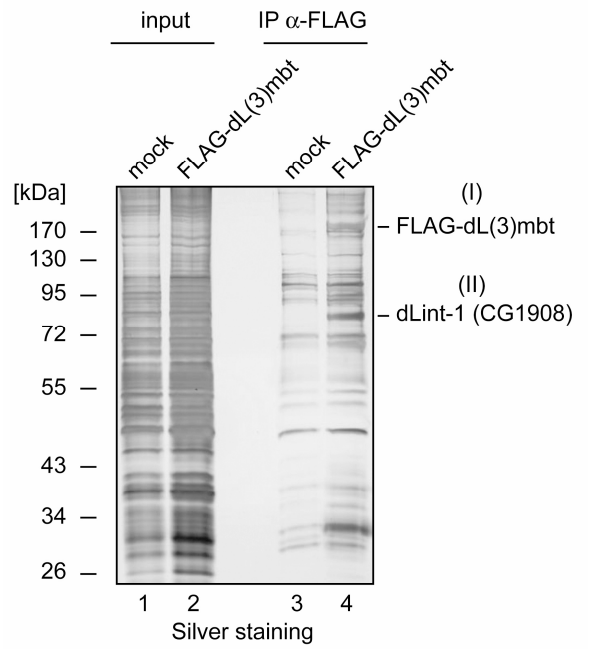


**Figure 4.6: dLint-1 (CG1908) co-purifies with FLAG-dL(3)mbt in FLAG affinity purification.** Nuclear extracts from control S2 cells (mock, lanes 1 and 3) and cells stably expressing FLAG-tagged dL(3)mbt (lanes 2 and 4) were subjected to FLAG affinity purification, elution with FLAG peptide (lanes 3 and 4), SDS-PAGE and silver staining. Input: 2 µg of nuclear extract (lanes 1 and 2). Proteins identified by mass spectrometry are denoted on the right (Table 4.1). IP: Immunoprecipitation.

Many polypeptides were recovered in both purifications (compare lanes 3 and 4), some of which appeared to be stained more intensively in the FLAG-dL(3)mbt purification. It seems likely, that a slightly higher input of FLAG-dL(3)mbt nuclear extract could account for this observation (compare lanes 1 and 2). Nevertheless, all polypeptides, which were present in both purifications (mock and FLAG-dL(3)mbt) were considered

to be contaminants, resulting from unspecific binding of proteins to α-FLAG agarose. This complication of unspecific binding was attributed to low expression levels of the recombinant FLAG-tagged protein.

Despite the high background caused by unspecific binding, two polypeptides were specifically enriched in the purification from FLAG-dL(3)mbt expressing cells, one with an apparent molecular weight higher than 170 kDa and one with approximately 85 kDa (Figure 4.6, compare lanes 3 and 4, polypeptides (I) and (II)). These polypeptides were excised from the gel and analysed by peptide mass fingerprinting. The larger polypeptide was identified as dL(3)mbt (see Figure 4.6 and Table 4.1). The 85 kDa polypeptide was identified as the gene product of *CG1908*, a protein of so far unknown function. In the following, the protein will be referred to as *Drosophila* L(3)mbt interacting protein 1 (dLint-1).

**Table 4.1: Peptide mass fingerprinting results from FLAG affinity purification of FLAG-dL(3)mbt.** Roman numerals denoting polypeptide bands refer to Figure 4.6. Mass spectrometry data are expressed as probability based molecular weight search (Mowse) scores, including the number of peptides, which matched the identified protein. Scores, greater than 60, are significant ($p<0.05$). Identified polypeptides are given with the according GI number in NCBI, the protein name, if available, the CG gene number, including the isoform and the corresponding organism. MW: molecular weight.

| Label | Probability based Mowse score | Number of peptides matched | Polypeptide identified | MW [kDa] |
|---|---|---|---|---|
| (I) | 184 | 26 | gi\|24650589, lethal (3) malignant brain tumour, CG5954-PA [*Drosophila melanogaster*] | 163.0 |
| (II) | 75 | 10 | gi\|18859817, CG1908-PA [*Drosophila melanogaster*] | 67.9 |

BLAST search identified homologues of dLint-1 in other *Drosophila* species, but not outside of the genus. Furthermore, conventional protein domain search tools failed to find conserved motifs within the dLint-1 amino acid sequence. Nevertheless, the C-terminus (amino acids 542 to 602) of dLint-1 is characterised by a cysteine/histidine-rich region, which contains a motif with similarity to the plant homeo domain (PHD) (R. Aasland, personal communication) (Figure 4.7).

Interestingly, PHD fingers are commonly found in nuclear proteins that play a role in chromatin regulation (Aasland et al., 1995). This PHD-like domain in dLint-1 has the typical Cys4HisCys3 (C4HC3) signature and the length (about 60 amino acids) in

common with canonical PHD fingers (Aasland et al., 1995; R. Aasland, personal communication). However, an aromatic residue, such as tryptophan, preceding the last cysteine pair that is conserved in classical PHD motifs (Bienz 2006) is missing. Moreover, the N-terminal part of the PHD-like domain contains a high density of charged residues, which is not typical for canonical PHD fingers. In summary, dLint-1 contains a domain that, despite some special features, shares significant similarities with PHD-fingers.

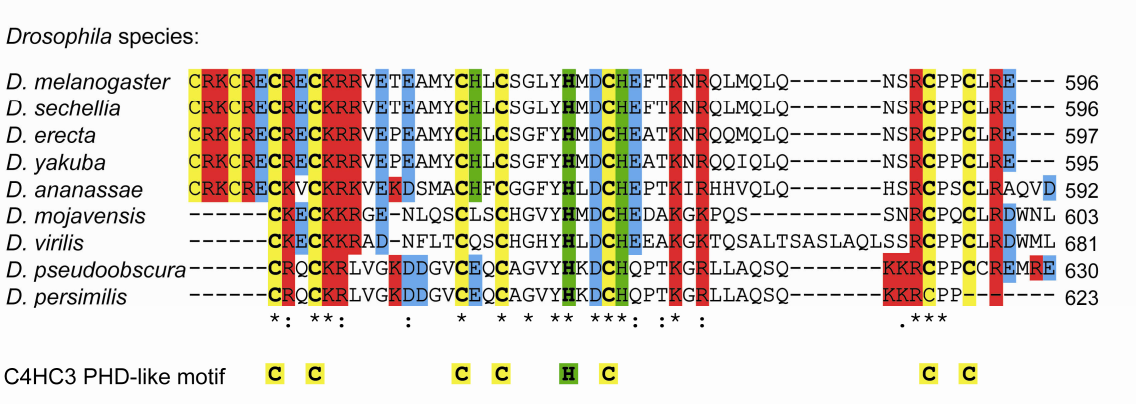


**Figure 4.7: Alignment of PHD-like motifs in *Drosophila* dLint-1 homologues.** Multiple sequence alignment of dLint-1 (CG1908) *Drosophila* homologues, generated with ClustalW2 (http://www.ebi.ac.uk/Tools/msa/clustalw2/) program. *Drosophila* species are denoted on the left. The C4HC3 PHD-like motif is written in bold and depicted below the alignment. Cys and His residues are colour-coded in yellow and green. Basic residues (Arg and Lys) are illustrated in red and acidic residues (Asp and Glu) in blue. Positions of amino acid residues (referring to the full length protein) of *D. melanogaster* and other *D.* species, are depicted on the right, respectively. Conservation of residues is displayed below the multiple alignment as follows: '*': Identical residues; ':': conserved substitutions; '.': semi-conserved substitutions.

#### 4.1.2.4 dL(3)mbt and dLint-1 interact in a robust manner

To verify the data of the α-FLAG affinity chromatography, in which dLint-1 was identified as a novel dL(3)mbt associating protein, the protein-protein interaction was assayed using several different approaches.

First, N-terminally FLAG-tagged dL(3)mbt, expressed in Sf9 insect cells using a recombinant baculovirus, was immobilised on α-FLAG agarose and incubated with *in vitro* translated, $^{35}$S-labelled dLint-1 (Figure 4.8 A). Autoradiography revealed that FLAG-dL(3)mbt bound dLint-1 very efficiently (upper panel), compared to the background resulting from unspecific binding of dLint-1 to the α-FLAG agarose (beads

control). In contrast, FLAG-dL(3)mbt failed to interact with *in vitro* translated Firefly-Luciferase confirming the specificity of the assay (lower panel).

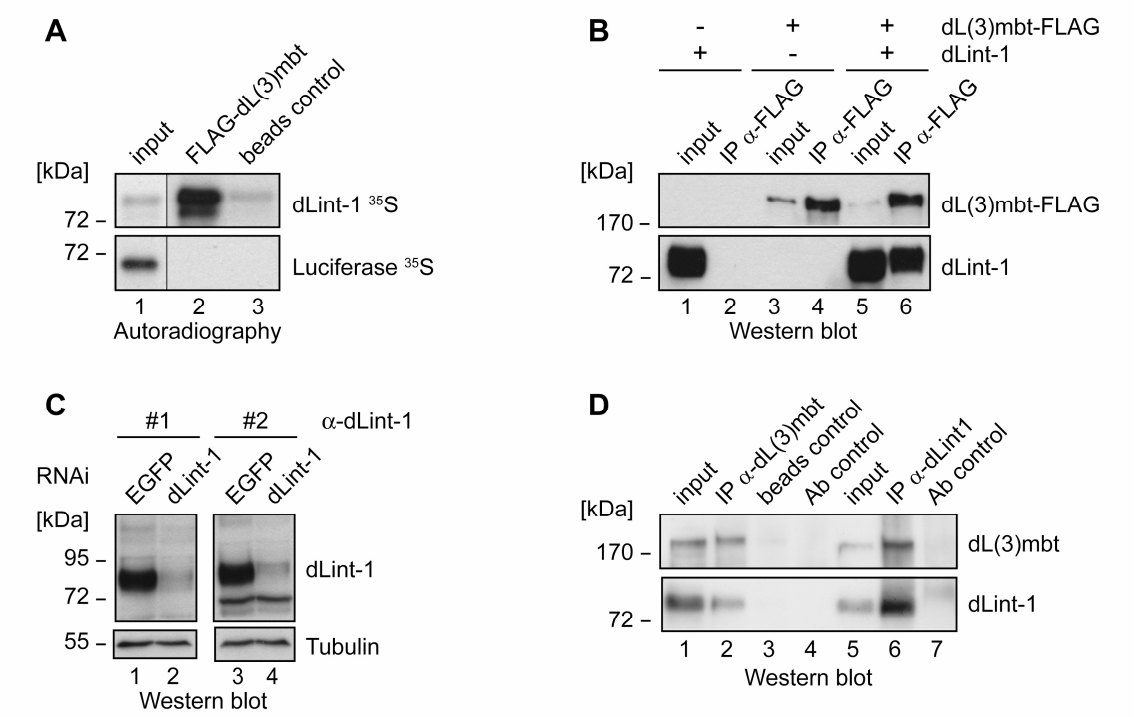


**Figure 4.8: dL(3)mbt and dLint-1 interact in a robust manner.** (A) *In vitro* translated, $^{35}$S-labelled dLint-1 (upper panel) or Luciferase (lower panel) were incubated with FLAG beads (beads control, lane 3) or FLAG beads loaded with baculoviral-expressed FLAG-dL(3)mbt (lane 2). Bound proteins were separated by SDS-PAGE and detected by auto-radiography. Input: 1% of *in vitro* translations (lanes 1). (B) Sf9 cells were co-infected with baculo-viruses expressing dL(3)mbt-FLAG or dLint-1 as indicated on top. Extracts from infected cells were immunoprecipitated with FLAG beads. Immunoprecipitates were subjected to Western blot using α-FLAG (rabbit) and α-Lint-1 antibody #1 (lanes 2, 4 and 6). Input: 5% of extracts (lanes 1, 3 and 5). (C) Specificity of dLint-1 antibodies. Nuclear extracts from cells treated with dsRNA directed against EGFP (lanes 1 and 3) and dLint-1 (lanes 2 and 4) were subjected to Western blot using dLint-1 #1 (left upper panel), dLint-1 #2 (right upper panel) and β-tubulin antibody (lower panels) as indicated. Detection of β-tubulin served as a loading control. (D) Nuclear extract from Kc167 cells was precipitated with ProtG beads loaded with dL(3)mbt antibody (lane 2), with dLint-1 antibody #2 (lane 6) or no antibody (beads control, lane 3). Immunoprecipitates were analysed by Western blot as indicated on the right. Ab control: dL(3)mbt- (lane 4) or dLint-1-specific (lane 7) antibody without extract. Input: 5% of nuclear extracts (lanes 1 and 5).

Next, Sf9 cells were co-infected with recombinant baculoviruses expressing C-terminally FLAG-tagged dL(3)mbt and untagged dLint-1. α-FLAG immunoaffinity purification of Sf9 whole cell extracts and Western blot analysis, demonstrated a strong interaction between both proteins (Figure 4.8 B, lane 6). As a control, dL(3)mbt-FLAG

and dLint-1 were also expressed individually and subjected to FLAG immunoprecipitation. However, in both controls no protein recognised by the dLint-1-specific antibody was recovered (compare lanes 2 and 4).

Up to that point, all binding assays were performed with overexpressed proteins. To rule out the possibility, that the interaction was driven by overexpression of proteins, it was indispensable to test for the interaction between endogenous dL(3)mbt and dLint-1.

For this purpose, two dLint-1-specific antibodies were generated. The specificity of these polyclonal antibodies was confirmed in Western blot, analysing nuclear extracts from Kc167 cells that were treated for 6 d with dsRNA directed against dLint-1 or EGFP as control (Figure 4.8 C). In line with the size of the 85 kDa band, which was identified as dLint-1 in peptide mass fingerprinting, both antibodies detected a protein between 72 and 95 kDa. Consistent with this protein being dLint-1, a strong decrease in signal intensity was observed after dLint-1 RNAi treatment (compare lanes 2 and 4 with lanes 1 and 3). Next, nuclear extract derived from Kc167 cells was immunoprecipitated both with dL(3)mbt- and dLint-1-specific antisera, respectively (Figure 4.8 D). In both cases endogenous dL(3)mbt and dLint-1 co-precipitated (compare lanes 2 and 6), whereas no dL(3)mbt and dLint-1 signals were detected in controls omitting either antibody (beads control, lane 3) or nuclear extract (antibody control, lanes 4 and 7). This result confirms that endogenous dL(3)mbt and dLint-1 interact *in vivo*.

To map the dLint-1 region required for binding to dL(3)mbt, immobilised GST-fusion proteins of full length dLint-1 and three deletion constructs (depicted in Figure 4.9 B) were incubated with recombinant baculoviral expressed dL(3)mbt-FLAG (Figure 4.9 A). This showed that the first N-terminal 301 residues of dLint-1 were required for binding to dL(3)mbt, whereas the C-terminal half of the protein (amino acids 302 to 602), including the Cys/His-rich PHD-like domain, was dispensable. The protein amounts of dLint-1-GST-fusions were controlled by Ponceau staining of the Western blot membrane (Figure 4.9 A, lower panel), demonstrating that the N-terminal dLint-1 construct was present in a lower protein concentration than the C-terminal constructs, but still capable of binding dL(3)mbt.

Taken together, the protein binding data strongly argue for a stable and presumably direct interaction between dL(3)mbt and dLint-1. Moreover, the dL(3)mbt interaction domain resides in the N-terminal half of the dLint-1 protein.

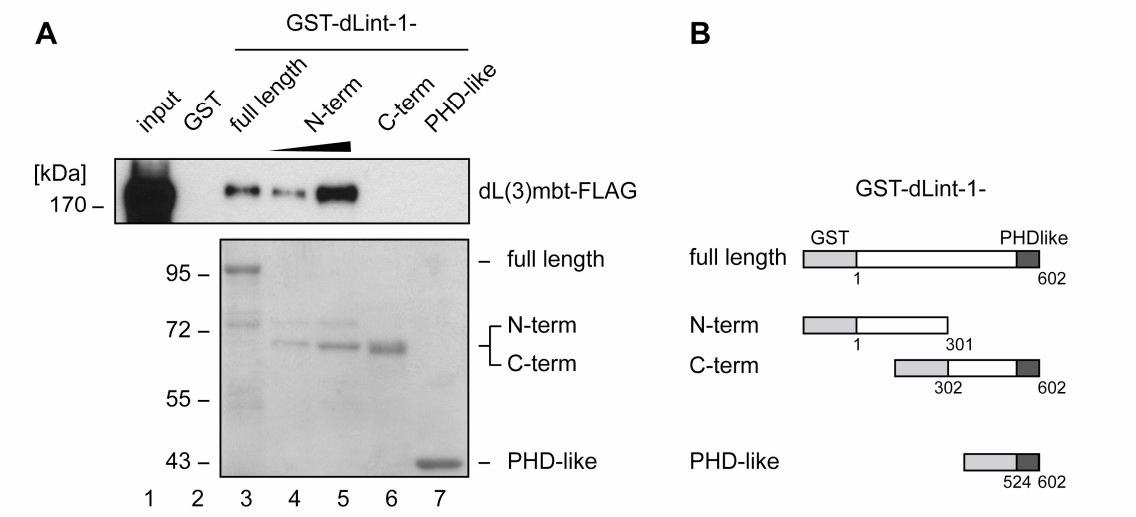


**Figure 4.9: The dL(3)mbt interaction domain of dLint-1 is located in the N-terminal half of the protein.** (A) Upper panel: GST and GST fusion proteins (lane 2: 4 µg GST; lane 3: 4 µg GST-dLint-1 full length; lane 4 and 5: 1 µg and 2 µg GST-dLint-1-N-term, respectively; lane 6: 4 µg GST-dLint-1-C-term; lane 7: 4 µg GST-dLint-1-PHD-like) as indicated on top were incubated with Sf9 extracts containing baculoviral expressed dL(3)mbt-FLAG. Bound proteins were analysed by Western blot using α-FLAG antibody. Input: 5% of Sf9 extract (lane 1). Lower panel: Ponceau-stained membrane of GST-dLint-1 fusion proteins used for binding experiment. (B) Scheme of GST-dLint-1 fusion proteins: The GST tag is depicted in grey, the PHD-like domain in black and the remaining dLint-1 protein in white. Numbers of amino acid residues are denoted below.

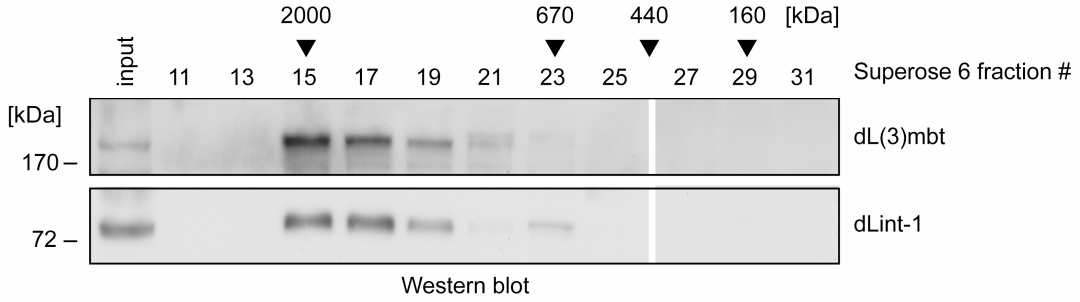


**Figure 4.10: dL(3)mbt and dLint-1 co-elute in gel filtration analysis.** Nuclear extract from Kc167 cells was fractionated over a Superose 6 column. Fractions were analysed by Western blotting using antibodies as indicated. Fraction numbers and gel filtration molecular weight standards are denoted on top. Input: 5% of extract loaded on the column.

Considering the robust association of dL(3)mbt and dLint-1, it seemed likely that dLint-1 is part of the high molecular weight complex, in which the bulk of dL(3)mbt resides. In order to address this issue, Kc167 nuclear extract was separated on a Superose 6 gel filtration column (Figure 4.10). Western blot analysis of the fractions suggested that the majority of dL(3)mbt and dLint-1 are associated in a large complex. A minor peak of

dLint-1 was observed in a fraction corresponding to a molecular weight of 670 kDa, indicating that a small amount of dLint-1 might exist as a smaller molecular weight species.

#### 4.1.2.5 Identification of dCoREST, dLsd1 and dRpd3 as additional dLint-1 associated proteins

The high apparent molecular weight of the dL(3)mbt- and dLint-1-containing complex, raised the question, whether dL(3)mbt is associated with additional polypeptides. In the α-FLAG immunoaffinity purification of FLAG-tagged dL(3)mbt high background binding of unspecific polypeptides prevented the identification of further interaction partners (Figure 4.6). As an alternative strategy to purify dL(3)mbt/dLint-1 associated proteins two S2 cells lines stably expressing FLAG-tagged dLint-1 (dLint-1-FLAG) were established. The two stable S2 cell lines varied in their dLint-1-FLAG expression levels (Figure 4.12 A, compare lanes 3 and 4 with 5 and 6).

To confirm the association of dLint-1-FLAG with high molecular weight complexes, nuclear extract from cell line #2 stably expressing recombinant dLint-1 was fractionated over a Superose 6 column (Figure 4.11). A proportion of FLAG-tagged dLint-1 was found to be present in high molecular weight fractions together with endogenous dL(3)mbt suggesting that the recombinant protein was incorporated into dL(3)mbt complexes. In addition, FLAG-tagged dLint-1 was also present in lower molecular weight fractions. dLint-1-FLAG, eluting in fractions with an apparent molecular weight smaller than 160 kDa (fractions 30 to 32), possibly corresponded to monomeric protein, which was not associated with complexes due to overexpression.

In agreement with the incorporation of recombinant dLint-1-FLAG into dL(3)mbt complexes, FLAG immunoprecipitation of nuclear extracts derived from the two cell lines co-precipitated endogenous dL(3)mbt (Figure 4.12 A, upper panel, compare lanes 4 and 6 with 2). Two chromatin-related proteins, the ATPase dMi-2 and the deacetylase dHDAC3, were not precipitated by FLAG immunoprecipitation (lower panels), demonstrating the specificity of the FLAG antibody and the dL(3)mbt-dLint-1 interaction.

Taken together, both gel filtration analysis and co-precipitations indicated that dLint-1-FLAG incorporated into dL(3)mbt complexes. Therefore the dLint-1-FLAG expressing cell line was a suitable tool to co-purify putative dLint-1/dL(3)mbt interacting proteins.

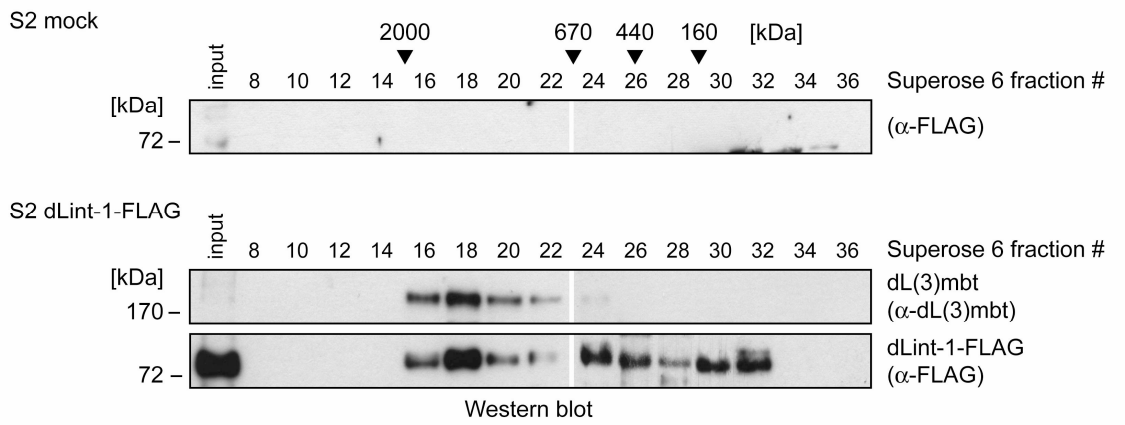


**Figure 4.11: Recombinant FLAG-tagged dLint-1 incorporates into high molecular weight complexes in S2 cells.** FLAG-tagged dLint-1 (encoded on pPac-dLint-1-FLAG) was stably transfected into S2 cells. Nuclear extracts from control S2 cells (mock, upper panel) and S2 dLint-1-FLAG cells (middle and lower panels) were fractionated over a Superose 6 gel filtration column. Eluted fractions were analysed by Western blot for the presence of endogenous dL(3)mbt (middle panel) and recombinant FLAG-tagged dLint-1 (upper and lower panels) using antibodies as indicated on the right. Fraction numbers and gel filtration molecular weight standards are denoted on top. Input: 5% of nuclear extract loaded.

To identify additional dLint-1/dL(3)mbt associated polypeptides, an FLAG immuno-affinity purification of FLAG-tagged dLint-1 from nuclear extract of the stable S2 cell line #2, characterised by a high expression level of the recombinant protein, was carried out (Figure 4.12 B). Several polypeptide bands were detected by silver staining that specifically co-purified with dLint-1-FLAG bound to α-FLAG resin, but not to resin incubated with mock nuclear extract (compare lanes 3 and 4). Input samples confirmed that equal amounts of both nuclear extracts have been applied (compare lanes 1 and 2).
In order to identify the corresponding proteins that co-purified with dLint-1-FLAG, bands were excised and subjected to peptide mass fingerprinting as before (compare Figure 4.12 and Table 4.2). For comparison, corresponding gel slices excised from the mock lane were analysed in parallel (data not shown).

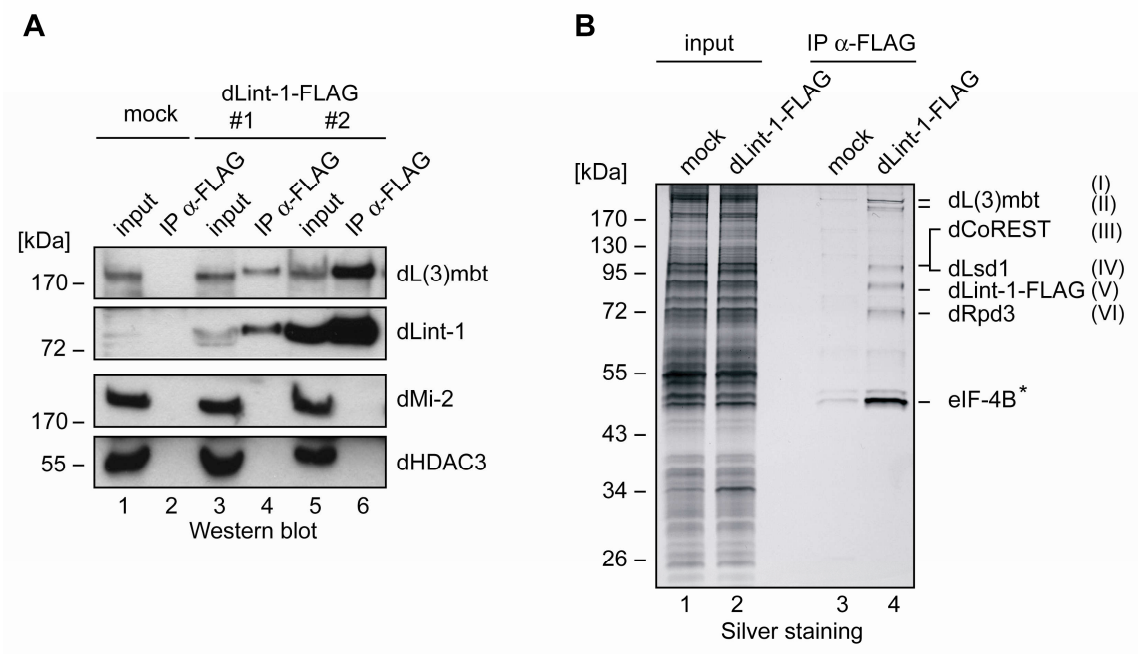


**Figure 4.12: Identification of dLint-1-FLAG associated proteins by FLAG affinity purification.** (A) Stable expression of FLAG-tagged dLint-1 in S2 cells. Nuclear extracts from control S2 cells (mock, lanes 1 and 2) and two S2 cell lines #1 and #2 stably expressing FLAG-tagged dLint-1 (lanes 3, 4, 5 and 6) were immunoprecipitated with α-FLAG agarose (lanes 2, 4 and 6). Immunoprecipitates were analysed by Western blotting with antibodies as indicated. Input: 5% of nuclear extracts (lanes 1, 2 and 3). (B) FLAG affinity purification. Nuclear extracts from control S2 cells (mock, lanes 1 and 3) and S2 cells stably expressing FLAG-tagged dLint-1 (cell line #2) (lanes 2 and 4) were subjected to FLAG affinity purification, elution with FLAG peptide (lanes 3 and 4), SDS-PAGE and silver staining. Input: 2 µg of nuclear extracts (lanes 1 and 2). Proteins identified by mass spectrometry are denoted on the right (see Table 4.2). The asterisk marks unspecifically bound protein. IP: immunoprecipitation.

Besides dLint-1 (V), polypeptides I and II were identified as dL(3)mbt (Figure 4.12 and Table 4.2). One is likely to correspond to the full length protein and the second one possibly originated from degradation, which occurred during the purification procedure. In addition, the histone deacetylase dRpd3 (VI), the corepressor dCoREST (III), and the histone demethylase dLsd1 (IV), were identified as dLint-1 associated polypeptides. Notably, the latter two were identified from the same gel slice as the top two specific hits in mass spectrometry. The intensively stained polypeptide band with a size between 43 kDa and 55 kDa was identified as the translation initiation factor eIF-4B, which was also bound to the resin of the mock FLAG purification, albeit at lower levels. Translation elongation and initiation factors belong to a class of proteins that commonly bind non-specifically to Sepharose/agarose beads (Trinkle-Mulcahy et al., 2008). Thus, eIF-4B was considered to be a cytoplasmic contaminant and not further investigated.

**Table 4.2: Peptide mass fingerprinting results from α-FLAG affinity purification of dLint-1-FLAG.** Roman numerals denoting the polypeptide bands refer to Figure 4.12 B. Mass spectrometry data are expressed as probability based molecular weight search (Mowse) scores, including the number of peptides, which matched the identified protein. Scores, greater than 32, are significant ($p<0.05$). Identified polypeptides are stated with the according GI number in NCBI, the protein name, the CG gene number, including the isoform and the corresponding organism. MW: molecular weight.

| Label | Probability based Mowse score | Number of peptides matched | Polypeptide identified | MW [kDa] |
|---|---|---|---|---|
| (I) | 6437 | 374 | gi\|3421009, tumour supressor [*Drosophila melanogaster*] | 163.0 |
| (II) | 3061 | 229 | gi\|3421009, tumour supressor [*Drosophila melanogaster*] | 163.0 |
| (III) | 3847 | 214 | gi\|62473829, CoREST, CG33525-PF [*Drosophila melanogaster*] | 62.7 |
| (IV) | 814 | 78 | gi\|21356479, Histone demethylase, CG17149-PA [*Drosophila melanogaster*] | 98.4 |
| (V) | 8391 | 466 | gi\|18859817, CG1908, CG1908-PA [*Drosophila melanogaster*] | 67.9 |
| (VI) | 4831 | 356 | gi\|24657891, Rpd3, CG7471-PA [*Drosophila melanogaster*] | 58.3 |

#### 4.1.2.6 dLint-1 associated proteins co-immunoprecipitate both in *Drosophila* embryonic cell lines and embryos

The FLAG immunoaffinity purification of dLint-1-FLAG led to the identification of three additional polypeptides that are associated with dLint-1 apart from dL(3)mbt. To validate the data obtained by mass spectrometry and to verify the complex composition, specific antibodies directed against dCoREST (Dallman et al., 2004) and dLsd1 (also referred to as Su(var)3-3) (Rudolph et al., 2007) were obtained. dL(3)mbt (this study, Scharf et al., 2009), dRpd3 (Brehm et al., 2000) and dLint-1 antibodies (this study) were available in the lab.

First, FLAG immunoprecipitations were carried out from nuclear extract derived from the stable S2 cell line (#2) expressing dLint-1-FLAG and subjected to Western blot (Figure 4.13). In agreement with mass spectrometry results, dL(3)mbt, dCoREST, dLsd1 and dRpd3 were detected in precipitates from FLAG-tagged dLint-1, but not from control extract (mock, compare lane 4 with lane 2). As an additional control for the specificity of this experiment FLAG immunoprecipitates were subjected to Western

blot using an HP1α-specific antibody and as a result no co-precipitation with dLint-1-FLAG was observed. The dCoREST protein exists in three splice variants, a small (S), a medium-sized (M) and a large (L) isoform, which will be referred to as dCoREST-S, dCoREST-M and dCoREST-L from hereon. The antibody used in this study recognises two of them, namely dCoREST-M and dCoREST-L, which exhibit the same domain composition, but differ in the length of the domain separating the two SANT domains (Dallman et al., 2004). The Western blot analysis clearly revealed that FLAG-tagged dLint-1 preferentially co-precipitated dCoREST-M (Figure 4.13), which was also the isoform identified by mass spectrometry. Moreover, Western blot analysis illustrated that the dCoREST-M splice variant and dLsd1 migrate, despite their different predicted molecular weights, at the same height upon SDS-PAGE. This is consistent with the fact that dLsd1 and dCoREST were identified by mass spectrometry from the same gel slice (compare Figure 4.12 and Table 4.2).

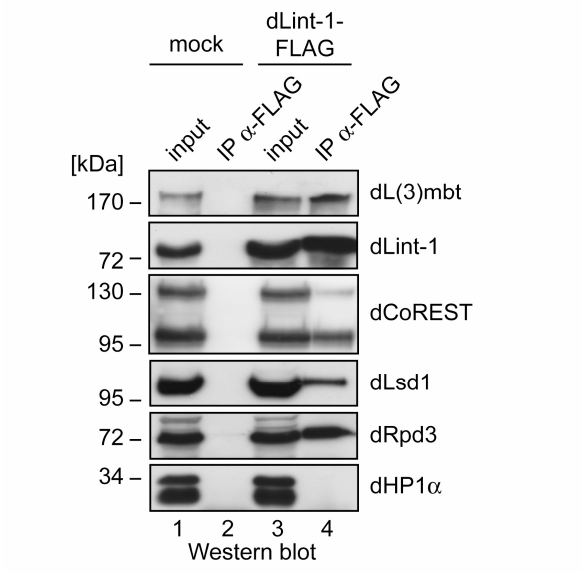


**Figure 4.13: Recombinant dLint-1-FLAG co-immunoprecipitated in addition to dL(3)mbt, dCoREST, dLsd1 and dRpd3.** Nuclear extracts from control S2 cells (mock, lanes 1 and 2) and S2 cells stably expressing FLAG-tagged dLint-1 (lanes 3 and 4) were precipitated with α-FLAG agarose. Immuno-precipitates were analysed by Western blot using antibodies as indicated on the right (lanes 2 and 4). Input: 5% of nuclear extracts (lanes 1 and 3).

In conclusion, the results obtained by FLAG affinity purification and subsequent peptide mass fingerprinting could be evidently confirmed by Western blot analysis, showing that immunoprecipitation of FLAG-tagged dLint-1 co-precipitated apart from dL(3)mbt also specifically dRpd3, dCoREST and dLsd1.

The association of dCoREST, dLsd1 and dRpd3 with dLint-1 was found after overexpression of a FLAG-tagged version of recombinant dLint-1 protein. To ensure that also the endogenous proteins interact with each other, nuclear extracts from Kc167

cells (Figure 4.14 A) and 0-12 hr old *Drosophila* embryos (Figure 4.14 B) were precipitated with dLint-1 and dCoREST-specific antisera.

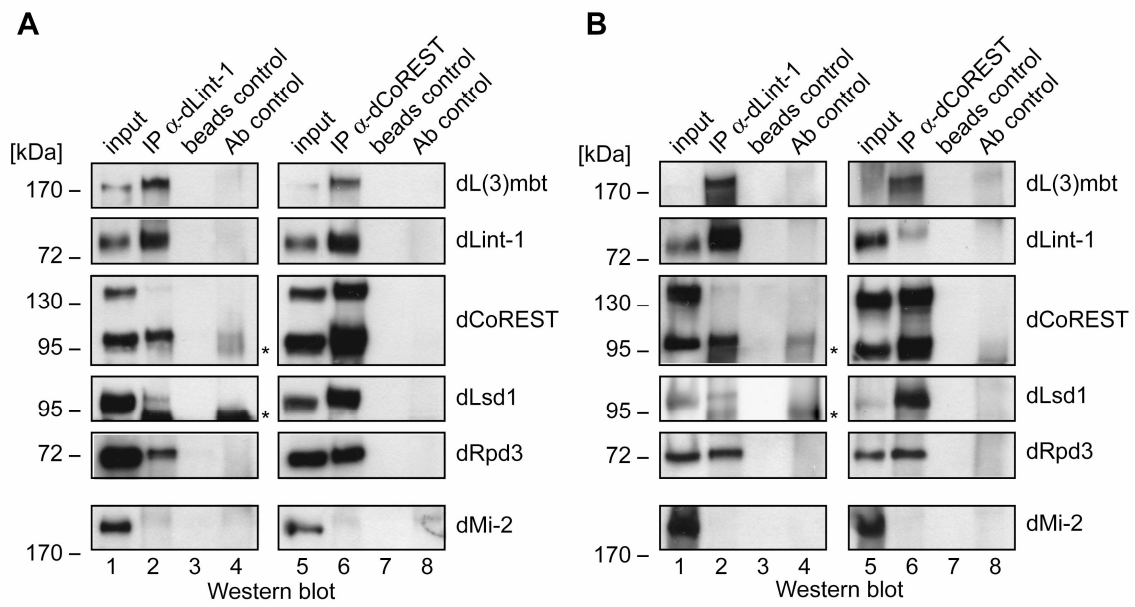


**Figure 4.14: Endogenous dLint-1 and dCoREST interact and co-immunoprecipitate dL(3)mbt, dRpd3 as well as dLsd1 in Kc167 cells and *Drosophila* embryos.** Nuclear extracts from Kc167 cells (A) and 0-12 hr old *Drosophila* embryos (B) were precipitated with ProtG beads loaded with dLint-1 antibody (lanes 2), with dCoREST antibody (lanes 6) or no antibody (beads control, lanes 3 and 7). Immunoprecipitates were analysed by Western blot as indicated on the right. Ab controls: contained dLint-1- (lanes 4) or dCoREST-specific (lanes 8) antibody, respectively. Input: 5% (lanes 1 and 5) of nuclear extracts. The asterisks mark signals that derive from unspecific antibody cross-reactions.

Indeed, both dLint-1- and dCoREST-specific antibodies co-precipitated all five proteins efficiently (Figure 4.14, compare lanes 2 and 6), compared to control precipitations, omitting either antibody (beads controls, lanes 3 and 7) or nuclear extract (antibody controls, lanes 4 and 8). This was the case not only for extract from embryonic Kc167 cells (Figure 4.14 A), but also for extract obtained from 0-12 hr old embryos (Figure 4.14 B), supporting the existence of these protein interactions *in vivo* in the *Drosophila* embryo.

The unrelated, highly abundant chromatin remodeler dMi-2 did not bind to either dLint-1 or dCoREST antibody, demonstrating the specificity of co-immunoprecipitations. In line with results obtained by FLAG immunoprecipitation (Figure 4.13), dLint-1 precipitated preferentially the dCoREST-M splice variant (lanes 2). In dLint-1 immuno-precipitations only a small percentage of dLsd1 appeared to precipitate (lanes 2). In

contrast, the dCoREST antibody, which recognised both splice variants (M and L), precipitated significantly more dLsd1 (lanes 6), while the dLint-1 signal was equal (Figure 4.14 A, lane 6) or even weaker (Figure 4.14 B, lane 6) compared with dLint-1 precipitates (lanes 2). This observation might imply the interaction of dCoREST and dLsd1 in other complexes independent of dLint-1/dL(3)mbt.

Taken together, immunoprecipitations clearly showed that all five proteins, which were identified in FLAG affinity immunopurification, co-precipitated with either dLint-1 or dCoREST on an endogenous level. This and the fact that all dLint-1 co-purifying proteins were identified with very high Mowse scores by mass spectrometry analysis (Table 4.2) strongly suggest that these proteins form stable protein complexes in *Drosophila*.

#### 4.1.2.7 dLint-1 interacting proteins co-elute in gel filtration analysis

The interaction of dLint-1 with dL(3)mbt, dCoREST, dLsd1 and dRpd3, documented extensively by immunoprecipitation experiments (Figures 4.13 and 4.14), supported the idea that these proteins are present in stable protein complexes. This hypothesis predicts that complex subunits co-elute during gel filtration. To test this hypothesis, nuclear extract from Kc167 cells was fractionated by gel filtration on a Superose 6 column (Figure 4.15) to separate protein complexes according to their molecular weight and shape and analysed by Western blot.

In line with previous results (Figure 4.10), the bulk of dL(3)mbt and dLint-1 eluted in a common peak, close to 2 MDa. However, a minor fraction of dLint-1 eluted at 670 kDa and below, indicating the association with other complexes aside from dL(3)mbt-containing ones. On the contrary to dL(3)mbt and dLint-1, Western blot analysis of gel filtration fractions using antibodies directed against dCoREST, dLsd1 and dRpd3 displayed more complex elution profiles, suggesting their presence in several independent complexes. Consistent with this observation dRpd3 has been shown to be part of multiple other chromatin-associated protein complexes, such as dNuRD (Kunert et al., 2009), SIN3–RPD3 (Pile and Wassarman, 2000) and ESC (Tie et al., 2001). In addition, gel filtration analysis of *Drosophila* embryo extract indicated, that dLsd1 also exists in numerous complexes (T. Rudolph, personal communication). Nevertheless, all three proteins were present in dL(3)mbt- and dLint-1-containing

fractions (compare fractions 15 to 19). However, while the peak fraction of dL(3)mbt and dLint-1 appeared to be in fraction 17, dLsd1 revealed a peak in fraction 15 and signal intensity decreased severely in fraction 17, arguing against their presence in the same complex. In case of dRpd3 no strong conclusions can be drawn, since the histone deacetylase was present in equal amounts in fractions 15 to 21. In contrast to this the dCoREST-M isoform, which was shown to preferentially bind to dLint-1 (Figures 4.13 and 4.14), co-eluted in fractions 15 to 19 with an identical profile as dL(3)mbt and dLint-1. By contrast these fractions contained only a small proportion of the dCoREST-L isoform present in the nuclear extract, which reveals rather a peak in the first protein-containing fraction similar to dLsd1 (fraction 17). These results provide further evidence that at least dL(3)mbt, dLint-1 and dCoREST are present in a common multi-subunit complex.

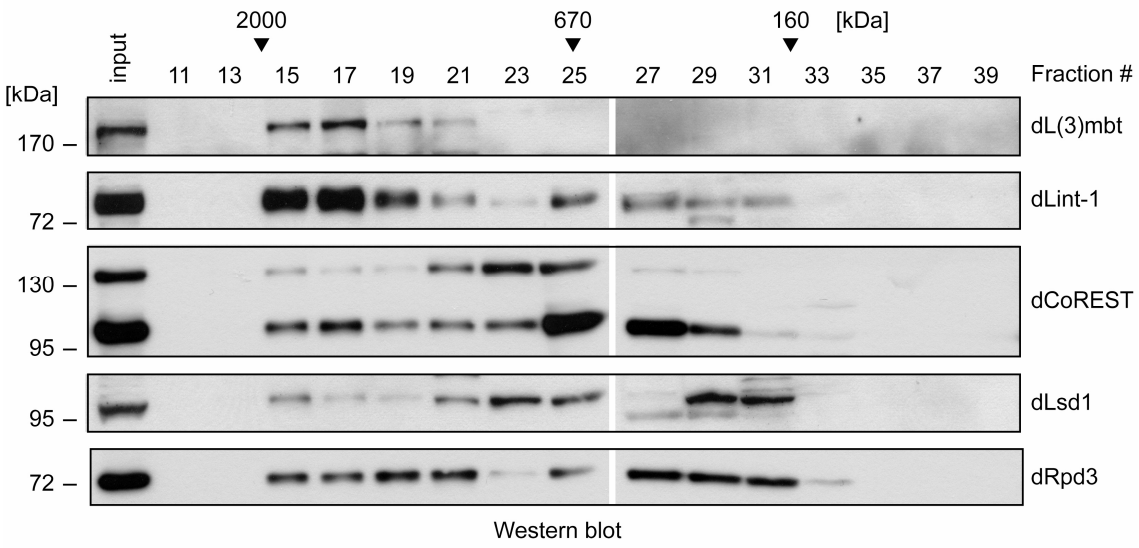


**Figure 4.15: dLint-1 interacting partners co-elute during gel filtration.** Nuclear extract from Kc167 cells was fractionated over a Superose 6 column. Fractions were analysed by Western blot as indicated on the right. Fraction numbers and molecular weight standards are denoted on top. Input: 5% of extract loaded on the column.

In order to assess more directly if dCoREST and dLsd1 are specifically associated with dL(3)mbt and dLint-1, Kc167 nuclear extract depleted of dL(3)mbt and dLint-1 by dL(3)mbt RNAi (see Figure 4.22 A) was separated by gel filtration (Figure 4.16).
Comparison of the input signals of dCoREST (panels 5 and 6) and dLsd1 (panels 7 and 8) protein in EGFP and dL(3)mbt RNAi-treated cells, revealed that protein levels were not affected by co-depletion of dL(3)mbt (compare panels 1 and 2) and dLint-1

(compare panels 3 and 4). However, the knockdown of dL(3)mbt and dLint-1 resulted in a pronounced shift of the dCoREST-M isoform peak (fraction 17, panel 5) from high molecular weight fractions to lower molecular weight fractions (compare panels 5 and 6, fractions 15 to 19). On the contrary, the dCoREST-L splice variant was still detectable in high molecular weight fractions after dL(3)mbt/dLint-1 co-depletion. Moreover the elution profile of dLsd1 remained unchanged upon RNAi treatment directed against dL(3)mbt compared to the EGFP control (compare panels 7 and 8). On first inspection the profiles of dRpd3 seemed to largely overlap in the presence and absence of dL(3)mbt/dLint-1 (compare panels 9 and 10). A closer look though revealed a shift of a dRpd3 portion to lower molecular weight fractions. While the peak of dRpd3 in EGFP dsRNA treated Kc167 cells in high molecular weight fractions resided in fraction 17 along with dL(3)mbt and dLint-1, the peak fraction in dL(3)mbt dsRNA treated cells is in fraction 19. This might indicate that dL(3)mbt/dLint-1-associated dRpd3 is incorporated in other complexes with lower molecular weight. Additionally as a control the analysis of an independent chromatin-related protein dMi-2 did not show a change in its elution profile (compare panels 11 and 12).

Taken together, these results support the idea that the dCoREST-M isoform, present in high molecular weight fractions, is stably associated with the dL(3)mbt/dLint-1 complex and that this complex disassembles upon dL(3)mbt and dLint-1 depletion. However, gel filtration analyses suggest that dLsd1 is not stably interacting with the dL(3)mbt/dLint-1 complex or that only sub-stoichiometric amounts are associated with the complex, which co-elute with other high molecular weight dLsd1 complexes in fractions 15 to 19. The results concerning dRpd3 are consistent with its presence in a dL(3)mbt/dLint-1 complex. However, to draw a substantive conclusion from gel filtration experiments is difficult, since dRpd3 is existent in numerous other multi-subunit complexes.

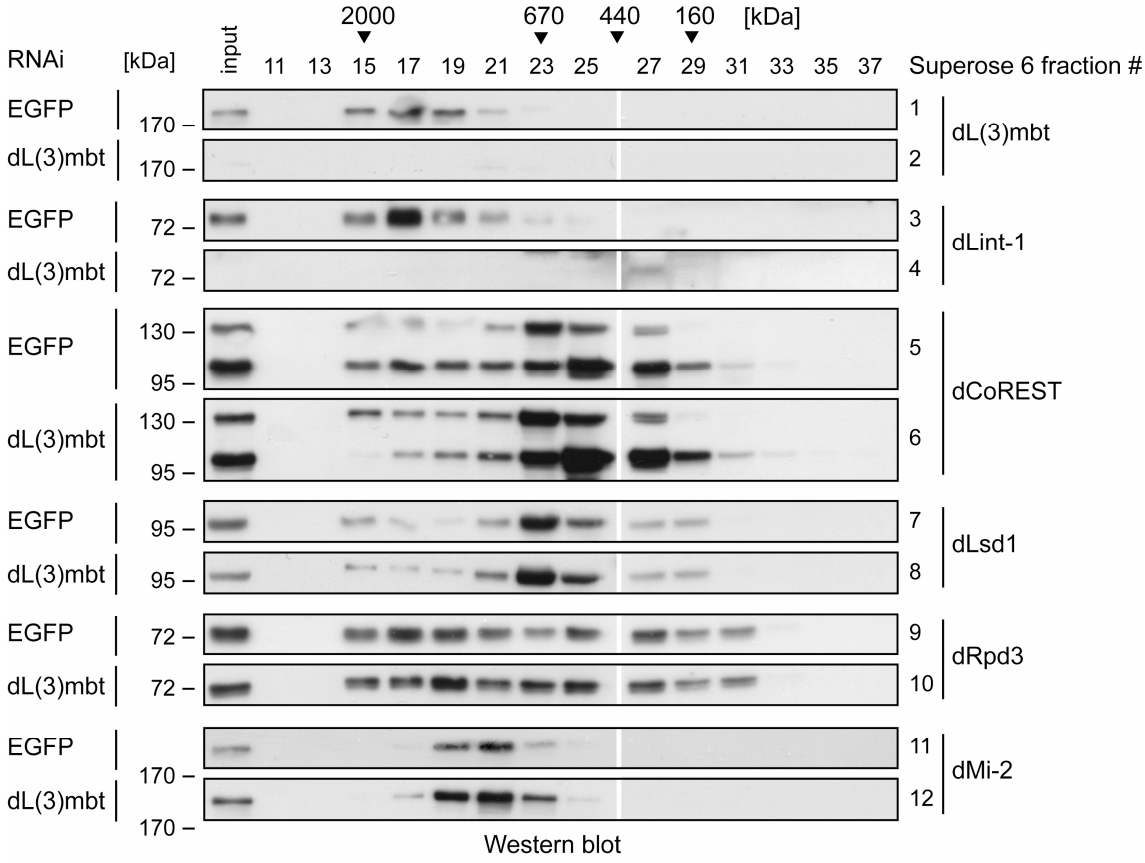


**Figure 4.16: Depletion of dL(3)mbt and dLint-1 results in a loss of dCoREST protein from high molecular weight fractions.** Nuclear extracts from Kc167 cells, treated with dsRNA directed against EGFP (panels 1, 3, 5, 7, 9 and 11) or dL(3)mbt (panels 2, 4, 6, 8, 10 and 12) were separated over a Superose 6 column and fractions were analysed by Western blot using dL(3)mbt (panels 1 and 2), dLint-1 (panels 3 and 4), dCoREST (panels 5 and 6), dLsd1 (panels 7 and 8), dRpd3 (panels 9 and 10) and dMi-2 (panels 11 and 12) antibodies as denoted on the right. Fraction numbers and molecular weight standards are shown on top. Input: 5% of extract loaded on the column. This experiment was designed by me and carried out under my supervision by M. Groh during an internship in the lab of Prof. A. Brehm.

#### 4.1.2.8 LINT is distinct from other dLint-1-, dCoREST- and dLsd1-containing complexes

Although dLsd1 co-immunoprecipitates with recombinant FLAG-tagged, as well as with endogenous Lint-1, gel filtration analyses of Kc167 nuclear extract imply that dLsd1 might not be stably associated with the dL(3)mbt-dLint-1-dCoREST complex. This is somewhat surprising, since in human CoREST and LSD1 have been found to co-exist in protein complexes in several purifications (Hakimi et al., 2003; Lee et al., 2005; Shi et al., 2005; You et al., 2001).

To gain a deeper insight into the composition of dL(3)mbt and dLint-1-containing complexes, Kc167 nuclear extract was subjected to classical sequential ion exchange chromatography (Figure 4.17 A).

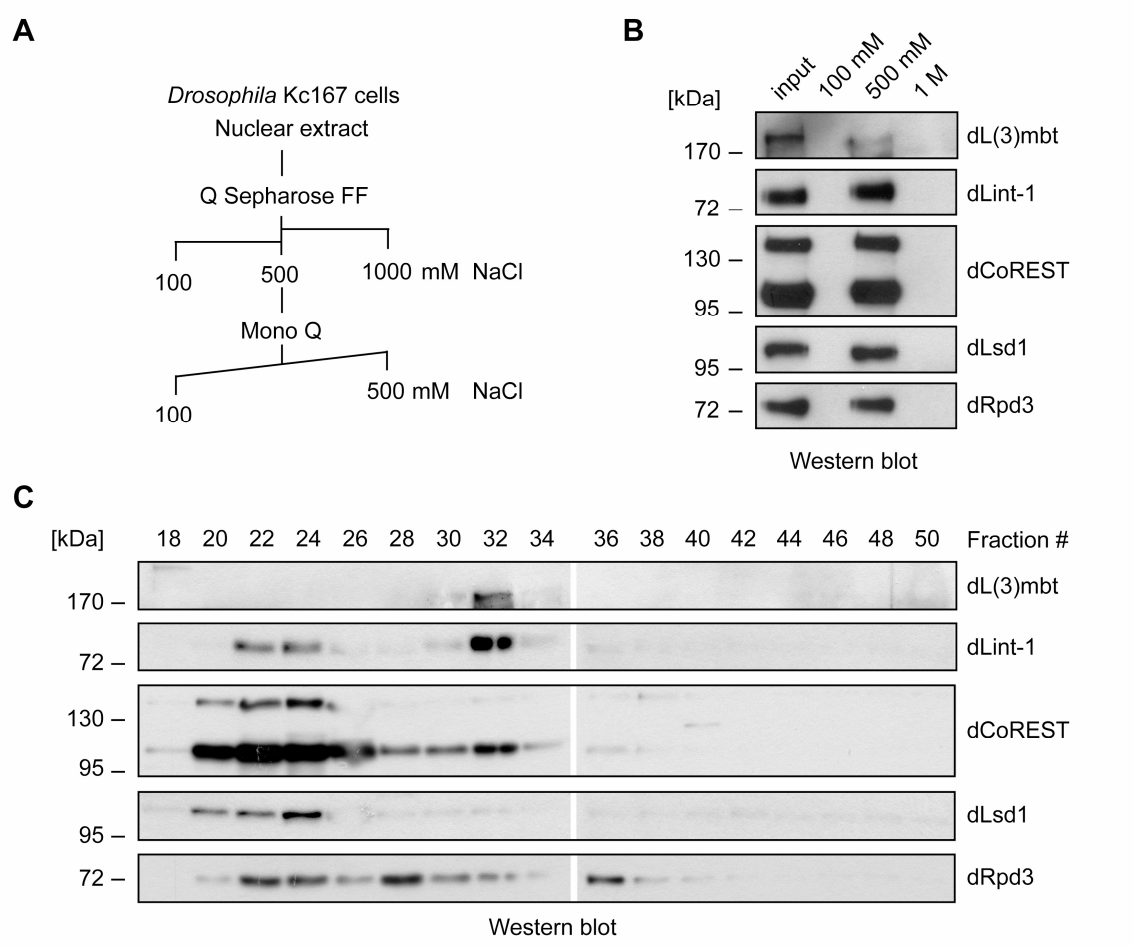


**Figure 4.17: The LINT core subunits dL(3)mbt, dLint-1 and dCoREST co-fractionate during ion exchange chromatography.** (A) Purification scheme: Nuclear extract from Kc167 cells was applied to sequential ion exchange chromatography. Extract was bound to a Q Sepharose anion exchange column in the presence of 100 mM salt (NaCl) and eluted stepwise with 500 mM and 1 M NaCl. The 500 mM salt eluate was applied to anion exchange chromatography using a Mono Q column and eluted gradually with 100 to 500 mM NaCl (fractions 1 to 50). Q Sepharose (B) and Mono Q (C) fractions were analysed by Western blot as indicated on the right. Salt concentrations (B) and fraction numbers (C) are denoted on top, respectively.

First, the nuclear extract was pre-fractionated in a first step using the anion exchange column Q Sepharose. As revealed by Western blot analysis (Figure 4.17 B) the proteins of interest eluted all at 500 mM NaCl and were therefore separated from proteins in the flow trough (100 mM) and from proteins eluting at 1 M NaCl. Moreover, this procedure removes nucleic acids present in the nuclear extract, since they bind strongly to the

anion exchange column due to their negative charge and are only eluted with 1 M salt. Second, the 500 mM Q Sepharose peak was fractionated over a Mono Q anion exchange column, which provides protein separation with a high resolution. For elution a salt gradient ranging from 100 to 500 mM (fractions 1 to 50) was applied. Signals specific for dL(3)mbt, dLint-1, dCoREST, dLsd1 and dRpd3 were only detected in fractions above 250 mM (Figure 4.17 C and data not shown). As judged by Western blot analysis, dL(3)mbt eluted in a single peak in fraction 32 together with dLint-1 and the dCoREST-M isoform at approximately 360 mM salt. The dRpd3 profile, however, is not informative. Although fraction 32 contained dRpd3 the signal did not coincide with a peak of dRpd3. Interestingly, the bulk of dLsd1 was separated from dL(3)mbt, eluting in fractions 22 to 24 along with a minor fraction of dLint-1, both splice variants of dCoREST (-M and -L) and dRpd3.

In summary, gel filtration and ion exchange chromatography experiments identified at least two dLint-1 complexes, one of which contains dCoREST and the bulk of dL(3)mbt. This novel three subunit complex will be referred to as the LINT complex from hereon (Figure 4.18). Moreover, ion exchange chromatography analysis along with results from immunoprecipitations suggests that dLint-1 resides in other complexes together with the histone demethylase dLsd1 and the histone deacetylase dRpd3.

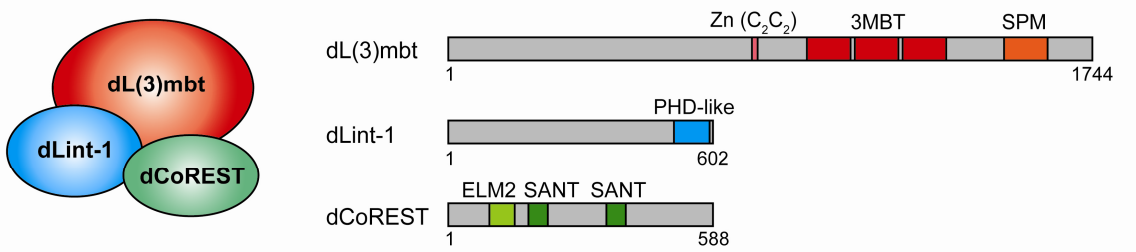


**Figure 4.18: LINT core complex composition.** Left panel: Schematic depiction of the LINT complex. Right panel: Schematic representation of the LINT subunits, depicting their domain structure. Top-down: dL(3)mbt, dLint-1, dCoREST-M. Protein sizes, in terms of amino acid residues, are denoted below the corresponding proteins.

#### 4.1.2.9 The LINT complex exists in the *Drosophila* larval brain

Up to this point biochemical data, identifying the LINT complex, had been obtained using extracts from *Drosophila* cell lines as a source, except for immunoprecipitations (α-dLint-1 and α-dCoREST) of endogenous proteins that have been also confirmed using *Drosophila* embryo extracts. Thus, it was important to further ensure that the LINT complex exists *in vivo* in the developing fly. A loss of function mutation of the *l(3)mbt* gene leads to the development of a malignant tumour in the brain of *Drosophila* larvae (Gateff et al., 1993; Wismar et al., 1995; Janic et al., 2010), uncovering the larval brain as a biological relevant tissue of dL(3)mbt protein function. Therefore, protein extracts were prepared from whole brains that were dissected from third instar larvae (Figure 4.19).

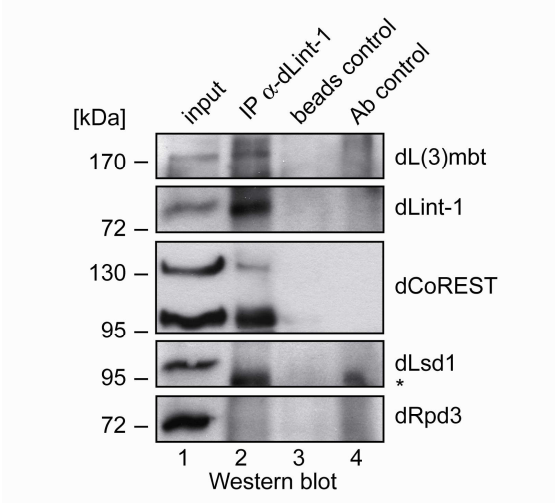


**Figure 4.19: The LINT core subunits dL(3)mbt, dLint-1 and dCoREST interact in third instar larval brain tissue.** Protein extracts from larval brains were precipitated with ProtG beads loaded with dLint-1 antibody (lane 2) or no antibody (beads control, lane 3). Ab control: contained dLint-1 antibody (lane 4). Immunoprecipitates were analysed by Western blot as indicated on the right. Input: 10% of brain extract (lane 1). The asterisk denotes a signal that derives from an un-specific antibody cross-reaction.

The extracts were imunoprecipitated using dLint-1 antibody and tested for co-immunoprecipitation of dL(3)mbt, dCoREST, dRpd3 and dLsd1 (Figure 4.19). In agreement with the LINT complex existing in the larval brain both dL(3)mbt and dCoREST co-precipitated with dLint-1 (lane 2). In contrast, dLsd1 and dRpd3 are not detected in the α-dLint-1 precipitate, despite robust input signals for both proteins, demonstrating that they are expressed in this tissue (compare lanes 1 and 2). In conclusion, the LINT complex exists in larval brain tissue and comprises the three core subunits dL(3)mbt, dLint-1 and dCoREST.

## 4.2 Identification of LINT complex target genes

Remarkably, the LINT complex contains with dL(3)mbt and dCoREST two known chromatin-regulating proteins, both exhibiting motifs, MBT and SANT domains, respectively, that have the potential to bind to histone tails (Bonasio et al., 2010; de la Cruz et al., 2004). In addition dL(3)mbt and dCoREST have known functions in transcriptional repression (Dallman et al., 2004; Lewis et al., 2004; Georlette et al., 2007). Therefore it was prompting to investigate the chromatin-associated role of the LINT complex in regulation of transcription.

### 4.2.1 dL(3)mbt and dLint-1 co-localise on many sites in the *Drosophila* genome

A special tool that is available in *Drosophila* third instar larvae, in order to investigate the localisation of chromatin binding proteins *in vivo* on a genome-wide level, is indirect immunofluorescent labelling of polytene chromosomes (Schwartz et al., 2004). During the third instar larval stage the genome of salivary gland cells undergoes repeated rounds of DNA replication without cell division (called endoreplication). A consequence of this is the production of giant polytene chromosomes that consist of up to thousand sister chromatids that remain synapsed. The centromeric regions of all chromosomes stay bundled together and form the so called chromocentre.

As a first step towards understanding whether the LINT complex that was purified from soluble Kc167 nuclear extract associates with chromatin *in vivo*, polytene chromosomes from $w^{1118}$ larvae were stained with dL(3)mbt and dLint-1 antibodies. However, no signals for endogenous dL(3)mbt above background levels could be detected with the available antibodies (Figure 4.20 B, upper panels).

Nevertheless, to investigate dL(3)mbt binding to chromatin despite this, a transgenic fly carrying an inducible UAS-dL(3)mbt transgene was generated using a germline-specific ϕC31 integrase-based integration system (Bischof et al., 2007). In this system, the expression of the transgene is regulated by an upstream activating sequence (UAS) element containing GAL4 binding sites. To induce transgene expression, flies carrying the UAS-transgene are mated to flies, which express the GAL4 transcription factor in a specific pattern (GAL4-driver strain) (Duffy, 2002). The progeny from these crosses express the UAS-dependent transgene in a transcriptional pattern that corresponds to the GAL4 expression pattern of the respective driver strain.

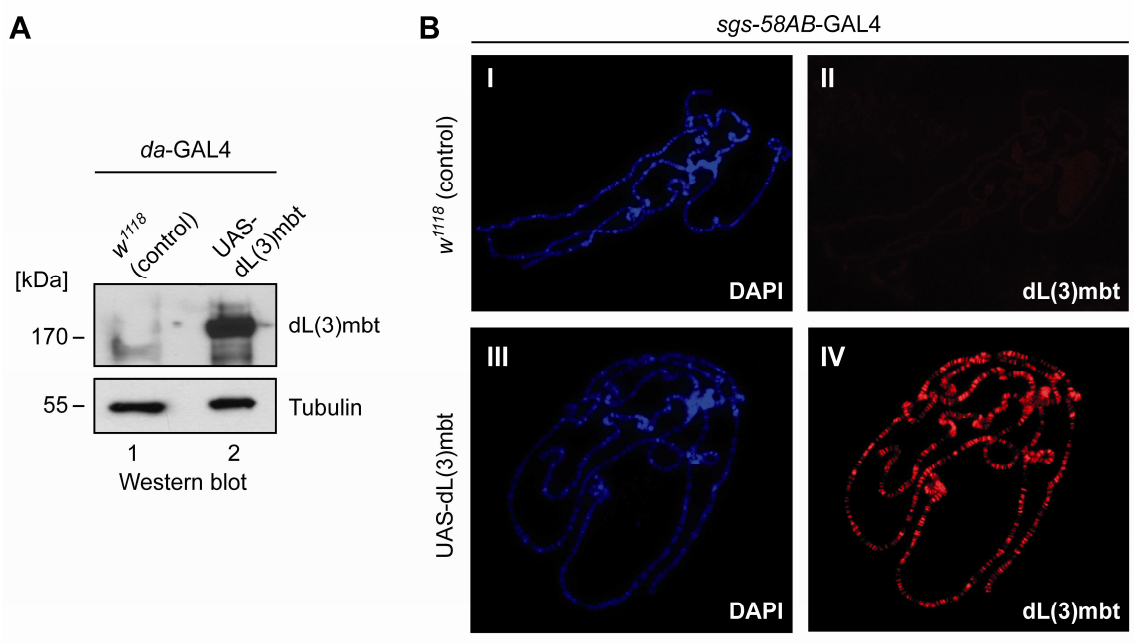


**Figure 4.20: Ectopically expressed recombinant dL(3)mbt reveals binding to multiple sites in the *Drosophila* genome.** (A) Verification of ectopic overexpression of the dL(3)mbt transgene in salivary gland extracts of third instar larvae by Western blot using dL(3)mbt (#3) and β-tubulin antibodies. $w^{1118}$ control flies and flies carrying a dL(3)mbt transgene under the control of UAS were crossed with a *da*-GAL4 driver strain. Western blot against β-tubulin served as a loading control. (B) $w^{1118}$ control flies (I, II) and flies carrying a UAS-dL(3)mbt transgene (III, IV) were crossed with an *sgs-58AB*-GAL4 driver strain. Polytene chromosomes were stained with DAPI (blue; left panels) and dL(3)mbt antibody (#P1 6E6) (red; right panels).

To verify the proper expression of the dL(3)mbt transgene upon site-specific insertion into the genome the resulting transgenic flies were crossed to a *daughterless*-GAL4 (*da*-GAL4) driver strain, which expresses GAL4 in an ubiquitous pattern. Western blot analysis of whole cell extracts from larval salivary glands using a dL(3)mbt-specific antibody confirmed the strong ectopic overexpression of dL(3)mbt in the progeny of these crosses (Figure 4.20 A, upper panel, compare lanes 1 and 2). In agreement with undetectable endogenous dL(3)mbt in immunostainings of polytene chromosomes (Figure 4.20 B, compare upper panels), no or little dL(3)mbt was detected by Western blot analysis in extracts obtained from control crosses (Figure 4.20, compare lane 1).

In order to get an insight into the ability of dL(3)mbt to bind to chromatin on a genome-wide level, flies carrying the UAS-dL(3)mbt transgene were crossed to the *sgs-58AB*-GAL4 driver strain, which expresses GAL4 in a salivary gland-specific expression pattern. Immunostaining of polytene chromosomes with a dL(3)mbt-specific antibody

highlighted numerous distinct bands occupied by recombinant dL(3)mbt (Figure 4.20 B, compare panels IV and II).

Next, to determine whether recombinant dL(3)mbt co-localises with LINT complex subunits polytene chromosomes were co-stained with dL(3)mbt and dLint-1 antibodies (Figure 4.21).

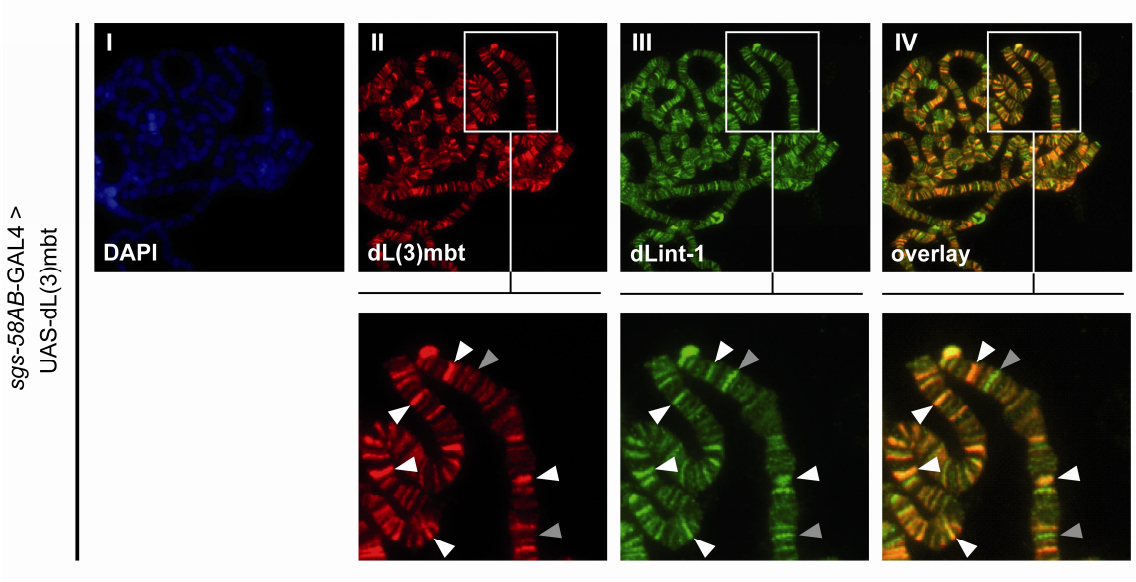


**Figure 4.21: Recombinant dL(3)mbt and endogenous dLint-1 co-localise on polytene chromosomes.** The *sgs-58AB*-GAL4 driver strain was crossed with UAS-dL(3)mbt transgenic flies. Upper panels: Polytene chromosomes were stained with DAPI (blue; panel I), dL(3)mbt (red; panel II) and dLint-1 (green; panel III) antibodies. An overlay of dL(3)mbt and dLint-1 signals is shown in panel IV. Lower panels: Close-up views of polytene stainings. White and grey arrowheads denote selected prominent bands of dL(3)mbt and dLint-1 co-localisation (white) or exclusive dLint-1 binding (grey).

Co-stainings revealed extensive co-localisation between the two proteins (Figure 4.21, compare panels II and III with panel IV). 466 bands were identified for dL(3)mbt and/or dLint-1 binding by visual inspection of immunofluorescence signals. 83% (386 bands) were stained by both dL(3)mbt and dLint-1 antibodies, 12% (55 bands) displayed dLint-1 but no or only very weak dL(3)mbt binding and 5% (25 bands) seemed to be occupied by dL(3)mbt alone. These results support the idea, gained by biochemical studies before, that the LINT subunits act in concert with each other and can bind together to many discrete genomic loci.

### 4.2.2 Expression profiling upon dL(3)mbt and dLint-1 depletion

Given that dL(3)mbt and dLint-1 co-occupy numerous chromosomal locations on polytene chromosomes it seemed very likely that the proteins of the LINT complex work in concert to co-regulate genes on the level of transcription.

To identify LINT regulated genes on a genome-wide level microarray expression analysis following the removal of complex subunits by RNAi in Kc167 cells was employed. Gel filtration analysis of the individual LINT subunits had suggested (Figures 4.10 and 4.15) that the bulk of dL(3)mbt and dLint-1 was present in the LINT complex, whereas dCoREST exists in other protein complexes. Therefore, to identify LINT complex-specific target genes, the two LINT-unique subunits dL(3)mbt and dLint-1 were depleted in Kc167 cells, respectively, by treating the cells with dsRNA targeting either dL(3)mbt or dLint-1 (Figure 4.22). For comparison, cells were treated with dsRNA directed against EGFP in parallel.

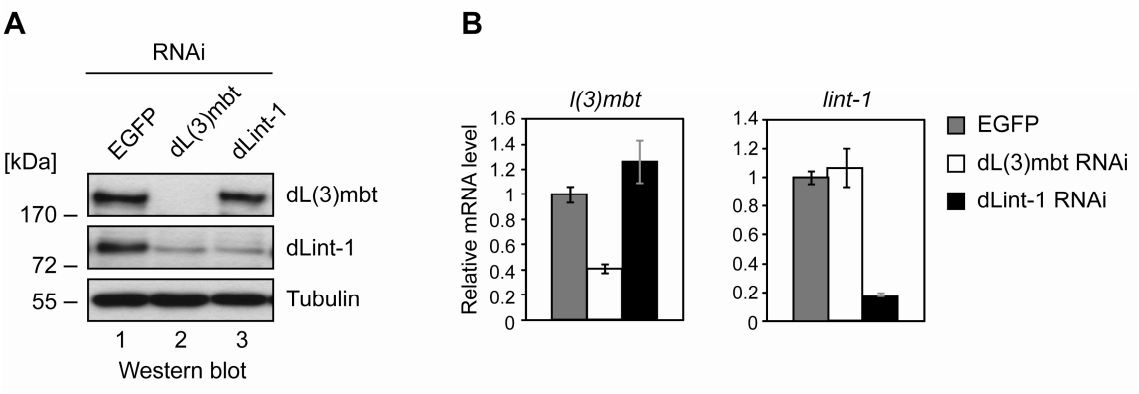


**Figure 4.22: Depletion of dL(3)mbt and dLint-1 in Kc167 cells.** Kc167 cells were treated with dsRNA directed against EGFP, dL(3)mbt or dLint-1 as indicated. (A) Protein levels of dL(3)mbt (upper panel) and dLint-1 (middle panel): Nuclear extracts from RNAi-treated cells were analysed by Western blot using antibodies as indicated on the right. Western blot against β-tubulin served as a loading control. (B) mRNA levels of *l(3)mbt* (left panel) and *lint-1* (right panel): mRNA isolated from RNAi treated cells was analysed by RT-qPCR. mRNA levels in EGFP dsRNA-treated cells were set to 1.

Efficiencies of RNAi-mediated knockdowns were controlled by Western blot (Figure 4.22 A). Detection of β-tubulin served as a loading control, to ensure that equal amounts of extract have been applied. Depletion of both dL(3)mbt and dLint-1 was efficient and resulted in strong decreases in protein level. Interestingly, dL(3)mbt knockdown resulted in co-depletion of dLint-1 but not vice versa. Quantification of mRNA levels

by RT-qPCR (Figure 4.22 B), however, revealed that dL(3)mbt depletion did not affect *lint-1* mRNA levels. This suggests that dLint-1 protein is destabilised by the loss of dL(3)mbt as a stable binding partner.

For microarray analysis knockdown experiments were conducted in biological triplicates and total RNA was prepared from dL(3)mbt, dLint-1 and EGFP RNAi-treated cells in each experiment. In cooperation with Gunther Doehlemann (MPI for Terrestrial Microbiology, Marburg) the total RNA was processed and hybridised to Affymetrix GeneChip *Drosophila* Genome 2.0 Arrays. Statistical analysis of the micro-array results was conducted by Florian Finkernagel (IMT, Marburg). Genes with a fold change of at least 1.5 (adjusted p-value ≤ 0.05) were considered to be deregulated (Figure 4.23).

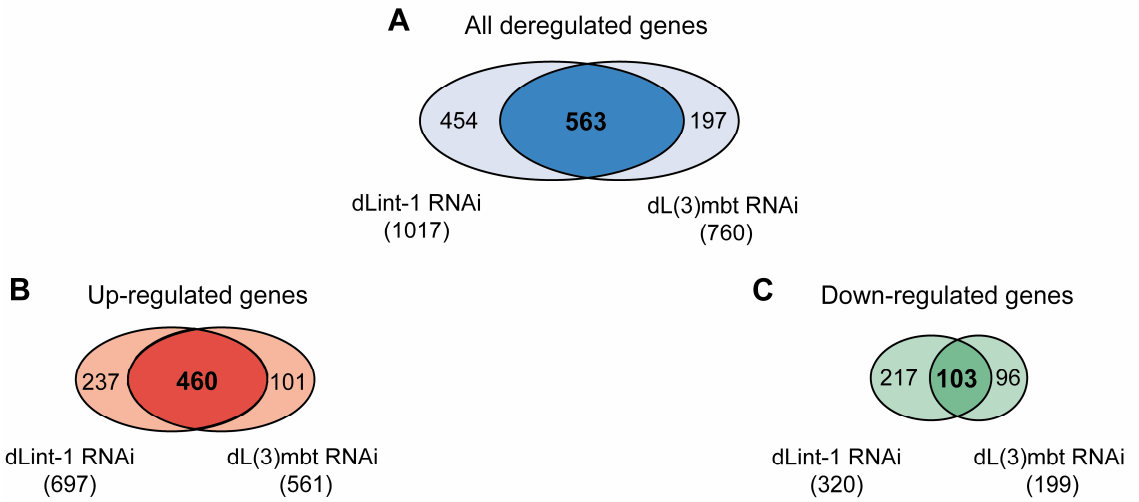


**Figure 4.23: Venn-diagrams displaying dL(3)mbt and dLint-1 regulated genes.** (A) Venn-diagrams representing all genes that were deregulated more than 1.5 fold (adj. p ≤ 0.05) upon dL(3)mbt or dLint-1 knockdown in Kc167 cells (blue). Deregulated genes were subdivided into (B) up-regulated (red) and (C) down-regulated (green) genes.

In dLint-1 depleted cells, 1017 genes were deregulated. From these 697 were up- and 320 were down-regulated. dL(3)mbt knockdown resulted in a deregulation of 760 genes, from these 561 genes were up-regulated, while 199 were down-regulated. Therefore, in both dL(3)mbt and dLint-1 depleted cells, approximately 2-fold more genes were up-regulated than down-regulated. Surprisingly, in dL(3)mbt RNAi-treated cells, less genes were deregulated overall compared to dLint-1 RNAi-treated cells, although co-depletion of dLint-1 in cells treated with dL(3)mbt-dsRNA seemed as

efficient as the loss of dLint-1 in cells treated with dLint-1 dsRNA (Figure 4.22, compare lanes 2 and 3).

Genes whose expression was changed in the same direction in both dL(3)mbt and dLint-1 depleted cells were considered as potential LINT complex target genes. For both dL(3)mbt and dLint-1 the majority of deregulated genes (74% and 53%, respectively) were found in both data sets. From these 563 coregulated genes 460 were up-regulated and 103 were down-regulated. The ratio between the numbers of up- and down-regulated genes (4.5 : 1) suggests a predominant role of LINT in transcriptional repression.

### 4.2.3 LINT represses ovary- and testis-specific genes

To gain insight into the type of target genes that were repressed by the LINT complex, genes strongly up-regulated upon dL(3)mbt and dLint-1 depletion were analysed. Interestingly, closer inspection of the top 50 genes derepressed upon dLint-1 RNAi using the FlyAtlas (http://flyatlas.org), a microarray-based atlas of gene expression in multiple adult tissues, revealed that 40% of the genes were expressed specifically in ovary or testis in the adult fly (Table 4.3). With the exception of eight, these genes were also among the top 50 up-regulated genes upon dL(3)mbt knockdown.

Among these were genes with established roles during germline development, such as *piwi* (Cox et al., 1998), *swallow* (*swa*) (Stephenson et al., 1988) and *nanos* (*nos*) (Lehmann and Nüsslein-Volhard, 1991), as well as in meiosis, such as *crossover suppressor on 2 of Manheim* (*c(2)M*) (Manheim and McKim, 2003). In contrast, a multitude of the top 50 deregulated genes displaying ovary- and testis-specific expression was annotated with unknown molecular function (i.e. *CG14516* and *skpB*).

**Table 4.3: Top 50 dLint-1 up-regulated genes.** Expression changes of genes upon knockdown of either dLint-1 or dL(3)mbt are expressed as log2 fold changes (FC). Genes were ranked according to decreasing FC. Genes are stated with their gene symbol and name. Specific expression of genes in ovary and/or testis is indicated.

| dLint-1 rank | dLint-1 log2 FC | dL(3)mbt rank | dL(3)mbt log2 FC | Gene symbol | Gene name | Ovary/Testis-specific expression |
|---|---|---|---|---|---|---|
| 1 | 7.9 | 3 | 7.6 | CG14516 | CG14516 | Ovary |
| 2 | 7.2 | 2 | 8.8 | CG30296 | CG30296 | |
| **3** | **6.5** | **4** | **7.6** | **piwi** | **P-element induced wimpy testis** | **Ovary** |
| 4 | 6.4 | 1 | 8.9 | CG11052 | CG11052 | Testis |
| 5 | 6.0 | 9 | 8.8 | CG17207 | CG17207 | Testis |
| 6 | 5.9 | 6 | 7.1 | CG5731 | CG5731 | |
| 7 | 5.9 | 10 | 6.7 | CG8589/tej | tejas/anon-fast-evolving-1D11 | Ovary |
| 8 | 5.7 | 5 | 7.1 | mthl14 | methuselah-like 14 | |
| 9 | 5.7 | 19 | 5.9 | hdm | hold'em | |
| 10 | 5.7 | 14 | 6.1 | eIF4E-6 | eIF4E-6 | |
| 11 | 5.7 | 18 | 5.9 | Acer | Angiotensin-converting enzyme-related | |
| 12 | 5.6 | 24 | 5.4 | CG1623 | CG1623 | |
| 13 | 5.4 | 16 | 5.9 | CG32313 | CG32313 | Testis |
| 14 | 5.4 | 20 | 5,9 | Rh4 | Rhodopsin 4 | |
| 15 | 5.2 | 17 | 5.9 | CG9875 | CG9875 | Testis |
| 16 | 5.1 | 25 | 5.3 | CG8008 | CG8008 | |
| 17 | 5.0 | 13 | 6.3 | skpB | skpB | Testis |
| 18 | 5.0 | 32 | 5.1 | Asph | Aspartyl β-hydroxylase | |
| 19 | 5.0 | 27 | 5.3 | CG11638 | CG11638 | |
| 20 | 4.9 | 8 | 6.9 | CG30380 | CG30380 | |
| 21 | 4.9 | 23 | 5.4 | CG5715 | CG5715 | |
| 22 | 4.9 | 28 | 5.3 | GNBP3 | Gram-neg. bacteria binding protein 3 | |
| 23 | 4.7 | 31 | 5.1 | osm-6 | osm-6 | Testis |
| 24 | 4.7 | 36 | 5.0 | CG15737 | CG15737 | Ovary |
| 25 | 4.7 | 30 | 5.2 | Cyp6g1 | Cyp6g1 | |
| 26 | 4.6 | 40 | 4.8 | Gbeta5 | Gbeta5 | |
| 27 | 4.6 | 12 | 6.3 | dpr19 | dpr19 | |
| 28 | 4.5 | 26 | 5.3 | TM4SF | Transmembrane 4 superfamily | |
| 29 | 4.5 | 38 | 4.9 | tok | tolkin | |
| 30 | 4.5 | 7 | 7.0 | CG4596 | CG4596 | |
| 31 | 4.4 | 46 | 4.5 | CG32436 | CG32436 | Testis |
| 32 | 4.4 | 11 | 6.4 | RpS5b | Ribosomal protein S5b | Ovary Testis |
| 33 | 4.4 | 39 | 4.8 | CG34232 | CG34232 | |

| | | | | | | |
|---|---|---|---|---|---|---|
| 34 | 4.4 | 15 | 6.0 | Ef1α100E | Elongation factor 1α100E | |
| **35** | **4.3** | **41** | **4.8** | **swa** | **swallow** | **Ovary** |
| 36 | 4.3 | 6 | 4.0 | CG9542 | CG9542 | |
| 37 | 4.3 | 45 | 4.5 | CG12698 | CG12698 | Testis |
| 38 | 4.3 | 51 | 4.3 | Hsp67Bc | Heat shock gene 67Bc | |
| 39 | 4.1 | 43 | 4.8 | CG8046 | CG8046 | |
| 40 | 4.1 | 79 | 3.8 | CG9961 | CG9961 | Testis |
| 41 | 4.1 | 52 | 4.3 | CG9427 | CG9427 | |
| 42 | 4.0 | 47 | 4.5 | CG2887 | CG2887 | Testis |
| 43 | 4.0 | 84 | 3.7 | CG17625 | CG17625 | Testis |
| **44** | **3.9** | **22** | **5.6** | **nos** | **nanos** | **Ovary** |
| 45 | 3.9 | 42 | 4.8 | CG40303 | CG40303 | |
| 46 | 3.9 | 90 | 3.5 | CG32187 | CG32187 | |
| **47** | **3.8** | **21** | **5.7** | **c(2)M** | **crossover suppressor on 2 of Manheim** | **Ovary** |
| 48 | 3.8 | 33 | 5.1 | CG34355 | CG34355 | |
| 49 | 3.7 | 71 | 3.9 | CG17032 | CG17032 | |
| 50 | 3.7 | 97 | 3.3 | CG6737 | CG6737 | Testis |

Continuation of Table 4.3.

For validation of the microarray results, nine genes with established roles during gametogenesis and axis formation of the oocyte or early embryo were selected. In microarray analysis, seven of these genes, *piwi*, *nanos* (*nos*), *swallow* (*swa*), *easter* (*ea*), *torso* (*tor*), *zero population growth* (*zpg*) and *bag of marbles* (*bam*), exhibited a significant derepression upon dL(3)mbt and dLint-1 knockdown, whereas the expression levels of *tudor* (*tud*) and *SpindleE* (*SpnE*) did not change. For verification, mRNA levels of these genes were determined in dL(3)mbt- and dLint-1-depleted cells by RT-qPCR in comparison to EGFP RNAi-treated cells (Figure 4.24; for knockdowns see Figure 4.22). Knockdown of dL(3)mbt and dLint-1 resulted in a derepression of *piwi*, *nos*, *swa*, *ea*, *tor*, *zpg* and *bam*, but had no significant effect on the expression of *tud* and *SpnE*, in agreement with microarray data. The magnitude of derepression ranged from 2.5-fold (*bam* expression in dLint-1 RNAi-treated cells) to 40-fold (*nos* expression in dL(3)mbt RNAi-treated cells).

In conclusion, these data support the idea that the LINT complex subunits contribute to the stable repression of germ cell-specific genes in Kc167 cells.

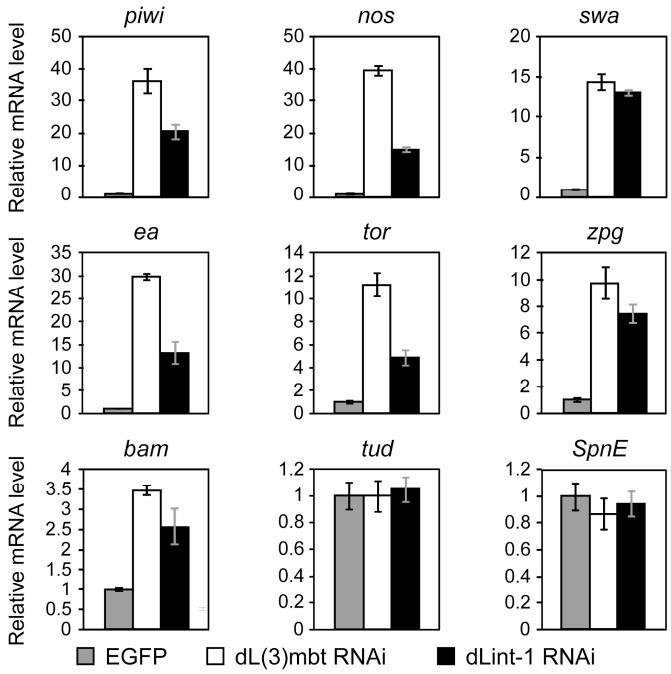


**Figure 4.24: Validation of dL(3)mbt and dLint-1 target genes by RT-qPCR.** Kc167 cells were treated with dsRNA directed against EGFP, dL(3)mbt or dLint-1 as indicated. Expression of *piwi, nanos* (*nos*), *swallow* (*swa*), *easter* (*ea*), *torso* (*tor*), *zero population growth* (*zpg*), *bag of marbles* (*bam*), *tudor* (*tud*) and *spindleE* (*SpnE*) were determined by RT-qPCR. mRNA levels in EGFP RNAi-treated cells were set to 1.

### 4.2.4 LINT represses germline-specific genes during fly development

The expression profiling by microarray analysis and the validation of candidate target genes had been performed in cell culture upon depletion of dL(3)mbt and dLint-1 by RNAi. To investigate whether LINT was also required for repression of germline-specific genes in the developing fly, RNAi fly lines of the Vienna Drosophila RNAi Center (VDRC) were used. These fly lines carry RNAi transgenes under the control of the upstream activating sequence (UAS) that can be conditionally expressed by crossing them to a GAL4-driver strain (Dietzl et al., 2007). This binary UAS-GAL4 system allowed the expression of RNAi transgenes to target *l(3)mbt* and *lint-1*, respectively. RNAi transgene transcription was driven by crossing in a driver strain expressing GAL4 under the control of the *daughterless* (*da*) gene. This should result in ubiquitous expression of the RNAi transgenes from early embryogenesis on in the pattern of the *da* gene (Cronmiller et al., 1988).

To quantify the knockdown efficiencies in third instar larvae of *da*-GAL4/UAS-RNAi crosses, expression levels of *l(3)mbt* and *lint-1* mRNA were determined by RT-qPCR

(Figure 4.25 A, left panels). As control, *UAS*-RNAi lines were crossed to the isogenic host strain of the RNAi library $w^{1118}$. Whereas, RNAi directed against dL(3)mbt led only to a mild reduction of dL(3)mbt mRNA (of about 40%), dLint-1 RNAi resulted in a robust reduction of dLint-1 mRNA levels (greater than 90%). In contrast to the situation in Kc167 cells (Figure 4.22 B), dLint-1 mRNA was also decreased (to 20%) upon dL(3)mbt depletion. Despite the robust effect on mRNA level, Western blot analysis of extract obtained from brains of third instar larvae revealed that dLint-1 protein levels were not strongly affected by dL(3)mbt RNAi (Figure 4.25 B).

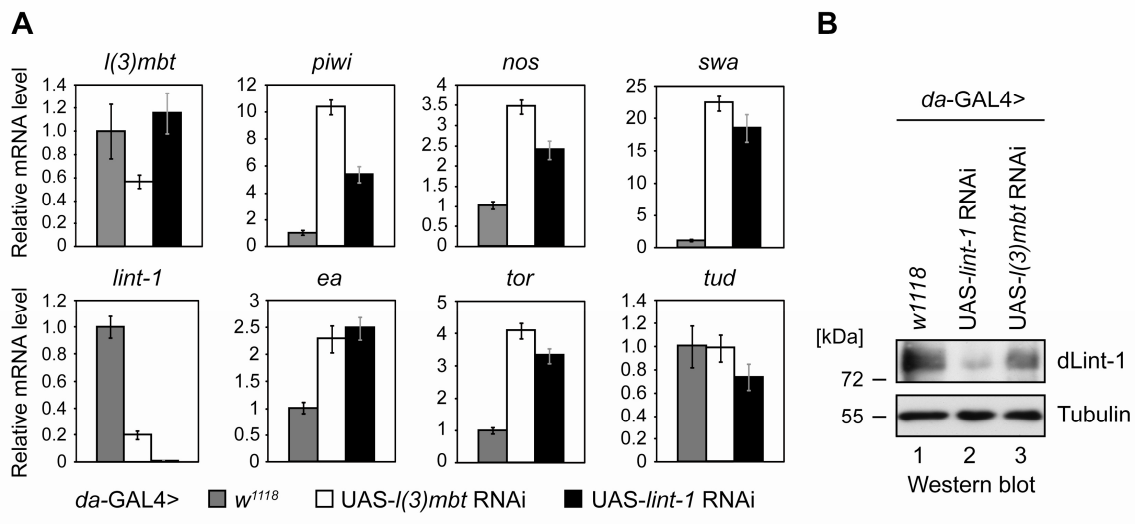


**Figure 4.25: Knockdown of dL(3)mbt and dLint-1 in the developing fly derepresses transcription of germline-specific genes.** RNAi depletion was achieved by crossing the *da*-GAL4 driver strain to $w^{1118}$ (as control), UAS-*l(3)mbt* RNAi and UAS-*lint-1* RNAi strains, respectively. (A) Expression of genes in third instar larvae was determined by RT-qPCR: *l(3)mbt*, *lint-1* (left panel) and germline-specific target genes (right panels), *piwi, nos, swa, ea, tor* and *tud* (control). mRNA levels in $w^{1118}$ crosses were set to 1. (B) Western blot demonstrating depletion of dLint-1 protein in the brain of third instar larvae. Western blot against β-tubulin served as a loading control.

Upon depletion of either dL(3)mbt or dLint-1 the transcription of *piwi*, *nos*, *swa*, *ea* and *tor* was derepressed in RNAi larvae, which is in good agreement with data obtained with Kc167 cells (Figure 4.25 B). In contrast, *tud* expression was not up-regulated. The magnitude of up-regulation ranged from 2.2-fold (*ea* transcription in dL(3)mbt RNAi larvae) to 22-fold (*swa* transcription in dL(3)mbt RNAi larvae).

Taken together these results strongly argue for an important role of LINT in the stable repression of germline-specific genes, both in *Drosophila* cell lines and in the developing fly.

### 4.2.5 LINT localises to promoter regions of target genes

The involvement of the LINT complex in repression of germ cell-specific genes raised the question, whether LINT binds directly to its target genes. Therefore, *swallow*, which was highly up-regulated upon dL(3)mbt and dLint-1 depletion, both in Kc167 cells and *Drosophila* larvae, was chosen as a model gene. To gain insight into the potential binding profile of LINT to specific chromatin regions, amplicons within the genomic *swallow* locus ranging from 3 kb upstream to 5.3 kb downstream of the transcription start site (TSS) were selected for qPCR analysis (Figure 4.26 A).

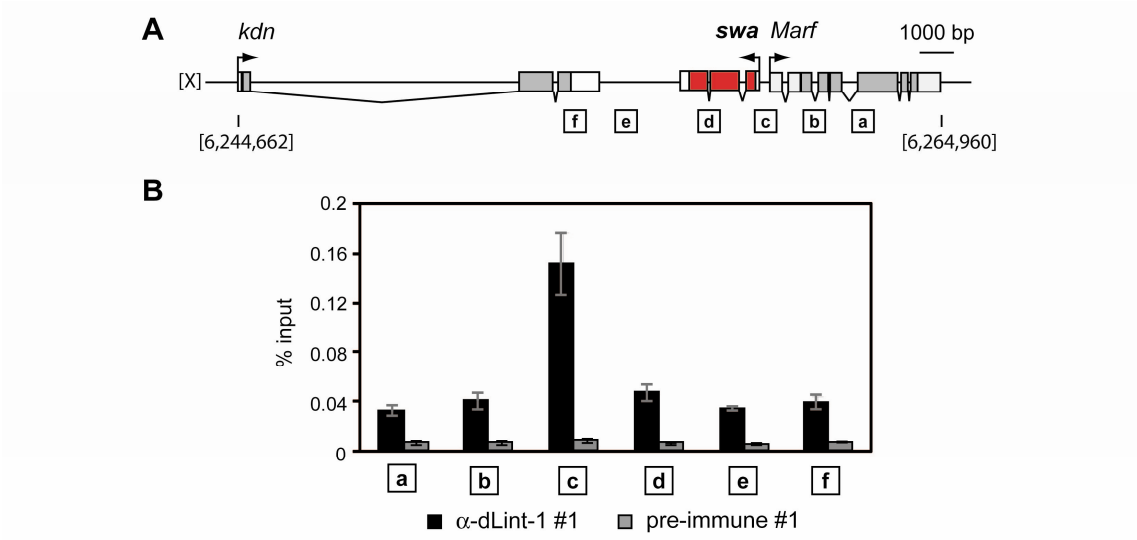


**Figure 4.26: dLint-1 binds to the promoter region of the *swallow* gene.** (A) Schematic representation of the genomic *swa* locus on chromosome [X]. The sequence location in bp is indicated below in squared brackets. 5' and 3' untranslated regions are shown in white, coding regions of *swa* and neighbouring genes are depicted in red and grey, respectively. Regions selected for amplification are indicated by framed letters (a to f). They have the following approximate distances from the TSS: a, 3 kb upstream; b, 1.5 kb upstream; c, 0-0.15 kb upstream (putative promoter); d, 1.5 kb downstream; e, 3.8 kb downstream; f, 5.3 kb downstream. (B) Chromatin was isolated from Kc167 cells. ChIP was performed with antisera indicated below. Immunoprecipitated DNA was quantified by qPCR using primers against regions as indicated (compare (A)). Mean values are expressed as percentage of input (% input).

Next, chromatin immunoprecipitations (ChIP) were carried out, using the dLint-1-specific antibody #1, to identify chromatin regions bound by LINT. The dL(3)mbt-specific antibodies could not be used, because they did not precipitate dL(3)mbt efficiently under ChIP conditions. Analysis of the immunoprecipitated DNA by qPCR, revealed that the dLint-1-specific antibody #1 precipitated generally higher levels of

DNA than the pre-immune serum control. This observation was independent of the chromatin region that was analysed (Figures 4.26 and 4.28). Nevertheless, a distinct peak of dLint-1 was detected by ChIP analysis at the putative promoter region of *swa* directly upstream of the TSS (region c). Compared with neighbouring regions (regions a, b, d, e and f) the immunoprecipitated DNA of the promoter region (c) was enriched by approximately 4-fold. This argues for a specific binding of dLint-1 to the promoter region of the *swa* gene.

To further support the specificity of the dLint-1 ChIP result, chromatin was also immunoprecipitated using the second dLint-1-specific antibody #2 and the corresponding pre-immune serum as control (Figure 4.27 B). Consistent with data obtained using the α-dLint-1 #1 antibody, the promoter region was at least 3-fold enriched, compared to amplicons localised 1.5 kb up- and downstream of the TSS.

Additionally, to ensure that the detected peak was indeed a result of dLint-1 protein as part of the LINT complex localising to the promoter region, ChIPs were carried out after co-depletion of dL(3)mbt/dLint-1 by RNAi directed against dL(3)mbt (see Figure 4.22 A). As control dLint-1 ChIPs were also done from chromatin of EGFP dsRNA-treated cells. In agreement with the idea that dLint-1 associates with the *swa* promoter, the corresponding dLint-1 peak decreased strongly (about 3-fold) upon co-depletion of dL(3)mbt and dLint-1, compared to the EGFP control. In addition, a decline of 2-fold was observed for the amplicon 1.5 kb downstream, indicating that also a proportion of ChIP signal in this region resulted from immunoprecipitation of dLint-1. On the contrary, analysis of an unrelated intergenic region revealed that the amount of immunoprecipitated DNA did not differ between EGFP and dL(3)mbt RNAi-treated cells, suggesting that this was the background level of DNA recovered by the dLint-1 antiserum.

In conclusion, the LINT subunit dLint-1 binds specifically to the putative promoter region of the *swa* gene directly upstream of the TSS.

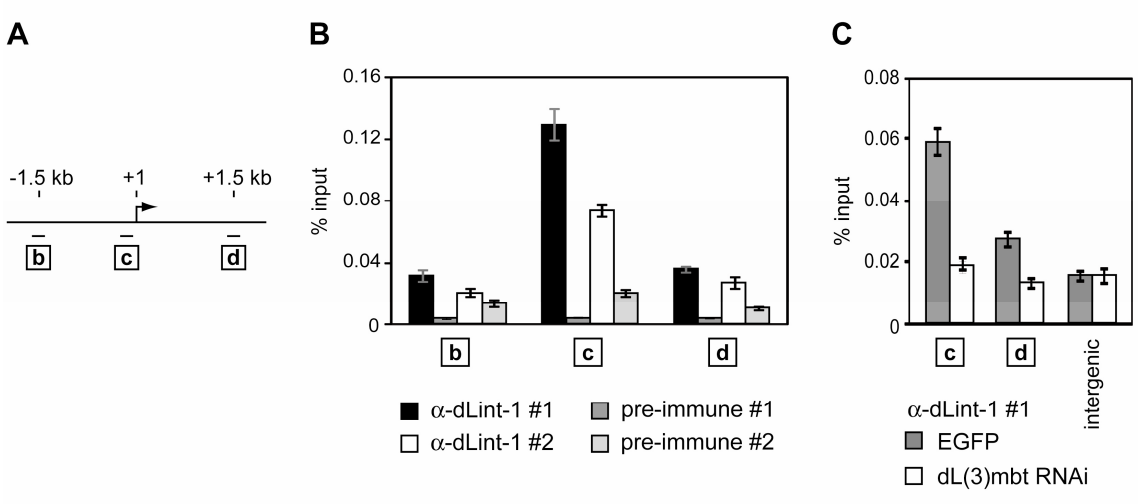


**Figure 4.27: Validation of dLint-1 ChIP results.** (A) Schematic representation of the amplified regions relative to the TSS. (B) Chromatin was prepared from Kc167 cells. ChIPs were carried out with antisera indicated below. (C) Chromatin was isolated from Kc167 cells treated with dsRNA directed against EGFP and dL(3)mbt. ChIPs were done using dLint-1-specific antibody #1. (B) and (C) Mean values are expressed as % input. Immunoprecipitated DNA was quantified by qPCR using primers against regions as indicated. Intergenic refers to an unrelated intergenic region on chromosome arm 2R.

To investigate if dLint-1 binds also to the promoter regions of other regulated genes, several putative LINT target genes were analysed by ChIP (Figure 4.28). Distinct peaks were detected over the promoters of *swa, nos, tolkin (tok)* and *crumbs (crb)* compared to regions 1.5 kb up- and downstream. In case of *piwi* elevated ChIP signals were detected at the putative promoter region directly upstream of the TSS and 1.5 kb upstream compared to 3 kb upstream and 1.5 kb downstream. As a second LINT subunit, association of dCoREST with these genes was tested. ChIP signals, obtained with the dCoREST-specific antibody, were generally lower than signals obtained using the α-dLint-1 antibody. Nevertheless, distinct dCoREST peaks were observed at the promoters of *swa, nos, tok* and *crb*. These results indicate that several target genes, which were identified by their derepression upon dL(3)mbt or dLint-1 knockdown, are directly bound by LINT complex subunits.

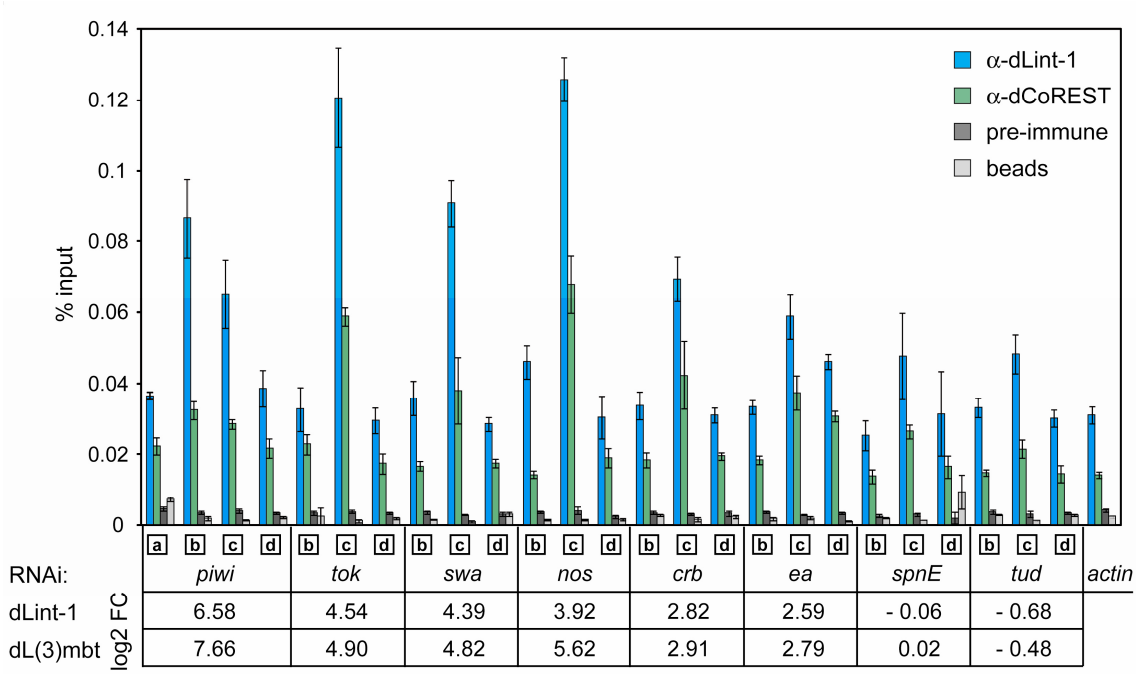


**Figure 4.28: dLint-1 and dCoREST bind to promoter regions of LINT target genes.** ChIPs were performed with antibodies indicated on the right. Genes analysed are denoted below the diagram. Regions selected for amplification are indicated by framed letters (a to d). They had the following approximate distances from the TSS: a, 3 kb upstream; b, 1.5 kb upstream; c, 0-0.15 kb upstream (putative promoter); d, 1.5 kb downstream. Derepression of transcription following RNAi-mediated depletion of dLint-1 and dL(3)mbt is shown as log2 FC (fold change) below the panel. Expression values for dLint-1 and dL(3)mbt RNAi are taken from microarray analysis.

## 4.3 Mechanism of gene repression by LINT

### 4.3.1 LINT occupied promoters display reduced nucleosome levels

It has been reported previously that the MBT domains of human L3MBTL1 can induce the compaction of nucleosomal arrays *in vitro* dependent on H4K20 or H1K26 mono- and di-methylation (Trojer et al., 2007). Therefore, the generation of compacted chromatin has been favoured as a mechanism for transcriptional repression by MBT domain-containing proteins. A prediction from this model is that the density of nucleosomes would be higher in the proximity of MBT protein-bound regions.

To determine if this applies to LINT target genes H3 occupancy as a parameter of nucleosome occupancy, was determined (Figure 4.29). In fact, ChIP results revealed that H3 ChIP signals are noticeably reduced at promoters of LINT target genes (*swa*, *piwi*, *nos*) (Figure 4.29 A) compared to regions up- and downstream (Figure 4.29 B, compare relative distances of amplicons). Hence, a negative correlation between LINT

binding to promoters and nucleosome density was observed. In case of the *swa* gene, not only regions 1.5 kb up- (b) and downstream (d), but also 3.0 kb up- (a), 3.8 kb down- (e) and 5.3 kb downstream (f) were analysed. Amplicons a, b and f were located in neighbouring genes *Marf* and *kdn*, respectively, which are actively transcribed in Kc167 cells, according to RNA-Seq data, obtained from the ModENCODE project (http://www.modencode.org/). These regions displayed similar nucleosome densities as detected in region b, situated in the body of the repressed *swa* gene. In summary, these data indicate that LINT regulated genes are not necessarily embedded into a highly compacted chromatin structure. In order to elucidate if dL(3)mbt plays a role in nucleosome positioning on LINT target genes, a thorough mapping analysis of nucleosomes remains to be done before and after dL(3)mbt RNAi.

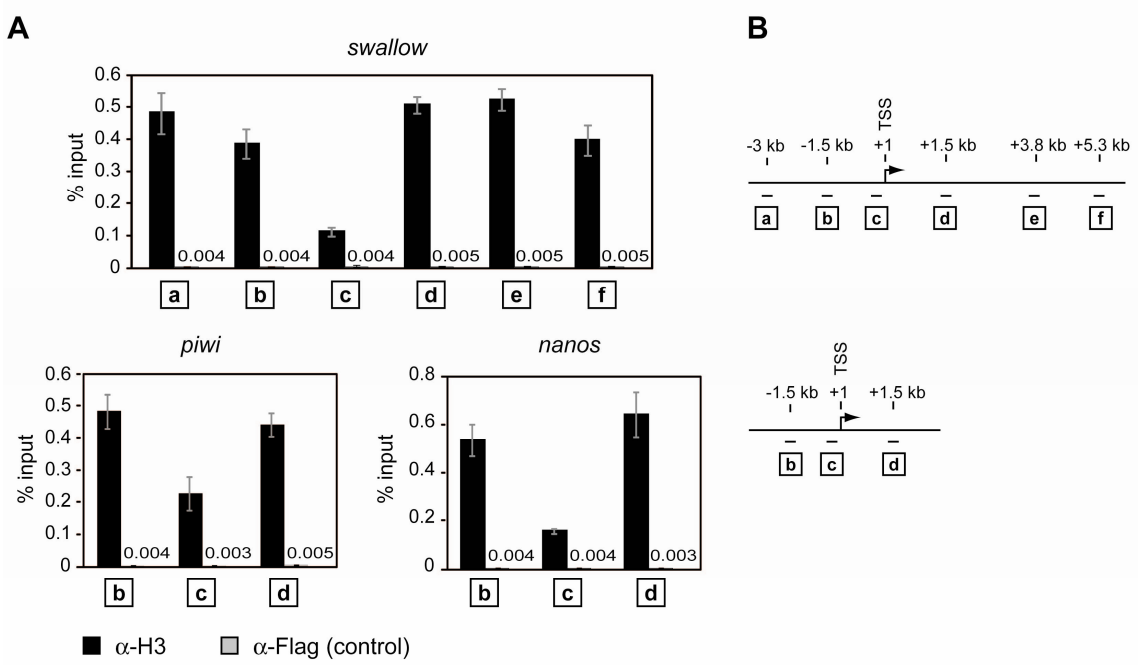


**Figure 4.29: LINT target gene promoters display reduced levels of H3.** (A) Chromatin from Kc167 cells was immunoprecipitated with α-H3 and α-FLAG (control) antibody. Immunoprecipitated DNA was quantified by qPCR using primers against regions a to f, as depicted in (B). Mean values are expressed as % input. (B) Schematic depiction of the approximate amplicon distances relative to the transcription start site (TSS; +1).

### 4.3.2 Depletion of dPR-Set7-mediated H4K20 mono-methylation does not affect LINT target gene repression

Previous publications have demonstrated that the MBT domains of the human dL(3)mbt homologue L3MBTL1 bind specifically to mono- and di-methylated H4K20 *in vitro* (Trojer et al., 2007). In this context, mono-methylation of H4K20, catalysed by PR-SET7 (Nishioka et al., 2002), was sufficient to mediate 3MBT domain-dependent compaction of oligo-nucleosomal arrays (Trojer et al., 2007). Moreover, it has been reported that L3MBTL1 and PR-SET7 can interact directly and that PR-SET7 promotes the repressive activity of L3MBTL1 in reporter assays. Furthermore, L3MBTL1 chromatin occupancy was decreased upon knockdown of PR-SET7 (Kalakonda et al., 2008).

In contrast to the situation in human, no interaction between dL(3)mbt and dPR-Set7 was detected in co-immunoprecipitations (Figure 4.31 A). Nevertheless, it was possible that binding of dL(3)mbt to methylated H4K20 could have an impact on the repressive function of LINT. Therefore, to verify that the MBT domains of dL(3)mbt indeed have the capability to bind to methylated H4 tails, their binding affinity to differentially methylated H4 peptides, comprising amino acids 16 to 25, was tested in *in vitro* peptide pulldown assays (Figure 4.30). As a positive control, immobilised H4 peptides were incubated with a recombinant GST fusion protein of the 3MBT domains of human L3MBTL1 (GST-h3MBT).

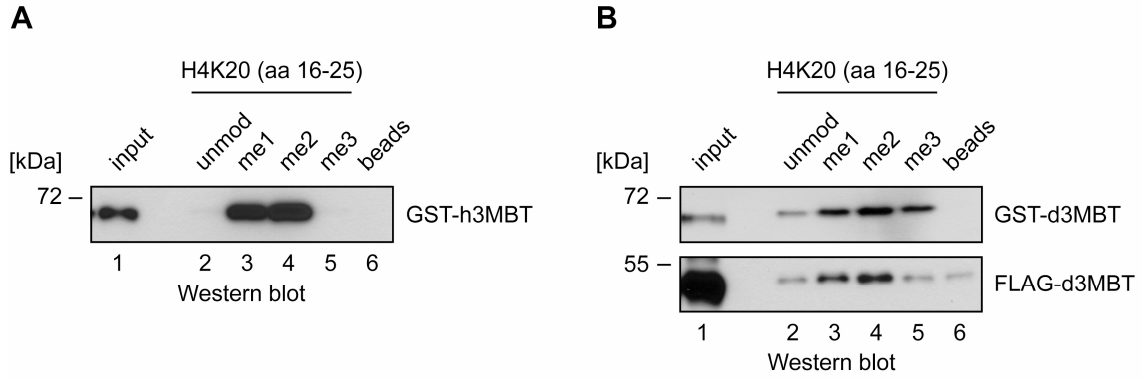


**Figure 4.30: The three MBT domains of dL(3)mbt bind preferentially to mono- and di-methylated H4K20 peptides.** Immobilised H4 peptides (aa 16-25), with unmodified (unmod), mono- (me1), di- (me2) or tri-methylated (me3) K20, were incubated with purified recombinant GST-h3MBT (A), GST-d3MBT (B, upper panel) or Sf9 extract containing FLAG-d3MBT (B, lower panel). Binding of GST-fusion or FLAG-tagged 3MBT proteins was analysed by Western blotting using α-FLAG or α-GST antibody, respectively. Input: 10% of GST fusion protein or Sf9 extract; beads: control without peptide. (B) Published in Scharf et al., 2009.

In agreement with published data (Trojer et al., 2007), the MBT domains of L3MBTL1 displayed a strong preference for H4 peptide mono- and di-methylated at lysine 20 (Figure 4.30 A). On the contrary, the MBT domains of dL(3)mbt (GST-d3MBT) bind to unmodified H4 peptide and showed increased binding to all three methylation states of H4K20 (Figure 4.30 B, upper panel). To preclude that incorrect protein folding or the lack of a post-translational modification, caused by expression of the GST fusion protein in bacteria, had any influence on the binding affinities, a FLAG-tagged construct of the MBT domains (FLAG-d3MBT) was expressed using the baculovirus system. In this case the histone peptides were incubated with Sf9 extract containing overexpressed FLAG-d3MBT. This FLAG-d3MBT construct recognised preferentially the mono- and di-methylated H4K20 peptide (Figure 4.30 B, lower panel), similarly to the human MBT domains. Collectively, the results from the peptide pulldown assays establish that the MBT domains of dL(3)mbt have the potential to bind to mono- and di-methylated H4K20 *in vitro*.

To further investigate whether dPR-Set7-mediated H4K20 mono-methylation has any impact on repression of LINT regulated genes dPR-Set7 was depleted by RNAi in Kc167 cells (Figure 4.31 B). The efficient knockdown of dPR-Set7 was controlled by analysing nuclear extract of dsRNA-treated cells by Western blot (Figure 4.31 B, upper panel). To monitor the effect of dPR-Set7 depletion on the global level of H4K20 mono-methylation histones were acid-extracted from the insoluble nuclear fraction. Western blotting revealed that RNAi against dPR-Set7 resulted in a strong decrease of H4K20me1 levels, while histone H3 levels were constant (Figure 4.31 A, middle and lower panels). Despite the efficient global reduction of H4K20 mono-methylation, no significant derepression of LINT target genes could be detected (Figure 4.31 B).

The observation that dPR-Set7 RNAi had no or little effect on LINT target gene expression, even though H4K20 mono-methylation levels were globally reduced, could have different reasons. There were two obvious possibilities to account for this: First, it was possible that the H4K20me1 mark was present at target genes, but the knockdown had no influence on repression by LINT. Second, it was equally conceivable, that this modification was not present at LINT target gene promoters.

Therefore, H4K20me1 levels were assessed by ChIP-qPCR (Figure 4.32 A). The *actin* gene was used as a positive control region to verify the efficiency of the immunoprecipitation. Indeed, robust H4K20me1 levels were detected at the *actin* gene with two independent antibodies (Figure 4.32 A). In comparison to this, H4K20me1

signals at the promoters of *swa* and *nos* were approximately 20-fold lower, similarly to an intergenic region that served as a negative control. Furthermore, H4K20me1 signals at *swa* and *nos* target genes did not significantly differ from signals obtained with the IgG control antibody.

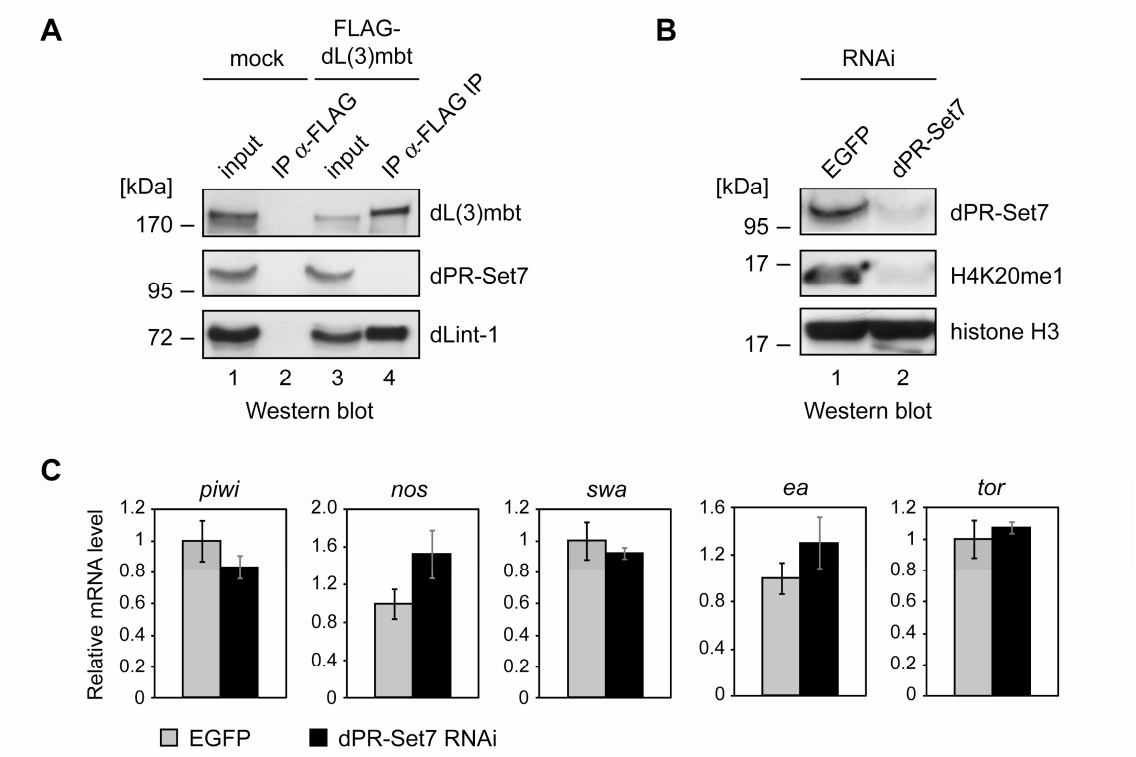


**Figure 4.31: dPR-Set7 does not contribute to repression of LINT target genes.** (A) Nuclear extracts from control S2 cells (mock, lanes 1 and 2) and S2 cells stably expressing FLAG-dL(3)mbt (lanes 3 and 4) were precipitated with FLAG agarose beads. Immunoprecipitates were analysed by Western blot using antibodies as indicated on the right (lanes 2 and 4). Input: 5% of nuclear extracts (lanes 1 and 3). dLint-1 served as a positive control. (B) and (C) Kc167 cells were treated with dsRNA directed against EGFP (control) or dPR-Set7. (B) Nuclear extracts or acid extracted histones were analysed by Western blot using antibodies as indicated on the right. Western blot against histone H3 served as a loading control. (C) Expression of LINT target genes was determined by RT-qPCR. Expression in EGFP RNAi-treated cells was set to 1.

The depletion of dPR-Set7 by RNAi led to strong decrease of H4K20me1 levels at the *actin* gene (Figure 4.32: left panel: 70%; right panel: 40%), but did not affect H4K20 mono-methylation signals at *swa* and *nos*.

In summary, these results suggest that the H4K20me1 mark appears to be absent from LINT target gene promoters and that binding of dL(3)mbt to mono-methylated H4K20 is not essential for the maintenance of stable repression of LINT target genes.

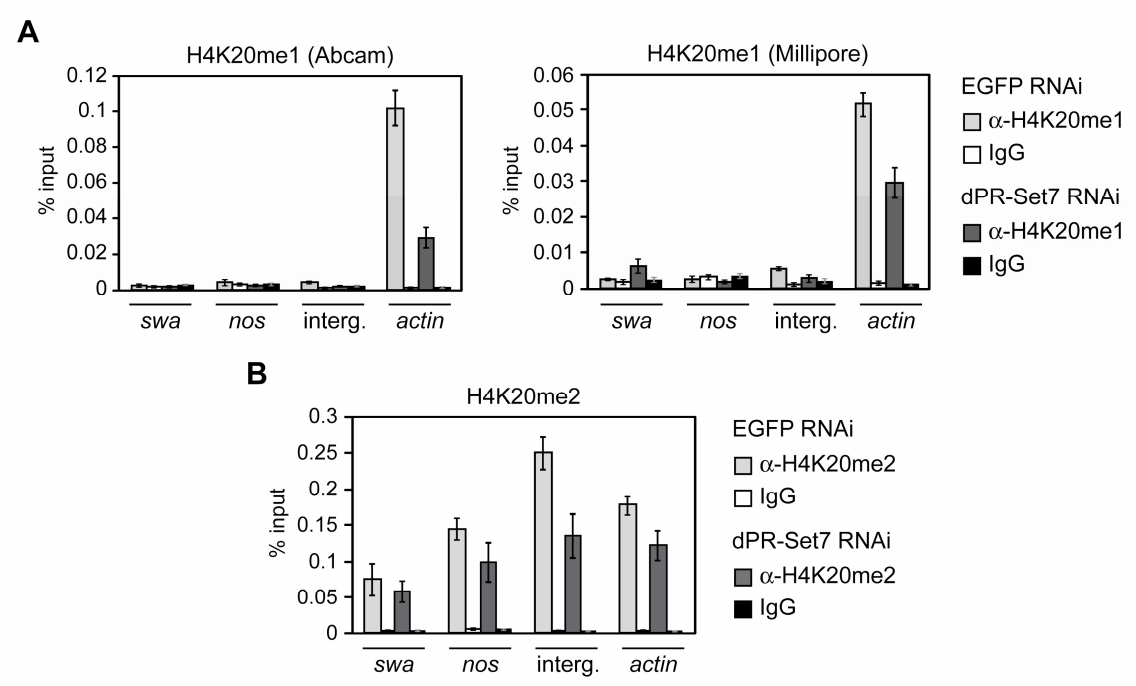


**Figure 4.32:** Kc167 cells were treated with RNAi directed against EGFP (control) or dPR-Set7. (A) Chromatin was precipitated with H4K20me1 (left panel: Abcam antibody; right panel: Millipore antibody) or IgG antibodies as indicated. (B) Chromatin was precipitated with H4K20me2 or IgG antibodies as indicated. (A) and (B) ChIP signals as % input are shown for *swa* and *nos* promoter regions, an intergenic region and the *actin* ORF as denoted below the panels.

Since the MBT domains of dL(3)mbt are also capable of binding H4K20 in its di-methylated state, ChIPs were also carried out to assess the levels of H4K20me2 at *swa* and *nos* promoters (Figure 4.32 B). It has been shown previously that H4K20me2 is the most abundant form of histone H4 in *Drosophila* as well as in mammals constituting 85-90% of total H4 (Schotta et al., 2008; Yang et al., 2008). Correspondingly, H4K20-me2-specific ChIPs showed robust signals for both *swa* and *nos* promoters and the two control regions relative to IgG signals (Figure 4.32 B). Knockdown of dPR-Set7 resulted in a partial loss of H4K20me2 levels at all four genomic regions. By comparison H4K20me2 levels differed by a factor of less than 3 between *swa*, *nos*, *actin* and intergenic region and were lowest at LINT target genes.

In conclusion, the H4K20me2 modification is detectable at target gene promoters. However, probably due to the abundance of this mark it is likely to be uniformely high along the genome and therefore H4K20me2 is also present at control regions that are not bound by LINT.

### 4.3.3 Derepression of LINT target genes is accompanied by changes in H3K4 methylation and H4 acetylation levels

Nucleosome occupancy profiles on genomic loci of LINT target genes and dPR-Set7 RNAi experiments demonstrated that chromatin compaction and dPR-Set7-dependent recruitment to H4K20me1 can be neglected as a major LINT repression mechanism.

The LINT complex does not appear to contain histone-modifying enzymes as stable subunits. Even though dLsd1 co-precipitated with dLint-1, the histone demethylase did not co-fractionate with the LINT subunits upon ion exchange chromatography (Figures 4.13, 4.14 and 4.17). The data about association of the histone deacetylase dRpd3 with LINT are more complex, since dRpd3 interacts efficiently with both dL(3)mbt and dLint-1 in immunoprecipitations carried out from S2, Kc167 or embryo nuclear extracts and is not clearly separated from the LINT subunits upon fractionation of Kc167 nuclear extract (Figures 4.2, 4.13, 4.14 and 4.17). However, dRpd3, as well as dLsd1, did not co-precipitate with dLint-1 from larval brain extract (Figure 4.19), suggesting that dRpd3 might be associated with LINT in a tissue-specific manner.

Although the LINT complex is devoid of histone modifier proteins, it was still conceivable that changes in histone modifications are involved in the regulation of LINT target genes. Therefore, changes of various histone marks were investigated by ChIP upon co-depletion of dL(3)mbt and dLint-1 in Kc167 cells by dL(3)mbt RNAi treatment (Figure 4.22), which leads to the disassembly of the complex (Figure 4.16) and a strong derepression of target genes (Figure 4.24). In the following, ChIP results are shown exemplary for *swa* as a direct target of LINT. Results obtained from analysis of the *nos* gene were comparable (not shown).

In EGFP dsRNA-treated control cells, H3K4me2 and H4 acetylation (antibody specific for H4 peptide acetylated at K5, 8, 12 and 16) levels were higher in the *swa* promoter region, compared to a region 1.5 kb downstream of the *swa* TSS, overlapping with the *swa* ORF, and an unrelated intergenic region on chromosome arm 2R (Figure 4.33).

Upon knockdown of dL(3)mbt, a strong increase in H3K4me2 levels both at the promoter and within the ORF was observed. Additionally, acetylation on H4 rose slightly at the promoter region, while it remained at low levels within the transcribed region. Both di-methylation of H3K4 and acetylation of H4 were not significantly changed upon dL(3)mbt depletion at the intergenic region, demonstrating the specificity of detected changes on the *swa* gene concomitant with derepression of transcription.

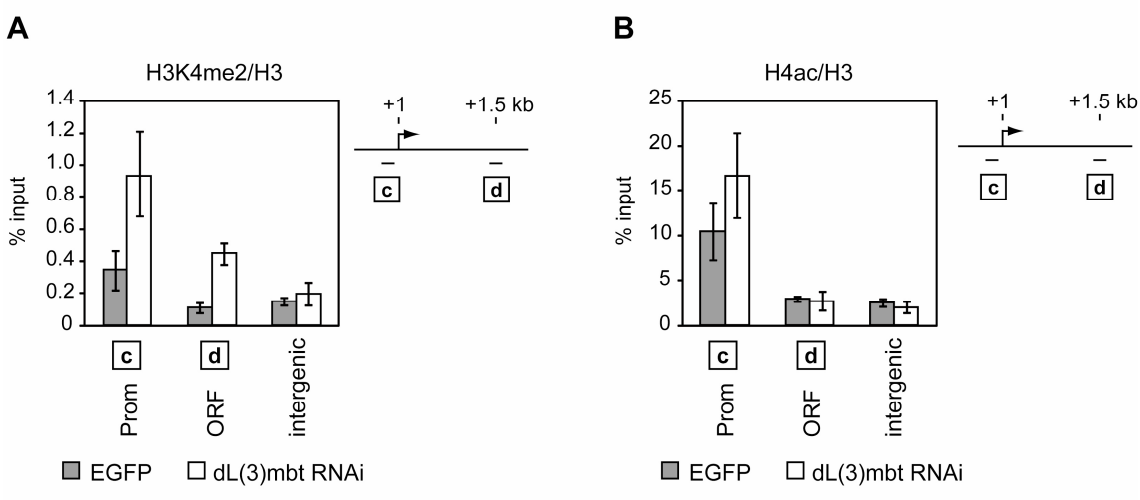


**Figure 4.33: LINT coordinates H3K4 methylation and H4 acetylation levels.** Kc167 cells were treated with dsRNA directed against EGFP (control) or dL(3)mbt. (A) ChIPs were carried out with α-H3K4me2 and α-H3 antibodies. (B) ChIPs were performed with α-H4ac and α-H3 antibodies. (A) and (B): Ratio of H3K4me2 or H4ac and H3 ChIP signals (mean values of qPCR triplicates as % input) is shown for *swa* promoter (c), *swa* ORF region (d) and an unrelated intergenic region, as indicated. The positions of the amplified *swa* regions relative to the TSS are depicted schematically on the right.

Taken together, derepression of LINT target genes is accompanied by elevated levels of histone marks associated with active transcription: A strong increase of H3K4me2 was observed, both at the promoter and within the ORF region. Additionally, H4 acetylation increased moderately in the promoter region of *swa*. These observations are in good agreement with LINT target genes being activated upon removal of the repressor complex.

### 4.3.4 Derepression of LINT target genes is accompanied by a decrease in H3K27me3 levels

The investigation of histone modification levels before and after derepression of LINT target genes in Kc167 cells did not only reveal a gain in active histone modifications (H3K4me2 and H4ac), but also a loss of the repressive histone mark H3K27me3 (Figure 4.34). In control cells, H3K27me3 levels were elevated in the transcribed region of *swa*, compared to the *swa* promoter (Figure 4.34 A). While H3K27me3 remained unchanged at the promoter, the modification declined strongly within the ORF of *swa*. Similar results were obtained using two independent H3K27me3-specific antibodies (Figure 4.34 A, left and right panels).

The enzyme that catalyses tri-methylation of H3K27 is the PcG protein Enhancer of zeste (E(z)) (Czermin et al., 2002; Kuzmichev et al., 2002). Correspondingly, depletion of E(z), which was controlled by Western blot (Figure 4.36 A), resulted also in a reduction of H3K27me3 levels in the transcribed region of *swa*, confirming the specificity of the H3K27me3 ChIP results (Figure 4.34 A). Whereas depletion of the H3K27 methylase E(z) led to a strong reduction of the H3K27me3 signal in Western blot analysing acid-extracted histone samples, dL(3)mbt RNAi did not decrease H3K27 tri-methylation levels in a global manner (Figure 4.34 B).

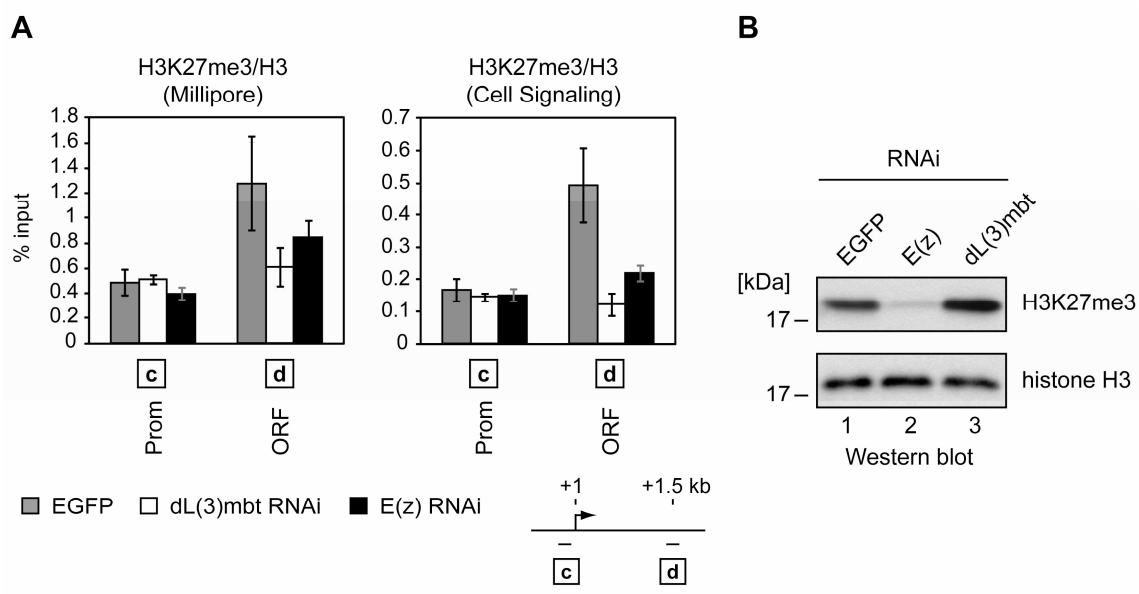


**Figure 4.34: Derepression of LINT target genes is accompanied by a decrease in H3K27 methylation in the transcribed region.** Kc167 cells were treated with dsRNA directed against EGFP (control), dL(3)mbt or E(z). (A) ChIPs were carried out with H3K27me3- and H3-specific antibodies. α-H3K27me3 antibodies were from Millipore (left panel) or Cell Signaling (right panel). Ratios of H3K27me3 and H3 ChIP signals (mean values of qPCR triplicates as % input) are shown for *swa* promoter (c) and ORF (d) regions. The positions of the amplified *swa* regions relative to the TSS are illustrated schematically on the right. (B) Acid extracted histones were analysed by Western blot using antibodies as indicated on the right. Western blot against histone H3 served as a loading control.

The reduction of H3K27me3 levels, mediated by dL(3)mbt/dLint-1 depletion and derepression of LINT regulated genes, raised the possibility that LINT interacts with the E(z) methylase. To address this hypothesis, nuclear extract from Kc167 cells was immunoprecipitated with dLint-1- (Figure 4.35 A) or E(z)-specific (Figure 4.35 B) antibodies. Although dLint-1 and dL(3)mbt were efficiently co-precipitated with the

dLint-1 antibody, no association of E(z) was detected (Figure 4.35 A, lane 2). Vice versa, E(z) antibody did not co-precipitate dL(3)mbt or dLint-1 above background levels (Figure 4.35 B, compare lanes 2 and 3). These results suggest that the effect of LINT depletion on H3K27me3 levels is not due to a direct interaction of LINT with E(z).

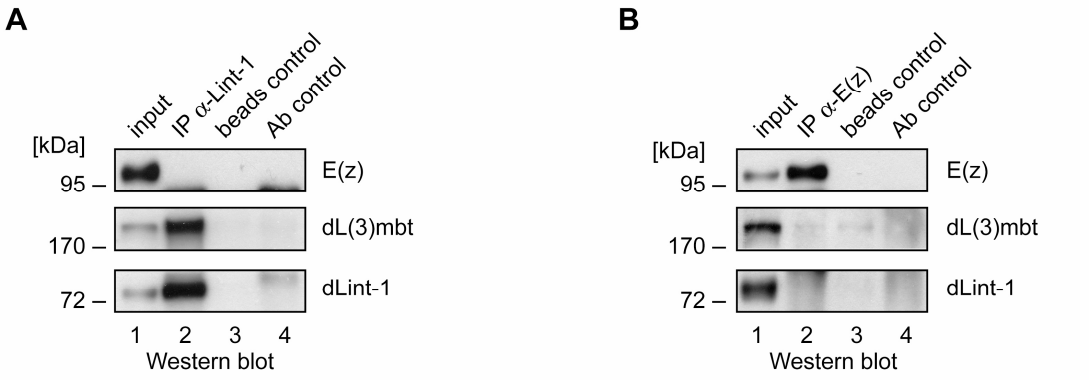


**Figure 4.35: LINT and E(z) do not co-immunoprecipitate in Kc167 cells:** (A) Nuclear extract from Kc167 cells was precipitated with ProtG beads loaded with α-dLint-1 antibody (A, lane 2), with α-E(z) 3TAF antibody (B, lane 2) or with no antibody (beads control, lanes 3). Immunoprecipitates were analysed by Western blot as indicated on the right.. Ab control: Contained E(z)- or dLint-1-specific antibody (lanes 4). Input: 5% of nuclear extract (lanes 1).

To confirm the presence of E(z) at LINT target genes, which was indicated by the H3K27me3 decrease upon E(z) depletion within the *swa* transcribed region, ChIP analysis was carried out using an E(z)-specific antibody (Figure 4.36). To demonstrate the specificity of the antibody used, E(z) was depleted in Kc167 cells using RNAi.

Western blot analysis of RNAi-treated cells confirmed that E(z) protein was depleted significantly (Figure 4.36 A). According to elevated levels of H3K27me3 1.5 kb downstream of the TSS compared to the promoter region, the E(z) antibody also precipitated more DNA in the transcribed region than in the promoter (Figure 4.36 B). In line with E(z) being associated with LINT target genes, E(z) ChIP signals were reduced upon RNAi knockdown both in promoter and ORF regions. In contrast, the knockdown of E(z) did only affect H3K27me3 levels within the transcribed region (Figure 4.34). Surprisingly, however, in dL(3)mbt RNAi cells (Figure 4.36 A) E(z) levels did not decrease, although the dL(3)mbt knockdown resulted in a significant loss of H3K27me3 at the *swa* gene (Figure 4.34).

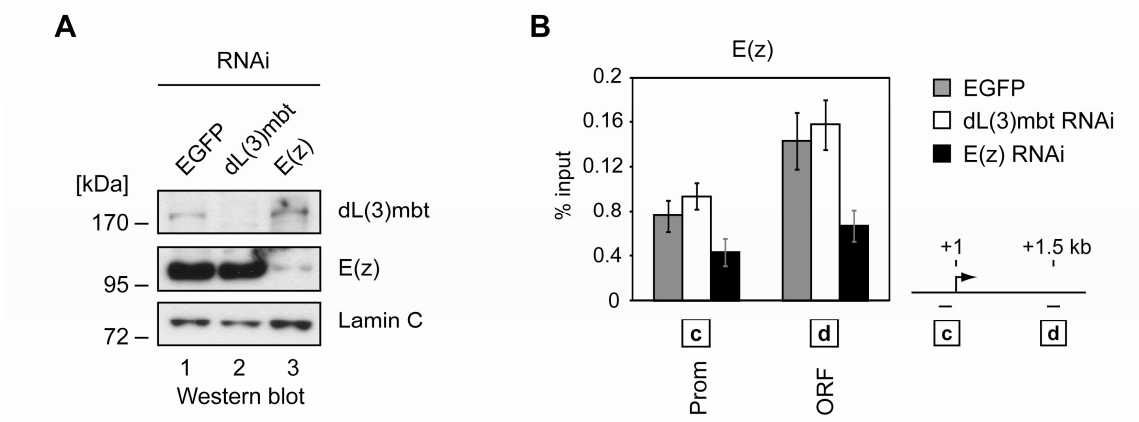


**Figure 4.36: E(z) is present at the *swa* target gene even in the absence of LINT.** Kc167 cells were treated with dsRNA directed against EGFP (control), dL(3)mbt or E(z). (A) Nuclear extracts were analysed by Western blot using antibodies as indicated. Western blot against Lamin C served as a loading control. (B) ChIPs were carried out using α-E(z) antibody (3TAD). Immunoprecipitated DNA was quantified by qPCR using primers against *swa* promoter and ORF regions. Mean values are expressed as % input. The positions of the amplified *swa* regions relative to the TSS are depicted schematically on the right.

In summary, derepression of LINT target genes results in a reduction of the E(z)-mediated repressive histone mark H3K27me3 in the transcribed region. Since E(z) binding is not affected by dL(3)mbt/dLint-1 co-depletion, there must be other mechanisms by which E(z) activity is inhibited or the balance of H3K27 methylation and demethylation is shifted towards the latter.

### 4.3.5 Histone-modifying enzymes are dispensable for maintenance of stable repression of LINT target genes

There is an ongoing debate in the chromatin field on whether histone modification changes are the cause of biological responses or rather the consequences of these processes, such as transcription or nucleosome remodelling (Henikoff and Shilatifard, 2011).

Therefore, the fact that LINT does not contain histone-modifying activities, however, the derepression of LINT target genes was accompanied by increased levels of activating (H3K4me2, H4ac) and a decrease in repressive (H3K27me3) histone modifications, raised the question if the loss of the corresponding enzymatic activities (dLsd1, dRpd3 and E(z), respectively) was sufficient to produce the observed changes in histone marks and transcription levels of LINT target genes. To address this issue,

first dLsd1 and E(z) were depleted by RNAi in Kc167 cells (Figure 4.36 A and 4.37 A, middle panels). To determine if dLsd1 depletion was affecting H3K4 methylation levels on LINT target genes, ChIPs targeting H3K4me2 were carried out after dLsd1 knockdown in comparison to dL(3)mbt or EGFP RNAi-treated cells (Figure 4.37 B). Again dL(3)mbt RNAi led to a specific increase of H3K4 di-methylation both in the promoter and the transcribed regions of *swa* and *nos*. dLsd1 depletion, however, failed to increase H3K4me2 levels, even though the knockdown seemed very efficient, judged by Western blot analysis (Figure 4.37 A). In contrast, knockdown of E(z) resulted, as shown above, in a reduction of H3K27me3 levels in the *swa* transcribed region (Figure 4.34).

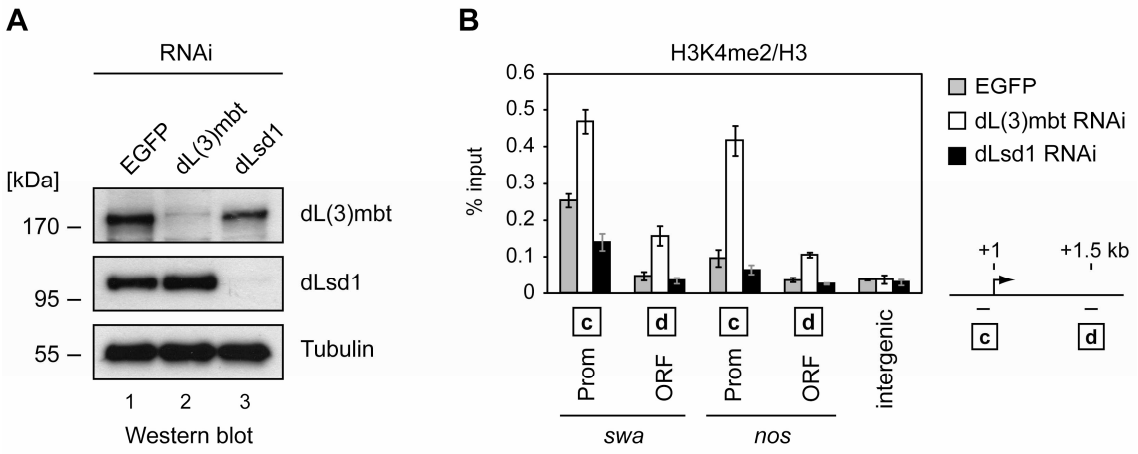


**Figure 4.37: H3K4me2 levels of LINT target genes do not increase upon dLsd1 knockdown.** Kc167 cells were treated with dsRNA directed against EGFP (control), dL(3)mbt and dLsd1. (A) Nuclear extracts were analysed by Western blot using antibodies as indicated. Detection of β-tubulin served as a loading control. (B) ChIPs were carried out using H3K4me2- and H3-specific antibodies. Immunoprecipitated DNA was quantified in triplicate by qPCR. Ratios of H3K4me2 and H3 ChIP signals (mean values of qPCR triplicates as % input) are shown for promoter (c) and ORF (d) regions of *swa* and *nos* and an unrelated intergenic region, as indicated. The positions of the amplified promoter and ORF regions relative to the TSS are depicted schematically on the right.

The opposite impacts of dLsd1 and E(z) depletion on their corresponding histone modifications, raised the question whether their knockdowns would have any consequences for the transcription of LINT target genes (Figure 4.38 and 4.39).

Even though the knockdown of E(z) resulted in a global loss of H3K27me3 levels and the decrease of this mark on the *swa* gene was comparable to the effect of dL(3)mbt

RNAi (Figure 4.34), LINT target genes were only mildly derepressed. The modest upregulation ranged from approximately 1.5- (*piwi*, *ea* and *tor*) to 2.5-fold (*swa*).

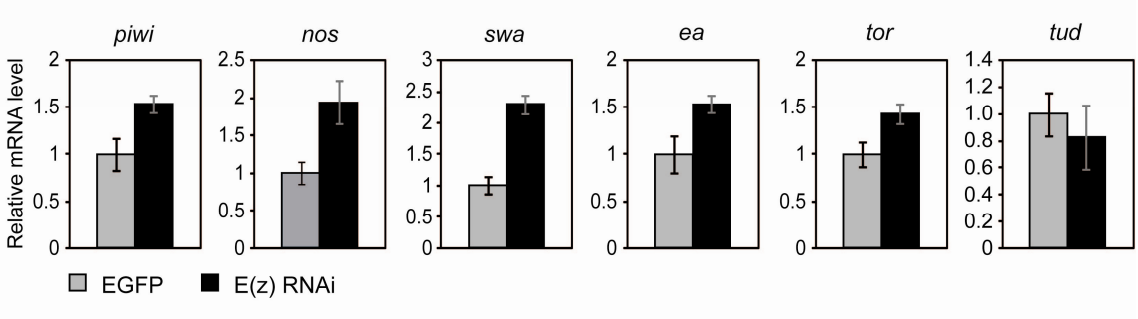


**Figure 4.38: LINT target genes are mildly derepressed upon E(z) depletion:** Kc167 cells were treated with dsRNA directed against EGFP (control) and E(z). Expression of LINT target genes was determined by RT-qPCR. Transcription in EGFP RNAi-treated cells was set to 1. For knockdown efficiency compare Western blots in Figure 4.36 A.

Next, all factors that associated with dLint-1 in the FLAG affinity purification, including dCoREST, dRpd3 and dLsd1 (Figure 4.12), were depleted by RNAi in Kc167 cells (Figure 4.39 A) to investigate which of them contribute to the repression of LINT target genes aside from dL(3)mbt and dLint-1. As shown before (Figure 4.24) dL(3)mbt and dLint-1 knockdown led in 6 out of 7 cases to a strong derepression of germline-specific target genes (dL(3)mbt RNAi: 10-fold (*zpg*) to 40-fold (*nos*); dLint-1 RNAi: 5-fold (*tor*) to 20-fold (*piwi*)) (Figure 4.39 B). In addition, the transcription of *bam* was up-regulated moderately, but significantly (dL(3)mbt RNAi: 3.5-fold; dLint-1 RNAi: 2.5 fold). Even though the depletion of dCoREST resulted only in a minor decrease of dCoREST protein levels (Figure 4.39 A, lane 3), the majority of LINT target genes were severely derepressed (dCoREST RNAi: 10-fold (*zpg*) to 20-fold (*piwi*)) (Figure 4.39 B). Again, in agreement with the effects of dL(3)mbt and dLint-1 RNAi, *bam* expression levels were up-regulated only 3-fold upon dCoREST knockdown. Therefore in most cases fold changes of deregulation of LINT target genes upon dCoREST RNAi were comparable with fold changes upon dL(3)mbt or dLint-1 depletion. One exception was the *ea* gene that was upregulated 13- and 30- fold after dLint and dL(3)mbt RNAi, respectively, but only 3-fold after dCoREST knockdown. In summary, these results revealed that all three LINT subunits are required for effective target gene silencing.

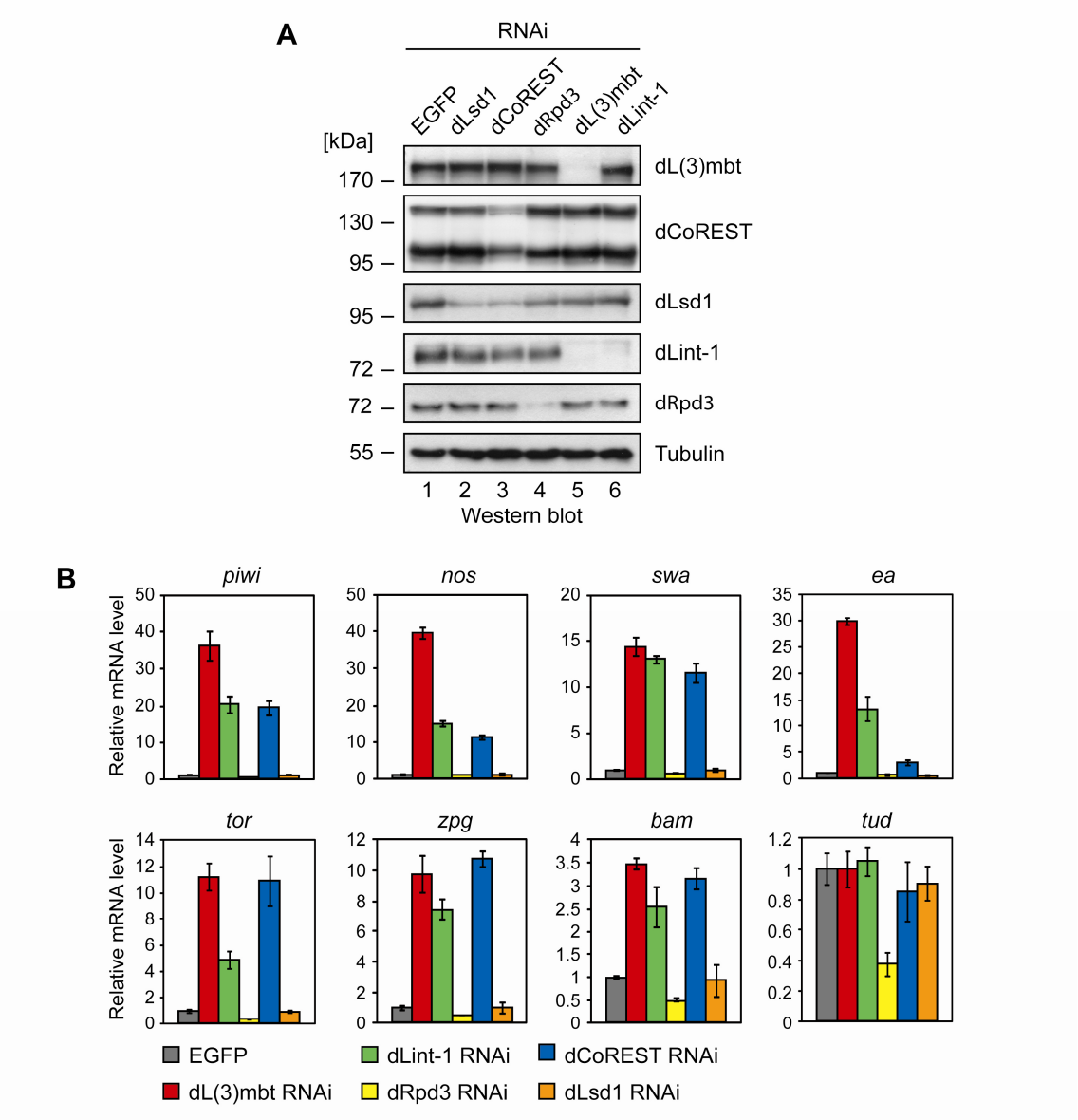


**Figure 4.39: LINT non-enzymatic subunits, but not the histone-modifying dLsd1 and dRpd3 enzymes, are required for repression of germline-specific target genes:** Kc167 cells were treated with dsRNA directed against EGFP (control), dLsd1, dCoREST, dRpd3, dLint-1 and dL(3)mbt. (A) Nuclear extracts were analysed by Western blot using antibodies as indicated. The detection of β-tubulin served as a loading control. (B) Expression of LINT target genes was determined by RT-qPCR. Analysis of *tud* served as a negative control. Transcription in EGFP RNAi-treated cells was set to 1.

Despite the fact that depletion of dLsd1 and dRpd3 appeared to be efficient judged by Western blot analysis (Figure 4.39 A, lanes 2 and 4), neither of them led to an up-regulation of LINT-specific target genes (Figure 4.39 B).

Interestingly, upon dCoREST knockdown it was noticeable that protein levels of dLsd1 were affected by a decrease that was comparable to the specific knockdown of dLsd1

itself (Figure 4.39, compare lanes 2 and 3). This is likely to be due to protein instability of dLsd1 upon loss of dCoREST. However, since dCoREST and dLsd1 do not co-exist in the LINT complex, this effect can be presumably attributed to the presence of these factors in other independent protein complexes that was already predicted from other experiments (see Figures 4.14, 4.15 and 4.17). By contrast, dL(3)mbt and dLint-1 protein levels remained unaltered upon dCoREST RNAi (Figure 4.39 A, compare lane 3).

Taken together, these results suggest that only the non-enzymatic LINT subunits, dL(3)mbt, dLint-1 and dCoREST, but not the histone-modifying factors dLsd1 and dRpd3 are required for stable repression of germline-specific target genes. This further implies that the histone modification changes of H3K4 methylation and H4 acetylation are likely to be consequences of active transcription taking place.

### 4.3.6 dL(3)mbt or dLint-1 promoter recruitment is sufficient for reporter gene silencing

The repression of the germline-specific LINT target genes, tested in this study, is strictly dependent on the presence of the three subunits, dL(3)mbt, dLint-1 and dCoREST. In contrast, the histone-modifying activities of dPR-Set7, E(z), as well as dLsd1 and dRpd3, of which the latter two are associated with dLint-1 or dL(3)mbt, are not required to maintain stable repression of these genes. The core LINT complex itself does not display any chromatin-modifying activities, but shows a strong preference to bind to the promoter regions of regulated genes (Figure 4.28). These observations raised the possibility that LINT represses transcription by sterically restricting the access for RNA polymerase II and/or activating transcription factors to promoter sequences.

To test this hypothesis, a LexA-dependent, plasmid-based reporter gene assay was used in order to recruit LINT subunits to a LexA binding site containing promoter upstream of a reporter gene encoding Firefly luciferase (Figure 4.40 A; Thompson and Travers, 2008). In the presence of LexA DNA binding domain alone the luciferase reporter gene is expressed at basal levels from the *Hsp70* promoter. To determine how dL(3)mbt and dLint-1 modulate transcription when tethered to the actively transcribed promoter of the reporter gene, both proteins were transiently expressed as LexA fusion proteins in Kc167 cells using increasing amounts of the pAc5.1 expression vectors (Figure 4.40 B). Immunoblotting with a LexA-specific antibody revealed that dL(3)mbt-LexA, as well as

dLint-1-LexA, were expressed at similar levels as LexA alone upon transfection of 500 or 1000 ng expression vector (panels 5 and 6). When less vector was used, expression was hardly detectable by Western blot (panels 1 to 4). Recruitment of either dL(3)mbt-LexA or dLint-1-LexA fusion protein to the reporter gene consistently resulted in a robust and dose-dependent repression of the *luciferase* gene (Figure 4.40 C) compared to LexA alone. The repressive activity of dL(3)mbt-LexA (upper panel) and dLint-1-LexA (lower panel) ranged from 4- to 12- and 2- to 10-fold, respectively. Comparison of the repressive activities with expression levels showed that even protein amounts of dL(3)mbt and dLint-1 LexA-fusions close or below the detection limit of Western blot were capable of repressing the reporter gene (Figure 4.40 B and C).

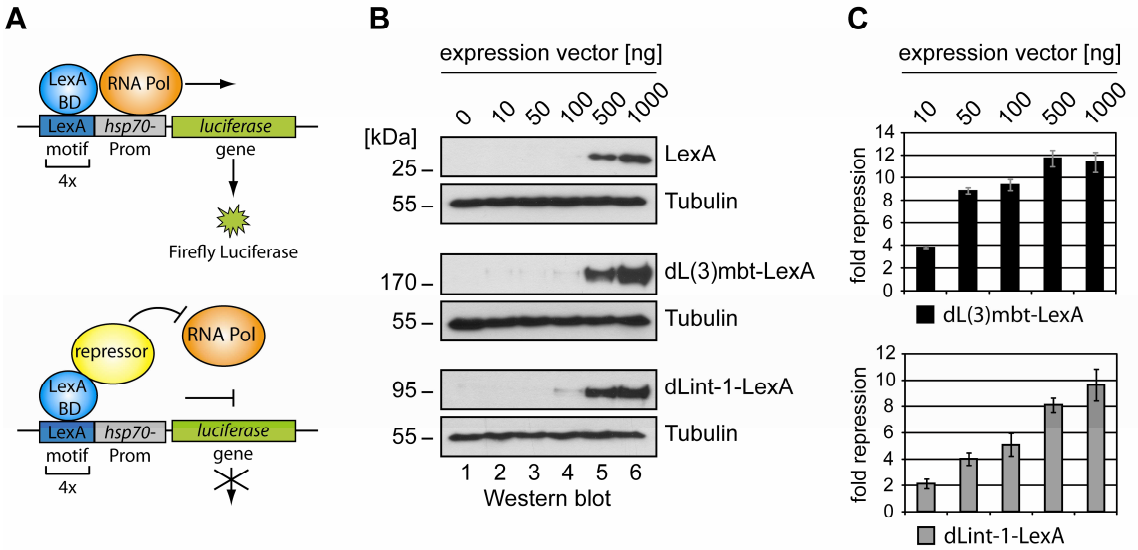


**Figure 4.40: dL(3)mbt and dLint-1 repress a luciferase reporter gene in a dose-dependent manner.** (A) Upper panel: LexA luciferase reporter gene assay (Thompson and Travers, 2008): The DNA binding domain of LexA (LexA DB) alone binds to sequence-specific recognition motifs (LexA motifs) upstream of the reporter gene. The *luciferase* gene, which is under the control of the *Hsp70* promoter, is expressed by RNA polymerase at basal levels. Firefly Luciferase protein is synthesised and its enzymatic activity can be measured. Lower panel: When a transcriptional repressor is fused to LexA, the fusion protein is tethered to the LexA motifs and efficient transcription of the *luciferase* gene is hindered (lower panel). (B) LexA (upper panels), dL(3)mbt-LexA (middle panels) and dLint-1-LexA (lower panels) were expressed transiently in Kc167 cells. Expression levels in the nuclear fraction of Kc167 cells were monitored by Western blot as indicated on the right using a LexA-specific antibody. Detection of β-tubulin served as a loading control. (C) Repressor activities of dL(3)mbt-LexA (upper panel) and dLint-1-LexA (lower panel) on the transcription of the *luciferase* reporter gene relative to LexA only samples. (B) and (C) The amount of expression vector used for transfections is denoted on top.

### 4.3.7 Reporter gene repression by dL(3)mbt and dLint-1 depends on LINT subunits

To unravel to which extent the integrity of the LINT complex plays a role for dL(3)mbt-LexA and dLint-1-LexA to function as repressors, dL(3)mbt, dLint-1 and dCoREST were depleted by RNAi prior to the luciferase reporter gene assay (Figure 4.41). In addition to the knockdown of LINT complex subunits, cells were treated with dsRNA directed against dLsd1 and other subunits of histone-modifying complexes, such as the H3K9 methyltransferase G9a and the Polycomb group proteins Pc, dRING, E(z) and Suz(12) (Figure 4.41 A and data not shown). The efficiencies of knockdowns were controlled by Western blot as far as antibodies were available (Figure 4.41 B) or by RT-qPCR (Figure 4.41 C).

As expected, since dsRNA probes were directed against sequences in the coding regions, RNAi against dL(3)mbt or dLint-1 had the strongest effects on dL(3)mbt-LexA or dLint-1-LexA, respectively, in terms of derepression of the reporter gene (Figure 4.41 A). The repressive activity of dL(3)mbt-LexA was reduced by a factor of at least 32, compared to mock and EGFP RNAi-treated cells, while repression by dLint-1-LexA was diminished approximately 8-fold. This result served as a positive control to confirm that RNAi treatment was effective within the chosen time frame.

In contrast to dL(3)mbt and dLint-1 knockdown, RNAi-mediated depletion of either G9a or Pc protein, both of which have an established function in transcriptional repression, did not abrogate repression of the reporter gene mediated by dL(3)mbt-LexA or dLint-1-LexA. Similarly, knockdown of dLsd1 had no or only a minor effect on dLint-1-LexA- or dL(3)mbt-mediated repression.

However, depletion of the LINT subunits dL(3)mbt and dCoREST led to a strong decrease of the repressive activity on the reporter by dLint-1-LexA of approximately 3-fold compared to mock and EGFP controls (Figure 4.41 A, right panel). Vice versa RNAi treatment against dLint-1 and CoREST also resulted in a partial derepression of the reporter gene in the presence of dL(3)mbt-LexA (Figure 4.41 A, left panel), but to a lesser extent compared with the effect on dLint-1-LexA upon LINT depletion.

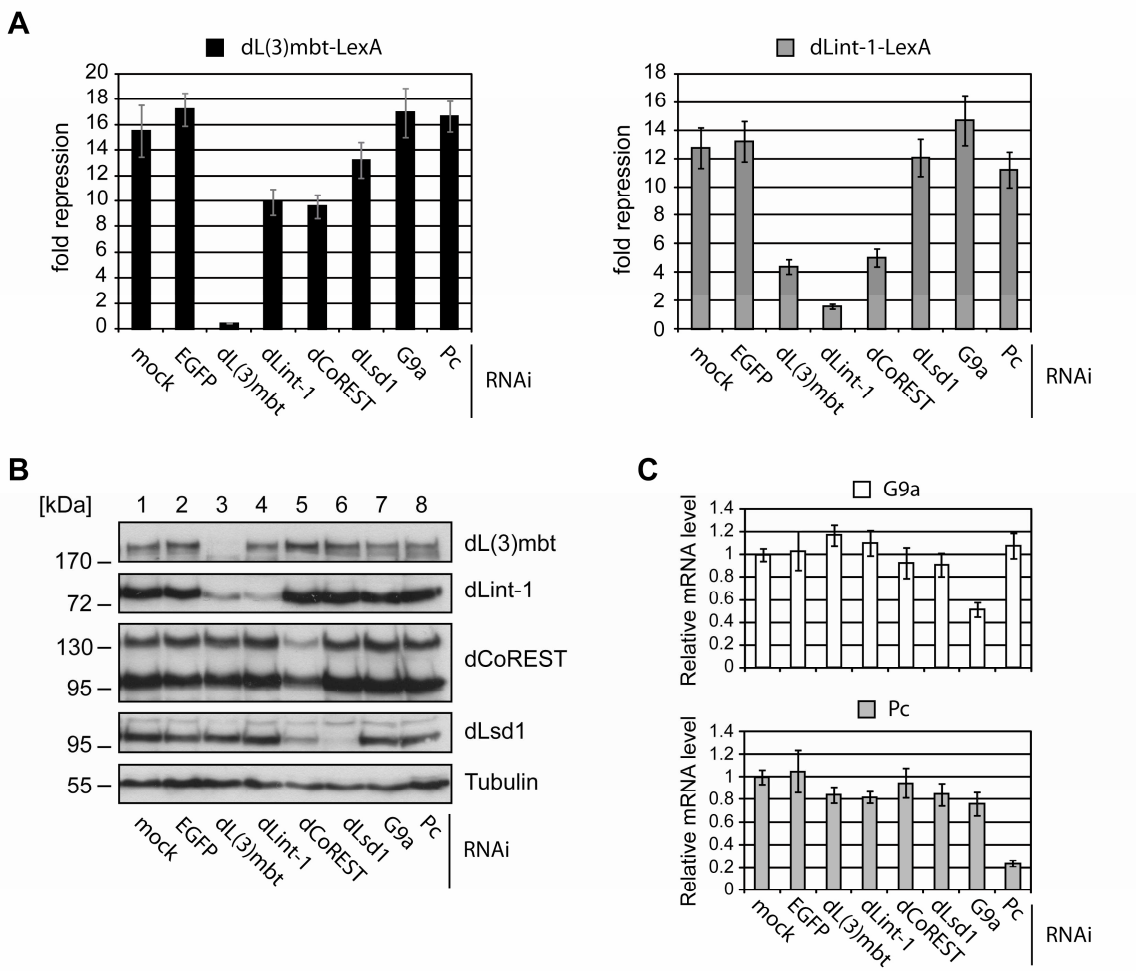


**Figure 4.41: The repressor activities of dL(3)mbt and dLint-1 is dependent on residual LINT subunits in a luciferase reporter gene assay.** (A) Kc167 cells were treated with dsRNA against various co-repressor proteins as indicated on the bottom. As negative controls cells were treated with no dsRNA (mock) or with dsRNA directed against EGFP. Luciferase reporter gene assays were carried out 48h after RNAi treatment. Repressor activity of dL(3)mbt-LexA (left panel) and dLint-1-LexA (right panel) on the *luciferase* reporter gene transcription compared to LexA only controls. (B) The knockdown efficiencies on endogenous dL(3)mbt, dLint-1, dCoREST and dLsd1 (as indicated on the right) in dsRNA treated cells (denoted below) were confirmed by Western blotting. (C) The knockdown efficiencies of G9a (upper panel) and Pc (lower panel) in RNAi-treated cells (denoted below) on the level of mRNA transcripts were monitored by RT-qPCR. The transcription level in untreated cell (mock) was set to 1.

Quantification of the effects of RNAi against LINT revealed that the repressive activity of dL(3)mbt-LexA was reduced from 16- (mock treated) or 17-fold (EGFP RNAi) to 10-fold (dLint-1 or dCoREST RNAi). In this context one might speculate that the dL(3)mbt-LexA fusion protein, which upon dLint-1 and dCoREST RNAi retains significant fold repression on the reporter, possesses an intrinsic activity to repress transcription that is independent on the LINT complex association. Furthermore, it is

noteworthy that the knockdown of dCoREST results additionally in decreased Lsd1 protein levels (see Figure 4.39). However, since dLsd1 RNAi did not release repression of dL(3)mbt and dLint-1, it can be concluded that the effects seen upon RNAi are dCoREST-specific. Surprisingly, the effect of dCoREST RNAi on repression by dL(3)mbt-LexA and dLint-1-LexA was comparable to dLint-1 and dL(3)mbt depletion, respectively, even though the knockdown, especially of the dCoREST-M, isoform appeared to be relatively inefficient as judged by Western blot (Figure 4.41 B).

In conclusion, both dL(3)mbt and dLint-1 displayed a robust and dose-dependent repressive activity on a luciferase reporter gene when tethered to its promoter in a LexA-dependent manner. Moreover, RNAi depletion experiments revealed that all three LINT subunits are required for maximal transcriptional repression when recruited to the promoter of a reporter gene, whereas dLsd1 and other repressive chromatin-associated proteins are dispensable for efficient repression.

# 5 Discussion

In this doctoral thesis, an interaction between dL(3)mbt and the HDAC dRpd3 has been identified that was found to play a role in the process of chromatin maturation (Scharf et al., 2009).

Moreover, LINT, a novel dL(3)mbt complex, has been purified by affinity purification and classical biochemical chromatography. Microarray analysis identified LINT target genes on a genome-wide level, which revealed that a subset of LINT targets constitutes germline-specific genes. An analysis of these regulated genes determined important molecular features of the repression mechanism by LINT.

## 5.1 dL(3)mbt is in a protein complex with dRpd3

### 5.1.1 The MBT domains as a protein interaction module

*dL(3)mbt interacts with the deacetylase dRpd3*

Both histone deacetylases and members of the MBT domain protein family have been implicated in chromatin compaction and transcriptional repression of genes. The assumption that dL(3)mbt as a MBT domain protein could cooperate with HDAC activity, proved to be indeed true. Both recombinant and endogenous dL(3)mbt was associated with significant amounts of HDAC activity (Figure 4.1). In agreement with this, dL(3)mbt co-immunoprecipitated dRpd3 (Figure 4.2), which can target various acetylated histone lysines (Rundlett et al., 1996). However, dL(3)mbt did not interact with dHDAC3, another member of the HDAC enzyme family in *Drosophila*. Nevertheless, an additional association with dHDAC4 and dHDAC6 cannot be excluded at this point, since antibodies against these enzymes were not available to test for a possible interaction.

*The MBT domains as a protein-protein interaction domain*

In the past, the MBT domains have been studied mainly in terms of their ability to function as histone tail binding modules (see introduction 2.2.1). A specific recognition of methylated H4K20 histone peptides was also confirmed for the MBT domains of dL(3)mbt (Figure 4.30 B). Therefore it is intriguing that the major dRpd3 interaction domain in dL(3)mbt was mapped also to the module of the three MBT domains (Figure

4.3 C). A recent publication provided good evidence that the interaction between MBT domain proteins and HDACs is highly conserved from *Drosophila* to man. The human L3MBTL2 protein has been reported to specifically associate with HDAC3 (Yoo et al., 2010). In accordance with the mapping data presented in this study, a construct containing only the four MBT domains of L3MBTL2 interacted with HDAC3.

Until recently, the methyl binding specificity of the MBT domains has been only studied in terms of binding to histone tails. However, for L3MBTL1 two studies have suggested a mono-methylation-dependent interaction with p53 (West et al., 2010) and pRB (Saddic et al., 2010), respectively. In both proteins specific lysine residues (pRB-K860 and p53-K382) have been identified that promote binding of L3MBTL1. The interaction of L3MBTL1 with methylated p53 appears to mediate repression of p53 target genes (such as p21) in the absence of DNA damage (West et al., 2010).

The specific interaction of the 3MBT region with dRpd3 and the fact that other interactions between a MBT domain protein and non-histone proteins are methylation-dependent, raises the possibility that dL(3)mbt binds to a dRpd3 product that has been post-translationally modified by methylation. This hypothesis has to be elucidated in future experiments. To this end one could investigate whether the dL(3)mbt-dRpd3 interaction still takes place upon treatment of cells with S-adenosyl-L-homocysteine (SAH). SAH is the product of all methyltransferases that use S-adenosyl-methionine (SAM) as a co-factor and acts as a competitive inhibitor for the methyl-transferase enzymatic activity.

### 5.1.2 A potential role of dL(3)mbt during chromatin assembly

*Histone modification changes during chromatin maturation*

As cells divide the DNA content doubles in S-phase of each cell cycle. The process of DNA replication entails the propagation of the chromatin structure to the daughter cells. The progression of the replication machinery temporarily disassembles the nucleosomes in front of the replication fork (Jackson and Chalkley, 1985; Sogo et al., 1986). Following replication, parental histones, as well as newly synthesised histones are re-assembled onto the two nascent DNA strands in a random manner, which requires the action of so called histone chaperones and chromatin remodelers (Avvakumov et al., 2011). The newly synthesised histones carry a specific histone modification pattern that distinguishes them from the histones found in mature chromatin (Loyola et al., 2006).

For instance, newly synthesised H4 has been shown to be acetylated at positions K5 and K12 (Sobel et al., 1995). Rapidly after deposition this acetylation pattern on H4 is removed.

The dynamics of histone modification changes during chromatin assembly were investigated by A. Scharf in the group of A. Imhof in an *in vitro* chromatin assembly assay (Scharf et al., 2009). This assay makes use of an extract obtained from *Drosophila* pre-blastoderm embryos that facilitates the efficient assembly of cloned DNA into chromatin (Becker and Wu, 1992). Immediately upon deposition of the histones, H4 becomes mono-methylated at K20, which is necessary for efficient deacetylation of the two acetylation marks at K5 and K12 (Scharf et al., 2009).

*A potential role of dL(3)mbt and dRpd3 during chromatin maturation*

As dL(3)mbt harbours the MBT domains as a reader module for recognition of mono-methylated K20 (this study and Scharf et al., 2009) dL(3)mbt was a candidate for the association with H4K20me1 and the recruitment of HDAC activity to newly assembled chromatin. In line with a possible role of the dL(3)mbt-dRpd3 complex (this study) during chromatin maturation, it gets efficiently recruited to newly assembled chromatin concomitant with H4K20 methylation and H4 deacetylation (Scharf et al., 2009). The association, however, is sensitive to the methyltransferase inhibitor SAH, suggesting that indeed association of dL(3)mbt-dRpd3 is dependent on H4K20 mono-methylation. Taken together, these data support a model, in which the mono-methylation of H4K20 marks properly assembled nucleosomes and recruits dL(3)mbt and dRpd3 HDAC activity, thereby contributing to the efficient deacetylation of the H4 tail required for chromatin maturation (Scharf et al., 2009).

The identification of the LINT complex raises the question, whether the dL(3)mbt-dRpd3 interaction and recruitment to newly assembled nucleosomes is independent of other dL(3)mbt complexes. Even though the core complex consists of only dL(3)mbt, dLint-1 and dCoREST a partial association with dRpd3 cannot be completely excluded (see 5.2.1). Therefore in terms of a role in chromatin maturation, a detailed analysis of composition of dL(3)mbt complexes in early embryos would be of special interest. So far the investigation of dL(3)mbt association in multi-protein complexes in *Drosophila* embryos by gel filtration and classical ion exchange chromatography was precluded by a weak and ‘smeary’ dL(3)mbt input signal (Figure 4.14).

*A role of MBT domain proteins in chromatin assembly*

In light of a possible role of dL(3)mbt in chromatin maturation, it is interesting that *l(3)mbt* mutant embryos display cell cycle defects, whereby the synchrony of nuclear divisions in the early embryo is disrupted (Yohn et al., 2003). Intriguingly, in mammals mono-methylation of H4K20 and the dL(3)mbt homologue L3MBTL1 have been implicated in the regulation of cell cycle. Thus, the depletion of PR-SET7, which causes a decrease in H4K20me1 levels, results in improper S-phase progression and replicative stress (Huen et al., 2008; Jørgensen et al., 2007; Tardat et al., 2007). The finding that PR-SET7 foci co-localise with sites of DNA synthesis supports a role of PR-SET7 and H4K20me1 directly at the replication fork (Tardat et al., 2007; Tardat et al., 2010). In line with an involvement of L3MBTL1 in DNA replication, L3MBTL1 was found to interact with several components of the DNA replication apparatus (Gurvich et al. 2010) and to be recruited to chromatin most prominently during S-phase (Koga et al., 1999). Just like PR-SET7, L3MBTL1 seems to be required for proper progression of the replication fork (Gurvich et al., 2010).

## 5.2 LINT – a novel chromatin-related protein complex

### 5.2.1 Identification of LINT as a high molecular weight complex

*The LINT complex is distinct from the Myb-MuvB/dREAM complex*

The gel filtration analysis of Kc167 nuclear extract (Figure 4.4) revealed that the bulk of dL(3)mbt is separated from the Myb-MuvB/dREAM complex-specific subunit RBF2 (Lewis et al., 2004; Korenjak et al., 2004). Therefore the data of this study strongly support the idea that LINT, the major dL(3)mbt complex purified from Kc167 cells, is biochemically independent of the Myb-MuvB/dREAM complex. The major conclusion from the biochemical analyses of the complex composition is that the LINT complex consists of three core subunits, the MBT domain protein dL(3)mbt, the previously uncharacterised protein dLint-1 and dCoREST (Figure 4.18). The latter is a known co-repressor protein, which assists Ttk88 to restrict expression of neuronal genes in non-neuronal tissues (Dallman et al., 2004).

However, the purification of dLint-1 using FLAG affinity purification co-purified in addition the H3K4me1/me2-specific demethylase dLsd1 (Rudolph et al., 2007; Shi et al, 2004) and the histone deacetylase dRpd3 (De Rubertis et al., 1996). In addition dLsd1

also co-precipitated with endogenous dLint-1, but in a rather inefficient manner compared to the input signal (Figure 4.14). Moreover, the combination of gel filtration analysis and sequential ion exchange chromatography of Kc167 nuclear extract revealed that the histone demethylase did not co-fractionate with the LINT subunits (Figures 4.15 and 4.17 C). In addition, the fractionation provides evidence that dLint-1 exists in at least one more protein complex, that is likely to contain dLsd1 but not dL(3)mbt (Figure 4.17 C).

*Possible association of dRpd3 with the LINT complex*

The biochemical data about the interaction of dRpd3 with LINT are less clear. Firstly, dRpd3 co-precipitated with both dL(3)mbt and dLint-1 in an efficient manner (Figure 4.2, 4.13 and 4.14). Secondly, even though the LINT subunits dL(3)mbt, dLint-1 and dCoREST got separated from several dRpd3 peaks (Figure 4.17 C, compare fractions 22, 28 and 36), the LINT-containing peak fraction was not devoid of dRpd3 (Figure 4.17 C, compare fraction 32). However, dRpd3, as well as dLsd1, did not co-precipitate with dLint-1 from larval brain extract, suggesting that LINT, at least in the larval brain, does not contain these histone-modifying proteins (Figure 4.19). Furthermore, although dRpd3 co-precipitated with dL(3)mbt and dLint-1 from nuclear extracts of cell lines, dRpd3 protein was dispensable for stable repression of LINT target genes (Figure 4.39). Nevertheless, it is conceivable that dRpd3 associates with LINT in a tissue-specific, developmental-specific or cell cycle-dependent manner. To test for this possibility it would be necessary to biochemically analyse the complex compositions of dL(3)mbt and dLint-1 complexes in different tissues, various developmental stages and in specific cell cycle stages.

*The size of the high molecular weight LINT complex*

The estimated molecular weight of the LINT complex, obtained by adding up the molecular weights of the single subunits dL(3)mbt (163 kDa), dLint-1, (67.9 kDa) and dCoREST (62.7 kDa), is approximately 300 kDa. Despite the theoretical molecular weight, however, LINT elutes from the gel filtration column sooner than expected, close to the void volume of 2 MDa (Figure 4.15).

In general, two major parameters determine the fractionation of proteins by gel filtration: the actual molecular weight and the three-dimensional shape of a protein or protein complex. Therefore, one possible reason that the calculated molecular weight of

the LINT complex does not correlate with the fractionation on the column might be an influence by the shape of the LINT complex. An alternative explanation could be that the LINT peak observed upon gel filtration does not correspond to a monomeric complex, but a dimer or even an oligomer of the complex. In fact, dL(3)mbt contains in its C-terminus an SPM domain that has been reported to facilitate homo- and hetero-dimerisation or oligomerisation (Kim et al., 2002; Kim et al., 2005; Peterson et al., 1997). This observation raises the question whether the SPM domain of dL(3)mbt can mediate dimerisation or oligomerisation of the LINT complex. Indeed, investigation of the role of the dL(3)mbt SPM domain in LINT supports its importance in the formation of oligomeric complexes (M. Reuter, diploma thesis, 2011). In this context it would be of great value to reconstitute the LINT complex biochemically *in vitro* using for example the MultiBac system for recombinant protein expression in Sf9 cells (Fitzgerald et al., 2006). This would facilitate to analyse the size of the purified wild-type complex, as well as an SPM deletion mutant, and compare it to the molecular weight of endogenous LINT in nuclear extract.

### 5.2.2 LINT complex composition

*L(3)mbt and CoREST complexes in Drosophila and mammals*

LINT is the first dL(3)mbt multi-subunit complex purified from *Drosophila*. Many other chromatin-related protein complexes that exist in *Drosophila* are also conserved in human. Exemplary are the complexes PRC2 (*Drosophila*: Czermin et al., 2002; Müller et al., 2002; human: Cao et al., 2002; Kuzmichev et al., 2002), dNuRD (*Drosophila*: Kunert et al., 2009; Reddy et al., 2010; human: Xue et al., 1998; Zhang et al., 1999) and dREAM (*Drosophila*: Korenjak et al., 2004; Lewis et al., 2004; human: Schmit et al., 2007).

However, the subunit compositions of the LINT complex and mammalian L3MBTL and CoREST protein complexes differ dramatically. On the one hand, L3MBTL1 co-precipitated pRB, HP1γ, H1B and core histones in a FLAG affinity purification (Trojer et al., 2007; Figure 5.1). None of these factors has been detected as dL(3)mbt or dLint-1 interacting proteins in the corresponding FLAG immunoaffinity purifications (Figures 4.6 and 4.12). On the other hand, all known CoREST complexes in the mammalian system that have been isolated from human cell lines contain LSD1 (also known as p110b or BHC110) as an integral subunit (You et al., 2001; Hakimi et al., 2003;

Lee et al., 2005; Shi et al., 2005). These purifications suggest that a core complex exists that is composed of CoREST, LSD1, HDAC1/2 and BHC80 (Figure 5.1). Additional proteins associated with this core include CtBP, BRAF35 and Zn-finger proteins (e.g. ZnF217, ZnF198). In *Drosophila*, an affinity purification of dLsd1 from nuclear extract of early (0-3 hr old) embryos identified the heterochromatin-associated factors HP1 and the H3K9 methyltransferase Su(var)3-9, as well as dRpd3 as interaction partners (Rudolph et al., 2007). However, also an interaction of dCoREST with dLsd1 and dRpd3 has been shown to be conserved in *Drosophila* previously (Dallman et al., 2004).

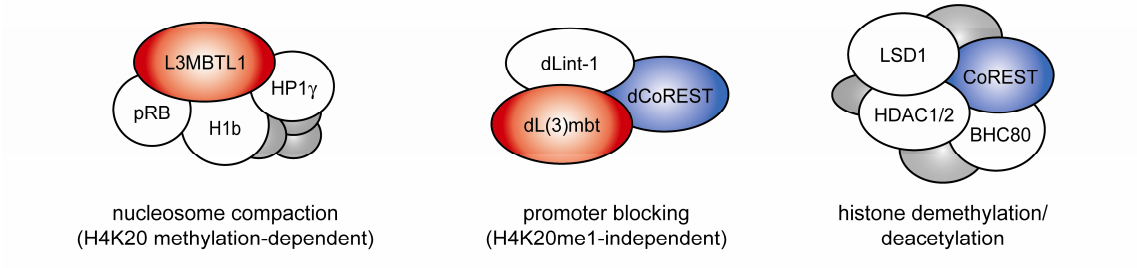


**Figure 5.1: L(3)mbt and CoREST complexes in *Drosophila melanogaster* and mammals.** Schematic representation of complex compositions of mammalian L3MBTL1 (left; Trojer et al., 2007), *Drosophila* LINT (middle) and mammalian LSD1/CoREST (right; Lee et al., 2005; Shi et al., 2005) complexes. Only core subunits are shown. Shared homologous subunits are indicated by color (red: L(3)mbt, blue: CoREST). Proposed repression mechanisms for each complex are indicated below.

*dLint-1 and dCoREST complexes in Drosophila aside from LINT*

This study provides further evidence that there are dCoREST complexes other than LINT. First, gel filtration analysis revealed that LINT only accounts for a fraction of dCoREST in nuclear extract of Kc167 cells (Figure 4.15). Second, a substantial amount of dCoREST-M and in fact the bulk of dCoREST-L splice variants are separated from LINT in extract fractionation by ion exchange chromatography (Figure 4.17). Thus, the majority of dCoREST protein was separated from LINT subunits dLint-1 and dL(3)mbt in both gel filtration and ion exchange chromatography. Intriguingly, the biochemical fractionations of Kc167 nuclear extract further disclosed that, while dL(3)mbt was apparently present only in a single peak together with the residual LINT subunits, dLint-1 eluted in a second broader peak that contained dLsd1, dRpd3 and again dCoREST (Figure 4.17 and data not shown, fractions 21-25). To unravel the exact distribution and composition of these additional dLint-1, dCoREST and dLsd1

complexes in *Drosophila*, further experiments are needed. One possible approach could be to establish another purification scheme using more or other types of ion exchange columns to figure out how many distinct complexes are indeed present in this second peak. Aside from this, additional immunoprecipitations of dLint-1, dCoREST or dLsd1, from single fractions after complex purification, analysed by Western blot or mass spectrometry, could shed light on the existence of other multi-subunit complexes.

In *Drosophila*, dCoREST exists in three splice variants (Dallman et al., 2004). The antibody, used in this study, recognises the dCoREST-M and -L isoforms, which exhibit the same domain composition, but differ in the length of the domain separating the two SANT domains (inter-SANT region) (Dallman et al., 2004). In co-immunoprecipitation experiments both FLAG-tagged dL(3)mbt (data not shown) and dLint-1 (Figure 4.13) preferentially bound the dCoREST-M isoform. Moreover, gel filtration analysis upon dL(3)mbt and dLint-1 co-depletion confirmed the specific association of the dCoREST-M variant with the LINT complex (Figure 4.16). It is tempting to speculate that the shorter inter-SANT region in dCoREST-M harbours a specific protein-protein interaction motif that mediates binding to the LINT complex. However an overall change in the structure of dCoREST by a variable length of the inter-SANT region could also be responsible for the specific interaction of LINT with the dCoREST-M splice variant.

Taken together, the novel LINT complex is exceptional in regards to its composition, since so far MBT and CoREST family members have not been found together in multi-subunit complexes (Figure 5.1).

### 5.2.3 dLint-1 – a novel PHD-like finger protein

*The PHD finger motif in dLint-1*

The LINT subunit dLint-1 is a novel protein containing a PHD-like domain in its C-terminus. The identification of the PHD-like domain was based on the discovery of a PHD finger-typical C4HC3 signature with the appropriate distances between the individual Cys/His residues (Aasland et al., 1995; see Figure 4.7) that is very likely to adopt a PHD finger fold (R. Aasland, personal communication).

The HHpred server (http://toolkit.tuebingen.mpg.de/hhpred) is a bioinformatical tool that was developed to detect even remote protein homologies and predict, based on published protein structures, secondary structures (Söding et al., 2005). In agreement

with the presence of a C4HC3 PHD signature, HHpred predicted the C-terminal region of dLint-1 (aa 501 to 602) to adopt with high probabilities similar structures as established PHD domains, among them the PHD fingers of the demethylase JARID1D, the co-repressor KAP-1, the ATP-remodeler CHD4 and BHC80 (also known as PHD finger protein 21A) (data not shown). The definite evidence for this would certainly be a structural analysis of the dLint-1 PHD-like domain using either nuclear magnetic resonance (NMR) or X-ray crystallography.

*PHD finger proteins in CoREST complexes*

As mentioned above, immunoprecipitations and fractionation of Kc167 nuclear extract revealed that dLint-1 is present in at least two distinct complexes, LINT and another that is likely to contain dLsd1 and dCoREST (Figures 4.13 and 4.17). Interestingly, BHC80, one of the PHD finger proteins that was identified by HHpred, is a subunit of mammalian CoREST/LSD1/HDAC complexes (Hakimi et al., 2002; Shi et al., 2005). However, an apparent homologous protein of the PHD-finger protein BHC80 is absent in *Drosophila* based on BLAST (Basic Local Alignment Search Tool) analysis. Vice versa, dLint-1 lacks an apparent homologue in mammals. In light of both BHC80 and dLint-1 containing a PHD and PHD-like domain, respectively, it is tempting to speculate that, although these proteins are not related based on their amino acid sequence, they possess a similar molecular function. Even though PHD fingers generally share a common topology, with two short β-strands bridging two Zn-binding motifs, which coordinate the Cys/His residues (Taverna et al., 2007), they exhibit flexibility in their histone peptide binding properties. Whereas the PHD fingers of human BPTF and inhibitor of growth family 2 (ING2) bind tri-methylated H3K4 (Shi et al., 2006; Wysocka et al., 2006), the BHC80 PHD domain was shown to specifically recognise unmethylated K4 within histone H3, the reaction product of LSD1 enzymatic activity, and discriminates higher methylated states of H3K4 (Lan et al., 2007b; Shi et al., 2004). Depletion of BHC80 led to the derepression of LSD1 target genes and the repression could be rescued by the re-introduction of wild-type BHC80, but not a PHD-finger mutant that was unable to bind H3 (Lan et al., 2007b).

*Potential chromatin-related roles PHD finger proteins*

On the basis of the primary sequence, it seems difficult to predict, whether an individual PHD finger functions as a histone-binding module and whether it recognises unmodified or methylated lysines, although a recent study made efforts to determine

sub-families of PHD fingers based on sequence alignments providing functional information (Slama and Geman, 2011). To investigate, whether the dLint-1 PHD-like domain belongs to the group of histone binding modules, GST-tagged or EGFP-tagged constructs of this domain were expressed in bacteria or HEK293 cells, respectively. A potential specificity for various histone lysine residues, including H3K4, H3K9, H3K27 and H4K20 in different methylation states, was tested in histone peptide binding assays (data not shown). However, reproducible and specific binding of the PHD-like domain to isolated histone tails could not be observed in these experiments. The failure in histone peptide binding could have several different reasons.

It is possible that either the histone substrate or/and the PHD-like binding module were not correctly chosen. The PHD-like domain might not be able to recognise free histone tails, but require additionally contacts to the globular domains of histones or to nucleosomes for efficient binding. Moreover, it is conceivable that the isolated PHD-like module was not sufficient for specific binding. The latter could be due to the lack of protein sequences within dLint-1 or dLint-1 interacting proteins that are required to stabilise or mediate histone peptide interaction.

However, the PHD-like domain does not necessarily need to belong to the group of histone readers. Instead, PHD fingers have been previously reported to have nucleosome-binding activity in human p300 (Ragvin et al., 2004) and *Drosophila* Acf1 (Eberharter et al., 2004). In both cases the PHD fingers seemed to cooperate with an adjacent Bromo domain. Therefore, it would be interesting to investigate whether PHD or PHD-like domains that are not linked to Bromo domains, such as the one of dLint-1, can also function as nucleosome-binding modules.

Furthermore, PHD fingers were also found to function as protein-protein interaction domains for non-histone proteins (O'Connell et al., 2001; Townsley et al., 2004). For instance, in *Drosophila* the PHD fingers of Polycomb-like (Pcl) mediate the interaction with E(z) (O'Connell et al., 2001). In case of dLint-1, the dL(3)mbt interaction domain resides in the N-terminal half of the protein, lacking the PHD-like domain (Figure 4.9). However, this does not exclude that the PHD-like domain can mediate interaction with the third LINT subunit dCoREST. To test this hypothesis, the dCoREST interaction domain(s) within dLint-1 or dL(3)mbt need(s) to be mapped in future experiments.

## 5.3 LINT as a repressor complex of genes driving brain tumour growth in *Drosophila*

### 5.3.1 dL(3)mbt as a tumour suppressor in the larval brain

*dL(3)mbt - a tumour suppressor protein*

Originally, brain tumour suppressor screens identified *l(3)mbt*, as a tumour suppressor gene in *Drosophila melanogaster*, since a temperature-sensitive mutation of the *l(3)mbt* gene (*l(3)mbt*$^{ts}$) led to the development of malignant tumour growth in the larval brain (Gateff et al., 1993; Wismar et al., 1995) (see introduction, 2.2.2). In this context it is noteworthy that most tissues in the *Drosophila* larva contain endo- or post-mitotic cells, and therefore only a limited number of actively dividing cells are in fact capable of neoplastic transformation, including adult optic neuroblasts and ganglion mother cells in the larval brain, imaginal disc and blood cells (Gateff, 1978). Thus, the malignant transformation caused by *l(3)mbt* mutation uncovered the larval brain as a biological relevant tissue of dL(3)mbt protein function, but this does not necessarily allow the conclusion that dL(3)mbt has a unique role in the brain.

In the course of this doctoral thesis two publications (Janic et al., 2010; Richter et al., 2011) contributed to our understanding of how dL(3)mbt acts as a tumour suppressor and identified two groups of target genes that are able to drive tumour growth in the *Drosophila* larval brain. The findings of these studies will be summarised in the following and discussed later in context of dL(3)mbt as a LINT subunit (see 5.3.2).

In order to get a deeper insight into the role of dL(3)mbt as a tumour suppressor Richter and co-workers (2011) characterised the origin of malignant overgrowth in *l(3)mbt* mutant larval brains in more detail. Before elucidating the results of these experiments I will give a short overview of the brain structure in the *Drosophila* larva.

*The nervous system of the Drosophila larval brain*

In *Drosophila*, all neurons of the central nervous system (CNS) originate from neuroblasts, which possess stem cell-like features (Neumüller and Knoblich, 2009). In the larva, these cells are subdivided in central brain (CB), optic lobe (OL) and ventral nerve cord (VNC) neuroblasts, dependent on their affiliation to one of these three main neurogenic regions (Figure 5.2 A). One important characteristic of neuroblasts is that they undergo multiple rounds of asymmetric cell divisions during larval stages, giving rise to two daughter cells. One of them remains a neuroblast, while the other differentiates further into a ganglion mother cell to ultimately generate two neurones

(Figure 5.2 B). While embryonic neuroblasts give rise to the neuroblasts of the CB and VNC, OL neuroblasts develop during larval stages from OL neuroepithelial cells.

One mechanism for the malignant transformation in *Drosophila* larval brain is believed to be the loss of cell polarity in neuroblasts leading to an increase in the neuroblast cell pool and the development of stem cell-derived tumours (Caussinus and Gonzalez, 2005). Defects in asymmetric cell divisions and loss of cell polarity are also found in human cancers and tightly correlate with the ability of tumours to invade and metastasise (Wodarz and Näthke, 2007). In contrast to human, where a multitude of mutations in genes that are required for essential cellular pathways needs to accumulate for the formation of tumours, in *Drosophila* mutations of single tumour suppressors, such as asymmetric cell division regulators, can initiate malignant transformation in the brain (Caussinus and Gonzalez, 2005).

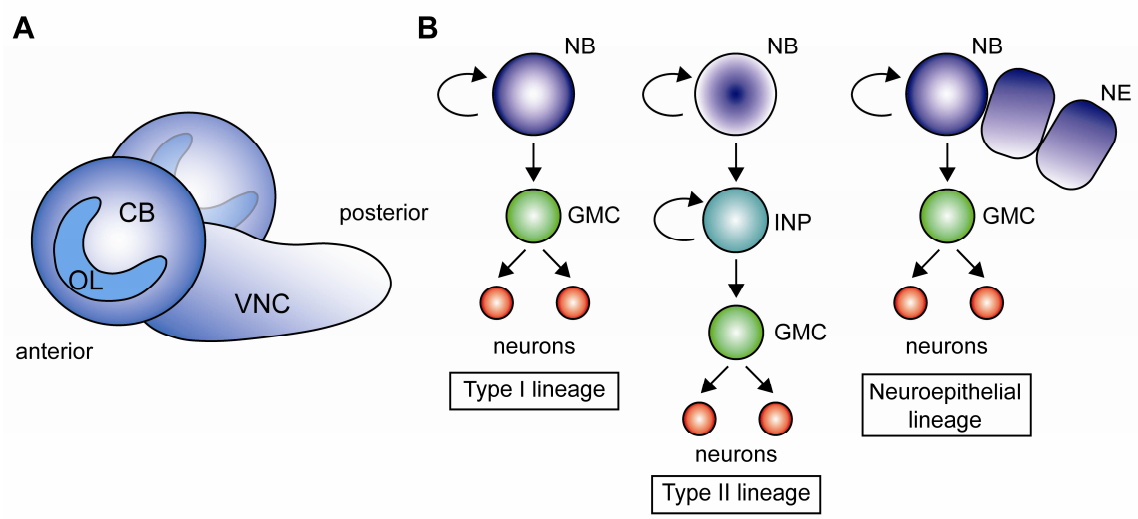


**Figure 5.2: The *Drosophila* larval brain.** (A) Schematic scheme of the *Drosophila* third instar larval brain (lateral view), which consists of three main neurogenic regions: The optic lobes (OL) are situated at the lateral surface of the two brain hemispheres. The central brain (CB) is located medially of the OL and descends into the ventral nerve cord (VNC) on the posterior side of the brain. (B) Asymmetric division of Type I, II and OL neuroblasts (NBs). Type I neuroblasts, which constitute the majority of NBs in the CB and VNC, divide asymmetrically into another NB and a mother ganglion cell (GMC) that terminally gives rise to two neurons. Type II NBs, which are located on the medial posterior surface of the brain lobes, generate transiently amplifying intermediate neural progenitor (INP) cells that produce in another asymmetric division GMCs. The NBs of the OL originate from OL neuroepithelial (NE) cells. Modified from Neumüller and Knoblich, 2009.

*The tumour phenotype of l(3)mbt mutant larval brains*

Using the neuroblast marker Deadpan to identify neural stem cells Richter et al. (2011) show that the number of Deadpan-positively stained cells is strongly increased in *l(3)mbt* mutant larval brains compared to wild-type causing an abnormal enlargement of the brain, in particular of the optic lobes. This expansion of the optic lobes appeared to result from an over-proliferation of the neuroepithelial cells of the inner and outer optic anlagen, which in late larval stages led to an elevated number in OL neuroblasts. In contrast to other mutants, exhibiting a tumour phenotype (such as *brat* and *lgl* mutants) (Betschinger et al., 2006; Lee et al., 2006a), *l(3)mbt* mutant brains did not reveal defects in the asymmetric segregation of determinants (Richter et al., 2011).

*dL(3)mbt target genes that drive tumour progression*

Using a candidate screen Richter and co-workers identified genes of the Salvador-Warts-Hippo (SWH) pathway (*ban*, *CycA*, *CycB*, *CycE*, *E2f*, *diap1*, *fj*, *ex*, *Mer*, *wg*, *Ser*), which was known to play a role in the regulation of proliferation and organ size (Harvey and Tapon, 2007; Zeng and Hong, 2008), to be important for tumour growth in *l(3)mbt* mutant larvae. As overexpression of Expanded or mutation of *ban* or *yki* could rescue the tumour phenotype, deregulation of target genes of the SWH pathway appears to be essential for the development of tumours (Richter et al., 2011). Out of eleven SWH pathway genes seven were identified as direct targets of dL(3)mbt binding, suggesting that derepression of SWH genes upon loss of dL(3)mbt function, leads to tumourigenesis.

Prior to the study by Richter et al. (2011) another set of genes, termed MBT signature (MBTS) genes, was already revealed to be required for tumour growth in *l(3)mbt* mutant larval brains by Janic et al. (2010). In an unbiased approach to identify mis-regulated genes that could be involved in the tumour growth genome-wide gene expression profiling was performed, comparing expression levels in *l(3)mbt* mutant larval brains at the restrictive temperature (29°C) to $w^{1118}$ control and *l(3)mbt* mutant larval brains at the permissive temperature (17°C). Intriguingly, from 102 genes, that were observed to be significantly up-regulated in *l(3)mbt* brain tumours, 26 are required in the germline, among them were also *swa*, *nos* and *piwi*. To investigate the contribution of mis-expression of germline genes to tumourigenesis Janic et al. (2010) quantified brain overgrowth in larvae that were mutant for $l(3)mbt^{ts}$ alone or double mutant for $l(3)mbt^{ts}$ and one of the germline-specific genes. The average brain size,

measured in total protein content, was approximately 7-fold larger in *l(3)mbt*$^{ts}$ mutants compared to *w*$^{1118}$ controls. Remarkably, the additional mutation of *piwi*, *nos*, *vasa* (*vas*) or *aubergine* (*aub*) prevented overgrowth, which resulted in normal sized brains in double mutant larvae, whereas mutation of other germline genes (e.g. *zpg*, *Pxt*) did not significantly reduce the brain size. These data revealed a striking correlation between the ectopic expression of some germline-specific genes and the *l(3)mbt*-mediated tumour growth in *Drosophila*.

Taking the data of the two studies of Richter et al. (2011) and Janic et al. (2010) into account, the most surprising result might be that the manipulation of single dL(3)mbt targets from both gene clusters (of SWH and MBTS genes), even though acting in completely different biological pathways, is able to rescue the tumourigenic phenotype in *l(3)mbt* mutant larvae. However, in none of the two publications, mentioned above, the authors address the question, whether dL(3)mbt as a repressor protein and tumour suppressor functions as a single protein or in context of a protein complex.

### 5.3.2 LINT and the regulation of genes driving brain tumour growth

*LINT represses MBTS genes*

Given that this study shows that LINT is the major dL(3)mbt complex in Kc167 cell nuclear extract and exists in the developing fly in embryos as well as in larval brain, it is likely that dL(3)mbt represses tumour-relevant genes in the context of the LINT complex. Supporting this idea RNA interference against dL(3)mbt or dLint-1 in Kc167 cells combined with gene expression profiling revealed that the majority of dL(3)mbt (74%) and dLint-1 (53%) deregulated genes overlapped between the two data sets (Figure 4.23). Intriguingly, 15 out of 32 germline-specific MBTS genes, which were up-regulated in tumourigenic *l(3)mbt* mutant larval brains (Janic et al., 2010), were also derepressed in Kc167 cells that were depleted of dL(3)mbt or dLint-1 (see Table 7.1 in the appendix). In addition, the MBTS genes *piwi*, *tej*, *hdm*, *CG32313*, *RpS5b*, *swa* and *nos* were among the top 50 genes that were most strongly up-regulated upon both dL(3)mbt and dLint-1 depletion (see Table 4.3). Among these, *piwi* and *nos* have been reported to contribute to malignant brain tumour growth (Janic et al., 2010). Moreover, 20 of the top 50 genes encode proteins that are expressed in an ovary- or testis-specific expression pattern (see Table 4.3).

By contrast, none of the SWH pathway genes that have been recently shown to be dL(3)mbt targets in *l(3)mbt* mutant brains (Richter et al., 2011) were found in microarrays to be up-regulated in dL(3)mbt and dLint-1 RNAi-treated cells. Discrepancies between the data presented in this study and the reports by Janic et al. (2010) and Richter et al. (2011) on dL(3)mbt target genes may arise from different reasons. It is possible that the depletion of dL(3)mbt or dLint-1 by RNAi, as opposed to a non-functional dL(3)mbt mutant protein, was not sufficient to derepress certain target genes under these conditions. The knockdown efficiencies were generally monitored in soluble nuclear extract, but not in the chromatin-bound fraction. It is therefore conceivable that even in case of an efficient depletion a protein fraction remains stably associated with chromatin. In addition, genes of the SWH pathway might be differently regulated in *Drosophila* larval brain compared to cell lines.

In line with the LINT complex regulating germ cell-specific target genes the expression of a selected subset of MBTS genes was strongly derepressed, not only upon dL(3)mbt and dLint-1, but also dCoREST knockdown (Figure 4.39). ChIP analysis, showing dLint-1 and dCoREST binding to promoter regions of the corresponding target genes confirmed that LINT represses them by a direct mechanism (Figure 4.28). A drawback of the dL(3)mbt-specific antibodies, which were raised in the course of this study, was that none of them worked in ChIP. Therefore the association of dL(3)mbt, the only subunit which appears to be specific for LINT (Figure 4.17), with target genes could not be tested. However, Richter and co-workers (2011) published a genome-wide ChIP-Seq analysis of dL(3)mbt binding sites using an independent antibody. In accordance with the LINT complex regulating germ cell-specific target genes, promoters that were bound by dLint-1 and dCoREST (Figure 4.28), also revealed peaks for dL(3)mbt association in the region upstream of the transcriptional start sites (ChIP-Seq data from Richter et al., 2011).

*Genome-wide binding of LINT subunits to chromatin*

Co-localisation studies on polytene chromosomes, preceding the identification of target genes, had already suggested that dL(3)mbt and dLint-1 binding sites overlap to a high extent, namely 83% of all bands were co-stained by both dL(3)mbt and dLint-1 antibodies (Figure 4.21). However, it was interesting to map global binding sites of LINT that are common to dL(3)mbt and dLint-1. To this end dLint-1 binding sites were determined in our lab using ChIP-Seq: Chromatin immunoprecipitations of dLint-1

were carried out by Eve-Lyne Mathieu in our lab, isolated DNA was subjected to Illumina sequencing by Maren Scharfe (Helmholtz Center for Infection Research, Braunschweig) and data were statistically analysed by Florian Finkernagel (IMT, Marburg). To gain insight into the co-localisation, dLint-1 (E. Mathieu, data not shown) and dL(3)mbt (Richter et al., 2011) ChIP-Seq results were compared. In good agreement with immunofluorescent polytene stainings, 80% of the dL(3)mbt peaks (2902 in number) overlapped with dLint-1 peaks. To gain a deeper insight in the distribution of LINT and other dLint-1 containing complexes on a genome-wide level it would be interesting to carry out dCoREST and dLsd1 ChIP-Seq analyses to be compared with existing dL(3)mbt (Richter et al., 2011) and dLint-1 (E. Mathieu, unpublished data) data sets. This has been so far precluded by the lack of adequate antibodies.

Taken together, the results presented in this work strongly support the idea that dL(3)mbt as part of the LINT complex directly silences germline-specific genes, whose ectopic expression contributes to the progression of tumour growth in the brain of larvae (Janic et al., 2010). This underlines furthermore the biological relevance of this novel protein complex. Since dLint-1 knockdown, similar to dL(3)mbt depletion, results in a strong derepression of germline-specific target genes, at least in the systems tested so far (Figures 4.24 and 4.25), it would be very interesting to investigate, whether mutation of the *lint-1* gene or ectopic depletion of dLint-1 protein by RNAi interference in the brain causes a similar tumourigenic phenotype.

*Germline-specific genes and tumourigenesis*

Interestingly, in human the aberrant expression of cancer-testis (CT) or cancer-germline (CG) genes, whose expression is normally restricted to gametes and trophoblasts, has been found in a range of tumour types (Simpson et al., 2005). Based on this study it is conceivable, that in human L3MBTL and CoREST proteins play a role in the silencing of CT and CG genes. Although the mechanism of how germline genes could induce tumourigenesis is poorly understood, a theory evolved that partial re-activation of the gametogenic gene-expression program equips somatic cells with germ cell-specific features contributing to immortality, invasiveness and metastatic capacity. In this context, a correlation between germ cell characteristics and lifespan was reported in the worm (Curran et al., 2009). *C. elegans* mutants with an increased longevity have been

shown to exhibit a soma-to-germline transformation, describing the mis-expression of germline-specific genes in somatic tissues.

*A germline-specific defect in L(3)mbt mutant embryos*

As many germ cell-specific genes are among the top LINT-regulated genes, it is worth noting that mutation of *l(3)mbt* in the fly has been reported to cause, aside from the malignant brain tumour phenotype, a defect in germline development (Yohn et al., 2003). However, it is difficult to judge how this relates to the silencing of germline-specific cells in somatic tissues. Embryos with a mutation in *l(3)mbt* had a decreased number of germline precursor pole cells (Yohn et al., 2003). These embryos already display defects in the synchrony of nuclear divisions at the onset of embryonic development. Thus it seems likely that defects in nuclear migration and hence germ cell formation are a direct consequence of disturbed nuclear divisions. Investigating the distribution of *l(3)mbt* mRNA by *in situ* hybridisation, Wismar et al. (1995) found that *l(3)mbt* mRNA is expressed throughout embryonic development in most tissues, but that pole cells were devoid of a hybridisation signal. This would support the idea that the abnormalities in the number of primordial germ cells (Yohn et al., 2003) is not due to a lack of dL(3)mbt in these cells, but through an indirect mechanism.

Although a high proportion of strongly up-regulated LINT target genes evidently display testis- or ovary-specific expression patterns, it is clear that the LINT complex is involved in the regulation of a large suite of genes functioning in diverse biological processes, which remains to be further investigated.

## 5.4 The role of MBT domains in transcriptional repression by LINT

Several *in vitro* binding studies have found that MBT domains specifically bind to mono- and di-methylated lysines within histone tails exhibiting a relatively low selectivity concerning the sequence context (Bonasio et al., 2010; Kalakonda et al., 2008; Li et al., 2007b; see introduction 2.2.1.2). These have been obtained using isolated MBT domain modules. However, few data exist on the binding properties of full length MBT proteins that potentially differ from the ones of isolated MBT modules. In line with this, there is a discrepancy between the specificity of the isolated four MBT domains of L3MBTL2 and the corresponding full-length protein in *in vitro* binding

assays. While the 4MBT region bound, similarly to the three MBT domains of L3MBTL1, specifically to mono- and di-methylated histone peptides (Guo et al., 2009), full-length L3MBTL2 recognised H4K20 preferentially in its un- and mono-methylated state (Trojer et al., 2011). In addition, Trojer et al. (2011) demonstrate a binding of L3MBTL2 (full length) to unmethylated H3 (aa 1-21) regardless of H3K4 or H3K9 mono- or di-methylation. In addition to the potential differences of the binding selectivity of MBT domains and full length MBT proteins, one should consider that the binding specificities of MBT domain proteins *in vivo* very likely also depend on many other factors, such as associated proteins influencing binding affinity and specificity to chromatin.

*Role of MBT domain binding to H4K20 methylation*

In human mono-methylation of H4K20 enhances chromatin association and promotes the repressive activity of L3MBTL1 (Trojer et al., 2007; Kalakonda et al., 2008). In fact the association of L3MBTL1 at the *cyclin E* promoter was shown to be reduced upon PR-SET7 knockdown, concomitant with an increase of the *cyclin E* mRNA levels (Kalakonda et al., 2008). Therefore, in this study the question was addressed whether loss of H4K20me1 has an impact on LINT repression. In agreement with dPR-Set7 being the sole methyltransferase in *Drosophila* (Nishioka et al., 2002), H4K20me1 levels were significantly reduced in a global manner (Figure 4.31 B). However, transcription levels of LINT target genes were unaffected (Figure 4.31 C). In agreement with this ChIP analysis suggests that the H4K20me1 modification is absent from promoters of LINT target genes *swa* and *nos* (Figure 4.32 A). This indicates that even though dL(3)mbt bound H4K20me1 with a higher affinity than unmethylated H4 peptide *in vitro* (Figure 4.30 B; Scharf et al., 2009) that the interaction between dL(3)mbt and H4K20me1 is not part of the repression mechanism of LINT.

There is one major difference between the L3MBTL1/H4K20me1 regulated *cyclin E* gene (Kalakonda et al., 2008) and the LINT target genes that were investigated in this study. While *cyclin E* is a cell cycle-dependent gene that needs to be dynamically regulated, the germline-specific LINT target genes are required to be constantly silenced in somatic cells. For this reason, it might well be that H4K20 methylation contributes to the modulation of other dL(3)mbt target genes in response to cell cycle progression or other biological pathways.

However, by using somatic Kc167 cells as a system, an associated drawback is that the repression of germ cell-specific LINT target genes is naturally already established. Therefore, it cannot be excluded that H4K20 mono-methylation plays an important role during the establishment of stable repression of germline-specific target genes.

In addition to mono-methylated H4K20, the MBT domains also specifically recognised H4K20me2 *in vitro* (Figure 4.30 B). Even though the H4K20me2 mark was present at LINT target gene promoters, the levels were not elevated in comparison to control regions (Figure 4.32 B). This observation was not surprising since two previous publications reported that 85-90% of all chromatin associated histone H4 molecules are di-methylated at lysine 20 (Schotta et al., 2008; Yang et al., 2008). This might implicate that the H4K20me2 mark is uniformely high along the chromosomes. Therefore, this modification is unlikely to recruit the LINT complex in a specific manner to its target genes. However, it is still conceivable that upon targeting of LINT by other means, a binding of dL(3)mbt to H4K20me2 contributes to transcriptional repression.

*Role of MBT domain binding to alternative histone modifications*

To explain the function of MBT domain proteins, such as Sfmbt, in the Polycomb system, it has been speculated that the MBT module could act as a so termed 'grappling hook' (Klymenko et al., 2006). Hence, in the untranscribed state H3K27, H3K9 and H4K20 are extensively tri-methylated throughout the *Ubx* locus, except for the promoter and the 5'-coding region (Papp and Müller, 2006). Given the specificity of MBT domains for mono- and di-methylated histone lysines Klymenko et al. (2006) favour a model, in which MBT proteins bound to PREs scan the neighbouring chromatin for lower methylated lysine residues. By tethering H3K27 to E(z)/PRC2 the MBT domains can then function like a 'grappling hook' to ensure that this histone mark becomes tri-methylated. However, in case of LINT regulated target genes this paradigm is difficult to envisage, since the binding peaks of LINT subunits and E(z) localise at diverging regions of target genes, at promoter and ORF, respectively. Therefore, a prerequisite for the functional interaction between dL(3)mbt and E(z) on chromatin would be the formation of a chromatin loop to bring dL(3)mbt and E(z) in close proximity. In order to test such a model, more sophisticated experiments would be necessary.

However, it is also tempting to speculate that dL(3)mbt within the LINT complex can bind specifically to the low-methylated state of activating histone modifications, such as

H3K4. *In vitro* binding assays of the three MBT domains of human L3MBTL1 revealed that the affinity towards H3K4me1 is a magnitude higher compared to H3K4me2 (Li et al., 2007b). In order to gain a better insight into the methylation status of H3K4 at LINT target promoters, it would be interesting to include an H3K4me1-specific antibody in ChIP analysis to investigate changes of H3K4me1 levels upon LINT disassociation.

## 5.5 LINT repression is independent of histone-modifying activities

*Changes of H3K4 methylation levels at LINT target genes*

The derepression of LINT target genes is accompanied by changes in histone modification patterns. It correlates with a modest increase of H4 acetylation at the promoter and a significant elevation of H3K4 di-methylation at the promoter and the ORF (Figure 4.33). Both histone marks are characteristic for active chromatin (see introduction). Although the LINT core complex does not contain any histone-modifying enzymes, dL(3)mbt and dLint-1 interact with the deacetylase dRpd3 and dLint-1 associates with the H3K4-specific demethylase dLsd1. The enzymatic activities of both proteins could have offered an explanation for the observed histone modification changes. However, depletion of the dLint-1 interacting dLsd1 and dRpd3 enzymes did not relieve the repression of LINT target genes (Figure 4.39). Moreover, knockdown of dLsd1 did not suppress repression of a reporter gene mediated by dL(3)mbt- and dLint-1-LexA fusion proteins (Figure 4.41). Also TSA-treatment of cells to inhibit HDAC activity did not reduce repressive potential of dL(3)mbt in the same reporter assay (D. Pagliarini, diploma thesis, 2008). These results suggest that the maintenance of germline-specific LINT target genes does not require these repressive histone-modifying enzymes. In contrast to loss of LINT from the promoter, a depletion of dLsd1 does not lead to an increase of H3K4me2 levels. Therefore it is most likely that the detected changes in histone modifications are a consequence of active transcription rather than a loss of histone-modifying enzymes that are associated with LINT target genes.

When discussing the relevance of histone modifications it seems indispensable to distinguish whether a certain modification pattern is cause or consequence of a specific biological event, such as transcription (Henikoff and Shilatifard, 2011). For instance, methylation of the H3K4 residue correlates highly with active transcription on a

genome-wide level (Schübeler et al., 2004; Roh et al., 2006). In most cases the modification of H3K4 by mono-, di- and tri-methylation is interpreted as a consequence of active transcription. In yeast it was demonstrated that the Set1 methyltransferase is recruited to sites of active transcription by the RNA Polymerase II elongating machinery (Krogan et al., 2003; Ng et al., 2003).

Even though LINT is devoid of histone-modifying enzymes, it is still conceivable that the dLint-1 interacting proteins dRpd3 and dLsd1, as well as other chromatin 'writers', are initially required to establish repressive chromatin patterns at LINT target genes. The data in this study indicate, however, that once gene silencing is established, the presence of LINT at the promoter is sufficient to protect repressive histone marks.

*Changes of H3K27 methylation levels at LINT target genes*

A third histone modification that was significantly affected by derepression of LINT target gene derepression was the repressive histone mark H3K27me3. Upon loss of LINT, the levels of tri-methylated H3K27 that is set by the PRC2 integral histone methyltransferase E(z) (Cao et al., 2002; Czermin et al., 2002; Kuzmichev et al., 2002; Müller et al., 2002) decreased significantly in the transcribed region (Figure 4.34). In accordance with the presence of H3K27me3, E(z) was detected specifically in the open reading frame of LINT target genes (Figure 4.36). In general high levels of H3K27me3 correlate with transcriptional silencing of Polycomb targets, such as the *Hox* genes (Nekrasov et al., 2007; Sarma et al., 2008). The repressive effect of this mark is in line with germline-specific genes targeted by LINT being turned off in somatic tissues. As described above, H3K4me2 levels were unaffected by dLsd1 knockdown. In contrast, H3K27me3 levels were indeed reduced upon depletion of E(z) (Figure 4.34). However, the expression levels of LINT target genes were also not significantly changed (Figure 4.38), arguing that the reduction of a single repressive mark is not sufficient for gene induction.

Surprisingly, although H3K27me3 levels strongly decreased upon derepression of target genes (Figure 4.33), E(z) was not displaced from the open reading frame (Figure 4.36). Hence, another mechanism must take effect to inhibit the enzymatic activity of PRC2.

A recent publication demonstrated that the enzymatic activity of E(z) in the PRC2 complex is inhibited by active chromatin modifications, such as methylated H3K36 and H3K4, in an allosteric manner (Schmitges et al., 2011). On the other hand PRC2 was shown to be stimulated by H3K27me3, the same mark that is deposited by its

catalytically subunit (Hansen et al., 2008; Margueron et al., 2009). This positive feed-back loop is thought to be involved in the efficient creation and epigenetic maintenance of H3K27me3 positive domains. The direct inhibition of PRC2 through active histone marks offers now a paradigm of how spreading of methylated H3K27 into active chromatin regions can be prevented (Schmitges et al., 2011).

With regard to this study the same mechanism may be responsible for a decrease in H3K27me3 despite the presence of E(z). Since the derepression of LINT target genes is accompanied by elevated levels of methylated H3K4 both in the promoter and the ORF (Figure 4.33), it is conceivable that this increase in active histone marks is efficient to inhibit the catalytic activity of E(z).

An alternative explanation for the decrease in the amount of H3K27me3 is that the enzymatic activity of E(z) is overcome by the counteracting H3K27me2/3 specific demethylase dUTX (Smith et al., 2008; Herz et al., 2010). Previously, Smith et al. (2008) demonstrated an interaction between dUTX and RNA polymerase II (RNA Pol II), as well as a co-localisation with the elongating form of RNA Pol II on polytene chromosomes. Using the heat shock gene *Hsp70* as a model for inducible gene activation, dUTX was shown to be recruited to the transcribed region upon heat shock induction of *Hsp70*. In conclusion, there are at least two mechanisms, which both occur on a co-transcriptional level, that could account for the H3K27me3 loss upon LINT target gene derepression.

## 5.6 Model of LINT-mediated gene repression

The data presented in this thesis favour the following model for target gene repression by the LINT complex (Figure 5.3).

The LINT core complex, consisting of dL(3)mbt, dLint-1 and dCoREST, stably represses genes, whose expression is normally restricted to the germline. All three subunits of LINT are crucial for the maintenance of stable silencing (Figure 4.39). The LINT complex binds specifically close to transcription start sites of target genes, suggesting that LINT might prevent transcription by restricting the access of RNA Pol II and activating transcription factors to promoters (Figures 5.1 and 5.2). In favour of this mechanism, recruitment of LINT subunits to the promoter region of a reporter gene is sufficient for repression even under conditions when repressive histone-modifying enzymes are depleted (Figure 4.41).

The derepression of target genes is accompanied by changes in histone modification patterns. Upon loss of LINT the levels of repressive H3K27me3 decrease, while active histone marks (H3K4me2 and H4 acetylation) increase. These changes are likely to occur as a consequence of active transcription (see 5.5).

In contrast to LINT, repression of mammalian CoREST/LSD1 complexes is considered to be triggered via histone demethylation and deacetylation, while the major repression mechanism of the mammalian L3MBTL1 complex is thought to be nucleosome compaction (Figure 5.1).

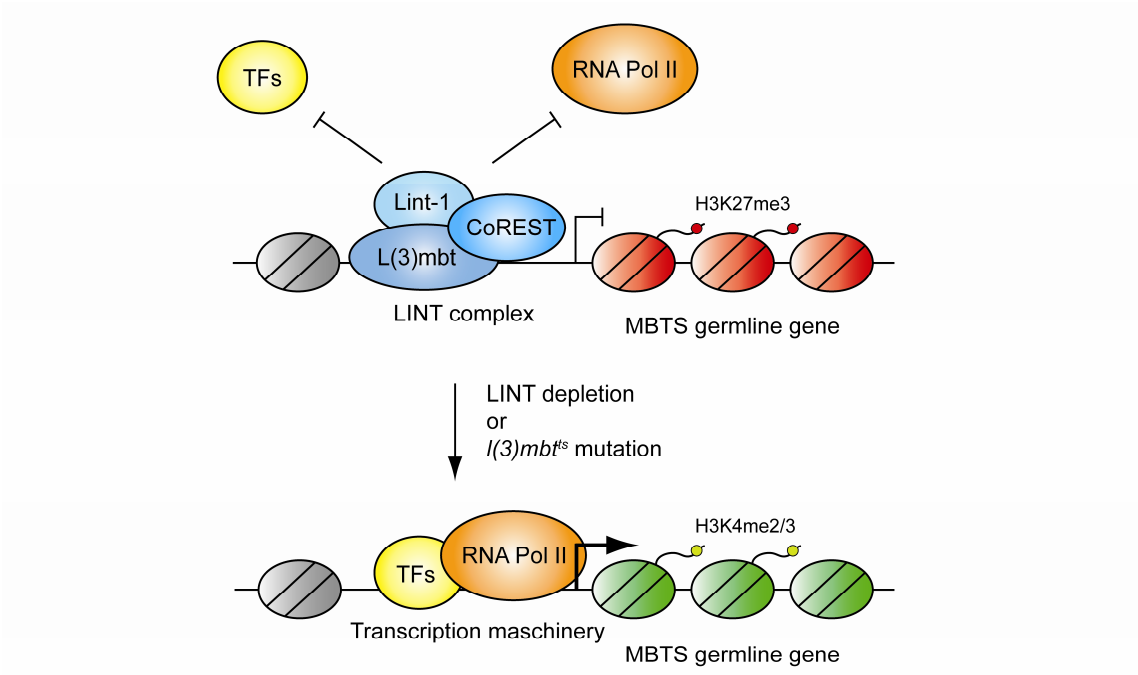


**Figure 5.3: Model of LINT-mediated transcriptional repression.** Upper panel: The LINT complex is associated with the promoter regions of repressed genes, such as the MBTS germline-specific genes, which precludes the access of RNA polymerase II (RNA Pol II) and/or activating transcription factors to the promoter. Lower panel: Inactivation or depletion of LINT complex subunits allows the binding of RNA Pol II and/or activating transcription factors to the promoter, facilitating transcription initiation and elongation. The derepression of LINT target genes is accompanied by a loss of repressive (H3K27me3) and a gain in active (H3K4me2) histone marks that are likely to occur co-transcriptionally.

In the future, further experiments are required to decipher the mechanism of LINT repression in more detail and determine the contribution of each LINT subunit, as well as of single protein domains of dL(3)mbt, dLint-1 and dCoREST.

## 5.7 Potential recruitment mechanisms of LINT to target genes

Although the LINT complex appears to bind directly to the promoter regions of target genes, the model presented here (Figure 5.3), does not imply that LINT features a DNA sequence-specific mode. About how LINT gets recruited to its binding sites can only be speculated and the exact mechanism of targeting remains to be elucidated in future experiments.

Like other repressor complexes (such as PRC1: Shao et al., 1999; PRC2: Czermin et al., 2002; Müller et al., 2002; and dNuRD: Kunert et al., 2009; Reddy et al., 2010), LINT lacks a DNA-sequence specific transcription factor as an integral subunit. Therefore, one possible mechanism for LINT targeting is that a transcriptional repressor specifically binds to its recognition site in the promoter of target genes and recruits LINT directly on the DNA as a co-repressor complex to silence transcription. As a candidate approach the promoter regions of genes, which were deregulated upon dL(3)mbt and dLint-1 depletion, were analysed statistically for the enrichment of known transcription factor binding motifs (F. Finkernagel). However, this analysis did not yield a significant result.

*Correlation between dL(3)mbt binding sites and insulator sequences*

A DNA motif search among the dL(3)mbt binding sites by Richter et al. (2011) led to the identification of four consensus sequences that matched consensus motifs of the chromatin insulators bound by CP190 (Negre et al., 2010), BEAF-32 (Zhao et al., 1995), CTCF (Holohan et al., 2007) and Su(Hw) (Adryan et al., 2007). Of these the latter three can directly bind to sequence-specific recognition sites. Insulator proteins have been implicated in the regulation of chromatin organisation and gene regulation by mediating the formation of chromatin loops (Yang and Corces, 2011). In agreement with an enrichment of insulator consensus sequences within dL(3)mbt-associated regions, binding sites of dL(3)mbt overlapped largely with bound CP190, BEAF-32, CTCF and to a lesser extent with Su(Hw) (Richter et al., 2011). The correlation between dL(3)mbt and insulator protein binding is particularly high within the *Hox* gene cluster of the Bithorax complex (Richter et al., 2011). Given that dLint-1 and dL(3)mbt ChIP-Seq peaks overlap to a great extent (approximately 80%, see 5.3.2) there is a high likelihood that also LINT shares a plethora of binding sites with insulator proteins. The statistical analysis to quantify this overlap remains to be done. However, questions that also need to be addressed in the future are for instance whether there is a biological

relevance for this overlap and whether insulator proteins can be involved in the targeting of dL(3)mbt to insulator sequences. Therefore, to term dL(3)mbt an insulator protein (Richter et al., 2011) seems premature at presence. Also one should keep in mind that ChIP data are always obtained from a cell population. Therefore the identification of regions that are positive for the binding of different factors does not necessarily imply that these sites are actually bound by all these factors concomitantly.

*Transcription factors as potential candidates to recruit LINT to target genes*

During the purification of the Myb-MuvB complex dL(3)mbt co-purified in a sub-stoichiometric manner from embryo extracts (Lewis et al., 2004). This led to the conclusion that dL(3)mbt is an optional subunit of Myb-MuvB. On the contrary the isolation of the dREAM complex, also from embryo extract, which is identical to the Myb-MuvB complex in its core subunit composition, was devoid of dL(3)mbt (Korenjak et al., 2004). Moreover, in this study the bulk of dL(3)mbt and RBF2 (a Myb-MuvB/dREAM subunit) clearly separated upon gel filtration analysis (Figure 4.4), arguing against a stable interaction and supporting an independent association of dL(3)mbt in the LINT complex. Nevertheless, gene expression analysis of Kc167 cells revealed an significant overlap within different gene classes, regulated by both Myb-MuvB and dL(3)mbt (Georlette et al., 2007). The fact that Myb-MuvB and dL(3)mbt share target genes and a probable proximity on the DNA might provide an explanation, why dL(3)mbt co-purified with Myb-MuvB in a sub-stoichiometric manner. If the Myb-MuvB complex with its two integral sequence-specific transcription factors E2F and dMyb is involved in the recruitment of dL(3)mbt and the LINT complex to common target genes, needs to be further investigated in the future.

In case of CoREST a recruitment mechanism has been elucidated for a certain set of target genes. In the mammalian system, as well as in *Drosophila*, the co-repressor CoREST, as part of a dLsd1-HDAC complex, is recruited by the transcription factors REST (repressor element I silencing transcription factor; in vertebrates) and Ttk88 (Tramtrack88; in *Drosophila*) (Andrés et al., 1999; Dallman et al., 2004), respectively. These transcription factors do not share a discernable homology, but in cooperation with CoREST-Lsd1-HDAC complexes, they both hinder the expression of neuronal-specific genes in non-neuronal cells. However, none of the neuronal genes, that were identified to be regulated by the Ttk88-dCoREST complex (Dallman et al., 2004), were up-regulated in dL(3)mbt depleted Kc167 cells (microarray analysis in this study, data not

shown), arguing against co-regulation of these genes by LINT. It is noteworthy, however, that the dCoREST-dLsd1-HDAC complex executes a similar function as the LINT complex by repressing the transcription of tissue-specific genes. While the dCoREST-dLsd1-HDAC complex silences neuronal-specific genes in non-neuronal cells, LINT represses germline-specific MBTS genes in somatic cells. Given that the same protein in two distinct chromatin-related complexes co-regulates different sets of target genes, it is tempting to speculate that one of the residual subunits determines the specificity for certain target genes, for instance by interacting with a sequence-specific transcription factor, while dCoREST fulfils a general repressive function.

To sum up, to unravel the exact mechanism of recruitment of LINT to target genes, more elaborate experimental and bioinformatical approaches are needed. For instance, a comparison of the microarray data upon depletion of dL(3)mbt or dLint-1, gained in this study, with dL(3)mbt (Richter et al., 2011) and dLint-1 (E. Mathieu, unpublished data) ChIP-Seq analysis could dismiss all indirectly deregulated genes. Accordingly, a DNA motif search within the promoter regions of direct target genes might be more meaningful and more likely result in an enrichment of LINT-bound consensus sequences. In this study I focused on identifying stoichiometric dL(3)mbt and dLint-1 complexes. However, the interaction with a targeting protein, like a transcriptional regulator, would probably be weak, especially in solution. Therefore, in order to isolate sub-stoichiometric interaction partners of the LINT complex, it would be reasonable to analyse the identity of all co-precipitating proteins in FLAG petide eluates from affinity purifications via mass spectrometry.

## 5.8 Chromatin compaction as a repressive mechanism

The compaction of chromatin is an appealing mechanism for gene silencing. In fact, transcriptional repressors that have been linked to chromatin compaction belong to Polycomb and MBT protein families.

Recently, human L3MBTL1 (Trojer et al., 2007) and L3MBTL2 (Trojer et al., 2011) have been shown to impact chromatin structure by compacting nucleosomal arrays *in vitro*. In these cases the ability to influence chromatin structure was attributed specifically to the MBT domains (Trojer et al., 2007 and 2011). In this context it is remarkable that both MBT proteins interact with HP1γ, a member of the

heterochromatin protein family (Eissenberg and Elgin, 2000). A prerequisite for L3MBTL1 compaction has been suggested to be mono- and di-methylation of histone H4K20 or H1bK26 (Trojer et al., 2007), whereas L3MBTL2 compacted chromatin in a modification independent manner (Trojer et al., 2011). However, one should take into account that results for L3MBTL1 were obtained using the isolated MBT module, while L3MBTL2 was studied as a full length protein.

Among the PcG proteins, the PRC1 complex has been revealed to induce packaging of oligo-nucleosomal arrays *in vitro*, thereby antagonising the remodelling activity of SWI/SNF-class chromatin remodelers (Shao et al., 1999; Francis et al., 2004). Evidence for this compaction by PRC1 *in vivo* has been provided in embryonic stem cells using a FISH 2D approach (Eskeland et al., 2010). Surprisingly, the ability to compact chromatin has been conserved in diverse PRC1 subunits in *Drosophila* and mammals, in Psc and the *Drosophila* Pc mouse homologue M33, respectively (Grau et al., 2011). The capability of chromatin compaction appears to require a region with a high positive charge. In addition to PRC1, the PcG family contains two more MBT domain proteins, namely Scm and Sfmbt, that are implicated in the formation of higher-order chromatin structures. Thus, MBT domain proteins and PRC1 subunits seem to have evolved independent modes of packaging chromatin.

Certainly, chromatin compaction by LINT mediated by dL(3)mbt would be a conceivable mechanism to explain access restriction of target gene promoters for RNA Pol II. As a consequence of chromatin compaction one might expect a local increase in nucleosome occupancy at the promoter regions of LINT target genes. However, H3 ChIP experiments have demonstrated that these promoters are generally depleted of nucleosomes (Figure 4.29) and that the content of H3 in the transcribed region of for instance *swa* is not elevated compared to neighbouring active genes (see 4.3.1 and Figure 4.29 B). These findings do not rule out the possibility that there is a local compaction that hinders transcription and is undetectable by H3 ChIP analysis. Nevertheless, the results obtained in this thesis favour a simpler model, namely that LINT association with promoter sequences prevents binding of activating transcription factors and RNA Pol II (see Figure 5.3). This hypothesis does not exclude a local impact on the chromatin structure by LINT mediated by dL(3)mbt. To get a first glimpse of how LINT influences chromatin structure one could investigate the effect of LINT and its single subunits on oligo-nucleosomal arrays by electron microscopy, as it has been done for the PRC1 complex (Francis et al., 2004). Furthermore, one might

gain a deeper insight by a nucleosome mapping analysis (Gévry et al., 2009) in the presence and absence of LINT, while blocking transcription, which itself induces chromatin structure changes like replication-independent histone turnover (Schwartz and Ahmad, 2005; Dion et al., 2007).

Even in terms of the intensively studied Polycomb/*Hox* gene system, the role of chromatin compaction is still difficult to envisage *in vivo* (Müller and Verrijzer, 2009). The PREs, bound by PcG proteins are depleted of nucleosomes and hypersensitive towards nuclease treatment (Mohd-Sarip et al., 2006; Papp and Müller, 2006). These so-called 'nucleosome-free regions' (NFRs), even though not completely devoid of nucleosomes, are suggested to be sites of high histone replacement, implying a continuous eviction and re-assembly of nucleosomes (Mito et al., 2007). Therefore it appears more feasible that PRC1 acts on chromatin in the flanking regions of PREs, such as promoters or coding regions of *Hox* genes, to create a lesser accessible chromatin structure. The exact location of chromatin compaction of Polycomb and MBT domain proteins remains to be elucidated in the future in more detail.

# 6 References

**Aasland**, R., Gibson, T.J., and Stewart, A.F. (**1995**). The PHD finger: implications for chromatin-mediated transcriptional regulation. Trends Biochem Sci 20, 56-59.

**Addou-Klouche**, L., Adélaïde, J., Finetti, P., Cervera, N., Ferrari, A., Bekhouche, I., Sircoulomb, F., Sotiriou, C., Viens, P., Moulessehoul, S., Bertucci, F., Birnbaum, D., and Chaffanet, M. (**2010**). Loss, mutation and deregulation of L3MBTL4 in breast cancers. Mol Cancer 9, 213.

**Adryan**, B., Woerfel, G., Birch-Machin, I., Gao, S., Quick, M., Meadows, L., Russell, S., and White, R. (**2007**). Genomic mapping of Suppressor of Hairy-wing binding sites in *Drosophila*. Genome Biol 8, R167.

**Agger**, K., Cloos, P.A., Christensen, J., Pasini, D., Rose, S., Rappsilber, J., Issaeva, I., Canaani, E., Salcini, A.E., and Helin, K. (**2007**). UTX and JMJD3 are histone H3K27 demethylases involved in HOX gene regulation and development. Nature 449, 731-734.

**Ahmad**, K., and **Henikoff**, S. (**2002**). The histone variant H3.3 marks active chromatin by replication-independent nucleosome assembly. Mol Cell 9, 1191-1200.

**Andrés**, M.E., Burger, C., Peral-Rubio, M.J., Battaglioli, E., Anderson, M.E., Grimes, J., Dallman, J., Ballas, N., and Mandel, G. (**1999**). CoREST: a functional corepressor required for regulation of neural-specific gene expression. Proc Natl Acad Sci U S A 96, 9873-9878.

**Annunziato**, A.T., Frado, L.L., Seale, R.L., and Woodcock, C.L. (**1988**). Treatment with sodium butyrate inhibits the complete condensation of interphase chromatin. Chromosoma 96, 132-138.

**Arai**, S., and **Miyazaki**, T. (**2005**). Impaired maturation of myeloid progenitors in mice lacking novel Polycomb group protein MBT-1. EMBO J 24, 1863-1873.

**Avvakumov**, N., Nourani, A., and Côté, J. (**2011**). Histone chaperones: modulators of chromatin marks. Mol Cell 41, 502-514.

**Bannister**, A.J., Zegerman, P., Partridge, J.F., Miska, E.A., Thomas, J.O., Allshire, R.C., and Kouzarides, T. (**2001**). Selective recognition of methylated lysine 9 on histone H3 by the HP1 chromo domain. Nature 410, 120-124.

**Becker**, P.B., and **Wu**, C. (**1992**). Cell-free system for assembly of transcriptionally repressed chromatin from *Drosophila* embryos. Mol Cell Biol 12, 2241-2249.

**Beisel**, C., Imhof, A., Greene, J., Kremmer, E., and Sauer, F. (**2002**). Histone methylation by the *Drosophila* epigenetic transcriptional regulator Ash1. Nature 419, 857-862.

**Bench**, A.J., Li, J., Huntly, B.J., Delabesse, E., Fourouclas, N., Hunt, A.R., Deloukas, P., and Green, A.R. (**2004**). Characterization of the imprinted polycomb gene L3MBTL, a candidate 20q tumour suppressor gene, in patients with myeloid malignancies. Br J Haematol 127, 509-518.

**Benting**, J., Lecat, S., Zacchetti, D., and Simons, K. (**2000**). Protein expression in *Drosophila* Schneider cells. Anal Biochem 278, 59-68.

**Berger**, J., Kurahashi, H., Takihara, Y., Shimada, K., Brock, H.W., and Randazzo, F. (**1999**). The human homolog of Sex comb on midleg (SCMH1) maps to chromosome 1p34. Gene 237, 185-191.

**Betschinger**, J., Mechtler, K., and Knoblich, J.A. (**2006**). Asymmetric segregation of the tumor suppressor brat regulates self-renewal in *Drosophila* neural stem cells. Cell 124, 1241-1253.

**Bhaumik**, S.R., Smith, E., and Shilatifard, A. (**2007**). Covalent modifications of histones during development and disease pathogenesis. Nat Struct Mol Biol 14, 1008-1016.

**Bienz**, M. (**2006**). The PHD finger, a nuclear protein-interaction domain. Trends Biochem Sci 31, 35-40.

**Bird**, A. (**2002**). DNA methylation patterns and epigenetic memory. Genes Dev 16, 6-21.

**Bischof**, J., Maeda, R.K., Hediger, M., Karch, F., and Basler, K. (**2007**). An optimized transgenesis system for *Drosophila* using germ-line-specific phiC31 integrases. Proc Natl Acad Sci U S A 104, 3312-3317.

**Blais**, A., and **Dynlacht**, B.D. (**2007**). E2F-associated chromatin modifiers and cell cycle control. Curr Opin Cell Biol 19, 658-662.

**Blum**, H., Beier, H., and Gross, H.J. (**1987**). Improved silver staining of plant proteins, RNA and DNA in polyacrylamide gels. Electrophoresis 8.

**Boccuni**, P., MacGrogan, D., Scandura, J.M., and Nimer, S.D. (**2003**). The human L(3)MBT polycomb group protein is a transcriptional repressor and interacts physically and functionally with TEL (ETV6). J Biol Chem 278, 15412-15420.

**Bonasio**, R., Lecona, E., and Reinberg, D. (**2010**). MBT domain proteins in development and disease. Semin Cell Dev Biol 21, 221-230.

**Bornemann**, D., Miller, E., and Simon, J. (**1996**). The *Drosophila* Polycomb group gene Sex comb on midleg (Scm) encodes a zinc finger protein with similarity to polyhomeotic protein. Development 122, 1621-1630.

**Botuyan**, M.V., Lee, J., Ward, I.M., Kim, J.E., Thompson, J.R., Chen, J., and Mer, G. (**2006**). Structural basis for the methylation state-specific recognition of histone H4-K20 by 53BP1 and Crb2 in DNA repair. Cell 127, 1361-1373.

**Boyer**, L.A., Plath, K., Zeitlinger, J., Brambrink, T., Medeiros, L.A., Lee, T.I., Levine, S.S., Wernig, M., Tajonar, A., Ray, M.K., Bell, G.W., Otte, A.P., Vidal, M., Gifford, D.K., Young, R.A., and Jaenisch, R. (**2006**). Polycomb complexes repress developmental regulators in murine embryonic stem cells. Nature 441, 349-353.

**Bradford,** M.M. (**1976**). A rapid and sensitive method for the quantitation of microgram quantities of protein utilizing the principle of protein-dye binding. Anal Biochem 72, 248-254.

**Braun**, H., Koop, R., Ertmer, A., Nacht, S., and Suske, G. (**2001**). Transcription factor Sp3 is regulated by acetylation. Nucleic Acids Res 29, 4994-5000.

**Breen**, T.R., and **Duncan**, I.M. (**1986**). Maternal expression of genes that regulate the bithorax complex of *Drosophila melanogaster*. Dev Biol 118, 442-456.

**Breen**, T.R., and **Harte**, P.J. (**1991**). Molecular characterization of the trithorax gene, a positive regulator of homeotic gene expression in *Drosophila*. Mech Dev 35, 113-127.

**Brehm**, A., Längst, G., Kehle, J., Clapier, C.R., Imhof, A., Eberharter, A., Müller, J., and Becker, P.B. (**2000**). dMi-2 and ISWI chromatin remodelling factors have distinct nucleosome binding and mobilization properties. EMBO J 19, 4332-4341.

**Brehm**, A., Miska, E.A., McCance, D.J., Reid, J.L., Bannister, A.J., and Kouzarides, T. (**1998**). Retinoblastoma protein recruits histone deacetylase to repress transcription. Nature 391, 597-601.

**Brent**, M.M., and **Marmorstein**, R. (**2008**). Ankyrin for methylated lysines. Nat Struct Mol Biol 15, 221-222.

**Brown**, J.L., Fritsch, C., Mueller, J., and Kassis, J.A. (**2003**). The *Drosophila* pho-like gene encodes a YY1-related DNA binding protein that is redundant with pleiohomeotic in homeotic gene silencing. Development 130, 285-294.

**Brown**, J.L., Mucci, D., Whiteley, M., Dirksen, M.L., and Kassis, J.A. (**1998**). The *Drosophila* Polycomb group gene pleiohomeotic encodes a DNA binding protein with homology to the

transcription factor YY1. Mol Cell 1, 1057-1064.

**Byrd**, K.N., and **Shearn**, A. (**2003**). ASH1, a *Drosophila* trithorax group protein, is required for methylation of lysine 4 residues on histone H3. Proc Natl Acad Sci U S A 100, 11535-11540.

**Cao**, R., Wang, L., Wang, H., Xia, L., Erdjument-Bromage, H., Tempst, P., Jones, R.S., and Zhang, Y. (**2002**). Role of histone H3 lysine 27 methylation in Polycomb-group silencing. Science 298, 1039-1043.

**Capili**, A.D., Schultz, D.C., RauscherIII, F.J., and Borden, K.L. (**2001**). Solution structure of the PHD domain from the KAP-1 corepressor: structural determinants for PHD, RING and LIM zinc-binding domains. EMBO J 20, 165-177.

**Caussinus**, E., and **Gonzalez**, C. (**2005**). Induction of tumor growth by altered stem-cell asymmetric division in *Drosophila melanogaster*. Nat Genet 37, 1125-1129.

**Chang**, B., Chen, Y., Zhao, Y., and Bruick, R.K. (**2007**). JMJD6 is a histone arginine demethylase. Science 318, 444-447.

**Chen**, G., Fernandez, J., Mische, S., and Courey, A.J. (**1999**). A functional interaction between the histone deacetylase Rpd3 and the corepressor groucho in *Drosophila* development. Genes Dev 13, 2218-2230.

**Cho**, Y., Griswold, A., Campbell, C., and Min, K.T. (**2005**). Individual histone deacetylases in *Drosophila* modulate transcription of distinct genes. Genomics 86, 606-617.

**Cho**, Y.W., Hong, T., Hong, S., Guo, H., Yu, H., Kim, D., Guszczynski, T., Dressler, G.R., Copeland, T.D., Kalkum, M., and Ge, K. (**2007**). PTIP associates with MLL3- and MLL4-containing histone H3 lysine 4 methyltransferase complex. J Biol Chem 282, 20395-20406.

**Clemens**, J.C., Worby, C.A., Simonson-Leff, N., Muda, M., Maehama, T., Hemmings, B.A., and Dixon, J.E. (**2000**). Use of double-stranded RNA interference in *Drosophila* cell lines to dissect signal transduction pathways. Proc Natl Acad Sci U S A 97, 6499-6503.

**Clements**, A., Poux, A.N., Lo, W.S., Pillus, L., Berger, S.L., and Marmorstein, R. (**2003**). Structural basis for histone and phosphohistone binding by the GCN5 histone acetyltransferase. Mol Cell 12, 461-473.

**Cox**, D.N., Chao, A., Baker, J., Chang, L., Qiao, D., and Lin, H. (**1998**). A novel class of evolutionarily conserved genes defined by piwi are essential for stem cell self-renewal. Genes Dev 12, 3715-3727.

**Cronmiller**, C., Schedl, P., and Cline, T.W. (**1988**). Molecular characterization of daughterless, a *Drosophila* sex determination gene with multiple roles in development. Genes Dev 2, 1666-1676.

**Curran**, S.P., Wu, X., Riedel, C.G., and Ruvkun, G. (**2009**). A soma-to-germline transformation in long-lived *Caenorhabditis elegans* mutants. Nature 459, 1079-1084.

**Cuthbert**, G.L., Daujat, S., Snowden, A.W., Erdjument-Bromage, H., Hagiwara, T., Yamada, M., Schneider, R., Gregory, P.D., Tempst, P., Bannister, A.J., and Kouzarides, T. (**2004**). Histone deimination antagonizes arginine methylation. Cell 118, 545-553.

**Czermin**, B., Melfi, R., McCabe, D., Seitz, V., Imhof, A., and Pirrotta, V. (**2002**). *Drosophila* enhancer of Zeste/ESC complexes have a histone H3 methyltransferase activity that marks chromosomal Polycomb sites. Cell 111, 185-196.

**Dallman**, J.E., Allopenna, J., Bassett, A., Travers, A., and Mandel, G. (**2004**). A conserved role but different partners for the transcriptional corepressor CoREST in fly and mammalian nervous system formation. J Neurosci 24, 7186-7193.

**de la Cruz**, X., Lois, S., Sánchez-Molina, S., and Martínez-Balbás, M.A. (**2005**). Do protein motifs read the histone code? Bioessays 27, 164-175.

**De Rubertis**, F., Kadosh, D., Henchoz, S., Pauli, D., Reuter, G., Struhl, K., and Spierer, P. (**1996**). The histone deacetylase RPD3 counteracts genomic silencing in *Drosophila* and yeast. Nature 384, 589-591.

**De Santa**, F., Totaro, M.G., Prosperini, E., Notarbartolo, S., Testa, G., and Natoli, G. (**2007**). The histone H3 lysine-27 demethylase Jmjd3 links inflammation to inhibition of polycomb-mediated gene silencing. Cell 130, 1083-1094.

**Dhalluin**, C., Carlson, J.E., Zeng, L., He, C., Aggarwal, A.K., and Zhou, M.M. (**1999**). Structure and ligand of a histone acetyltransferase bromodomain. Nature 399, 491-496.

**Di Lorenzo**, A., and **Bedford**, M.T. (**2010**). Histone arginine methylation. FEBS Lett 585(13), 2024-2031.

**Di Stefano**, L., Ji, J.Y., Moon, N.S., Herr, A., and Dyson, N. (**2007**). Mutation of *Drosophila* Lsd1 disrupts H3-K4 methylation, resulting in tissue-specific defects during development. Curr Biol 17, 808-812.

**Di Stefano**, L., Walker, J.A., Burgio, G., Corona, D.F., Mulligan, P., Näär, A.M., and Dyson, N.J. (**2011**). Functional antagonism between histone H3K4 demethylases *in vivo*. Genes Dev 25, 17-28.

**Dietzl**, G., Chen, D., Schnorrer, F., Su, K.C., Barinova, Y., Fellner, M., Gasser, B., Kinsey, K., Oppel, S., Scheiblauer, S., Couto, A., Marra, V., Keleman, K., and Dickson, B.J. (**2007**). A genome-wide transgenic RNAi library for conditional gene inactivation in *Drosophila*. Nature 448, 151-156.

**Dion**, M.F., Kaplan, T., Kim, M., Buratowski, S., Friedman, N., and Rando, O.J. (**2007**). Dynamics of replication-independent histone turnover in budding yeast. Science 315, 1405-1408.

**Duffy**, J.B. (**2002**). GAL4 system in *Drosophila*: a fly geneticist's Swiss army knife. Genesis 34, 1-15.

**Eberharter**, A., Vetter, I., Ferreira, R., and Becker, P.B. (**2004**). ACF1 improves the effectiveness of nucleosome mobilization by ISWI through PHD-histone contacts. EMBO J 23, 4029-4039.

**Echalier**, G., and **Ohanessian**, A. (**1970**). In vitro culture of *Drosophila melanogaster* embryonic cells. In Vitro 6, 162-172.

**Eissenberg**, J.C., and **Elgin**, S.C. (**2000**). The HP1 protein family: getting a grip on chromatin. Curr Opin Genet Dev 10, 204-210.

**Eissenberg**, J.C., James, T.C., Foster-Hartnett, D.M., Hartnett, T., Ngan, V., and Elgin, S.C. (**1990**). Mutation in a heterochromatin-specific chromosomal protein is associated with suppression of position-effect variegation in *Drosophila melanogaster*. Proc Natl Acad Sci U S A 87, 9923-9927.

**Eissenberg**, J.C., Lee, M.G., Schneider, J., Ilvarsonn, A., Shiekhattar, R., and Shilatifard, A. (**2007**). The trithorax-group gene in *Drosophila* little imaginal discs encodes a trimethylated histone H3 Lys4 demethylase. Nat Struct Mol Biol 14, 344-346.

**Eryilmaz**, J., Pan, P., Amaya, M.F., Allali-Hassani, A., Dong, A., Adams-Cioaba, M.A., Mackenzie, F., Vedadi, M., and Min, J. (**2009**). Structural studies of a four-MBT repeat protein MBTD1. PLoS One 4, e7274.

**Eskeland**, R., Leeb, M., Grimes, G.R., Kress, C., Boyle, S., Sproul, D., Gilbert, N., Fan, Y., Skoultchi, A.I., Wutz, A., and Bickmore, W.A. (**2010**). Ring1B compacts chromatin structure and represses gene expression independent of histone ubiquitination. Mol Cell 38, 452-464.

**Fay**, D.S., and **Yochem**, J. (**2007**). The SynMuv genes of *Caenorhabditis elegans* in vulval development and beyond. Dev Biol 306, 1-9.

**Feng**, Q., Wang, H., Ng, H.H., Erdjument-Bromage, H., Tempst, P., Struhl, K., and Zhang, Y. (**2002**). Methylation of H3-lysine 79 is mediated by a new family of HMTases without a SET domain. Curr Biol 12, 1052-1058.

**Fire**, A., Xu, S., Montgomery, M.K., Kostas, S.A., Driver, S.E., and Mello, C.C. (**1998**). Potent and specific genetic interference by double-stranded RNA in *Caenorhabditis elegans*. Nature 391, 806-811.

**Fischle**, W., Tseng, B.S., Dormann, H.L., Ueberheide, B.M., Garcia, B.A., Shabanowitz, J., Hunt, D.F., Funabiki, H., and Allis, C.D. (**2005**). Regulation of HP1-chromatin binding by histone H3 methylation and phosphorylation. Nature 438, 1116-1122.

**Fischle**, W., Wang, Y., Jacobs, S.A., Kim, Y., Allis, C.D., and Khorasanizadeh, S. (**2003**). Molecular basis for the discrimination of repressive methyl-lysine marks in histone H3 by Polycomb and HP1 chromodomains. Genes Dev 17, 1870-1881.

**Fitzgerald**, D.J., Berger, P., Schaffitzel, C., Yamada, K., Richmond, T.J., and Berger, I. (**2006**). Protein complex expression by using multigene baculoviral vectors. Nat Methods 3, 1021-1032.

**Francis**, N.J., Kingston, R.E., and Woodcock, C.L. (**2004**). Chromatin compaction by a polycomb group protein complex. Science 306, 1574-1577.

**Francis**, N.J., Saurin, A.J., Shao, Z., and Kingston, R.E. (**2001**). Reconstitution of a functional core polycomb repressive complex. Mol Cell 8, 545-556.

**Frolov**, M.V., and **Dyson**, N.J. (**2004**). Molecular mechanisms of E2F-dependent activation and pRB-mediated repression. J Cell Sci 117, 2173-2181.

**Gardner**, K.E., Allis, C.D., and Strahl, B.D. (**2011**). OPERating ON Chromatin, a Colorful Language where Context Matters. J Mol Biol 409(1), 36-46.

**Gateff**, E. (**1978**). Malignant neoplasms of genetic origin in *Drosophila melanogaster*. Science 200, 1448-1459.

**Gateff**, E., Löffler, T., and Wismar, J. (**1993**). A temperature-sensitive brain tumor suppressor mutation of *Drosophila melanogaster*: developmental studies and molecular localization of the gene. Mech Dev 41, 15-31.

**Georlette**, D., Ahn, S., MacAlpine, D.M., Cheung, E., Lewis, P.W., Beall, E.L., Bell, S.P., Speed, T., Manak, J.R., and Botchan, M.R. (**2007**). Genomic profiling and expression studies reveal both positive and negative activities for the *Drosophila* Myb MuvB/dREAM complex in proliferating cells. Genes Dev 21, 2880-2896.

**Gévry**, N., Svotelis, A., Larochelle, M., and Gaudreau, L. (**2009**). Nucleosome mapping. Methods Mol Biol 543, 281-291.

**Gildea**, J.J., Lopez, R., and Shearn, A. (**2000**). A screen for new trithorax group genes identified little imaginal discs, the *Drosophila melanogaster* homologue of human retinoblastoma binding protein 2. Genetics 156, 645-663.

**Goto**, H., Tomono, Y., Ajiro, K., Kosako, H., Fujita, M., Sakurai, M., Okawa, K., Iwamatsu, A., Okigaki, T., Takahashi, T., and Inagaki, M. (**1999**). Identification of a novel phosphorylation site on histone H3 coupled with mitotic chromosome condensation. J Biol Chem 274, 25543-25549.

**Graham**, F.L., and **van der Eb**, A.J. (**1973a**). A new technique for the assay of infectivity of human adenovirus 5 DNA. Virology 52, 456-467.

**Graham**, F.L., and **van der Eb**, A.J. (**1973b**). Transformation of rat cells by DNA of human adenovirus 5. Virology 54, 536-539.

**Grau**, D.J., Chapman, B.A., Garlick, J.D., Borowsky, M., Francis, N.J., and Kingston, R.E. (**2011**). Compaction of chromatin by diverse Polycomb group proteins requires localized regions of high charge. Genes Dev 25, 2210-2221.

**Grimm**, C., de Ayala Alonso, A.G., Rybin, V., Steuerwald, U., Ly-Hartig, N., Fischle, W., Müller, J., and Müller, C.W. (**2007**). Structural and functional analyses of methyl-lysine binding by the malignant brain tumour repeat protein Sex comb on midleg. EMBO Rep 8, 1031-1037.

**Grimm**, C., Matos, R., Ly-Hartig, N., Steuerwald, U., Lindner, D., Rybin, V., Müller, J., and Müller, C.W. (**2009**). Molecular recognition of histone lysine methylation by the Polycomb group repressor dSfmbt. EMBO J 28, 1965-1977.

**Guo**, Y., Nady, N., Qi, C., Allali-Hassani, A., Zhu, H., Pan, P., Adams-Cioaba, M.A., Amaya, M.F., Dong, A., Vedadi, M., Schapira, M., Read, R.J., Arrowsmith, C.H., and Min, J. (**2009**). Methylation-state-specific recognition of histones by the MBT repeat protein L3MBTL2. Nucleic Acids Res 37, 2204-2210.

**Gurvich**, N., Perna, F., Farina, A., Voza, F., Menendez, S., Hurwitz, J., and Nimer, S.D. (**2010**). L3MBTL1 polycomb protein, a candidate tumor suppressor in del(20q12) myeloid disorders, is essential for genome stability. Proc Natl Acad Sci U S A 107, 22552-22557.

**Hagemeier**, C., Cook, A., and Kouzarides, T. (**1993**). The retinoblastoma protein binds E2F residues required for activation *in vivo* and TBP binding in vitro. Nucleic Acids Res 21, 4998-5004.

**Hakimi**, M.A., Bochar, D.A., Chenoweth, J., Lane, W.S., Mandel, G., and Shiekhattar, R. (**2002**). A core-BRAF35 complex containing histone deacetylase mediates repression of neuronal-specific genes. Proc Natl Acad Sci U S A 99, 7420-7425.

**Hakimi**, M.A., Dong, Y., Lane, W.S., Speicher, D.W., and Shiekhattar, R. (**2003**). A candidate X-linked mental retardation gene is a component of a new family of histone deacetylase-containing complexes. J Biol Chem 278, 7234-7239.

**Han**, Z., Guo, L., Wang, H., Shen, Y., Deng, X.W., and Chai, J. (**2006**). Structural basis for the specific recognition of methylated histone H3 lysine 4 by the WD-40 protein WDR5. Mol Cell 22, 137-144.

**Hansen**, K.H., Bracken, A.P., Pasini, D., Dietrich, N., Gehani, S.S., Monrad, A., Rappsilber, J., Lerdrup, M., and Helin, K. (**2008**). A model for transmission of the H3K27me3 epigenetic mark. Nat Cell Biol 10, 1291-1300.

**Harrison**, M.M., Ceol, C.J., Lu, X., and Horvitz, H.R. (**2006**). Some *C. elegans* class B synthetic multivulva proteins encode a conserved LIN-35 Rb-containing complex distinct from a NuRD-like complex. Proc Natl Acad Sci U S A 103, 16782-16787.

**Harrison**, M.M., Lu, X., and Horvitz, H.R. (**2007**). LIN-61, one of two *Caenorhabditis elegans* malignant-brain-tumor-repeat-containing proteins, acts with the DRM and NuRD-like protein complexes in vulval development but not in certain other biological processes. Genetics 176, 255-271.

**Harvey**, K., and **Tapon**, N. (**2007**). The Salvador-Warts-Hippo pathway - an emerging tumour-suppressor network. Nat Rev Cancer 7, 182-191.

**Henikoff**, S., and **Shilatifard**, A. (**2011**). Histone modification: cause or cog? Trends Genet 27, 389-396.

**Herz**, H.M., Madden, L.D., Chen, Z., Bolduc, C., Buff, E., Gupta, R., Davuluri, R., Shilatifard, A., Hariharan, I.K., and Bergmann, A. (**2010**). The H3K27me3 demethylase dUTX is a suppressor of Notch- and Rb-dependent tumors in *Drosophila*. Mol Cell Biol 30, 2485-2497.

**Holohan**, E.E., Kwong, C., Adryan, B., Bartkuhn, M., Herold, M., Renkawitz, R., Russell, S., and White, R. (**2007**). CTCF genomic binding sites in *Drosophila* and the organisation of the bithorax complex. PLoS Genet 3, e112.

**Huang**, Y., Fang, J., Bedford, M.T., Zhang, Y., and Xu, R.M. (**2006**). Recognition of histone H3 lysine-4 methylation by the double tudor domain of JMJD2A. Science 312, 748-751.

**Huen**, M.S., Sy, S.M., van Deursen, J.M., and Chen, J. (**2008**). Direct interaction between SET8 and proliferating cell nuclear antigen couples H4-K20 methylation with DNA replication. J Biol Chem 283, 11073-11077.

**Huisinga**, K.L., Brower-Toland, B., and Elgin, S.C. (**2006**). The contradictory definitions of heterochromatin: transcription and silencing. Chromosoma 115, 110-122.

**Issaeva**, I., Zonis, Y., Rozovskaia, T., Orlovsky, K., Croce, C.M., Nakamura, T., Mazo, A., Eisenbach, L., and Canaani, E. (**2007**). Knockdown of ALR (MLL2) reveals ALR target genes and leads to alterations in cell adhesion and growth. Mol Cell Biol 27, 1889-1903.

**Jackson**, V., and **Chalkley**, R. (**1985**). Histone segregation on replicating chromatin. Biochemistry 24, 6930-6938.

**James**, T.C., and **Elgin**, S.C. (**1986**). Identification of a nonhistone chromosomal protein associated with heterochromatin in *Drosophila melanogaster* and its gene. Mol Cell Biol 6, 3862-3872.

**Janic**, A., Mendizabal, L., Llamazares, S., Rossell, D., and Gonzalez, C. (**2010**). Ectopic expression of germline genes drives malignant brain tumor growth in *Drosophila*. Science 330, 1824-1827.

**Jeanmougin**, F., Wurtz, J.M., Le Douarin, B., Chambon, P., and Losson, R. (**1997**). The bromodomain revisited. Trends Biochem Sci 22, 151-153.

**Jenuwein**, T., and **Allis**, C.D. (**2001**). Translating the histone code. Science 293, 1074-1080.

**Jørgensen**, S., Elvers, I., Trelle, M.B., Menzel, T., Eskildsen, M., Jensen, O.N., Helleday, T., Helin, K., and Sørensen, C.S. (**2007**). The histone methyltransferase SET8 is required for S-phase progression. J Cell Biol 179, 1337-1345.

**Kalakonda**, N., Fischle, W., Boccuni, P., Gurvich, N., Hoya-Arias, R., Zhao, X., Miyata, Y., Macgrogan, D., Zhang, J., Sims, J.K., Rice, J.C., and Nimer, S.D. (**2008**). Histone H4 lysine 20 monomethylation promotes transcriptional repression by L3MBTL1. Oncogene 27, 4293-4304.

**Karytinos**, A., Forneris, F., Profumo, A., Ciossani, G., Battaglioli, E., Binda, C., and Mattevi, A. (**2009**). A novel mammalian flavin-dependent histone demethylase. J Biol Chem 284, 17775-17782.

**Kavi**, H.H., and **Birchler**, J.A. (**2009**). *Drosophila* KDM2 is a H3K4me3 demethylase regulating nucleolar organization. BMC Res Notes 2, 217.

**Kehle**, J., Beuchle, D., Treuheit, S., Christen, B., Kennison, J.A., Bienz, M., and Müller, J. (**1998**). dMi-2, a hunchback-interacting protein that functions in polycomb repression. Science 282, 1897-1900.

**Kelly**, A.E., Ghenoiu, C., Xue, J.Z., Zierhut, C., Kimura, H., and Funabiki, H. (**2010**). Survivin reads phosphorylated histone H3 threonine 3 to activate the mitotic kinase Aurora B. Science 330, 235-239.

**Kennison**, J.A. (**1995**). The Polycomb and trithorax group proteins of *Drosophila*: trans-regulators of homeotic gene function. Annu Rev Genet 29, 289-303.

**Ketel**, C.S., Andersen, E.F., Vargas, M.L., Suh, J., Strome, S., and Simon, J.A. (**2005**). Subunit contributions to histone methyltransferase activities of fly and worm polycomb group complexes. Mol Cell Biol 25, 6857-6868.

**Kim**, C.A., and **Bowie**, J.U. (**2003**). SAM domains: uniform structure, diversity of function. Trends Biochem Sci 28, 625-628.

**Kim**, C.A., Gingery, M., Pilpa, R.M., and Bowie, J.U. (**2002**). The SAM domain of polyhomeotic forms a helical polymer. Nat Struct Biol 9, 453-457.

**Kim**, C.A., Sawaya, M.R., Cascio, D., Kim, W., and Bowie, J.U. (**2005**). Structural organization

of a Sex-comb-on-midleg/polyhomeotic copolymer. J Biol Chem 280, 27769-27775.

**Kim**, J., Daniel, J., Espejo, A., Lake, A., Krishna, M., Xia, L., Zhang, Y., and Bedford, M.T. (**2006**). Tudor, MBT and chromo domains gauge the degree of lysine methylation. EMBO Rep 7, 397-403.

**Klymenko**, T., and **Müller**, J. (**2004**). The histone methyltransferases Trithorax and Ash1 prevent transcriptional silencing by Polycomb group proteins. EMBO Rep 5, 373-377.

**Klymenko**, T., Papp, B., Fischle, W., Köcher, T., Schelder, M., Fritsch, C., Wild, B., Wilm, M., and Müller, J. (**2006**). A Polycomb group protein complex with sequence-specific DNA-binding and selective methyl-lysine-binding activities. Genes Dev 20, 1110-1122.

**Koester-Eiserfunke**, N., and **Fischle**, W. (**2011**). H3K9me2/3 binding of the MBT domain protein LIN-61 is essential for *Caenorhabditis elegans* vulva development. PLoS Genet 7, e1002017.

**Koga**, H., Matsui, S., Hirota, T., Takebayashi, S., Okumura, K., and Saya, H. (**1999**). A human homolog of *Drosophila* lethal(3)malignant brain tumor (l(3)mbt) protein associates with condensed mitotic chromosomes. Oncogene 18, 3799-3809.

**Korenjak**, M., and **Brehm**, A. (**2005**). E2F-Rb complexes regulating transcription of genes important for differentiation and development. Curr Opin Genet Dev 15, 520-527.

**Korenjak**, M., Taylor-Harding, B., Binné, U.K., Satterlee, J.S., Stevaux, O., Aasland, R., White-Cooper, H., Dyson, N., and Brehm, A. (**2004**). Native E2F/RBF complexes contain Myb-interacting proteins and repress transcription of developmentally controlled E2F target genes. Cell 119, 181-193.

**Kornberg**, R.D. (**1977**). Structure of chromatin. Annu Rev Biochem 46, 931-954.

**Kouzarides**, T. (**2007**). Chromatin modifications and their function. Cell 128, 693-705.

**Krogan**, N.J., Dover, J., Wood, A., Schneider, J., Heidt, J., Boateng, M.A., Dean, K., Ryan, O.W., Golshani, A., Johnston, M., Greenblatt, J.F., and Shilatifard, A. (**2003**). The Paf1 complex is required for histone H3 methylation by COMPASS and Dot1p: linking transcriptional elongation to histone methylation. Mol Cell 11, 721-729.

**Kunert**, N., and **Brehm**, A. (**2008**). Mass production of *Drosophila* embryos and chromatographic purification of native protein complexes. Methods Mol Biol 420, 359-371.

**Kunert**, N., Wagner, E., Murawska, M., Klinker, H., Kremmer, E., and Brehm, A. (**2009**). dMec: a novel Mi-2 chromatin remodelling complex involved in transcriptional repression. EMBO J 28, 533-544.

**Kuzmichev**, A., Nishioka, K., Erdjument-Bromage, H., Tempst, P., and Reinberg, D. (**2002**). Histone methyltransferase activity associated with a human multiprotein complex containing the Enhancer of Zeste protein. Genes Dev 16, 2893-2905.

**Kuzmin**, A., Han, Z., Golding, M.C., Mann, M.R., Latham, K.E., and Varmuza, S. (**2008**). The PcG gene Sfmbt2 is paternally expressed in extraembryonic tissues. Gene Expr Patterns 8, 107-116.

**Lai**, J.S., and **Herr**, W. (**1992**). Ethidium bromide provides a simple tool for identifying genuine DNA-independent protein associations. Proc Natl Acad Sci U S A 89, 6958-6962.

**LaJeunesse**, D., and **Shearn**, A. (**1995**). Trans-regulation of thoracic homeotic selector genes of the Antennapedia and bithorax complexes by the trithorax group genes: absent, small, and homeotic discs 1 and 2. Mech Dev 53, 123-139.

**Lan**, F., Bayliss, P.E., Rinn, J.L., Whetstine, J.R., Wang, J.K., Chen, S., Iwase, S., Alpatov, R., Issaeva, I., Canaani, E., Roberts, T.M., Chang, H.Y., and Shi, Y. (**2007a**). A histone H3 lysine 27 demethylase regulates animal posterior development. Nature 449, 689-694.

**Lan**, F., Collins, R.E., De Cegli, R., Alpatov, R., Horton, J.R., Shi, X., Gozani, O., Cheng, X., and Shi, Y. (**2007b**). Recognition of unmethylated histone H3 lysine 4 links BHC80 to LSD1-mediated gene repression. Nature 448, 718-722.

**Lee**, C.Y., Robinson, K.J., and Doe, C.Q. (**2006a**). Lgl, Pins and aPKC regulate neuroblast self-renewal versus differentiation. Nature 439, 594-598.

**Lee**, M.G., Villa, R., Trojer, P., Norman, J., Yan, K.P., Reinberg, D., Di Croce, L., and Shiekhattar, R. (**2007a**). Demethylation of H3K27 regulates polycomb recruitment and H2A ubiquitination. Science 318, 447-450.

**Lee**, M.G., Wynder, C., Cooch, N., and Shiekhattar, R. (**2005**). An essential role for CoREST in nucleosomal histone 3 lysine 4 demethylation. Nature 437, 432-435.

**Lee**, N., Zhang, J., Klose, R.J., Erdjument-Bromage, H., Tempst, P., Jones, R.S., and Zhang, Y. (**2007b**). The trithorax-group protein Lid is a histone H3 trimethyl-Lys4 demethylase. Nat Struct Mol Biol 14, 341-343.

**Lee**, T.I., Jenner, R.G., Boyer, L.A., Guenther, M.G., Levine, S.S., Kumar, R.M., Chevalier, B., Johnstone, S.E., Cole, M.F., Isono, K., et al. (**2006b**). Control of developmental regulators by Polycomb in human embryonic stem cells. Cell 125, 301-313.

**Lehmann**, R., and **Nüsslein-Volhard**, C. (**1991**). The maternal gene nanos has a central role in posterior pattern formation of the *Drosophila* embryo. Development 112, 679-691.

**Levine**, S.S., Weiss, A., Erdjument-Bromage, H., Shao, Z., Tempst, P., and Kingston, R.E. (**2002**). The core of the polycomb repressive complex is compositionally and functionally conserved in flies and humans. Mol Cell Biol 22, 6070-6078.

**Lewis**, P.W., Beall, E.L., Fleischer, T.C., Georlette, D., Link, A.J., and Botchan, M.R. (**2004**). Identification of a *Drosophila* Myb-E2F2/RBF transcriptional repressor complex. Genes Dev 18, 2929-2940.

**Li**, B., Carey, M., and Workman, J.L. (**2007a**). The role of chromatin during transcription. Cell 128, 707-719.

**Li**, H., Fischle, W., Wang, W., Duncan, E.M., Liang, L., Murakami-Ishibe, S., Allis, C.D., and Patel, D.J. (**2007b**). Structural basis for lower lysine methylation state-specific readout by MBT repeats of L3MBTL1 and an engineered PHD finger. Mol Cell 28, 677-691.

**Li**, H., Ilin, S., Wang, W., Duncan, E.M., Wysocka, J., Allis, C.D., and Patel, D.J. (**2006**). Molecular basis for site-specific read-out of histone H3K4me3 by the BPTF PHD finger of NURF. Nature 442, 91-95.

**Li**, J., Bench, A.J., Vassiliou, G.S., Fourouclas, N., Ferguson-Smith, A.C., and Green, A.R. (**2004**). Imprinting of the human L3MBTL gene, a polycomb family member located in a region of chromosome 20 deleted in human myeloid malignancies. Proc Natl Acad Sci U S A 101, 7341-7346.

**Liang**, G., Lin, J.C., Wei, V., Yoo, C., Cheng, J.C., Nguyen, C.T., Weisenberger, D.J., Egger, G., Takai, D., Gonzales, F.A., and Jones, P.A. (**2004**). Distinct localization of histone H3 acetylation and H3-K4 methylation to the transcription start sites in the human genome. Proc Natl Acad Sci U S A 101, 7357-7362.

**Liu**, W., Tanasa, B., Tyurina, O.V., Zhou, T.Y., Gassmann, R., Liu, W.T., Ohgi, K.A., Benner, C., Garcia-Bassets, I., Aggarwal, A.K., Desai, A., Dorrestein, P.C., Glass, C.K., and Rosenfeld, M.G. (**2010**). PHF8 mediates histone H4 lysine 20 demethylation events involved in cell cycle progression. Nature 466, 508-512.

**Lloret-Llinares**, M., Carré, C., Vaquero, A., de Olano, N., and Azorín, F. (**2008**). Characterization of *Drosophila melanogaster* JmjC+N histone demethylases. Nucleic Acids Res 36, 2852-2863.

**Loyola**, A., Bonaldi, T., Roche, D., Imhof, A., and Almouzni, G. (**2006**). PTMs on H3 variants before chromatin assembly potentiate their final epigenetic state. Mol Cell 24, 309-316.

**Lu**, J., Ruhf, M.L., Perrimon, N., and Leder, P. (**2007**). A genome-wide RNA interference screen identifies putative chromatin regulators essential for E2F repression. Proc Natl Acad Sci U S A 104, 9381-9386.

**Luco**, R.F., Pan, Q., Tominaga, K., Blencowe, B.J., Pereira-Smith, O.M., and Misteli, T. (**2010**). Regulation of alternative splicing by histone modifications. Science 327, 996-1000.

**Luger**, K., Mäder, A.W., Richmond, R.K., Sargent, D.F., and Richmond, T.J. (**1997**). Crystal structure of the nucleosome core particle at 2.8 A resolution. Nature 389, 251-260.

**Lyko**, F., Ramsahoye, B.H., and Jaenisch, R. (**2000**). DNA methylation in *Drosophila melanogaster*. Nature 408, 538-540.

**MacGrogan**, D., Kalakonda, N., Alvarez, S., Scandura, J.M., Boccuni, P., Johansson, B., and Nimer, S.D. (**2004**). Structural integrity and expression of the L3MBTL gene in normal and malignant hematopoietic cells. Genes Chromosomes Cancer 41, 203-213.

**Manheim**, E.A., and **McKim**, K.S. (**2003**). The Synaptonemal complex component C(2)M regulates meiotic crossing over in *Drosophila*. Curr Biol 13, 276-285.

**Mantri**, M., Krojer, T., Bagg, E.A., Webby, C.A., Butler, D.S., Kochan, G., Kavanagh, K.L., Oppermann, U., McDonough, M.A., and Schofield, C.J. (**2010**). Crystal Structure of the 2-Oxoglutarate- and Fe(II)-Dependent Lysyl Hydroxylase JMJD6. J Mol Biol.

**Margueron**, R., Justin, N., Ohno, K., Sharpe, M.L., Son, J., Drury, W.J., Voigt, P., Martin, S.R., Taylor, W.R., De Marco, V., Pirrotta, V., Reinberg, D., and Gamblin, S.J. (**2009**). Role of the polycomb protein EED in the propagation of repressive histone marks. Nature 461, 762-767.

**Maurer-Stroh**, S., Dickens, N.J., Hughes-Davies, L., Kouzarides, T., Eisenhaber, F., and Ponting, C.P. (**2003**). The Tudor domain 'Royal Family': Tudor, plant Agenet, Chromo, PWWP and MBT domains. Trends Biochem Sci 28, 69-74.

**McKittrick**, E., Gafken, P.R., Ahmad, K., and Henikoff, S. (**2004**). Histone H3.3 is enriched in covalent modifications associated with active chromatin. Proc Natl Acad Sci U S A 101, 1525-1530.

**Milne**, T.A., Briggs, S.D., Brock, H.W., Martin, M.E., Gibbs, D., Allis, C.D., and Hess, J.L. (**2002**). MLL targets SET domain methyltransferase activity to Hox gene promoters. Mol Cell 10, 1107-1117.

**Min**, J., Allali-Hassani, A., Nady, N., Qi, C., Ouyang, H., Liu, Y., MacKenzie, F., Vedadi, M., and Arrowsmith, C.H. (**2007**). L3MBTL1 recognition of mono- and dimethylated histones. Nat Struct Mol Biol 14, 1229-1230.

**Min**, J., Zhang, Y., and Xu, R.M. (**2003**). Structural basis for specific binding of Polycomb chromodomain to histone H3 methylated at Lys 27. Genes Dev 17, 1823-1828.

**Mito**, Y., Henikoff, J.G., and Henikoff, S. (**2007**). Histone replacement marks the boundaries of cis-regulatory domains. Science 315, 1408-1411.

**Mohd-Sarip**, A., van der Knaap, J.A., Wyman, C., Kanaar, R., Schedl, P., and Verrijzer, C.P. (**2006**). Architecture of a polycomb nucleoprotein complex. Mol Cell 24, 91-100.

**Montini**, E., Buchner, G., Spalluto, C., Andolfi, G., Caruso, A., den Dunnen, J.T., Trump, D., Rocchi, M., Ballabio, A., and Franco, B. (**1999**). Identification of SCML2, a second human gene homologous to the *Drosophila* sex comb on midleg (Scm): A new gene cluster on Xp22. Genomics 58, 65-72.

**Moshkin**, Y.M., Kan, T.W., Goodfellow, H., Bezstarosti, K., Maeda, R.K., Pilyugin, M., Karch, F., Bray, S.J., Demmers, J.A., and Verrijzer, C.P. (**2009**). Histone chaperones ASF1 and NAP1

differentially modulate removal of active histone marks by LID-RPD3 complexes during NOTCH silencing. Mol Cell 35, 782-793.

**Murawska**, M., Kunert, N., van Vugt, J., Längst, G., Kremmer, E., Logie, C., and Brehm, A. (**2008**). dCHD3, a novel ATP-dependent chromatin remodeler associated with sites of active transcription. Mol Cell Biol 28, 2745-2757.

**Müller**, J., Hart, C.M., Francis, N.J., Vargas, M.L., Sengupta, A., Wild, B., Miller, E.L., O'Connor, M.B., Kingston, R.E., and Simon, J.A. (**2002**). Histone methyltransferase activity of a *Drosophila* Polycomb group repressor complex. Cell 111, 197-208.

**Müller**, J., and **Kassis**, J.A. (**2006**). Polycomb response elements and targeting of Polycomb group proteins in *Drosophila*. Curr Opin Genet Dev 16, 476-484.

**Müller**, J., and **Verrijzer**, P. (**2009**). Biochemical mechanisms of gene regulation by polycomb group protein complexes. Curr Opin Genet Dev 19, 150-158.

**Nagy**, L., Kao, H.Y., Chakravarti, D., Lin, R.J., Hassig, C.A., Ayer, D.E., Schreiber, S.L., and Evans, R.M. (**1997**). Nuclear receptor repression mediated by a complex containing SMRT, mSin3A, and histone deacetylase. Cell 89, 373-380.

**Nègre**, N., Brown, C.D., Shah, P.K., Kheradpour, P., Morrison, C.A., Henikoff, J.G., Feng, X., Ahmad, K., Russell, S., White, R.A., Henikoff, S., Kellis, M., and White, K.P. (**2010**). A comprehensive map of insulator elements for the *Drosophila* genome. PLoS Genet 6, e1000814.

**Nekrasov**, M., Klymenko, T., Fraterman, S., Papp, B., Oktaba, K., Köcher, T., Cohen, A., Stunnenberg, H.G., Wilm, M., and Müller, J. (**2007**). Pcl-PRC2 is needed to generate high levels of H3-K27 trimethylation at Polycomb target genes. EMBO J 26, 4078-4088.

**Nekrasov**, M., Wild, B., and Müller, J. (**2005**). Nucleosome binding and histone methyltransferase activity of *Drosophila* PRC2. EMBO Rep 6, 348-353.

**Neumüller**, R.A., and **Knoblich**, J.A. (**2009**). Dividing cellular asymmetry: asymmetric cell division and its implications for stem cells and cancer. Genes Dev 23, 2675-2699.

**Ng**, H.H., Robert, F., Young, R.A., and Struhl, K. (**2003**). Targeted recruitment of Set1 histone methylase by elongating Pol II provides a localized mark and memory of recent transcriptional activity. Mol Cell 11, 709-719.

**Nishioka**, K., Rice, J.C., Sarma, K., Erdjument-Bromage, H., Werner, J., Wang, Y., Chuikov, S., Valenzuela, P., Tempst, P., Steward, R., Lis, J.T., Allis, C.D., and Reinberg, D. (**2002**). PR-Set7 is a nucleosome-specific methyltransferase that modifies lysine 20 of histone H4 and is associated with silent chromatin. Mol Cell 9, 1201-1213.

**Northcott**, P.A., Nakahara, Y., Wu, X., Feuk, L., Ellison, D.W., Croul, S., Mack, S., Kongkham, P.N., Peacock, J., Dubuc, A., et al., and Taylor, M.D. (**2009**). Multiple recurrent genetic events converge on control of histone lysine methylation in medulloblastoma. Nat Genet 41, 465-472.

**Nowak**, S.J., and **Corces**, V.G. (**2004**). Phosphorylation of histone H3: a balancing act between chromosome condensation and transcriptional activation. Trends Genet 20, 214-220.

**O'Connell**, S., Wang, L., Robert, S., Jones, C.A., Saint, R., and Jones, R.S. (**2001**). Polycomblike PHD fingers mediate conserved interaction with enhancer of zeste protein. J Biol Chem 276, 43065-43073.

**Ogawa**, H., Ishiguro, K., Gaubatz, S., Livingston, D.M., and Nakatani, Y. (**2002**). A complex with chromatin modifiers that occupies E2F- and Myc-responsive genes in G0 cells. Science 296, 1132-1136.

**Oktaba**, K., Gutiérrez, L., Gagneur, J., Girardot, C., Sengupta, A.K., Furlong, E.E., and Müller, J. (**2008**). Dynamic regulation by polycomb group protein complexes controls pattern formation and the cell cycle in *Drosophila*. Dev Cell 15, 877-889.

**Owen**, D.J., Ornaghi, P., Yang, J.C., Lowe, N., Evans, P.R., Ballario, P., Neuhaus, D., Filetici, P., and Travers, A.A. (**2000**). The structural basis for the recognition of acetylated histone H4 by the bromodomain of histone acetyltransferase gcn5p. EMBO J 19, 6141-6149.

**Pagliarini**, D. (**2008**). Struktur-/Funktionsanalysen der MBT-Domänen des *Drosophila* Proteins L(3)mbt. Diploma thesis (Philipps-Universität Marburg).

**Papp**, B., and **Müller**, J. (**2006**). Histone trimethylation and the maintenance of transcriptional ON and OFF states by trxG and PcG proteins. Genes Dev 20, 2041-2054.

**Pascual**, J., Martinez-Yamout, M., Dyson, H.J., and Wright, P.E. (**2000**). Structure of the PHD zinc finger from human Williams-Beuren syndrome transcription factor. J Mol Biol 304, 723-729.

**Perna**, F., Gurvich, N., Hoya-Arias, R., Abdel-Wahab, O., Levine, R.L., Asai, T., Voza, F., Menendez, S., Wang, L., Liu, F., Zhao, X., and Nimer, S.D. (**2010**). Depletion of L3MBTL1 promotes the erythroid differentiation of human hematopoietic progenitor cells: possible role in 20q- polycythemia vera. Blood 116, 2812-2821.

**Peterson**, A.J., Kyba, M., Bornemann, D., Morgan, K., Brock, H.W., and Simon, J. (**1997**). A domain shared by the Polycomb group proteins Scm and ph mediates heterotypic and homotypic interactions. Mol Cell Biol 17, 6683-6692.

**Peterson**, A.J., Mallin, D.R., Francis, N.J., Ketel, C.S., Stamm, J., Voeller, R.K., Kingston, R.E., and Simon, J.A. (**2004**). Requirement for sex comb on midleg protein interactions in *Drosophila* polycomb group repression. Genetics 167, 1225-1239.

**Pile**, L.A., and **Wassarman**, D.A. (**2000**). Chromosomal localization links the SIN3-RPD3 complex to the regulation of chromatin condensation, histone acetylation and gene expression. EMBO J 19, 6131-6140.

**Pokholok**, D.K., Harbison, C.T., Levine, S., Cole, M., Hannett, N.M., Lee, T.I., Bell, G.W., Walker, K., Rolfe, P.A., Herbolsheimer, E., Zeitlinger, J., Lewitter, F., Gifford, D.K., and Young, R.A. (**2005**). Genome-wide map of nucleosome acetylation and methylation in yeast. Cell 122, 517-527.

**Ponting**, C.P. (**1995**). SAM: a novel motif in yeast sterile and *Drosophila* polyhomeotic proteins. Protein Sci 4, 1928-1930.

**Preuss**, U., Landsberg, G., and Scheidtmann, K.H. (**2003**). Novel mitosis-specific phosphorylation of histone H3 at Thr11 mediated by Dlk/ZIP kinase. Nucleic Acids Res 31, 878-885.

**Pérez-Cadahía**, B., Drobic, B., and Davie, J.R. (**2009**). H3 phosphorylation: dual role in mitosis and interphase. Biochem Cell Biol 87, 695-709.

**Qin**, J., Van Buren, D., Huang, H.S., Zhong, L., Mostoslavsky, R., Akbarian, S., and Hock, H. (**2010**). Chromatin protein L3MBTL1 is dispensable for development and tumor suppression in mice. J Biol Chem 285, 27767-27775.

**Ragvin**, A., Valvatne, H., Erdal, S., Arskog, V., Tufteland, K.R., Breen, K., ØYan, A.M., Eberharter, A., Gibson, T.J., Becker, P.B., and Aasland, R. (**2004**). Nucleosome binding by the bromodomain and PHD finger of the transcriptional cofactor p300. J Mol Biol 337, 773-788.

**Reddy**, B.A., Bajpe, P.K., Bassett, A., Moshkin, Y.M., Kozhevnikova, E., Bezstarosti, K., Demmers, J.A., Travers, A.A., and Verrijzer, C.P. (**2010**). *Drosophila* transcription factor Tramtrack69 binds MEP1 to recruit the chromatin remodeler NuRD. Mol Cell Biol 30, 5234-5244.

**Reuter**, L.M. (**2011**). Analyse von Proteininteraktionen im *Drosophila* LINT-Komplex. Diploma thesis (Philipps-Universität Marburg).

**Richter**, C., Oktaba, K., Steinmann, J., Müller, J., and Knoblich, J.A. (**2011**). The tumour

suppressor L(3)mbt inhibits neuroepithelial proliferation and acts on insulator elements. Nat Cell Biol 13, 1029-1039.

**Roh**, T.Y., Cuddapah, S., Cui, K., and Zhao, K. (**2006**). The genomic landscape of histone modifications in human T cells. Proc Natl Acad Sci U S A 103, 15782-15787.

**Roh**, T.Y., Cuddapah, S., and Zhao, K. (**2005**). Active chromatin domains are defined by acetylation islands revealed by genome-wide mapping. Genes Dev 19, 542-552.

**Roseman**, R.R., Morgan, K., Mallin, D.R., Roberson, R., Parnell, T.J., Bornemann, D.J., Simon, J.A., and Geyer, P.K. (**2001**). Long-range repression by multiple polycomb group (PcG) proteins targeted by fusion to a defined DNA-binding domain in *Drosophila*. Genetics 158, 291-307.

**Rudolph**, T., Yonezawa, M., Lein, S., Heidrich, K., Kubicek, S., Schäfer, C., Phalke, S., Walther, M., Schmidt, A., Jenuwein, T., and Reuter, G. (**2007**). Heterochromatin formation in *Drosophila* is initiated through active removal of H3K4 methylation by the LSD1 homolog SU(VAR)3-3. Mol Cell 26, 103-115.

**Rundlett**, S.E., Carmen, A.A., Kobayashi, R., Bavykin, S., Turner, B.M., and Grunstein, M. (**1996**). HDA1 and RPD3 are members of distinct yeast histone deacetylase complexes that regulate silencing and transcription. Proc Natl Acad Sci U S A 93, 14503-14508.

**Ruthenburg**, A.J., Li, H., Patel, D.J., and Allis, C.D. (**2007**). Multivalent engagement of chromatin modifications by linked binding modules. Nat Rev Mol Cell Biol 8, 983-994.

**Saddic**, L.A., West, L.E., Aslanian, A., Yates, J.R., Rubin, S.M., Gozani, O., and Sage, J. (**2010**). Methylation of the retinoblastoma tumor suppressor by SMYD2. J Biol Chem 285, 37733-37740.

**Saiki**, R.K., Gelfand, D.H., Stoffel, S., Scharf, S.J., Higuchi, R., Horn, G.T., Mullis, K.B., Erlich, H.A. (**1988**). Primer-directed enzymatic amplification of DNA with a thermostable DNA polymerase. Science 239, 487-491

**Sakabe**, K., Wang, Z., and Hart, G.W. (**2010**). Beta-N-acetylglucosamine (O-GlcNAc) is part of the histone code. Proc Natl Acad Sci U S A 107, 19915-19920.

**Sambrook**, J., and **Russel**, D.W. (**2001**). Molecular Cloning - A Laboratory Manual. Cold Spring Habor, New York, CSHL Press.

**Santiveri**, C.M., Lechtenberg, B.C., Allen, M.D., Sathyamurthy, A., Jaulent, A.M., Freund, S.M., and Bycroft, M. (**2008**). The malignant brain tumor repeats of human SCML2 bind to peptides containing monomethylated lysine. J Mol Biol 382, 1107-1112.

**Sarma**, K., Margueron, R., Ivanov, A., Pirrotta, V., and Reinberg, D. (**2008**). Ezh2 requires PHF1 to efficiently catalyze H3 lysine 27 trimethylation *in vivo*. Mol Cell Biol 28, 2718-2731.

**Sathyamurthy**, A., Allen, M.D., Murzin, A.G., and Bycroft, M. (**2003**). Crystal structure of the malignant brain tumor (MBT) repeats in Sex Comb on Midleg-like 2 (SCML2). J Biol Chem 278, 46968-46973.

**Saurin**, A.J., Shao, Z., Erdjument-Bromage, H., Tempst, P., and Kingston, R.E. (**2001**). A *Drosophila* Polycomb group complex includes Zeste and dTAFII proteins. Nature 412, 655-660.

**Scharf**, A.N., Meier, K., Seitz, V., Kremmer, E., Brehm, A., and Imhof, A. (**2009**). Monomethylation of lysine 20 on histone H4 facilitates chromatin maturation. Mol Cell Biol 29, 57-67.

**Schindler**, U., Beckmann, H., and Cashmore, A.R. (**1993**). HAT3.1, a novel Arabidopsis homeodomain protein containing a conserved cysteine-rich region. Plant J 4, 137-150.

**Schmit**, F., Korenjak, M., Mannefeld, M., Schmitt, K., Franke, C., von Eyss, B., Gagrica, S., Hänel, F., Brehm, A., and Gaubatz, S. (**2007**). LINC, a human complex that is related to pRB-

containing complexes in invertebrates regulates the expression of G2/M genes. Cell Cycle 6, 1903-1913.

**Schmitges**, F.W., Prusty, A.B., Faty, M., Stützer, A., Lingaraju, G.M., Aiwazian, J., Sack, R., Hess, D., Li, L., Zhou, S., Chan, H., Gu, J., Gut, H., Fischle, W., Müller, J., and Thomä, N.H. (**2011**). Histone methylation by PRC2 is inhibited by active chromatin marks. Mol Cell 42, 330-341.

**Schneider**, I. (**1972**). Cell lines derived from late embryonic stages of *Drosophila melanogaster*. J Embryol Exp Morphol 27, 353-365.

**Schnitzler**, G.R. (**2008**). Control of nucleosome positions by DNA sequence and remodeling machines. Cell Biochem Biophys 51, 67-80.

**Schotta**, G., Ebert, A., Dorn, R., and Reuter, G. (**2003**). Position-effect variegation and the genetic dissection of chromatin regulation in *Drosophila*. Semin Cell Dev Biol 14, 67-75.

**Schotta**, G., Sengupta, R., Kubicek, S., Malin, S., Kauer, M., Cellén, E., Celeste, A., Pagani, M., Opravil, S., De La Rosa-Velazquez, I.A., Espejo, A., Bedford, M.T., Nussenzweig, A., Busslinger, M., and Jenuwein, T. (**2008**). A chromatin-wide transition to H4K20 monomethylation impairs genome integrity and programmed DNA rearrangements in the mouse. Genes Dev 22, 2048-2061.

**Schwartz**, B.E., and **Ahmad**, K. (**2005**). Transcriptional activation triggers deposition and removal of the histone variant H3.3. Genes Dev 19, 804-814.

**Schwartz**, B.E., Werner, J.K., and Lis, J.T. (**2004**). Indirect immunofluorescent labeling of *Drosophila* polytene chromosomes: visualizing protein interactions with chromatin *in vivo*. Methods Enzymol 376, 393-404.

**Schwartz**, Y.B., Kahn, T.G., Nix, D.A., Li, X.Y., Bourgon, R., Biggin, M., and Pirrotta, V. (**2006**). Genome-wide analysis of Polycomb targets in *Drosophila melanogaster*. Nat Genet 38, 700-705.

**Schübeler**, D., MacAlpine, D.M., Scalzo, D., Wirbelauer, C., Kooperberg, C., van Leeuwen, F., Gottschling, D.E., O'Neill, L.P., Turner, B.M., Delrow, J., Bell, S.P., and Groudine, M. (**2004**). The histone modification pattern of active genes revealed through genome-wide chromatin analysis of a higher eukaryote. Genes Dev 18, 1263-1271.

**Shahbazian**, M.D., and **Grunstein**, M. (**2007**). Functions of site-specific histone acetylation and deacetylation. Annu Rev Biochem 76, 75-100.

**Shao**, Z., Raible, F., Mollaaghababa, R., Guyon, J.R., Wu, C.T., Bender, W., and Kingston, R.E. (**1999**). Stabilization of chromatin structure by PRC1, a Polycomb complex. Cell 98, 37-46.

**Shi**, X., Hong, T., Walter, K.L., Ewalt, M., Michishita, E., Hung, T., Carney, D., Peña, P., Lan, F., Kaadige, M.R., et al., and Gonzani, O. (**2006**). ING2 PHD domain links histone H3 lysine 4 methylation to active gene repression. Nature 442, 96-99.

**Shi**, Y., Lan, F., Matson, C., Mulligan, P., Whetstine, J.R., Cole, P.A., and Casero, R.A. (**2004**). Histone demethylation mediated by the nuclear amine oxidase homolog LSD1. Cell 119, 941-953.

**Shi**, Y.J., Matson, C., Lan, F., Iwase, S., Baba, T., and Shi, Y. (**2005**). Regulation of LSD1 histone demethylase activity by its associated factors. Mol Cell 19, 857-864.

**Shogren-Knaak**, M., Ishii, H., Sun, J.M., Pazin, M.J., Davie, J.R., and Peterson, C.L. (**2006**). Histone H4-K16 acetylation controls chromatin structure and protein interactions. Science 311, 844-847.

**Shogren-Knaak**, M., and **Peterson**, C.L. (**2006**). Switching on chromatin: mechanistic role of histone H4-K16 acetylation. Cell Cycle 5, 1361-1365.

**Simon**, J., Chiang, A., and Bender, W. (**1992**). Ten different Polycomb group genes are required for spatial control of the abdA and AbdB homeotic products. Development 114, 493-505.

**Simpson**, A.J., Caballero, O.L., Jungbluth, A., Chen, Y.T., and Old, L.J. (**2005**). Cancer/testis antigens, gametogenesis and cancer. Nat Rev Cancer 5, 615-625.

**Slama**, P., and **Geman**, D. (**2011**). Identification of family-determining residues in PHD fingers. Nucleic Acids Res 39, 1666-1679.

**Smith**, E.R., Lee, M.G., Winter, B., Droz, N.M., Eissenberg, J.C., Shiekhattar, R., and Shilatifard, A. (**2008**). *Drosophila* UTX is a histone H3 Lys27 demethylase that colocalizes with the elongating form of RNA polymerase II. Mol Cell Biol 28, 1041-1046.

**Smith**, M., Mallin, D.R., Simon, J.A., and Courey, A.J. (**2011**). Small Ubiquitin-like Modifier (SUMO) Conjugation Impedes Transcriptional Silencing by the Polycomb Group Repressor Sex Comb on Midleg. J Biol Chem 286, 11391-11400.

**Sobel**, R.E., Cook, R.G., Perry, C.A., Annunziato, A.T., and Allis, C.D. (**1995**). Conservation of deposition-related acetylation sites in newly synthesized histones H3 and H4. Proc Natl Acad Sci U S A 92, 1237-1241.

**Sofueva**, S., Du, L.L., Limbo, O., Williams, J.S., and Russell, P. (**2010**). BRCT domain interactions with phospho-histone H2A target Crb2 to chromatin at double-strand breaks and maintain the DNA damage checkpoint. Mol Cell Biol 30, 4732-4743.

**Sogo**, J.M., Stahl, H., Koller, T., and Knippers, R. (**1986**). Structure of replicating simian virus 40 minichromosomes. The replication fork, core histone segregation and terminal structures. J Mol Biol 189, 189-204.

**Stephenson**, E.C., Chao, Y.C., and Fackenthal, J.D. (**1988**). Molecular analysis of the swallow gene of *Drosophila melanogaster*. Genes Dev 2, 1655-1665.

**Stewart**, M.D., Li, J., and Wong, J. (**2005**). Relationship between histone H3 lysine 9 methylation, transcription repression, and heterochromatin protein 1 recruitment. Mol Cell Biol 25, 2525-2538.

**Stielow**, B., Sapetschnig, A., Krüger, I., Kunert, N., Brehm, A., Boutros, M., and Suske, G. (**2008a**). Identification of SUMO-dependent chromatin-associated transcriptional repression components by a genome-wide RNAi screen. Mol Cell 29, 742-754.

**Stielow**, B., Sapetschnig, A., Wink, C., Krüger, I., and Suske, G. (**2008b**). SUMO-modified Sp3 represses transcription by provoking local heterochromatic gene silencing. EMBO Rep 9, 899-906.

**Strahl**, B.D., and **Allis**, C.D. (**2000**). The language of covalent histone modifications. Nature 403, 41-45.

**Suganuma**, T., and **Workman**, J.L. (**2008**). Crosstalk among Histone Modifications. Cell 135, 604-607.

**Söding**, J., Biegert, A., and Lupas, A.N. (**2005**). The HHpred interactive server for protein homology detection and structure prediction. Nucleic Acids Res 33, W244-248.

**Tamkun**, J.W., Deuring, R., Scott, M.P., Kissinger, M., Pattatucci, A.M., Kaufman, T.C., and Kennison, J.A. (**1992**). brahma: a regulator of *Drosophila* homeotic genes structurally related to the yeast transcriptional activator SNF2/SWI2. Cell 68, 561-572.

**Tanaka**, Y., Katagiri, Z., Kawahashi, K., Kioussis, D., and Kitajima, S. (**2007**). Trithorax-group protein ASH1 methylates histone H3 lysine 36. Gene 397, 161-168.

**Tardat**, M., Brustel, J., Kirsh, O., Lefevbre, C., Callanan, M., Sardet, C., and Julien, E. (**2010**). The histone H4 Lys 20 methyltransferase PR-Set7 regulates replication origins in mammalian cells. Nat Cell Biol 12, 1086-1093.

**Tardat**, M., Murr, R., Herceg, Z., Sardet, C., and Julien, E. (**2007**). PR-Set7-dependent lysine methylation ensures genome replication and stability through S phase. J Cell Biol 179, 1413-1426.

**Taunton**, J., Hassig, C.A., and Schreiber, S.L. (**1996**). A mammalian histone deacetylase related to the yeast transcriptional regulator Rpd3p. Science 272, 408-411.

**Taverna**, S.D., Li, H., Ruthenburg, A.J., Allis, C.D., and Patel, D.J. (**2007**). How chromatin-binding modules interpret histone modifications: lessons from professional pocket pickers. Nat Struct Mol Biol 14, 1025-1040.

**Thoma**, F., Koller, T., and Klug, A. (**1979**). Involvement of histone H1 in the organization of the nucleosome and of the salt-dependent superstructures of chromatin. J Cell Biol 83, 403-427.

**Thompson**, E.C., and **Travers**, A.A. (**2008**). A *Drosophila* Smyd4 homologue is a muscle-specific transcriptional modulator involved in development. PLoS One 3, e3008.

**Tie**, F., Furuyama, T., Prasad-Sinha, J., Jane, E., and Harte, P.J. (**2001**). The *Drosophila* Polycomb Group proteins ESC and E(Z) are present in a complex containing the histone-binding protein p55 and the histone deacetylase RPD3. Development 128, 275-286.

**Townsley**, F.M., Thompson, B., and Bienz, M. (**2004**). Pygopus residues required for its binding to Legless are critical for transcription and development. J Biol Chem 279, 5177-5183.

**Trinkle-Mulcahy**, L., Boulon, S., Lam, Y.W., Urcia, R., Boisvert, F.M., Vandermoere, F., Morrice, N.A., Swift, S., Rothbauer, U., Leonhardt, H., and Lamond, A. (**2008**). Identifying specific protein interaction partners using quantitative mass spectrometry and bead proteomes. J Cell Biol 183, 223-239.

**Trojer**, P., Cao, A.R., Gao, Z., Li, Y., Zhang, J., Xu, X., Li, G., Losson, R., Erdjument-Bromage, H., Tempst, P., Farnham, P.J., and Reinberg, D. (**2011**). L3MBTL2 protein acts in concert with PcG protein-mediated monoubiquitination of H2A to establish a repressive chromatin structure. Mol Cell 42, 438-450.

**Trojer**, P., Li, G., Sims, R.J., Vaquero, A., Kalakonda, N., Boccuni, P., Lee, D., Erdjument-Bromage, H., Tempst, P., Nimer, S.D., Wang, Y.H., and Reinberg, D. (**2007**). L3MBTL1, a histone-methylation-dependent chromatin lock. Cell 129, 915-928.

**Trojer**, P., and **Reinberg**, D. (**2008**). Beyond histone methyl-lysine binding: how malignant brain tumor (MBT) protein L3MBTL1 impacts chromatin structure. Cell Cycle 7, 578-585.

**Tse**, C., Sera, T., Wolffe, A.P., and Hansen, J.C. (**1998**). Disruption of higher-order folding by core histone acetylation dramatically enhances transcription of nucleosomal arrays by RNA polymerase III. Mol Cell Biol 18, 4629-4638.

**Tsukada,** Y., and **Zhang**, Y. (**2006**). Purification of histone demethylases from HeLa cells. Methods 40, 318-326.

**Upadhyay**, A.K., and **Cheng**, X. (**2011**). Dynamics of histone lysine methylation: structures of methyl writers and erasers. Prog Drug Res 67, 107-124.

**Usui**, H., Ichikawa, T., Kobayashi, K., and Kumanishi, T. (**2000**). Cloning of a novel murine gene Sfmbt, Scm-related gene containing four mbt domains, structurally belonging to the Polycomb group of genes. Gene 248, 127-135.

**Varga-Weisz**, P.D., and **Becker**, P.B. (**1998**). Chromatin-remodeling factors: machines that regulate? Curr Opin Cell Biol 10, 346-353.

**Vaughn**, J.L., Goodwin, R.H., Tompkins, G.J., and McCawley, P. (**1977**). The establishment of two cell lines from the insect Spodoptera frugiperda (Lepidoptera; Noctuidae). In Vitro 13, 213-217.

**Veigaard**, C., Nørgaard, J.M., and Kjeldsen, E. (**2011**). Genomic profiling in high hyperdiploid

acute myeloid leukemia: a retrospective study of 19 cases. Cancer Genet 204, 516-521.

**Wang**, L., Brown, J.L., Cao, R., Zhang, Y., Kassis, J.A., and Jones, R.S. (**2004**). Hierarchical recruitment of polycomb group silencing complexes. Mol Cell 14, 637-646.

**Wang**, L., Jahren, N., Miller, E.L., Ketel, C.S., Mallin, D.R., and Simon, J.A. (**2010**). Comparative analysis of chromatin binding by Sex Comb on Midleg (SCM) and other polycomb group repressors at a *Drosophila* Hox gene. Mol Cell Biol 30, 2584-2593.

**Wang**, W.K., Tereshko, V., Boccuni, P., MacGrogan, D., Nimer, S.D., and Patel, D.J. (**2003**). Malignant brain tumor repeats: a three-leaved propeller architecture with ligand/peptide binding pockets. Structure 11, 775-789.

**Wang**, Y., Reddy, B., Thompson, J., Wang, H., Noma, K., Yates, J.R., and Jia, S. (**2009**). Regulation of Set9-mediated H4K20 methylation by a PWWP domain protein. Mol Cell 33, 428-437.

**Webby**, C.J., Wolf, A., Gromak, N., Dreger, M., Kramer, H., Kessler, B., Nielsen, M.L., Schmitz, C., Butler, D.S., Yates, J.R., et al., and Böttger, A. (**2009**). Jmjd6 catalyses lysyl-hydroxylation of U2AF65, a protein associated with RNA splicing. Science 325, 90-93.

**Wei**, Y., Mizzen, C.A., Cook, R.G., Gorovsky, M.A., and Allis, C.D. (**1998**). Phosphorylation of histone H3 at serine 10 is correlated with chromosome condensation during mitosis and meiosis in Tetrahymena. Proc Natl Acad Sci U S A 95, 7480-7484.

**West**, L.E., Roy, S., Lachmi-Weiner, K., Hayashi, R., Shi, X., Appella, E., Kutateladze, T.G., and Gozani, O. (**2010**). The MBT repeats of L3MBTL1 link SET8-mediated p53 methylation at lysine 382 to target gene repression. J Biol Chem 285, 37725-37732.

**Winter**, S., and **Fischle**, W. (**2010**). Epigenetic markers and their cross-talk. Essays Biochem 48, 45-61.

**Wismar**, J. (**2001**). Molecular characterization of h-l(3)mbt-like: a new member of the human mbt family. FEBS Lett 507, 119-121.

**Wismar**, J., Löffler, T., Habtemichael, N., Vef, O., Geissen, M., Zirwes, R., Altmeyer, W., Sass, H., and Gateff, E. (**1995**). The *Drosophila melanogaster* tumor suppressor gene lethal(3)malignant brain tumor encodes a proline-rich protein with a novel zinc finger. Mech Dev 53, 141-154.

**Wodarz**, A., and **Näthke**, I. (**2007**). Cell polarity in development and cancer. Nat Cell Biol 9, 1016-1024.

**Wu**, S., Trievel, R.C., and Rice, J.C. (**2007**). Human SFMBT is a transcriptional repressor protein that selectively binds the N-terminal tail of histone H3. FEBS Lett 581, 3289-3296.

**Wysocka**, J., Swigut, T., Xiao, H., Milne, T.A., Kwon, S.Y., Landry, J., Kauer, M., Tackett, A.J., Chait, B.T., Badenhorst, P., Wu, C., and Allis, C.D. (**2006**). A PHD finger of NURF couples histone H3 lysine 4 trimethylation with chromatin remodelling. Nature 442, 86-90.

**Xue**, Y., Wong, J., Moreno, G.T., Young, M.K., Côté, J., and Wang, W. (**1998**). NURD, a novel complex with both ATP-dependent chromatin-remodeling and histone deacetylase activities. Mol Cell 2, 851-861.

**Yang**, J., and **Corces**, V.G. (**2011**). Chromatin insulators: a role in nuclear organization and gene expression. Adv Cancer Res 110, 43-76.

**Yang**, M., Gocke, C.B., Luo, X., Borek, D., Tomchick, D.R., Machius, M., Otwinowski, Z., and Yu, H. (**2006**). Structural basis for CoREST-dependent demethylation of nucleosomes by the human LSD1 histone demethylase. Mol Cell 23, 377-387.

**Yang**, H., Pesavento, J.J., Starnes, T.W., Cryderman, D.E., Wallrath, L.L., Kelleher, N.L., and Mizzen, C.A. (**2008**). Preferential dimethylation of histone H4 lysine 20 by Suv4-20. J Biol Chem 283, 12085-12092.

**Yang**, Y., Sun, Y., Luo, X., Zhang, Y., Chen, Y., Tian, E., Lints, R., and Zhang, H. (**2007**). Polycomb-like genes are necessary for specification of dopaminergic and serotonergic neurons in *Caenorhabditis elegans*. Proc Natl Acad Sci U S A 104, 852-857.

**Yohn**, C.B., Pusateri, L., Barbosa, V., and Lehmann, R. (**2003**). l(3)malignant brain tumor and three novel genes are required for *Drosophila* germ-cell formation. Genetics 165, 1889-1900.

**Yoo**, J.Y., Choi, K.C., Kang, H., Kim, Y.J., Lee, J., Jun, W.J., Kim, M.J., Lee, Y.H., Lee, O.H., and Yoon, H.G. (**2010**). Histone deacetylase 3 is selectively involved in L3MBTL2-mediated transcriptional repression. FEBS Lett 584, 2225-2230.

**Yoshida**, M., Kijima, M., Akita, M., and Beppu, T. (**1990**). Potent and specific inhibition of mammalian histone deacetylase both *in vivo* and in vitro by trichostatin A. J Biol Chem 265, 17174-17179.

**You**, A., Tong, J.K., Grozinger, C.M., and Schreiber, S.L. (**2001**). CoREST is an integral component of the CoREST- human histone deacetylase complex. Proc Natl Acad Sci U S A 98, 1454-1458.

**Yuan**, G.C., Liu, Y.J., Dion, M.F., Slack, M.D., Wu, L.F., Altschuler, S.J., and Rando, O.J. (**2005**). Genome-scale identification of nucleosome positions in *S. cerevisiae*. Science 309, 626-630.

**Yuan**, W., Xu, M., Huang, C., Liu, N., Chen, S., and Zhu, B. (**2011**). H3K36 Methylation Antagonizes PRC2-mediated H3K27 Methylation. J Biol Chem 286, 7983-7989.

**Zeng**, Q., and **Hong**, W. (**2008**). The emerging role of the hippo pathway in cell contact inhibition, organ size control, and cancer development in mammals. Cancer Cell 13, 188-192.

**Zeng**, L., Zhang, Q., Li, S., Plotnikov, A.N., Walsh, M.J., and Zhou, M.M. (**2010**). Mechanism and regulation of acetylated histone binding by the tandem PHD finger of DPF3b. Nature 466, 258-262.

**Zhang**, K., Chen, Y., Zhang, Z., and Zhao, Y. (**2009**). Identification and verification of lysine propionylation and butyrylation in yeast core histones using PTMap software. J Proteome Res 8, 900-906.

**Zhang**, Y., Malone, J.H., Powell, S.K., Periwal, V., Spana, E., Macalpine, D.M., and Oliver, B. (**2010**). Expression in aneuploid *Drosophila* S2 cells. PLoS Biol 8, e1000320.

**Zhang**, Y., Ng, H.H., Erdjument-Bromage, H., Tempst, P., Bird, A., and Reinberg, D. (**1999**). Analysis of the NuRD subunits reveals a histone deacetylase core complex and a connection with DNA methylation. Genes Dev 13, 1924-1935.

**Zhao**, K., Hart, C.M., and Laemmli, U.K. (**1995**). Visualization of chromosomal domains with boundary element-associated factor BEAF-32. Cell 81, 879-889.

# 7 Appendix

## Microarray results: dL(3)mbt and dLint-1 deregulated genes

**Table 7.1: Overlap of dL(3)mbt and dLint-1 co-regulated genes:** List of genes identified by microarray analysis that are co-regulated in both dL(3)mbt and dLint-1 depleted Kc167 cells (log2 FC: ≥ 0.5 and ≤ -0.5). Genes were put in order according to decreasing log2 fold changes (log2 FC) in dLint-1 RNAi-treated cells. Deregulated MBTS genes are labelled with a grey background.

| Affy_ID | dL3MBT RNAi log2 FC | dLint1 RNAi log2 FC | Gene Symbol | Gene Title |
|---|---|---|---|---|
| 1634302_s_at | 7.6925 | 7.9155 | CG14516 | CG14516 |
| 1639028_a_at | 8.8067 | 7.2829 | CG30296 | CG30296 |
| 1641305_at | 7.6564 | 6.5804 | piwi | P-element induced wimpy testis |
| 1630749_at | 8.9467 | 6.4546 | CG11052 | CG11052 |
| 1627235_at | 6.8328 | 6.0472 | CG17207 | CG17207 |
| 1635163_at | 7.1200 | 5.9691 | CG5731 | CG5731 |
| 1638729_at | 6.7737 | 5.9535 | CG8589 / tej | CG8589 / tejas / anon-fast-evolving-1D11 |
| 1625450_at | 7.1608 | 5.7951 | mthl14 | methuselah-like 14 |
| 1628036_at | 5.9196 | 5.7478 | hdm | hold'em |
| 1633137_at | 6.1735 | 5.7432 | eIF4E-6 | eIF4E-6 |
| 1640031_at | 5.9197 | 5.7306 | Acer | Angiotensin-converting enzyme-related |
| 1636899_s_at | 5.4052 | 5.6217 | CG1623 | CG1623 |
| 1640961_at | 5.9902 | 5.4461 | CG32313 | CG32313 |
| 1626251_at | 5.9181 | 5.4130 | Rh4 | rhodopsin |
| 1631174_at | 5.9198 | 5.2046 | CG9875 | CG9875 |
| 1632490_at | 5.3525 | 5.1476 | CG8008 | CG8008 |
| 1636591_at | 6.3343 | 5.0894 | skpB | skpB |
| 1629597_a_at | 5.1300 | 5.0775 | Asph | Aspartyl beta-hydroxylase |
| 1637913_at | 5.3428 | 5.0032 | CG11638 | CG11638 |
| 1627272_at | 6.9354 | 4.9460 | CG30380 | CG30380 |
| 1633920_at | 5.4937 | 4.9150 | CG5715 | CG5715 |
| 1635470_at | 5.3212 | 4.9113 | GNBP3 | Gram-negative bacteria binding protein 3 |
| 1640025_at | 5.1533 | 4.7864 | osm-6 | osm-6 |
| 1631125_at | 5.0375 | 4.7619 | CG15737 | CG15737 |
| 1625697_at | 5.2593 | 4.7415 | Cyp6g1 | CYP6-like |
| 1625454_at | 4.8588 | 4.6507 | Gbeta5 | Gbeta5 |
| 1641390_at | 6.3524 | 4.6145 | dpr19 | dpr19 |
| 1633696_at | 5.3490 | 4.5591 | TM4SF | Transmembrane 4 superfamily |
| 1641053_s_at | 4.9014 | 4.5371 | tok | Tolkin |
| 1633126_at | 7.0239 | 4.5360 | CG4596 | CG4596 |
| 1630191_at | 4.5037 | 4.4814 | CG32436 | CG32436 |
| 1640104_at | 6.4902 | 4.4284 | RpS5b | Ribosomal protein S5b |
| 1632600_at | 4.8760 | 4.4245 | CG34232 | --- |
| 1624989_s_at | 6.0270 | 4.4083 | Ef1alpha100E | elongation factor 1-alpha F2 |
| 1633458_at | 4.8220 | 4.3879 | swa | swallow |
| 1638866_at | 4.0106 | 4.3443 | CG9542 | CG9542 |
| 1622940_at | 4.5716 | 4.3269 | CG12698 | CG12698 |

| | | | | |
|---|---|---|---|---|
| 1638484_at | 4.3197 | 4.3132 | Hsp67Bc | Gene 3 |
| 1624467_a_at | 4.8002 | 4.1979 | CG8046 | CG8046 |
| 1638121_at | 3.8750 | 4.1362 | CG9961 | CG9961 |
| 1627645_at | 4.3139 | 4.1208 | CG9427 | CG9427 |
| 1640846_at | 4.5030 | 4.0802 | CG2887 | CG2887 |
| 1628925_at | 3.7627 | 4.0513 | CG17625 | CG17625 |
| 1632713_at | 5.6229 | 3.9161 | nos | nanos |
| 1633377_at | 4.8050 | 3.9145 | --- | --- |
| 1625582_at | 3.5798 | 3.9020 | CG32187 | CG32187 |
| 1624856_at | 5.7646 | 3.8970 | c(2)M | crossover suppressor on 2 of Manheim |
| 1636063_at | 5.1226 | 3.8716 | CG34355 | CG34355 |
| 1639353_at | 3.9377 | 3.7828 | CG17032 | CG17032 |
| 1625639_at | 3.3813 | 3.7066 | CG6737 | CG6737 |
| 1624763_at | 3.9457 | 3.7051 | CG2556 | CG2556 |
| 1624628_at | 3.8907 | 3.6745 | CG10396 | CG10396 |
| 1634464_at | 3.7449 | 3.6591 | RpS19b | Ribosomal protein S19b |
| 1629468_at | 3.8971 | 3.6231 | CG9372 | CG9372 |
| 1624197_a_at | 3.9959 | 3.6002 | CG6652 | CG6652 |
| 1627051_at | 4.0280 | 3.5358 | Lcp9 | Larval cuticle protein 9 |
| 1641534_at | 4.1092 | 3.4932 | CG11842 | CG11842 |
| 1623971_at | 3.5584 | 3.4924 | CG9150 | CG9150 |
| 1624310_s_at | 3.6255 | 3.4857 | CG4753 | CG4753 |
| 1623712_at | 4.1017 | 3.4756 | CG10132 | CG10132 |
| 1635980_s_at | 4.0331 | 3.4009 | CG12991 | CG12991 |
| 1634933_s_at | 4.0823 | 3.3741 | CG17207 | CG17207 |
| 1634882_at | 3.6649 | 3.3395 | Acp63F | Accessory gland protein 63F |
| 1634402_at | 3.7653 | 3.3319 | Scgbeta | Sarcoglycan beta |
| 1626271_at | 4.2489 | 3.2746 | CG9634 | CG9634 |
| 1629015_a_at | 3.8365 | 3.2697 | DAAM | Dishevelled Associated Activator of Morphogenesis |
| 1624377_s_at | 3.9682 | 3.2369 | CG32594 | E protein |
| 1625688_at | 3.3574 | 3.2159 | CG6293 | CG6293 |
| 1634788_at | 3.1321 | 3.2107 | CG4872 | CG4872 |
| 1639936_at | 3.0000 | 3.1957 | Sas | N-acetylneuraminic acid phosphate synthase |
| 1632321_a_at | 3.6488 | 3.1907 | mthl7 | Mth-like 7 |
| 1623961_at | 4.0643 | 3.1483 | Arpc3B | Arpc3B |
| 1633615_at | 3.9173 | 3.1320 | CG15330 | CG15330 |
| 1635940_at | 4.2164 | 3.1297 | CG5367 | CG5367 |
| 1626044_at | 3.9587 | 3.1234 | CG7628 | CG7628 |
| 1633893_at | 4.4560 | 3.1130 | CG31217 | predicted gene W |
| 1635256_s_at | 3.3079 | 3.0822 | CG1275 | CG1275 |
| 1626600_at | 3.0082 | 3.0711 | CG30016 | CG30016 |
| 1623613_at | 2.9774 | 3.0336 | CG13762 | CG13762 |
| 1634733_at | 2.3848 | 3.0270 | CG3831 | CG3831 |
| 1630366_at | 3.9608 | 3.0228 | CG31149 | CG31149 |
| 1635831_at | 2.6828 | 2.9702 | CG14036 | CG14036 |
| 1637463_a_at | 3.5252 | 2.9489 | Nrg | neuroglian |
| 1636961_a_at | 2.6571 | 2.9429 | CG9027 | CG9027 |
| 1629430_s_at | 2.5436 | 2.9006 | regucalcin | regucalcin |
| 1636510_a_at | 2.9620 | 2.8945 | Lsd-1 | Lipid storage droplet-1 |
| 1637256_at | 2.9847 | 2.8847 | CG34349 | CG11819 |
| 1632688_s_at | 2.3021 | 2.8663 | CG11594 | CG11594 |
| 1630585_s_at | 2.8297 | 2.8602 | --- | --- |
| 1633227_s_at | 2.7559 | 2.8324 | CG14945 | CG14945 |
| 1628146_at | 2.9076 | 2.8184 | --- | --- |
| 1636247_at | 2.9029 | 2.8181 | CG32354 | CG32354 |

| | | | | |
|---|---|---|---|---|
| 1637404_at | 3.9025 | 2.8141 | CG10262 | CG10262 |
| 1638885_at | 4.1302 | 2.8099 | --- | --- |
| 1625572_s_at | 2.2315 | 2.7891 | Dbi | diazepam binding inhibitor |
| 1627619_at | 3.2158 | 2.7844 | CG15332 | CG15332 |
| 1632873_at | 2.4292 | 2.7824 | MtnA | metallothionein N |
| 1634093_at | 5.0666 | 2.7729 | CG32017 | CG32017 |
| 1639406_at | 2.7197 | 2.7548 | lbm | Late Bloomer |
| 1630239_at | 5.0973 | 2.7534 | --- | --- |
| 1629119_at | 4.9504 | 2.7373 | CG33221 | CG33221 |
| 1622906_at | 2.4611 | 2.7151 | CG9027 | CG9027 |
| 1622990_at | 3.4265 | 2.6872 | CG5381 | CG5381 |
| 1629889_s_at | 2.3878 | 2.6823 | regucalcin | regucalcin |
| 1624718_a_at | 4.2700 | 2.6630 | CG42299 / CG42300 | CG42299 / CG42300 |
| 1634557_at | 2.8743 | 2.6478 | Rhp | Rhophilin |
| 1636785_at | 3.2313 | 2.6424 | --- | --- |
| 1624720_s_at | 3.1794 | 2.6289 | CG6043 | CG6043 |
| 1635643_at | 2.8349 | 2.6285 | Rab23 | Rab23 |
| 1641657_s_at | 3.8622 | 2.6213 | CG12424 | CG12424 |
| 1639867_at | 2.7898 | 2.5923 | ea | Easter |
| 1624982_s_at | 2.4759 | 2.5496 | CG5080 | CG5080 |
| 1634739_a_at | 2.6202 | 2.5257 | Pfk | 6-phosphofructokinase |
| 1639478_at | 3.9344 | 2.5253 | CG5091 / CG5096 | CG5091 / CG5096 |
| 1635313_at | 3.1816 | 2.5227 | CG10405 | CG10405 |
| 1626228_a_at | 3.1972 | 2.5176 | CG6967 | CG6967 |
| 1630476_s_at | 3.2214 | 2.5130 | nahoda | nahoda |
| 1630217_at | 2.8464 | 2.5019 | CG13650 | CG13650 |
| 1624706_at | 3.1450 | 2.4996 | CG34349 | CG11819 |
| 1633710_at | 2.4035 | 2.4704 | ChLD3 | CG17905 |
| 1626559_s_at | 2.0116 | 2.4630 | CG13148 | CG13148 |
| 1638368_at | 1.8948 | 2.4301 | CG31674 | CG31674 |
| 1627799_at | 2.5016 | 2.4246 | CG12161 | CG12161 |
| 1638417_at | 2.3389 | 2.4203 | CG31373 | CG31373 |
| 1636410_at | 1.9583 | 2.4176 | CG3505 | CG3505 |
| 1634993_at | 3.2603 | 2.4151 | CG40498 | CG40498 |
| 1624846_at | 3.9166 | 2.4093 | CG10764 | CG10764 |
| 1637538_s_at | 2.3126 | 2.4056 | CG9485 | CG9485 |
| 1623347_at | 2.4913 | 2.4006 | CG11674 | CG11674 |
| 1636733_at | 1.2546 | 2.3887 | CG32135 | CG32135 |
| 1639396_s_at | 2.4471 | 2.3853 | CDase | Ceramidase |
| 1622970_at | 2.8858 | 2.3515 | form3 | formin 3 |
| 1641009_at | 3.2860 | 2.3504 | --- | --- |
| 1632011_at | 3.0630 | 2.3463 | CG31274 / MESK4 | CG31274 / Misexpression suppressor of KSR 4 |
| 1633572_at | 2.4569 | 2.3373 | CG42336 | CG42336 |
| 1628298_at | 1.9390 | 2.3342 | Dox-A3 | prophenoloxidase |
| 1626524_at | 3.1284 | 2.3173 | CG16996 | CG16996 |
| 1635591_at | 2.1484 | 2.2841 | NijA | ninjurin A |
| 1629010_at | 3.1712 | 2.2816 | rho-5 | rhomboid-5 |
| 1638778_at | 2.8726 | 2.2605 | CG10352 | CG10352 |
| 1636146_at | 3.4896 | 2.2570 | Nrg | neuroglian |
| 1640972_at | 2.8721 | 2.2541 | CycJ | Cyclin-dependent kinase interactor 5 |
| 1623746_a_at | 2.1906 | 2.2513 | PICK1 | PICK1 |
| 1637794_at | 2.6981 | 2.2450 | CG4927 | CG4927 |
| 1630140_at | 2.5242 | 2.2351 | CG14931 | CG14931 |
| 1632019_s_at | 2.2408 | 2.2335 | CG9008 | CG9008 |
| 1637632_at | 4.4942 | 2.2246 | CG12194 | CG12194 |
| 1635416_at | 4.1936 | 2.2031 | CG31100 | CG31100 |

| | | | | |
|---|---|---|---|---|
| 1636564_at | 2.1022 | 2.1974 | CG14757 | CG14757 |
| 1622959_at | 1.9383 | 2.1821 | CG12928 | CG12928 |
| 1638220_at | 2.0355 | 2.1761 | CG16888 | CG16888 |
| 1641265_at | 3.4615 | 2.1571 | tty | tweety |
| 1633645_at | 1.0967 | 2.1498 | CG13512 | CG13512 |
| 1632574_at | 2.0238 | 2.1463 | CG6574 | CG6574 |
| 1640097_at | 1.2798 | 2.1460 | Pxn | peroxidasin |
| 1627537_at | 1.7860 | 2.1458 | CG3085 | CG3085 |
| 1628579_at | 2.4513 | 2.1189 | --- | --- |
| 1639251_at | 2.2301 | 2.1136 | CG17462 | CG17462 |
| 1630085_s_at | 1.6529 | 2.1127 | Peritrophin-A | peritrophin A |
| 1635300_at | 4.0608 | 2.1121 | CG1268 | CG1268 |
| 1626152_at | 2.6932 | 2.1093 | Ror | Ror |
| 1624849_at | 2.0905 | 2.0891 | Prosap | Prosap |
| 1623769_at | 1.9746 | 2.0651 | CG7322 | CG7322 |
| 1637654_at | 3.0555 | 2.0647 | CG10566 | CG10566 |
| 1633982_at | 1.8321 | 2.0484 | CG32088 | CG32088 |
| 1626268_at | 2.6959 | 2.0469 | Klp54D | Kinesin-like protein at 54D |
| 1634036_at | 1.7296 | 2.0226 | CG8788 | CG8788 |
| 1637003_at | 2.1031 | 2.0156 | CG6927 | CG6927 |
| 1636906_s_at | 2.1338 | 2.0073 | Sans | Sans |
| 1634756_at | 2.7443 | 2.0007 | nAcRalpha-80B | Dalpha4 |
| 1626552_at | 2.7830 | 1.9997 | CG3568 | CG3568 |
| 1629572_a_at | 2.3165 | 1.9996 | fat-spondin | fat-spondin |
| 1631076_at | 2.1885 | 1.9533 | CG13771 | CG13771 |
| 1623342_at | 1.6430 | 1.9505 | CG8369 | CG8369 |
| 1626897_at | 4.3727 | 1.9459 | HisCl1 | Histamine-gated chloride channel subunit 1 |
| 1631228_a_at | 1.8773 | 1.9425 | sPLA2 | secretory Phospholipase A2 |
| 1635930_at | 2.3549 | 1.9402 | btn | buttonless |
| 1640477_at | 2.3338 | 1.9401 | tilB | touch insensitive larva B |
| 1637561_at | 2.0999 | 1.9359 | lectin-33A | lectin-33A |
| 1625292_at | 2.3665 | 1.9070 | CG12200 | CG12200 |
| 1633998_s_at | 2.5724 | 1.9046 | --- | --- |
| 1636255_s_at | 1.8152 | 1.8599 | CG7997 | CG7997 |
| 1641530_s_at | 2.5070 | 1.8508 | CG2264 | CG2264 |
| 1634336_at | 2.2068 | 1.8426 | bam | bag-of-marbles |
| 1624744_a_at | 2.4766 | 1.8346 | nuf | nuclear-fallout |
| 1641304_s_at | 2.1563 | 1.8215 | CG9801 | CG9801 |
| 1629802_at | 1.7213 | 1.8206 | CG15484 | CG15484 |
| 1632525_at | 3.7480 | 1.8164 | CG9925 | CG9925 |
| 1633880_s_at | 2.0468 | 1.8043 | CG8533 | CG8533 |
| 1634553_at | 1.8404 | 1.7957 | CG13602 | CG13602 |
| 1640845_at | 1.7952 | 1.7936 | CG10581 | CG10581 |
| 1637806_at | 1.9534 | 1.7926 | Ada | Adenosine deaminase |
| 1629804_s_at | 1.8722 | 1.7888 | CG6329 | CG6329 |
| 1640281_s_at | 1.4613 | 1.7884 | CG17129 | CG17129 |
| 1634325_a_at | 2.4876 | 1.7828 | MESK2 | Misexpression suppressor of KSR 2 |
| 1626079_a_at | 2.4727 | 1.7705 | CG2201 | CG2201 |
| 1627301_s_at | 2.9443 | 1.7640 | CG7208 | CG7208 |
| 1630999_at | 2.1925 | 1.7565 | CG7724 | CG7724 |
| 1629831_at | 2.0082 | 1.7555 | CG17801 | CG17801 |
| 1624425_at | 2.1987 | 1.7545 | CG7384 | CG7384 |
| 1632070_at | 1.5302 | 1.7543 | Ugt58Fa | lectin-58Fg |
| 1628197_at | 3.3645 | 1.7468 | CG13177 | CG13177 |
| 1623312_s_at | 1.5794 | 1.7163 | CG11836 | CG11836 |
| 1633167_s_at | 1.8986 | 1.6907 | CG32496 / CG6788 | CG32496 / CG6788 |

| | | | | |
|---|---|---|---|---|
| 1630797_at | 1.8675 | 1.6899 | CG32582 | CG32582 |
| 1632345_at | 1.2979 | 1.6831 | CG8353 | CG8353 |
| 1637000_at | 1.9552 | 1.6755 | Vha68-1 | Vha68-1 |
| 1627862_at | 2.8946 | 1.6709 | CG15267 | CG15267 |
| 1631098_at | 1.7104 | 1.6706 | CG7194 | CG7194 |
| 1641204_at | 1.5659 | 1.6660 | CG14864 | CG14864 |
| 1631756_at | 1.4518 | 1.6574 | CG10859 | CG10859 |
| 1633994_at | 3.8917 | 1.6513 | CG34402 | CG17793 |
| 1634310_at | 2.0130 | 1.6359 | TpnC4 | TpnC4 |
| 1624568_at | 1.6605 | 1.6350 | CG7985 | CG7985 |
| 1635223_at | 2.4339 | 1.6339 | CG30285 / rap | CG30285 / fizzy-related |
| 1629444_at | 2.0608 | 1.6339 | CG11756 | CG11756 |
| 1627176_at | 1.8279 | 1.6333 | CG31431 | CG31431 |
| 1630811_at | 2.2517 | 1.6324 | CG31624 | CG31624 |
| 1628964_at | 2.0401 | 1.6160 | CG4804 | CG4804 |
| 1628493_at | 1.4035 | 1.6152 | kal-1 | Kallmann |
| 1627837_at | 1.4916 | 1.6107 | CG5527 | CG5527 |
| 1631606_at | 1.4311 | 1.6102 | CG14285 | CG14285 |
| 1637843_at | 2.0446 | 1.6075 | --- | --- |
| 1627574_at | 1.4728 | 1.6011 | CG4623 | CG4623 |
| 1636535_at | 1.5538 | 1.5889 | CG15912 | CG15912 |
| 1627420_s_at | 1.1387 | 1.5840 | CG7702 | connectin-like |
| 1626640_at | 1.9760 | 1.5741 | CG4565 | CG4565 |
| 1639640_at | 1.3630 | 1.5701 | CG32485 | CG32485 |
| 1626619_at | 1.7740 | 1.5663 | CG9919 | CG9919 |
| 1622932_s_at | 1.7280 | 1.5651 | sn | fascin |
| 1628918_at | 1.7860 | 1.5646 | CG17478 | CG17478 |
| 1641722_at | 0.9268 | 1.5632 | Reg-2 | rhythmically expressed gene 2 |
| 1638882_at | 1.2924 | 1.5539 | ry | Xanthine DH |
| 1628143_a_at | 1.3147 | 1.5445 | --- | --- |
| 1640303_a_at | 1.8083 | 1.5437 | pst | pastrel |
| 1631638_at | 1.1820 | 1.5388 | Pvf1 | PDGF- and VEGF-related factor 1 |
| 1641232_s_at | 1.3519 | 1.5381 | CG32706 / CG6999 | CG32706 / CG6999 |
| 1629160_s_at | 1.4012 | 1.5376 | --- | --- |
| 1625835_at | 1.4442 | 1.5286 | yellow-f2 | yellow-f2 |
| 1631377_a_at | 1.4367 | 1.5256 | Adk1 | Adenylate kinase-1 |
| 1631179_s_at | 1.9973 | 1.5251 | CG6680 | CG6680 |
| 1631782_at | 1.3786 | 1.5023 | CG14312 | CG14312 |
| 1638587_at | 2.7113 | 1.4902 | tor | torso |
| 1630605_at | 1.5638 | 1.4876 | CG16947 | CG16947 |
| 1626886_at | 1.0778 | 1.4765 | CG3663 | CG3663 |
| 1625817_at | 1.1744 | 1.4549 | CG14868 | CG14868 |
| 1636244_s_at | 1.5558 | 1.4545 | CG5191 | CG5191 |
| 1624466_a_at | 1.6443 | 1.4492 | CG15117 | CG15117 |
| 1628567_at | 2.4824 | 1.4483 | CG13565 | CG13565 |
| 1640291_at | 1.8280 | 1.4472 | CG11848 | CG11848 |
| 1633483_a_at | 1.2973 | 1.4390 | CG14207 | small heat shock protein hsp20 family |
| 1641339_at | 1.3219 | 1.4380 | CG10137 | CG10137 |
| 1629536_at | 1.3796 | 1.4366 | CG14079 | CG14079 |
| 1636997_at | 1.8946 | 1.4342 | CG18528 | CG18528 |
| 1640747_s_at | 1.4610 | 1.4290 | CG8547 | CG8547 |
| 1629778_s_at | 1.6725 | 1.4273 | CG5130 | CG5130 |
| 1639956_at | 1.4849 | 1.4168 | CG17760 | CG17760 |
| 1639210_at | 1.9836 | 1.4126 | Fcp3C | Follicle cell protein 3C |
| 1624884_at | 1.2211 | 1.4073 | CG32712 | CG32712 |
| 1630985_at | 2.3281 | 1.4000 | CG30441 | CG30441 |
| 1629916_at | 1.3714 | 1.3994 | debcl | deborg |

| | | | | |
|---|---|---|---|---|
| 1636925_at | 1.2928 | 1.3892 | CG31477 | CG31477 |
| 1638064_a_at | 1.4324 | 1.3817 | dgo | diego |
| 1635541_s_at | 1.8664 | 1.3783 | MESK2 | Misexpression suppressor of KSR 2 |
| 1626027_at | 1.7218 | 1.3734 | Sr-CII | Scavenger Receptor |
| 1633741_at | 1.0550 | 1.3707 | CR31032 | CR31032 |
| 1626255_at | 1.4224 | 1.3654 | Gr61a | Gustatory receptor 61a |
| 1636603_a_at | 2.1410 | 1.3583 | CG9297 | CG9297 |
| 1630145_s_at | 1.5324 | 1.3518 | Tsp42Ea | tetraspanin 42E |
| 1639996_at | 2.2390 | 1.3482 | tomb | tombola |
| 1631486_at | 1.5572 | 1.3468 | p38c | p38c |
| 1630285_at | 1.6143 | 1.3445 | RhoGAP100F | RhoGAP100F |
| 1634125_at | 1.7975 | 1.3385 | CG30440 | CG30440 |
| 1623065_at | 1.5462 | 1.3368 | CG13692 | CG13692 |
| 1641268_at | 1.0779 | 1.3304 | CG13313 | CG13313 |
| 1635813_at | 1.4092 | 1.3292 | mia | TBP-associated factor 60kD-2 |
| 1627900_at | 1.0563 | 1.3193 | Dim1 | CG3058 |
| 1639431_at | 2.0115 | 1.3132 | synaptogyrin | synaptogyrin |
| 1634890_at | 0.8249 | 1.3006 | UK114 | UK114 |
| 1627593_at | 1.5743 | 1.3004 | CG2678 | transcript B |
| 1630370_at | 1.5367 | 1.2965 | CG9796 | CG9796 |
| 1640729_s_at | 1.8725 | 1.2850 | nrv3 | Nervana 3 |
| 1641294_a_at | 0.9992 | 1.2816 | CG3625 | CG3625 |
| 1625617_at | 0.8711 | 1.2767 | Roc2 | Roc2 |
| 1635131_at | 1.1470 | 1.2737 | CG4525 | CG4525 |
| 1637056_s_at | 0.9761 | 1.2700 | CG11200 | CG11200 |
| 1635969_at | 0.9613 | 1.2654 | CG11590 | CG11590 |
| 1637826_at | 1.2098 | 1.2550 | CG10623 | selenocysteine methyltransferase |
| 1631933_at | 1.2150 | 1.2490 | CG8526 | CG8526 |
| 1634738_s_at | 1.5436 | 1.2364 | --- | --- |
| 1632119_s_at | 1.6804 | 1.2353 | ltd | lightoid |
| 1623957_s_at | 1.4071 | 1.2222 | GstS1 | glutathione-S-transferase |
| 1625543_s_at | 1.7272 | 1.2181 | CYLD | CYLD |
| 1639516_at | 1.4649 | 1.2171 | CG30187 | CG30187 |
| 1626721_at | 1.5259 | 1.2157 | CG11762 | CG11762 |
| 1623743_at | 1.5368 | 1.2143 | CG3191 | CG3191 |
| 1633630_at | 1.8354 | 1.2114 | CG4324 | CG4324 |
| 1635473_at | 0.5887 | 1.2110 | Apf | diadenosine tetraphosphate hydrolase |
| 1635765_at | 1.5564 | 1.2091 | CG31161 | CG31161 |
| 1628251_at | 0.8961 | 1.2057 | CG33054 | CG33054 |
| 1625756_at | 1.2641 | 1.1969 | CG6656 | CG6656 |
| 1639059_s_at | 1.2054 | 1.1927 | exu | exuperantia |
| 1635527_at | 1.0549 | 1.1908 | CG5039 | CG5039 |
| 1626953_at | 1.6009 | 1.1900 | Fmo-1 | Flavin-containing monooxygenase 1 |
| 1637737_at | 1.0061 | 1.1885 | l(1)G0230 | lethal (1) G0230 |
| 1625280_at | 1.4362 | 1.1714 | amon | amontillado |
| 1631608_at | 1.3086 | 1.1691 | CG6954 | CG6954 |
| 1629546_at | 0.7178 | 1.1501 | CG7054 | CG7054 |
| 1632717_a_at | 0.9283 | 1.1463 | CG14341 | CG14341 |
| 1634608_at | 1.3113 | 1.1353 | CG30383 | CG30383 |
| 1634631_at | 1.3295 | 1.1319 | CG3105 | CG3105 |
| 1625568_a_at | 0.9706 | 1.1165 | CG15111 | CG15111 |
| 1636313_at | 1.4472 | 1.1162 | CG4914 | CG4914 |
| 1628547_at | 1.3606 | 1.1083 | CG5167 | CG5167 |
| 1629568_at | 0.8775 | 1.1079 | CG33276 | CG33276 |
| 1625443_a_at | 1.0438 | 1.1044 | CG33054 | CG33054 |

| | | | | |
|---|---|---|---|---|
| 1624357_at | 1.7099 | 1.0993 | cona | corona |
| 1632882_at | 1.2841 | 1.0977 | CG11671 | CG11671 |
| 1624012_at | 0.6105 | 1.0946 | mRpL10 | mitochondrial ribosomal protein L10 |
| 1625947_at | 1.1923 | 1.0897 | GLaz | Glial Lazarillo |
| 1631077_at | 1.1094 | 1.0862 | CG16957 | CG16957 |
| 1627826_s_at | 0.7295 | 1.0840 | CG12744 | CG12744 |
| 1622943_s_at | 1.1225 | 1.0813 | CG2371 | CG2371 |
| 1624663_a_at | 1.6417 | 1.0755 | vis | vismay |
| 1631173_at | 0.9835 | 1.0681 | dob | CG5560 |
| 1632373_s_at | 0.7834 | 1.0676 | CG34015 | CG34015 |
| 1635684_a_at | 1.5764 | 1.0627 | unc-13 | lethal (4) ry16 |
| 1628959_at | 0.8346 | 1.0503 | gatA | benedict |
| 1628738_at | 0.8338 | 1.0447 | CG31251 | CG31251 |
| 1625345_at | 1.4776 | 1.0427 | CG18508 | CG18508 |
| 1640059_at | 1.1107 | 1.0411 | CG6040 | CG6040 |
| 1628290_s_at | 0.8950 | 1.0308 | CG17292 | CG17292 |
| 1639597_at | 0.7868 | 1.0292 | Obp44a | Odorant-binding protein 44a |
| 1627354_at | 1.2959 | 1.0270 | CG11779 / CG5835 | CG11779 / CG5835 |
| 1639133_at | 0.9355 | 1.0163 | CG1939 | CG1939 |
| 1624813_s_at | 0.6618 | 1.0149 | CG34008 | CG34008 |
| 1626186_at | 1.1790 | 1.0109 | CG18193 | CG18193 |
| 1631867_at | 0.9300 | 1.0099 | Idgf5 | Imaginal disc growth factor 5 |
| 1636089_at | 1.4318 | 1.0091 | comm | commissureless |
| 1640492_at | 0.6652 | 1.0080 | CG10672 | CG10672 |
| 1637691_at | 0.9938 | 1.0069 | CG4570 | CG4570 |
| 1624937_at | 1.0582 | 1.0055 | CG12288 | CG12288 |
| 1623560_at | 0.7475 | 1.0053 | CG18048 | CG18048 |
| 1635964_at | 1.0943 | 1.0002 | niki | nimA-like kinase |
| 1629625_at | 0.8187 | 0.9958 | CG42336 | CG42336 |
| 1623238_at | 1.0007 | 0.9948 | CG5618 | CG5618 |
| 1639944_at | 1.4167 | 0.9889 | Cyp9f2 | Cyp9f2 |
| 1630624_s_at | 1.1325 | 0.9867 | CG10151 | CG10151 |
| 1640842_at | 0.8324 | 0.9831 | CG34159 / CG5739 | CG34159 / CG5739 |
| 1639109_a_at | 1.3128 | 0.9799 | CRMP | dihydropyrimidine amidohydrolase |
| 1628802_at | 0.7372 | 0.9754 | CG32554 | CG32554 |
| 1626023_at | 0.7280 | 0.9726 | CG14932 | CG14932 |
| 1630421_at | 1.0434 | 0.9622 | CG33170 | CG33170 |
| 1624203_s_at | 1.3174 | 0.9620 | Gli | gliotactin |
| 1633059_at | 1.8217 | 0.9490 | CG6357 | CG6357 |
| 1627884_at | 0.7830 | 0.9404 | CG5281 | CG5281 |
| 1636943_s_at | 0.9788 | 0.9339 | Spn5 | serpin 5 |
| 1629977_at | 0.7650 | 0.9281 | CG9921 | CG9921 |
| 1639848_at | 0.5809 | 0.9281 | topi | matotopetli |
| 1632762_s_at | 0.9794 | 0.9272 | CG3176 / CG32817 | CG3176 / CG32817 |
| 1635687_at | 0.6087 | 0.9250 | CG8490 | CG8490 |
| 1627105_at | 2.0793 | 0.9221 | TrxT | thioredoxin |
| 1635517_at | 1.6207 | 0.9168 | CG1667 | CG1667 |
| 1638564_at | 0.6142 | 0.9162 | CG12279 | CG12279 |
| 1623216_s_at | 0.5910 | 0.9159 | CG9629 | CG9629 |
| 1641066_s_at | 0.6191 | 0.9101 | fbp | fructose-1,6-bisphosphatase |
| 1629492_s_at | 1.3919 | 0.9095 | CG31626 | CG31626 |
| 1625857_at | 0.8688 | 0.9094 | CG8451 | CG8451 |
| 1632855_at | 1.0483 | 0.9039 | CG7352 | CG7352 |
| 1635486_at | 1.1470 | 0.9038 | CG33468 | CG33468 |
| 1624435_at | 1.0526 | 0.9016 | Tsp42Ej | CG12143 |
| 1641714_at | 0.8110 | 0.8983 | CG12338 | CG12338 |
| 1623257_a_at | 0.8429 | 0.8949 | CG17665 | CG17665 |

| | | | | |
|---|---|---|---|---|
| 1629906_s_at | 0.8802 | 0.8922 | --- | --- |
| 1623883_at | 0.9842 | 0.8906 | CG18661 | CG18661 |
| 1634621_at | 0.8731 | 0.8848 | CG13599 | CG13599 |
| 1640775_a_at | 1.0662 | 0.8802 | Nmdmc | NAD-dependent methylene-tetrahydrofolate dehydrogenase |
| 1626928_at | 1.0227 | 0.8800 | CG13190 | CG13190 |
| 1637236_at | 1.5189 | 0.8795 | CG41284 | --- |
| 1639645_at | 0.7682 | 0.8776 | CG9740 | CG9740 |
| 1636788_a_at | 1.0261 | 0.8700 | loqs | loquacious |
| 1629732_at | 1.2308 | 0.8648 | CG8791 | CG8791 |
| 1625370_s_at | 1.0431 | 0.8631 | gem | persephone |
| 1634351_at | 0.6280 | 0.8578 | CG7860 | CG7860 |
| 1633861_at | 0.7575 | 0.8554 | CG8145 | CG8145 |
| 1629879_at | 0.7383 | 0.8553 | Nnf1a | CG13434 |
| 1628500_at | -1.0267 | 0.8519 | CG32483 | CG32483 |
| 1639257_s_at | 0.8172 | 0.8512 | CG11739 | CG11739 |
| 1635203_at | 1.1550 | 0.8488 | Dip2 | dorsal interacting protein 2 |
| 1636718_s_at | 1.1097 | 0.8443 | CG4502 | CG4502 |
| 1631363_at | 0.6649 | 0.8405 | Nuf2 | CG8902 |
| 1641648_at | 0.6621 | 0.8386 | CG3939 | CG3939 |
| 1638543_at | 1.7135 | 0.8386 | CG33775 | CG33775 |
| 1630754_at | 0.6252 | 0.8355 | ORMDL | ORMDL |
| 1638265_s_at | 0.5893 | 0.8354 | --- | --- |
| 1637469_at | 0.8568 | 0.8347 | pen-2 | presenilin enhancer |
| 1632646_at | 1.0586 | 0.8328 | Ptth | prothoracicotropic hormone |
| 1630845_at | 0.6978 | 0.8320 | Sod | superoxide-dismutase |
| 1632613_at | 0.6510 | 0.8239 | Spn6 | serpin 6 |
| 1626417_at | 0.8895 | 0.8226 | --- | --- |
| 1635638_s_at | 0.6773 | 0.8215 | tomosyn | tomosyn |
| 1634620_a_at | 0.5989 | 0.8165 | stl | stall |
| 1639111_at | 0.7052 | 0.8160 | CG15362 | CG15362 |
| 1631030_at | 0.6092 | 0.8123 | Dbp80 | Helicase 80 |
| 1637727_at | 0.6420 | 0.8091 | CG7049 | CG7049 |
| 1630768_s_at | 1.1435 | 0.8070 | achi / vis | achintya / vismay |
| 1631984_at | 0.6514 | 0.8061 | CG3639 | CG3639 |
| 1635887_at | 0.6640 | 0.8051 | CG30094 | CG30094 |
| 1631775_at | 0.5949 | 0.8014 | CG11137 | CG11137 |
| 1633272_at | 1.1451 | 0.7974 | CG9090 | CG9090 |
| 1625750_at | 0.6010 | 0.7931 | CG17272 | CG17272 |
| 1624183_a_at | 0.7878 | 0.7907 | Fas1 | fasciclin I |
| 1639868_at | 0.7530 | 0.7902 | CG1702 | CG1702 |
| 1638652_at | 0.9863 | 0.7857 | CG40006 | CG40006 |
| 1626918_at | 0.7079 | 0.7848 | CG13879 | CG13879 |
| 1640430_s_at | 0.6031 | 0.7833 | CG15881 | CG15881 |
| 1639485_at | 0.6089 | 0.7832 | CG3893 | CG3893 |
| 1626304_at | 0.6753 | 0.7805 | CG32446 | CG32446 |
| 1625973_a_at | 1.0785 | 0.7774 | CG3038 | CG3038 |
| 1637645_at | 0.8068 | 0.7741 | miple2 | miple2 |
| 1641235_at | 0.6687 | 0.7675 | CG14102 | CG14102 |
| 1633870_at | 0.5929 | 0.7671 | CG9436 | CG9436 |
| 1626227_at | 1.0515 | 0.7631 | CG5337 | CG5337 |
| 1624725_at | 1.7151 | 0.7619 | CG9626 | CG9626 |
| 1624901_at | 0.8564 | 0.7590 | CG9272 | CG9272 |
| 1641408_at | 0.9901 | 0.7583 | --- | --- |
| 1638052_at | 0.8957 | 0.7537 | CG41128 | CG41128 |
| 1631456_at | 0.6634 | 0.7502 | CG6812 | CG6812 |
| 1641733_a_at | 0.8135 | 0.7497 | cerv | CG15645 |
| 1629666_at | 0.6347 | 0.7350 | dgt4 | CG4865 |

| | | | | |
|---|---|---|---|---|
| 1638801_at | 0.7555 | 0.7350 | CG14229 | CG14229 |
| 1641603_s_at | 0.9578 | 0.7330 | CG9611 | gp150-like |
| 1640778_at | 0.7835 | 0.7306 | --- | --- |
| 1626052_at | 0.7410 | 0.7166 | MP1 | Melanization Protease 1 |
| 1628097_at | 0.7495 | 0.7166 | elk | eag-like K[+] channel |
| 1632979_at | 0.6159 | 0.7148 | CG11784 | CG11784 |
| 1631536_at | 0.8597 | 0.7124 | Dip3 | Dorsal interacting protein 3 |
| 1639856_at | 0.9450 | 0.7119 | CG5727 | CG5727 |
| 1624617_at | 0.6042 | 0.7095 | CG1665 | CG1665 |
| 1638278_s_at | 0.5917 | 0.6880 | Myo61F | myosin61F |
| 1635074_s_at | 1.1320 | 0.6832 | --- | --- |
| 1623508_at | 1.0617 | 0.6813 | CG30466 | CG30466 |
| 1633626_at | 0.6136 | 0.6798 | CG14104 | CG14104 |
| 1627843_at | 0.7257 | 0.6793 | CG12253 | CG12253 |
| 1634570_at | 1.7582 | 0.6760 | CG5375 | CG5375 |
| 1628445_at | 0.9610 | 0.6736 | CG33213 | CG33213 |
| 1631101_at | 0.6639 | 0.6711 | CG6480 | CG6480 |
| 1630730_at | 0.7513 | 0.6617 | CG6808 | CG6808 |
| 1628453_at | 0.6171 | 0.6609 | l(1)G0289 | lethal (1) G0289 |
| 1637461_at | 0.6535 | 0.6595 | CG9527 | CG9527 |
| 1638344_at | 0.7893 | 0.6569 | CG5287 | CG5287 |
| 1626615_at | 0.7644 | 0.6532 | CG31156 | CG31156 |
| 1631183_at | 0.7454 | 0.6477 | RhoL | Rho-like |
| 1627302_at | 0.6820 | 0.6410 | Fmo-2 | Flavin-containing monooxygenase 2 |
| 1636730_at | 0.6045 | 0.6345 | CG13373 | CG13373 |
| 1623904_a_at | 0.8428 | 0.6306 | Rpt3R | Rpt3R |
| 1623022_at | 0.8046 | 0.6210 | CG15820 | CG15820 |
| 1641117_a_at | 0.8063 | 0.6153 | CG17600 | CG17600 |
| 1627854_at | 0.6181 | 0.6115 | CG9914 | Enoyl-CoA hydratase mitochondrial |
| 1623887_at | 1.2932 | 0.6097 | Pimet | CG12367 |
| 1623271_a_at | 0.5912 | 0.5977 | janA | janus A |
| 1641455_at | 0.8489 | 0.5862 | CG6762 | CG6762 |
| 1637815_s_at | -0.8570 | -0.5859 | Cka | connector of kinase to AP-1 |
| 1629835_at | -0.8112 | -0.5990 | CG5048 | CG5048 |
| 1637928_at | -0.9457 | -0.5999 | gb / Oatp58Db | CG6070 / Organic anion transporting polypeptide 58Db |
| 1625992_s_at | -0.6284 | -0.6025 | CG34413 | CG32836 |
| 1638171_s_at | -0.7851 | -0.6311 | CG1753 | CG1753 |
| 1635399_s_at | -0.6195 | -0.6435 | CG11006 | CG11006 |
| 1632963_at | -0.6514 | -0.6515 | CG4963 | anon-fast-evolving-2H5 |
| 1627888_at | -0.7302 | -0.6554 | CG6672 | CG6672 |
| 1632098_at | -0.8236 | -0.6626 | CG4364 | CG4364 |
| 1637703_a_at | -0.8560 | -0.6723 | Socs36E | Suppressor of cytokine signaling at 36E |
| 1640905_at | -0.9685 | -0.6741 | wibg | within bgcn |
| 1628807_at | -1.0074 | -0.6779 | CG5205 | CG5205 |
| 1641576_a_at | -1.2820 | -0.6917 | CG5205 | CG5205 |
| 1622909_at | -0.5917 | -0.7065 | Pi3K21B | dPI 3-kinase |
| 1631006_a_at | -0.7350 | -0.7123 | CG10171 | CG10171 |
| 1636149_at | -1.0581 | -0.7165 | CG31705 | CG31705 |
| 1625791_s_at | -0.9043 | -0.7240 | --- | --- |
| 1627704_a_at | -0.7820 | -0.7267 | Traf4 | TNF Receptor Associated Factor 1 |
| 1641059_at | -0.9559 | -0.7268 | Ca-P60A | organellar-type Ca-ATPase |
| 1626606_at | -2.2609 | -0.7288 | CG10630 | CG10630 |
| 1631527_at | -0.6813 | -0.7290 | CG5642 | CG5642 |
| 1627454_a_at | -0.6859 | -0.7301 | cora | Coracle |

| | | | | |
|---|---|---|---|---|
| 1625744_at | -0.7559 | -0.7317 | GstE6 | Glutathione S transferase E6 |
| 1637055_s_at | -0.8695 | -0.7421 | --- | --- |
| 1637612_at | -0.5893 | -0.7424 | Hip14 | htt-interacting protein 14 |
| 1639048_a_at | -0.7242 | -0.7444 | CG8229 | CG8229 |
| 1636745_at | -0.7040 | -0.7478 | Art4 | *Drosophila* arginine methyl-transferase 4 |
| 1638274_s_at | -0.8298 | -0.7541 | pix | pixie |
| 1637510_s_at | -1.2060 | -0.7718 | Hexo1 | Hexosaminidase 1 |
| 1639215_at | -0.6561 | -0.7748 | Csat | *D.melanogaster* nucleotide sugar transporter |
| 1629324_at | -0.7689 | -0.7782 | CG6870 | cytochrome B5 |
| 1633252_at | -0.6522 | -0.7819 | CG31714 | CG31714 |
| 1630515_s_at | -1.4784 | -0.7957 | Glt | glutactin |
| 1626563_at | -0.7008 | -0.7984 | Taf6 | Suppressor of Ras85D 3-4B |
| 1625856_at | -0.8156 | -0.8035 | dm | diminutive |
| 1640884_at | -0.6817 | -0.8105 | CG15784 | CG15784 |
| 1630091_at | -0.8239 | -0.8191 | CG31296 | CG31296 |
| 1626621_at | -0.6774 | -0.8338 | CG1407 | CG1407 |
| 1640567_at | -0.7926 | -0.8441 | CG7337 | CG7337 |
| 1627142_at | -1.0690 | -0.8621 | CG2943 | CG2943 |
| 1625885_at | -0.8182 | -0.8723 | betaTub97EF | beta tubulin |
| 1636302_s_at | -0.7759 | -0.9000 | Su(dx) | Suppressor of deltex |
| 1640065_at | -0.8571 | -0.9041 | GstE7 | Glutathione S transferase E7 |
| 1636968_at | -0.9213 | -0.9088 | CG5559 | CG5559 |
| 1637060_a_at | -0.6527 | -0.9190 | Nopp140 | Nopp140 |
| 1625945_a_at | -0.9598 | -0.9214 | CG1233 | CG1233 |
| 1629846_at | -1.0410 | -0.9276 | CG11619 | CG11619 |
| 1622926_at | -0.7760 | -0.9277 | CG5776 | CG5776 |
| 1637370_at | -1.3887 | -0.9389 | yellow-f | yellow f |
| 1623320_at | -0.9114 | -0.9456 | CG3711 | CG3711 |
| 1632465_s_at | -0.7436 | -0.9702 | CG6424 | CG6424 |
| 1633473_s_at | -1.0151 | -0.9733 | Ald | aldolase |
| 1633641_a_at | -1.0767 | -0.9955 | CG15611 | CG15611 |
| 1640489_at | -1.7766 | -1.0064 | CG18522 | CG18522 |
| 1634167_a_at | -0.9641 | -1.0177 | sage | salivary gland-expressed bHLH |
| 1625489_at | -0.9037 | -1.0191 | --- | --- |
| 1641548_at | -0.7579 | -1.0342 | CG10289 | CG10289 |
| 1629776_a_at | -0.9815 | -1.0560 | CG6643 | CG6643 |
| 1641068_a_at | -1.4281 | -1.0614 | spz | Spaetzle |
| 1623415_at | -1.0754 | -1.0749 | dl | dorsal |
| 1634731_at | -1.0202 | -1.0949 | Cyp4p3 | Cyp4p3 |
| 1637188_s_at | -1.5477 | -1.0986 | CG30492 | CG30492 |
| 1637936_at | -1.0374 | -1.1062 | CG32512 | CG32512 |
| 1633237_at | -1.8793 | -1.1713 | Idgf1 | Imaginal disc growth factor1 |
| 1628613_a_at | -1.3817 | -1.1746 | CG30492 / CG30494 | CG30492 / CG30494 |
| 1635714_s_at | -0.6911 | -1.1825 | fdl | fused lobes |
| 1623663_a_at | -1.5868 | -1.1854 | CG18063 | CG18063 |
| 1638708_s_at | -0.8571 | -1.2593 | gpp | grappa |
| 1635028_s_at | -1.3175 | -1.2859 | Fuca | alpha-L-fucosidase |
| 1635462_at | -1.2174 | -1.3364 | rho | rhomboid |
| 1634048_a_at | -1.6744 | -1.3394 | bgm | bubblegum |
| 1627312_at | -0.8411 | -1.3682 | RpL12 | Ribosomal protein L12 |
| 1635512_at | -1.4638 | -1.3778 | CG11893 | CG11893 |
| 1633964_at | -0.7880 | -1.3994 | CG3626 | CG3626 |
| 1636323_at | -1.3718 | -1.4120 | CG2249 | CG2249 |
| 1635630_a_at | -1.4942 | -1.4349 | spir | spire |
| 1627513_at | -0.9962 | -1.4363 | --- | --- |
| 1633905_at | -1.6198 | -1.4666 | RpL28 | Ribosomal protein L28 |

| | | | | |
|---|---|---|---|---|
| 1629484_s_at | -1.0079 | -1.4769 | chinmo | Chronologically inappropriate morphogenesis |
| 1630412_at | -1.4859 | -1.4805 | nimB5 | CG16873 |
| 1637347_at | -2.0855 | -1.6057 | CG34164 / CG5317 | CG34164 / CG5317 |
| 1631123_at | -1.7171 | -1.6778 | Corin | DCorin |
| 1633459_a_at | -1.7201 | -1.6862 | fau | fau |
| 1629771_at | -1.2399 | -1.7365 | Cyp12a5 | Cyp12a5 |
| 1625388_at | -1.6575 | -1.7661 | CG4893 | CG4893 |
| 1638859_at | -2.0157 | -1.7806 | CG14741 | CG14741 |
| 1634002_at | -2.1558 | -1.7817 | CG13315 | CG13315 |
| 1640856_at | -1.8191 | -1.8016 | CG14755 | CG14755 |
| 1631222_at | -2.5403 | -1.8303 | pdm3 | pou domain motif 3 |
| 1628890_at | -1.6279 | -1.9595 | CG11873 | CG11873 |
| 1639495_at | -2.4164 | -1.9655 | Cyp9b1 | Cytochrome P450-9b1 |
| 1639321_s_at | -2.0132 | -2.0115 | Tl | toll |
| 1639692_s_at | -2.0482 | -2.0473 | dl | dorsal |
| 1639834_at | -2.0699 | -2.0838 | CG14291 | CG14291 |
| 1637012_at | -2.2272 | -2.1204 | m2 | E(spl) region transcript m2 |
| 1625873_at | -2.7727 | -2.4568 | CG15661 | CG15661 |
| 1637962_at | -1.5755 | -2.5169 | spir | spire |
| 1631701_a_at | -3.1035 | -2.5682 | Cpr49Ac | CG8502 |
| 1626048_at | -2.7214 | -2.5741 | HLHmgamma | split locus enhancer protein mB |
| 1640202_at | -3.4350 | -2.7265 | Idgf2 | Imaginal disc growth factor 2 |
| 1639637_a_at | -3.9943 | -3.1120 | CG3376 | CG3376 |
| 1640654_at | -5.7820 | -5.7820 | He | Hemese |

## Abbreviations and acronyms

Amino acids are abbreviated with the common single or three letter code. The nucleotides Adenine, Guanine, Cytosine, Thymine and Uracil are abbreviated with A, G, C, T and U, respectively. Posttranslational modifications of histones are referred to with the abbreviation of the corresponding histone (H1, H3, H4, H2A or H2B), the amino acid residue in the single letter code including its position within the amino acid sequence and the modification status (e.g. me1, me2, me3, ac, ph). Therefore histone modifications are abbreviated for instance as H4K20me1 or H3K27me3.

| | |
|---|---|
| α | anti |
| aa | amino acid |
| Ab | antibody |
| ac | acetyl/acetylated |
| Acf1 | ATP-dependent chromatin assembly factor 1 |
| ADP | adenosine diphosphate |
| AKT | murine thymoma viral oncogene or protein kinase B |
| AML | acute myeloid leukemia |
| Ash1 | Absent, small, or homeotic discs 1 |
| ATP | adenosine triphosphate |
| BD | binding domain |
| BEAF-32 | Boundary element-associated factor 32 |
| BHC80 | BRAF-histone deacetylase complex 80 |
| BLAST | basic local alignment search tool |
| bp | base pair |
| 53BP1 | p53 binding protein 1 |
| BPTF | Bromo domain PHD finger transcription factor |
| c | *Caenorhabditis* |
| C- | carboxy-/carboxyl- |
| Caf1 | Chromatin assembly factor 1 |
| cDNA | complementary DNA |
| del | deletion |
| *C. elegans* | *Caenorhabditis elegans* |
| CG x | computed gene x |
| CG | cancer-germline |
| ChIP | chromatin immunoprecipitation |
| ChIP-Seq | ChIP sequencing |
| CoREST | REST corepressor |
| CP190 | Centrosomal protein 190 |
| cpm | counts per minute |
| Ct | cycle threshold |

| | |
|---|---|
| CT | cancer-testis |
| CTCF | CCCTC-binding factor |
| CTD | C-terminal domain |
| d | Drosophila |
| *D. melanogaster* | *Drosophila melanogaster* |
| *da* | *daughterless* |
| Da | dalton |
| DAPI | 4',6-diamidino-2-phenylindole |
| DDR | DNA damage response |
| DMSO | dimethyl sulfoxide |
| DNA | deoxyribonucleic acid |
| DNMT | deoxyribonucleic acid methyltransferase |
| dNTP | deoxyribonucleotide triphosphate |
| DP | Dimerisation partner |
| dREAM | *Drosophila* RBF, dE2F2, and dMyb-interacting proteins |
| DRM | DP, RB and MuvB |
| DSB | double strand break |
| dsRNA | Double-stranded ribonucleic acid |
| DTT | dithiotreithol |
| EtBr | ethidium bromide |
| *E. coli* | *Escherichia coli* |
| Esc | Extra sex combs |
| Escl | Esc-like |
| EDTA | ethylene diamine tetra acetic acid |
| EED | Early embryonic death |
| EGFP | Enhanced green fluorescent protein |
| EGTA | ethylene glycol tetra acetic acid |
| EMS | ethyl methane sulfonate |
| Epo | erythropoietin |
| Ets | E-26 transforming specific |
| E(z) | Enhancer of zeste |
| FBS | fetal bovine serum |
| FC | fold change |
| FCS | fetal calf serum |
| FOXO | Forkhead box O-class |
| fw | forward |
| g | gram |
| Gcn5p | General control of amino acid synthesis 5 protein |
| G0-phase | gap phase 0 |
| G1-phase | gap phase 1 |
| GMC | ganglion mother cell |
| GST | glutathione-S-transferase |
| h | human |
| HAT | histone acetyltransferase |

| | |
|---|---|
| HDAC | histone deacetylase |
| Hepes | 4-(2-hydroxyethyl)-1-piperazineethanesulfonic acid |
| HKMT | histone lysine methyltransferase |
| Hox | *Homeobox*-containing |
| HP1 | Heterochromatin protein 1 |
| HPLC | high performance liquid chromatography |
| hr | hour |
| HRP | horseradish peroxidase |
| *Hsp70* | *Heat shock protein 70* |
| HSPC | hematopoietic stem/progenitor cells |
| IEX | ion exchange chromatography |
| Ig | immunoglobuline |
| INP | intermediate neural progenitor |
| IP | immunoprecipitation |
| IPTG | iso-propyl-ß-D-thiogalactopyranoside |
| ISWI | Imitation switch |
| ITC | isothermal titration calorimetry |
| *iv*T | *in vitro* transcription |
| JmjC | Jumonji C |
| JMJD | Jumonji domain containing |
| kDa | kilo dalton |
| KDM2 | Lysine-specific demethylase 2 |
| LB | lysogeny broth |
| Lid | Little imaginal discs |
| Lint-1 | L(3)mbt interacting |
| L(3)mbt | Lethal 3 malignant brain tumour |
| L3MBTL | Lethal 3 malignant brain tumour-like |
| Lsd1 | Lysine-specific demethylase 1 |
| M | molar |
| MAPK | Mitogen-activated protein kinase |
| MBT | malignant brain tumour |
| MBTS | MBT signature |
| MDa | mega dalton |
| MDS | myelodysplastic syndromes |
| me | methyl/methylated |
| Mec | MEP-1-containing complex |
| MES | 2-(N-morpholino)ethane sulfonic acid |
| Mi-2 | Mitchell-2 |
| min | minute |
| MLL | mixed-lineage leukemia |
| mRNA | messenger ribonucleic acid |
| MPD | myeloproliferative disorders |
| M-phase | mitosis phase |
| MS | mass spectrometry |

| | |
|---|---|
| Muv | multivulva |
| N- | amino- |
| NB | neuroblast |
| NCBI | National Center for Biotechnology Information |
| NE | nuclear extract |
| NFR | nucleosome free region |
| NMR | nuclear magnetic resonance |
| NuRD | Nucleosome remodelling and histone deacetylase |
| NURF | Nucleosome remodelling factor |
| Nurf55 | Nucleosome remodelling factor 55 |
| OL | optic lobe |
| ORF | open reading frame |
| PAA | polyacrylamide |
| PADI | peptidylarginine deiminase |
| PAGE | polyacrylamide gel electrophoresis |
| PBS | phosphate buffered saline |
| Pc | Polycomb |
| Pcl | Polycomb-like |
| P/CAF | p300/CBP-associated factor |
| PcG | Polycomb group |
| PCR | polymerase chain reaction |
| pdb | protein data base |
| Pen/Strep | penicillin/streptomycin |
| PEV | positional-effect variegation |
| ph | phosphate/phosporylated |
| Ph | polyhomeotic |
| PHD | plant homeo domain |
| Pho | Pleiohomeotic |
| PhoRC | Pho-repressive complex |
| PMSF | phenylmethylsulfonyl fluoride |
| Pol | polymerase |
| pRB | retinoblastoma protein |
| PRC1 | Polycomb repressor complex 1 |
| PRC2 | Polycomb repressor complex 2 |
| PRE | Polycomb response element |
| PRMT | protein arginine methyltransferase |
| PR-Set7 | PR/SET domain-containing |
| Psc | Posterior sex combs |
| PTM | post-translational modification |
| PV | polycythaemia vera |
| PVDF | polyvinyl difluoride |
| qPCR | quantitative PCR |
| RBF | Retinoblastoma family protein |
| RNA | ribonucleic acid |

| | |
|---|---|
| RNAi | RNA interference |
| RNA Pol II | RNA polymerase II |
| Rpd3 | Reduced potassium dependency 3 |
| rpm | revolutions per minute |
| RSCB | Research Collaboratory for Structural Bioinformatics |
| RT | room temperature |
| RT-qPCR | real time-quantitative PCR |
| rv | reverse |
| s | second |
| SAH | S-adenosyl-L-homocysteine |
| SAM | S-adenosyl-methionine |
| SAM domain | sterile alpha motif domain |
| Sce | Sex combs extra |
| *S. cerevisiae* | *Saccharomyces cerevisiae* |
| Scm | Sex comb on midleg |
| SDS | sodium dodecyl sulphate |
| sec | second |
| SET | Su(var)3-9, E(z) and Trx |
| Sfmbt | Scm-related gene containing four mbt domains |
| sgs | salivary gland-specific |
| Sp3 | Specificity protein 3 |
| S-phase | DNA synthesis phase |
| SPM domain | Scm, Ph and MBT homology domain |
| STAT5 | Signal transducer and activator of transcription |
| SUMO | Small ubiquitin-like modifier |
| Su(Hw) | Suppressor of Hairy-wing |
| Su(var) | Suppressor of variegation |
| Su(z)12 | Suppressor of zeste 12 |
| synMuv | synthetic multivulva |
| SWH | Salvador-Warts-Hippo |
| SWI/SNF | Switch/Sucrose NonFermentable |
| Temed | tetramethylethylenediamine |
| Tris | tris(hydroxyl-methyl)aminomethane |
| Trx | Trithorax |
| trxG | trithorax group |
| ts | temperature sensitive |
| TSA | trichostatin A |
| UTX | Ubiquitously transcribed tetratricopeptide repeat on X chromosome |
| VDRC | Vienna Drosophila RNAi Center |
| VNC | ventral nerve cord |
| v/v | volume per volume |
| w/v | weight per volume |
| Zn | zinc |

## Curriculum vitae

## List of academic teachers

My academic teachers at the University of Bayreuth were the following professors:

Alt, Bauer-Catanese, Beck, Dettner, Gradzielski, Gremer, Haarer, Hillebrecht, Hoffmann, Komor, Krausch, Krauss, Lehner, Meyer, Morys, Peternell, Platz, Rösch, Schmid, Schobert, Schumann, Seifert, Sprinzl, Unverzagt, Völkl.

## Acknowledgements

At this point, I would like to thank and acknowledge all people, who have supported me in the course of this thesis and have contributed indirectly or directly to this study.

## Ehrenwörtliche Erklärung